Guidance and Neuronal Properties of Dental Pulp Stem Cells:

A thesis submitted for the degree of Doctor of Philosophy

Agnieszka Stokowski, B.Sc (Hons.)

School of Molecular and Biomedical Science, Genetics discipline
Centre for the Molecular Genetics of Development
University of Adelaide University, Australia
Institute of Medical and Veterinary Science, Haematology department

November 2006

Contents

Table of Figures

Declaration

I declare that this thesis contains no material that has been accepted for the award of any other degree or diploma in any university or other tertiary institution. To the best of my knowledge and belief, this thesis contains no material previously published or written by another person, except where due reference has been made in the text.

I consent to this copy of my thesis, when deposited in the University of Adelaide library, being made available for photocopying and loan if accepted for the award of Doctor of Philosophy.

November 2006

Personal Bibliography

EphB/ephrin-B interaction mediates adult stem cell attachment, spreading and migration: implications for dental tissue repair

A Stokowski, S Shi, T Sun, PM Bartold, SA Koblar, S Gronthos

In Press, Stem Cell Journal, accepted 20th September 2006.

In preparation:

- Development of the Ikaros assay, Nature Biotechnology
- Adult stem cell potential for stroke therapy. Journal Clinical Neuroscience
- Eph/ephrin expression in the DRG. Journal to be decided.

Abstract

Human adult dental pulp stem cells (DPSC) reside within the perivascular niche of dental pulp and are thought to originate from migrating cranial neural crest (CNC) cells. During development, CNC cells respond to the environmental cues to migrate and differentiate into the different cell types that contribute to the formation of craniofacial structures and the peripheral nervous system. The Eph family of receptor tyrosine kinases and their ligands, the ephrin molecules, play an essential role in the migration of neural crest cells during development and postnatal stem cell (SC) niche maintenance.

The present study demonstrated multiple Eph receptors expressed primarily on DPSC within the perivascular niche, while the surrounding pulp tissue expressed ephrin-B ligands. EphB/ephrin-B bi-directional signalling inhibited DPSC attachment and spreading, while DPSC migration was restricted through uni-directional ephrin-B1 activated EphB forward signalling *in vitro*. Furthermore, we observed that ephrin-B1 was down-regulated in diseased adult teeth compared to paired uninjured controls. Collectively, these studies suggest that EphB/ephrin-B molecules play a role in restricting DPSC attachment and migration in order to maintain DPSC within their SC niche under steady-state conditions. These results may have implications for dental pulp development and regeneration of the dentine matrix following injury or disease.

The present study also examined the neural potential of human DPSC. The data demonstrated that *ex vivo* expanded human adult DPSC responded to both neuronal inductive conditions and enforced transcriptional activation, acquiring a neuronal morphology and expressing neuronal specific markers at both the gene and protein levels. An *in vivo* avian transplantation assay was developed, "Ikaros Assay", to examine the response of human DPSC to endogenous neural environmental cues. DPSC expressed neuronal markers and acquired a neuronal morphology, following transplantation into the mesencephalon of embryonic day two chick embryos. This was also observed for other SC populations derived from deciduous teeth (SHED) and partially for bone marrow stromal stem cells (BMSSC) but not skin fibroblasts (SFB). Furthermore, axonal processes of the avian peripheral nervous system redirected their migration towards transplanted DPSC, implying that DPSC expressed factors important for axonal outgrowth. In summary, it is proposed that adult human DPSC may be an alternative exogenous source of neural SC and/or reservoirs of neurotrophic factors for the treatment of neural diseases, such as stroke.

Acknowledgements

I would like to thank a number of people for their support and help during this PhD. First and foremost, I would like to thank my fiancé, Craig Arthur, for believing in me, supporting and encouraging me throughout the PhD, especially during the writing process, and for keeping me sane.

I would like to say a huge thank you to my family, my parents (Helena and Jerzy), my brother (Darek), my sister (Joanna) and her family (Ken, Casey and Ryan). They have supported me, believed in me, and helped me enormously, I'm sure that I couldn't have done it without them.

Enormous thanks must go to both of my supervisors - Dr. Simon Koblar and Dr. Stan Gronthos – both of whom have been instrumental in my development as an autonomous and analytical scientist. Thankyou for your guidance, advice and support during my PhD.

Thank you to all the lab members both past and present of both the Koblar and Gronthos labs and also to Andrew Zannatino and his lab members. The scientific discussions over the years have helped me to develop creative and novel ideas. It has been a real pleasure working with you all. I would also like to especially thank Dr. Anne-Hamilton Bruce for assisting in the editing process of the thesis, your time and effort was greatly appreciated and to Dr. Tao Sun for assisting me with the avian embryo injections.

I would like to thank the Genetics department at the University of Adelaide and also the Haematology department at the IMVS for making me feel welcome. I would especially like to thank Velta Vingelis and Helli Meinecke for their lengthy discussions of life in general.

Finally, I would like to thank my close friends, especially Nadia, Kylie, Natalie for their constant encouragement and support. I truly appreciate your friendship.

Abbreviations

ALPase	alkaline phosphatase
BDNF	brain derived neurotrophic factor
bHLH	basic helix-loop-helix
BMP	bone morphogenic protein
BMSSC	bone marrow stromal stem cells
BrdU	bromodeoxyuridine
BSA	bovine serum albumin
CAP	cbl-associated protein
Cdks	cyclin dependent kinases
cDNA	complementary deoxyribonucleic acid
CHX	cyclohexamide
CNC	cranial neural crest
CNS	central nervous system
DAPI	4',6-diamidino-2-phenylindole dihydrochloride
DG	dentate gyrus
DMSO	dimethyl-sulfoxide
DNA	deoxyribonucleic Acid
DPC	dental pulp cells
DPSC	dental pulp stem cells
DPP	dentin sialoprotein
DRG	dorsal root ganglion
DSP	dentin phosphoprotein
DSPP	dentin sialophosphoprotein
ECM	extracellular matrix
EGF	epithelial growth factor
ELIZA	enzyme-linked immunosorbent assay
EMT	epithelial to mesenchymal transition
ERK	extracellular signal-regulated kinase
ERM	Est-related molecule
ESC	embryonic stem cells
Fc	fusion protein
FGF	fibroblast growth factor
FCS	foetal calf serum
GABA	gamma amino butyric acid
GAP	GTPase-activating protein
G-CSF	granulocyte colony-stimulating factor
GEF	guanine exchange factor
GFAP	glial fibrillary acidic protein
GFP	green fluorescent protein
GTPase	guanosine triphosphatase
Hox	homeobox type 1 transcription factor
HSC	haematopoietic stem cells
IC	intestinal crypt
ISC	intestinal stem cells
LAB	living autologous fibrous bone
LB	luria broth
LGE	lateral ganglionic eminence
LIF	leukemia inhibitory factor
MAPK	mitogen activated protein kinase
MEK	MAPK/ERK kinase
MEPE	matrix extracellular glycoprotein
MGE	medial ganglionic eminence
mRNA	messenger ribonucleic acid
MSC	mesenchymal stem cells
NCSC	neural crest stem cells
NDRF	NeuroD related factor

NeuroD	neurogenic differentiation
NF	neurofilament
NF-M	neurofilament medium chain
NF-H	neurofilament heavy chain
NGF	nerve growth factor
Ngn-1	neurogenin-1
NHT	normal human teeth
NIA	neural induction assay
NLS	nuclear localisation signal
NMDA	N-methyl-D-aspartate
NSC	neural stem cells
NSE	neural specific enolase
NT	neurotrophin
OB	olfactory bulb
OPN	osteopontin
P	passage
PBS	phosphate buffered saline
PBS-T	phosphate buffered saline + 0.1% Tween-20
PBS-TX	phosphate buffered saline + 0.3% triton-X 100
PDGF	platelet-derived growth factor
PDL	periodontal ligament
PDZ	postsynaptic density, discs-large, zona occludens-1
PFA	paraformaldehyde
PGP 9.5	protein gene product 9.5
PI	Post injection
PI3K	phosphoinositide 3- kinase
PNS	Peripheral Nervous System
PP2	Src kinase kinase inhibitor
PSA-NCAM	Polyasetylated – N cell adhesion molecule
PTZ	pentylenetetrazol
r	rhombomere
RA	retinoic acid
RMS	rostral migratory stream
RTK	receptor tyrosine kinase
RT-PCR	real time polymerase chain reaction
SBP	stromal bone producing
SC	stem cells
SCF	stem cell factor
SDF-1	stromal derived factor 1
SDS	sodium dodecyl sulfate
SEM	standard error of the mean
SFB	skin fibroblasts
SGZ	sub-granular zone
SHED	stem cells from human exfoliated deciduous teeth
SH	Src homology
Shh	sonic hedgehog
SIC	spreading initiation centre
SMP	Schwann cell myelin protein
SOCS	suppressor of cytokine signalling
SPARC	Secreted protein acidic and rich in cytokine
STRO-1	early mesenchymal stem cell marker
SVZ	sub-ventricular zone
TAC	transient amplifying cells
TG (or V)	trigeminal ganglion
TGF	transforming growth factor
TNC	trunk neural crest
TNF	tumour necrosis factor
TRITC	tetramethylrhodamine β isothiocyanate
TUJ1	β-tubulin III clone
μ	microns
U0126	ERK/MEK inhibitor
VZ	ventricular zone
Wnt	wingless related proteins
WST-1	tetrazolium salt

Chapter 1 - Introduction

1.1 Stem cells

Stem cells (SC) have the capacity to self-renew and develop into numerous cell types via asymmetric cell division. The different SC populations can be broadly clustered into two groups (1) totipotent embryonic stem cells (ESC) and (2) pluri or multipotent adult tissue specific SC. The properties that define a SC and what regulates it "stemness" are thought to involve a subset of 216 genes that were identified by a microarray analysis comparing ESC and two adult SC populations, hematopoietic and neural SC (HSC and NSC, respectively) (Ramalho-Santos et al., 2002). This microarray analysis provided insight that adult SC may possess greater plasticity then first anticipated. The differentiation potential of adult SC has been clearly demonstrated with mesenchymal SC (MSC) with both *in vitro* and transplantation experiments (Jiang et al., 2002). It therefore appears that adult or multi-potent SC from different sources have similar phenotypic and functional properties and may encompass a broader potential or plasticity than initially proposed.

1.1.1 Purpose and function of stem cells

Totipotent ESC are the least restricted population of SC in relation to cell growth and differentiation. ESC can give rise to any cell type that is ultimately derived from the three embryonic layers: endoderm, mesoderm and ectoderm (Gage, H., 2000; Henningson et al., 2003). Most adult SC, however, are pluri or multipotent and are believed to have restricted growth potentials and differentiation capacities. For example neural SC have the potential to differentiate into astrocytes, oligodendrocytes and neurons (Reynolds et al., 1992).

Recently, it has been suggested that multipotent SC are also capable of undergoing trans-differentiation, the process by which SC can develop into cell types derived from different germ layers (Bjornson et al., 1999). The debate continues between the differentiation of SC into cell types of other germ layers and whether this trait is attributed to fusion, trans-differentiation or de-differentiation (Weissman et al., 2001). The question that needs to be addressed is whether these SC require a more primitive state, similar to ESC, as an

intermediate in trans-differentiation (Tsai et al., 2002), or whether simple instructive factors in culture or from the host would be sufficient.

Current research suggests that instructive environmental factors, in culture or *in vivo* are essential for trans-differentiation of adult SC types and, may therefore be potentially an ideal source for cellular based therapeutic treatments. Multiple studies have shown that when *ex vivo* expanded MSC were transplanted *in vivo*, they responded to endogenous environmental cues. The MSC cells differentiated into neural cell types when engrafted into the lateral vertical of neonatal mice (Kopen et al., 1999) or contributed to most somatic cell types when transplanted into the early blastocyst stage in the embryo (Jiang et al., 2002). Multipotent adult SC are located in many organs within the body including the epidermis, intestine, bone marrow, liver, neural and neural crest, and most recently identified dental tissues (Alvarez-Buylla et al., 2004; Gronthos et al., 2000; Morrison et al., 1999; Seo et al., 2004; Wagers et al., 2002; Weissman et al., 2001; Young et al., 2002; Zhang et al., 2003). SC reside in specialised regions within their respective organs, often referred to as a SC "niche" (Scadden, T., 2006).

1.1.2 The stem cell niche

Dexter and colleagues, who investigated the bone marrow stromal support of hematopoietic SC, were the first considered the concept of a SC niche. These researchers noted that SC maintenance was dependent on the microenvironment surrounding the SC (Dexter et al., 1977). Schofield took this concept further in 1978, proposing that the microenvironment, which he termed "niche", would need to exist within organs to allow a self-renewing cell to maintain its plasticity within a tissue-type, while still allowing the daughter cell to differentiate (Schofield, R., 1978; Schofield, R., 1983). This concept of the SC niche was extrapolated to studies of the gonads of *Drosophila melanogaster* and *Caenorhabditis elegans* (Crittenden et al., 2002; Xie et al., 2000) and later in mammals (Hess et al., 2006). The most current understanding of a SC niche is that of a specialised physical location, which constitutes a 3-dimensional microenvironment provided by support cells. In this microenvironment, SC and transient amplifying cells (TAC) are protected and controlled in their self-renewing capacity, retaining SC in their undifferentiated state or subsequent differentiation. The homeostasis or the balance of SC relative to the needs of the organism is

maintained by an intricate signalling process (Fuchs et al., 2004; Hess et al., 2006; Moore et al., 2006; Scadden, T., 2006).

A SC niche is not believed to be static in function or number; it can be created or made to change in response to specific conditions such as stress or injury (Scadden, T., 2006). Thus clearly identifying and understanding the components that control SC niche function would contribute to the development of future therapeutic strategies to enhanced repair following injury. The signals involved in maintaining the SC niche, the self-renewal and differentiation processes are believed to require a range of physical, structural and paracrine factors, metabolic processes and indirect communication between the niche and the sympathetic nervous system (reviewed by (Scadden, T., 2006)).

The physical structure of the niche is vital to provide a specialised microenvironment, a residence for the quiescent SC, or alternatively, a place that allows for their change in location. Paracrine factors, such as wingless related proteins (Wnt) and associated morphogens, Notch, BMP, FGF and sonic hedgehog (Shh), are expressed by the supportive cells of a range of SC niches including the haematopoietic, intestine, hair follicle, ovary, and the brain to name a few. These factors are believed to be essential for the establishment and maintenance of SC within their niche (Holmberg et al., 2006; Lim et al., 2000; Martino et al., 2006; Niemann, C., 2006; Ross et al., 2006; Scadden, T., 2006; Tsai et al., 2002). Equally important are the molecules that retain the architectural organization of established niche structures; this component of the SC niche is not well defined. It has been suggested that cell adhesion molecules (Wang et al., 2006) and chemokines (Papayannopoulou, T., 2004) contribute to the anchorage of the SC niche, while guidance molecules (Holmberg et al., 2006) are important for the organization of the niche structure. The Eph family of receptor tyrosine kinases (RTKs), are important mediators of neural and vascular structural boundary formation, and have been implicated in intestinal epithelial SC niche organization (Holmberg et al., 2006). Eph/ephrin interactions have also been shown to act as negative regulators of neural SC/progenitor proliferation (Depaepe et al., 2005; Holmberg et al., 2005).

A major discovery was recently made demonstrating that the peripheral nervous system (PNS) coordinates the localisation of HSC to their niche within the bone (Katayama et al., 2006). During development and as adults, the HSC exit and re-engage their niche. It was postulated that the sympathetic nervous system activates granulocyte colony-stimulating

factor (G-CSF). G-CSF then triggers the release of proteases that degrade adhesion molecules and chemokines, which normally retain HSC within the bone marrow (Papayannopoulou, T., 2004), thus allowing HSC to leave their SC niche (Katayama et al., 2006; Papayannopoulou, T., 2004; Semerad et al., 2005). It therefore appears that the bone marrow, the bone and the nervous system integrate signals to regulate the HSC niche. More significantly, Lapidot and colleagues showed that the HSC niche is regulated by bone lining cells and bone resorbing osteoclasts (Kollet et al., 2006). As the nervous system connects anatomically to all tissue of an organism, this finding could have some bearing on the SC response to change in the environment, eg, following mechanical injury or disease.

Another inherent system that connects or engages with all tissue types is the vascular system. It has also been suggested that the perivascular environment influences SC niche function (Hackney et al., 2002). The peri-vasculature and MSC populations associate with many organs of the body (Meirelles et al., 2006). Palmer and colleagues investigated the association of neurogenesis with a vascular niche and identified that within the sub-granular zone (SGZ), clusters of proliferative cells assemble around small capillaries (Palmer et al., 2000). It has been postulated that within these clusters neurogenesis occurred concurrently with vascular recruitment and remodelling (Palmer et al., 2000). It was proposed that two hierarchies of signalling must exist, extrinsic somatic cues and intrinsic central nervous system (CNS) cues, which act together to modulate neurogenesis. BMSSC, periodontal ligament SC (PDLSC) and dental pulp stem cells (DPSC) have also been shown to reside within the microvasculature of their specific organ (Gronthos et al., 2000; Gronthos et al., 2003; Seo et al., 2004; Shi et al., 2003). More specifically, immunohistochemical analysis showed that BMSSC, PDLSC and DPSC localise with vascular and endothelial markers CD146, smooth muscle actin and von Willebrand factor, while 14% of BMSSC and 63% of DPSC also co-localised with pericyte marker 3G5, and thus are thought to reside within a perivascular niche (Chen et al., 2006; Gronthos et al., 2003; Shi et al., 2003). Pericytes reside in and are integral to the microvasculature; they are thought to be important for angiogenesis. It has been demonstrated that pericytes have similar properties (Doherty et al., 1998; Schor et al., 1995) and functions to MSC and maybe precursor cells of MSC in bone marrow and other tissues.

The above-mentioned studies indicate that four distinctly different SC populations, NSC, BMSSC, PDLSC and DPSC, associate within a vasculature niche environment. Extensive

research has been conducted into BMSSC, their proliferation, differentiation and maintenance within a microenvironment. Furthermore, studies investigating the association of a vascular niche with NSC have indicated a role for the niche in self-renewal of NSC. The recently discovered PDLSC and DPSC populations have also been shown to reside within a perivascular niche, however there is limited knowledge about their purpose or function.

1.2 Dental Pulp Stem Cells

1.2.1 Tooth development

Tooth formation initiates from the reciprocal interaction between CNC derived mesenchymal cells and epithelial tissue, (Chai et al., 2000; Imai et al., 1996). The developing tooth undergoes a number of developmental stages, namely the bud, cap and bell stages, within the mandibular arch before it erupts through the gum to function as a mature tooth (Fig. 1.1) (Cate, R., 1989; Fejerskov, Josephsen, K., 1986). Four main signalling molecules implicated in neurogenesis, BMPs, FGF, Shh and Wnt, are involved in the proliferation and differentiation throughout these stages of tooth development (Peters et al., 1999; Thesleff et al., 1999). The mature tooth comprises mainly the enamel, dentine and dental pulp among other structures (Fig. 1.2). The enamel, made by ameloblasts, is a hard acellular mineralized tissue that can not be replaced or regenerated, because the ameloblasts undergo apoptosis following the formation of the enamel layer. The dentine is a specialized mineralised tissue synthesized by odontoblasts, which forms the bulk of the tooth and supports the enamel. It is avascular, enclosing a central pulp chamber of soft connective tissue in the centre of the tooth, giving rise to the odontoblasts that form the dentine. The vascularized pulp tissue also nourishes the dentine and carries nerves that allow sensitivity to pain and a signalling mechanism to signal the requirement for new dentine formation. The tooth is secured within the jaw by the periodontal ligaments (PDL), which are derived from the dental follicle. Sharpey's Fibers, which are connective tissue fibres, are embedded between the cementum and the inner wall of the alveolar bone socket (Cate, R., 1989; Fejerskov et al., 1986) (Fig. 1.2).

Unlike bone, teeth do not normally regenerate or undergo turnover, but do display a limited capacity to repair dentine and PDL. If reparative activity exists, by what means does this occur? Two populations of SC have been identified in the tooth that demonstrate self-renewal capacity and differentiation potential, DPSC, located within the dental pulp, (Gronthos et al., 2000) and PDLSC, within the periodontal ligament (Seo et al., 2004).

Figure. 1.1 Cranial neural crest cells are required in all stages of tooth development and formation.

Cranial neural crest (CNC) derived cells (dark blue) populate the mesenchyme that resides under the dental lamina. Odontogensis is initiated by the thickening of the oral epithelium, which forms the dental lamina. The dental lamina condenses and grows into the CNC derived mesenchyme to form the tooth bud (bud and cap stages). Following the bud stage, the epithelial tissue undergoes specific folding that produce ameloblasts, which make the enamel. At the same time the CNC derived cells condense at the epithelial mesenchymal interface (dark blue) to form the dental sac, otherwise known as the dental papilla. The dental papilla eventually gives rise to the dental pulp and the dentine-secreting odontoblasts, the dentine and cementum in the adult tooth (adapted from (Chai et al., 2000)).

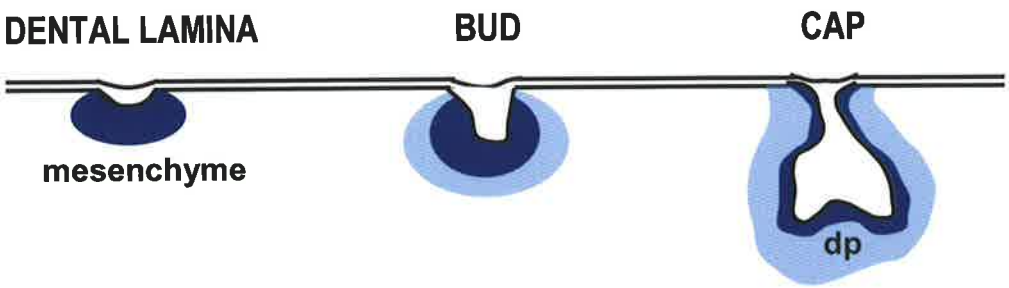

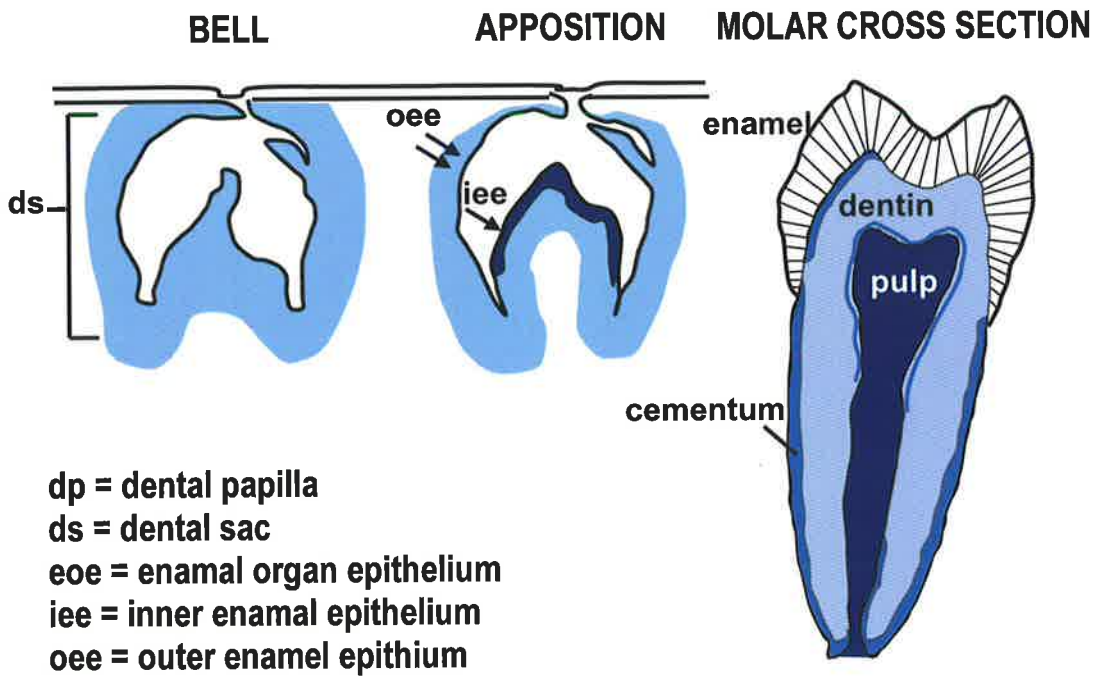

dp = dental papilla
ds = dental sac
eoe = enamal organ epithelium
iee = inner enamal epithelium
oee = outer enamel epithium

Figure 1.2 A schematic diagram detailing the main structures of an adult tooth.

The enamel is the hard inert tissue on the surface of the tooth that resides above the gum, within the crown region. The connective tissue that supports the enamel is known as the dentine; this tissue is avascular and is made from odontoblasts. The pulp is the soft connective tissue in the centre of the tooth, giving rise to the odontoblasts that form the dentine. The pulp tissue contains stem cells, is vascularised and carries nerves that give it sensitivity to pain. The tooth is secured within the jaw, in the root region of the tooth, by the periodontal ligaments. The periodontal ligament is secured by connective tissue fibres known as Sharpey's Fibers that are embedded between the thin mineralized outer layer of cementum and the inner wall of the alveolar bone.

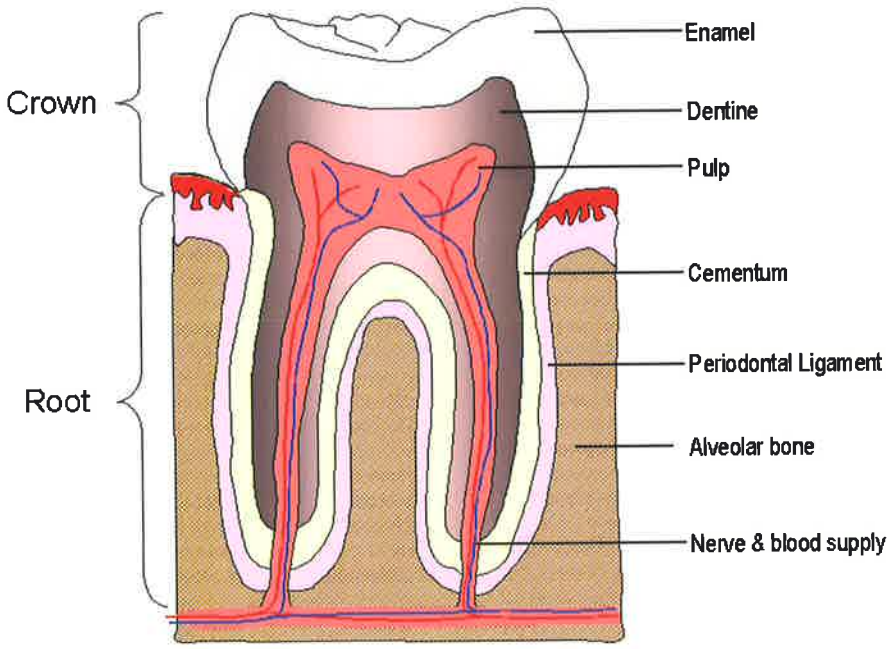
Crown
Root
Enamel
Dentine
Pulp
Cementum
Periodontal Ligament
Alveolar bone
Nerve & blood supply

1.2.2 Properties of adult human Dental Pulp Stem Cells

The proliferation and differentiation potential of the dental pulp cells (DPC), which comprise all cell types within the pulp, presumably including DPSC, has been reported previously with *in vitro* assays (Denholm et al., 1998; Lyaruu et al., 1999; Mooney et al., 1996; Shiba et al., 1998). Gronthos and colleagues identified a subset of DPC within the pulp tissue using early mesenchymal SC markers, STRO-1 and CD146, and the pericyte marker, 3G5. These DPSC encapsulate nerve bundles, in addition to their perivascular niche localisation within the pulp (Gronthos et al., 2002; Gronthos et al., 2000; Shi et al., 2003). The dental SC niche has also been identified in rodent incisors (Harada et al., 2004); however rodent and human teeth differ, as rodent teeth are continuously growing. The location of the SC identified in the rodent dental pulp is termed the 'apical bud', as the eternal tooth bud that gives rise to the dental progeny dwells at the apical end of continuously growing teeth (Harada et al., 1999; Harada et al., 2002b; Ohshima et al., 1992). More primitive SC populations have also been identified in porcine third molar tooth buds that have the potential to develop into organised tooth structures comprised of enamel, cementum, dentin and fibrous pulp tissues (Young et al., 2002).

Adult derived DPSC have been compared to BMSSC, as both SC types have been isolated with the same early mesenchymal SC markers, STRO-1 and CD146, and share similar mesenchymal characteristics, such as the capacity to generate mineralised tissues *in vitro* and *in vivo*. Additionally, both populations displayed a common gene expression profile as identified by cDNA microarray analysis (Gronthos et al., 2000; Shi et al., 2001). Therefore, these studies suggest that the differentiation of DPSC into odontoblasts and BMSC into osteoblasts may be mediated by common biochemical pathways (Shi et al., 2001).

Gronthos and colleagues (Gronthos et al., 2002; Gronthos et al., 2000) demonstrated that DPSC possess properties characteristic of SC, due to the capacity of DPSC for self-renewal, high proliferative potential and multi-lineage differentiation. The self-renewal capacity was demonstrated when cells from harvested primary human DPSC transplants, (which generated tooth-like structures), were isolated and sorted using human specific antibodies and then re-sorted into secondary transplants, which also generated tooth-like structures (Gronthos et al., 2002). Additionally, DPSC exhibit a higher proliferation rate of 20-30% and a longer lifespan

of greater than 20 population doublings *in vitro* when compared to BMSSC. The higher proliferation of DPSC may be attributed to the developmental state of third molars, which are the last permanent teeth to develop and as such are "younger" developmentally than the SC of bone marrow. Alternatively, it is possible that there is a lower demand on the SC population in teeth than bone marrow, as bone is turned over throughout life, which doesn't occur with human teeth.

1.2.3 Differentiation potential of Dental Pulp Stem Cells

1.2.3.1 The potential to recapitulate a tooth-like structure and bone formation

Loss of teeth due to disease or injury affects many individuals. Tooth replacement or regeneration of teeth or tooth structures is currently being investigated. Yelick and colleagues were able to bioengineer tooth structures by combining a biodegradable scaffold and cultured rat or porcine tooth bud cells within a rat host (Duailibi et al., 2004; Young et al., 2002). These researchers suggest that the bud cells comprised dental epithelia and MSC that were able to generate the bioengineered tooth structure comprising dentin, odontoblasts, pulp and enamel. Gronthos and colleagues support the concept of MSC within the tooth and demonstrate that human DPSC when transplanted under the skin of immuno-compromised mice were able to regenerate a dentine-pulp-like complex. The complex was composed of mineralised matrix characteristic of dentine, with tubules lined with an odontoblast layer and vascularized fibrous tissue. The formation of dentine and blood vessels within the newly generated structure was similar to an endogenous developing dentine-pulp complex (Batouli et al., 2003; Gronthos et al., 2002; Gronthos et al., 2000).

Various factors known to stimulate the growth of pulp cells or odontoblast progenitors are also thought to promote proliferation and differentiation of DPSC. These factors include TGF-β, basic FGF, EGF, platelet-derived growth factor (PDGF), tumour necrosis factor (TNF)-α and interleukin-1β, all with characteristically different patterns of action on proliferation, matrix synthesis and differentiation (Shiba et al., 1998). The effects of these cytokines and growth factors on the synthesis of DNA of cultured DPC were examined by Northern and Western blot analysis. Laminin, type 1 collagen, fibronectin, alkaline phosphatase (ALPase) and secreted protein acidic and rich in cysteine (SPARC) (Shiba et al.,

1998). Dentine sialophosphoprotein (DSPP), a gene that encodes the matrix proteins dentin sialoprotein (DSP) and dentin phosphoprotein (DPP), was expressed predominately following pre-dentin matrix formation, but before mineralization, known as dentinogenesis (Feng et al., 1998). DSPP is only expressed by mature odontoblasts cultures and not by DPSC, suggesting that DPSC represent an undifferentiated pre-odontogenic phenotype prior to differentiation (Gronthos et al., 2004; Gronthos et al., 2000). Matrix extracellular phosphoglycoprotein (MEPE), a member of the integrin-binding ligand N-linked glycoprotein, was the only marker identified that down-regulated following DPSC odontoblast differentiation and subsequent mineral formation. This was in contrast to DSP expression, which was up-regulated following differentiation (Liu et al., 2005). The researchers suggested that MEPE is an inhibitor of DPSC odontoblast formation as it decreased expression following DPSC differentiation. MEPE in conjunction with DSP could be used as markers to monitor the differentiation state of DPSC in culture or during tissue engineering (Liu et al., 2005).

The majority of research investigating pulp tissue has been directed towards dental repair. Dental pulp tissue is able to proliferate and form new tissue resembling that of the native pulp *in vitro* and a vascularized pulp-like chamber following transplantation *in vivo* (Duailibi et al., 2004; Lyaruu et al., 1999; Mooney et al., 1996; Young et al., 2002). The regeneration of the dental-pulp complex was observed when BMP-7 *ex vivo* gene transfer into dermal fibroblasts of inflamed dental pulp induced reparative dentinogenesis (Rutherford, B., 2001). Findings from a rodent dental defect model suggested that allogenic DPC were able to survive and localise to the pulp chamber if sufficient blood supply was available, following transplantation (Kim et al., 2006). However, these investigations failed to address the regenerative capacity of endogenous DPSC. About and colleagues demonstrated that cells within the vasculature of dental pulp tissue proliferated in response to injury of the dentine or pulp, as demonstrated by BrdU staining (Tecles et al., 2005). Interestingly, these BrdU positive cells were found to migrate towards the injury sites. While it was not determined that the BrdU cells were multipotential DPSC, it was postulated that endogenous odontogenic precursor cells may have the capacity to proliferate, migrate and differentiate to regenerate damaged dentine matirx (Shi et al., 2005) following injury (Tecles et al., 2005).

Recently, it was proposed that a population of stromal bone producing (SBP) cells could be isolated from DPSC, referred to as SBP/DPSC, based on the phenotype $kit^{+}/CD34^{+}/CD45^{-}$, using flow cytometry. These SBP/DPSC retained their self-renewal properties and were able

to produce living autologous fibrous bone tissue (LAB) both *in vitro* and following transplantation into immuno-compromised mice (Laino et al., 2005). $Kit^+/CD34^+/STRO\text{-}1^+$ DPSC isolated from individuals of 6-10 years of age commenced bone differentiation both *in vitro* and following transplantation into immuno-compromised mice, where transplanted DPSC remodelled into lamellar bone (Laino et al., 2006). Interestingly, Gronthos and colleagues did not observe bone formation in their adult DPSC transplant experiments as reported by Laino and colleagues. However, stem cells from human exfoliated deciduous teeth (SHED) cells do induce bone formation *in vivo* (Miura et al., 2003). Notably, the SC populations investigated by the two researchers were isolated differently and possibly identifying different cell populations, which perhaps could explain the discrepancy in the results. Lino and colleagues suggest that SBP/DPSC could be isolated when selecting for $kit^+/CD34^+/CD45^-$ cells. Gronthos and colleagues noted that their DPSC population were CD34 and c-kit negative (personal communication Dr. Gronthos), where CD34 identifies hematopoietic SC and endothelial cells but not MSC. Therefore the purity of the SBP/DPSC population needs to be determined in order to discount the possibility of contaminating $CD34^+/c\text{-}kit^+$ endothelial cells.

1.2.3.2 The neural potential of DPSC

In addition to the function of DPSC in tooth formation and bone differentiation, cultured DPSC also differentiate into fat-laden adipocytes, when selected with either STRO-1, $kit^+/CD34^+/CD45^-$ or $kit^+/CD34^+/STRO\text{-}1^+$; or myotubes when selected with $kit^+/CD34^+/STRO\text{-}1^+$ (Gronthos et al., 2002; Laino et al., 2005; Laino et al., 2006). Interestingly, non-selected DPSC expressed neural markers nestin and glial fibrillary acidic protein (GFAP) (Gronthos et al., 2002). Furthermore, DPSC under neural inductive conditions expressed post-mitotic neuronal marker NeuN (Gronthos et al., 2004). However, the investigation into the neuronal potential of adult DPSC is limited to these two studies.

1.2.4 Stem cells from human exfoliated deciduous teeth (SHED)

The SC population identified in deciduous (primary teeth) teeth is another potential source of isolating SC in a non-invasive manner. During this process the majority of nerves and vasculature retract, due to the resorption of the dental follicle (Christensen et al., 1993) allowing the teeth to fall out naturally. Deciduous teeth contain multipotent SC within the remnant pulp tissue, referred to as SHED (Miura et al., 2003). SHED were isolated with two early MSC associated markers, STRO-1 and CD146. These markers were also co-localised around the blood vessels within the remnant pulp tissue, suggesting that SHED may originate from a perivascular micro-environment, consistent with the findings of DPSC, PDLSC and BMSSC (Seo et al., 2004; Shi et al., 2003). SHED are highly proliferative, clonogenic cells capable of differentiating into a variety of cell types including odontoblasts, adipocytes and neural cells, indicating multi-differentiation potential *in vitro*. Furthermore, SHED were able to form new human dentin and induce murine endogenous bone formation *in vivo*. In addition, human SHED have been shown to survive over time as differentiated neurons following transplantation into the brains of immuno-compromised mice, as demonstrated by the co-expression of the neurofilament and human specific mitochondrial antibodies (Miura et al., 2003). However, the functional significance of these observations has yet to be determined.

The developmental processes, tissue structure and function differ between deciduous and adult teeth. Deciduous teeth exist for a shorter period of time in comparison to adult teeth as deciduous teeth undergo resorption whereas adult teeth are premanent. It is not surprising then that these tissues also differ in their resident stem cell populations. SHED have a higher proliferation rate, increased cell-population doublings, and the capacity to form sphere-like cell-clusters when compared to DPSC. Furthermore, SHED demonstrated osteo-inductive capacity *in vivo* but failed to reconstitute a mature dentin-pulp-like complex and or differentiate into osteoblasts (Miura et al., 2003). Studies conducted by Laino and colleagues suggested that $kit^+/CD34^+/STRO\text{-}1^+$ isolated DPSC from 6-10 year old donors produced fibrous bone *in vitro*. However, the Laino study failed to definitively demonstrate that the mineral production they observed was generated from bone or dentine. Furthermore, while the Laino study also documented lamellar bone formation following the transplantation of these differentiated cells into immuno-compromised mice, it was not demonstrated that the transplanted cells produced the bone *in vivo*. The study does suggest though, that this dental

stromal SC population localised within a "sealed niche" within the pulp and were highly clonogenic, with extensive proliferation capacity (Laino et al., 2006).

1.2.5 Are Dental Pulp Stem Cells of Cranial Neural Crest Origin?

It has been postulated that DPSC are either mesodermal or ectodermal in origin. Both DPSC and BMSSC express smooth muscle and endothelial markers, suggesting that they and a number of other SC populations may arise from developing blood vessels (Bianco et al., 1999). As previously mentioned, DPSC express pericyte associated marker, 3G5 (Shi et al., 2003), where pericytes reside within blood vessels (Carlile et al., 2000). Furthermore, STRO-1 also recognises stromal cell precursors of pericyte cells (Gronthos, S., 2004). Interestingly, pericytes are of neural crest origin (Schor and Canfield., 1998). Therefore it is plausible to suggest that DPSC share both mesenchymal and neural crest characteristics, as this SC population has been isolated with an early MSC marker, STRO-1, but reside in a region of neural crest origin.

A number of studies have indicated that structures within the tooth originate from CNC cells, using antibody staining and DiI labelling (Christensen et al., 1993; Hainfellner et al., 2001; Imai et al., 1996), however these studies were not conclusive. Other groups have shown that teeth are unable to form without the presence of CNC cells (Lumsden, G., 1988; Mitsiadis et al., 2003). Recently, an elegant study used a two-component genetic system marking the progeny of CNC during tooth and mandible development. The study showed the location of CNC cells within the tooth (Fig. 1.1), where CNC contributed to a number of cell types within the dental pulp, dentine matrix, cementum and periodontal ligament tissues (Chai et al., 2000). Furthermore, Fontaine-Pérus and colleagues showed that transplantation of mouse neural crest cells isolated from the developing neural tube into the equivalent region of the chicken embryo resulted in the development of a tooth-like structure (Mitsiadis et al., 2003). This experiment provided strong evidence that CNC are critical for tooth development, as birds lost the ability to produce teeth 70-80 million years ago (Chen et al., 2000). Neural crest stem cells (NCSC) also contribute to the development of the PNS, sympathetic and parasympathetic nervous systems, in addition to facial structures via CNC cells (Douarin et al., 1999b; Douarin et al., 1999c; Douarin et al., 1999f). Therefore, it could be postulated that

if DPSC possess properties similar to neural crest, then DPSC may be an alternative source of adult neural SC.

1.3 Neural Crest Development

1.3.1 Trunk and cranial neural crest derivatives

During development, neural crest cells are located within the dorsal region of the forming neural tube along the length of the vertebrate axis (Fig. 1.3a) (Bronner-Fraser, M., 2002). As the neural tube thickens, the most rostral regions develop into the brain and CNS, while the caudal regions form the spinal cord. The neural crest cells that reside in and caudal to somite 5 are considered to be sacral or trunk neural crest (TNC), while neural crest cells that localise rostral to somite 5, within rhombomeres (r), diencephalic and mesencephalic regions are referred to as mesencephalic or CNC (Fig. 1.3b) (Abzhanov et al., 2003; Bronner-Fraser, M., 1995; Douarin, M., 2004; Douarin et al., 1999e).

Neural crest cells are a unique population of cells and although they arise from the neural ectoderm, they are sometimes regarded as a separate or fourth germ layer because of their contribution to multiple cell derivatives (Hall, K., 2000). In general neural crest cells are considered a transient embryonic neural-derived precursor population. TNC cells are able to differentiate into neurons, glia and Schwann cells that form the PNS. Another major cell population from the TNC are melanocytes of the skin. CNC retain further plasticity, generating the above-mentioned derivatives, while also contributing to the formation of facial structures. These include skeletal derivatives (cartilage, bone and teeth), connective tissue, pericytes, structures of the heart including the endothelium of aortic arteries and the septum and further derivatives of the PNS (cranial ganglia, sympathetic and parasympathetic ganglia) (Abzhanov et al., 2003; Aquino et al., 2006; Baroffio et al., 1991; Bronner-Fraser, M., 1995; Chai et al., 2000; Douarin, M., 2004; Douarin et al., 1999f; Kruger et al., 2002; Morrison et al., 1999; Trentin et al., 2004).

1.3.1.1 Neural differentiation potential of cranial neural crest

The fate of CNC is in part dependent on the signals in the local environment (Douarin et al., 2004, Abzhanov et al., 2003, Anderson, J., 1997, Bronner-Fraser, M., 1995, Baroffio, et al., 1991). Instructive signals from the surrounding tissue, such as the neuroepithelium, head surface ectoderm and paraxial head mesoderm, ECM molecules, guidance molecules, morphogens and transcription factors all contribute to the fate of CNC cells (Anderson, J., 1997; Couly et al., 2002; Dunn et al., 2000; Francis-West et al., 1998; Golding et al., 2002; Shah et al., 1996; Trainor et al., 2002; Zhang et al., 1997).

Chicken/quail chimera experiments have generated extensive knowledge on the specific location of CNC within the neural tube, their designated location and cell fate following emigration from the neural tube. CNC reside in specific segments within the hindbrain called rhombomeres (r). CNC cells migrate as streams when they leave the hindbrain and enter their specified branchial arch. Three streams have been identified, the trigeminal, hyoid and post-otic streams. Early migrating CNC within these streams give rise to mesenchymal derivatives, while a second wave of migrating CNC differentiate into neurons and glia, and contribute to cranial ganglia (Fig. 1.3b) (Baker et al., 1997). The CNC cells in the trigeminal stream originate from the mesencephalon region and r1-3. These CNC migrate to the first branchial arch, condense and differentiate into neurons that produce the TG. CNC from r3-5 form the hyoid stream and become neurons of a number of cranial nerves in the second branchial arch. Additionally, CNC migrate from r6-8 in the post-otic stream, differentiate into neurons forming a number of ganglia that reside in the third and forth branchial arches (Baker et al., 2001; Douarin et al., 1999c; Lumsden et al., 1991; Schilling et al., 1994). (Fig. 1.3b). The patterning of rhombomeres and the subsequent migration of the CNC into their respective branchial arches is initially dependent on HOX gene expression (Krumlauf et al., 1993) and boundary formation created by Eph/ephrin receptor tyrosine kinase contact-dependent guidance molecules (Robinson et al., 1997).

Figure 1.3 Neural crest cells originate in the dorsal neural tube and migrate along specifically defined pathways in response to guidance cues.

(a) A schematic sagittal view of neurulation. Neural crest cells reside within the dorsal (D) portion of the neuroepithelium, at the junction between the neural tube (NT) and the lateral ectoderm, the notochord (NC) is located ventrally (V). (b) Shortly after closure, neural crest cells start to emigrate in a head-to-tail wave along the length of the embryo along specified migratory paths. Cranial neural crest cells from the mesencephalon region to rhombomere 8 (r8, or somite 5) contribute to structures within the head region. These cranial neural crest cells specifically migrate from the dorsal region of the neural tube to enter their respective branchial arches (BA), where they respond to the local environment and differentiate into a number of cell types. (c) The trigeminal ganglion (TG) is one sensory ganglion to which the cranial neural crest cells contribute. The axonal processes of the TG migrate to their correct destination in response to inhibitory cues (red) and permissive or attractive cues (green). These cues prevent the inappropriate migration or selectively promote the migration of the processes to their correct destination, respectively. Cranial and trunk neural crest cells also respond to similar guidance directing their specific navigation to their final destination (adapted from (a) (Bronner-Fraser, M., 2002) (b) (Douarin, M., 2004) (c) (Jayasena et al., 2005)).

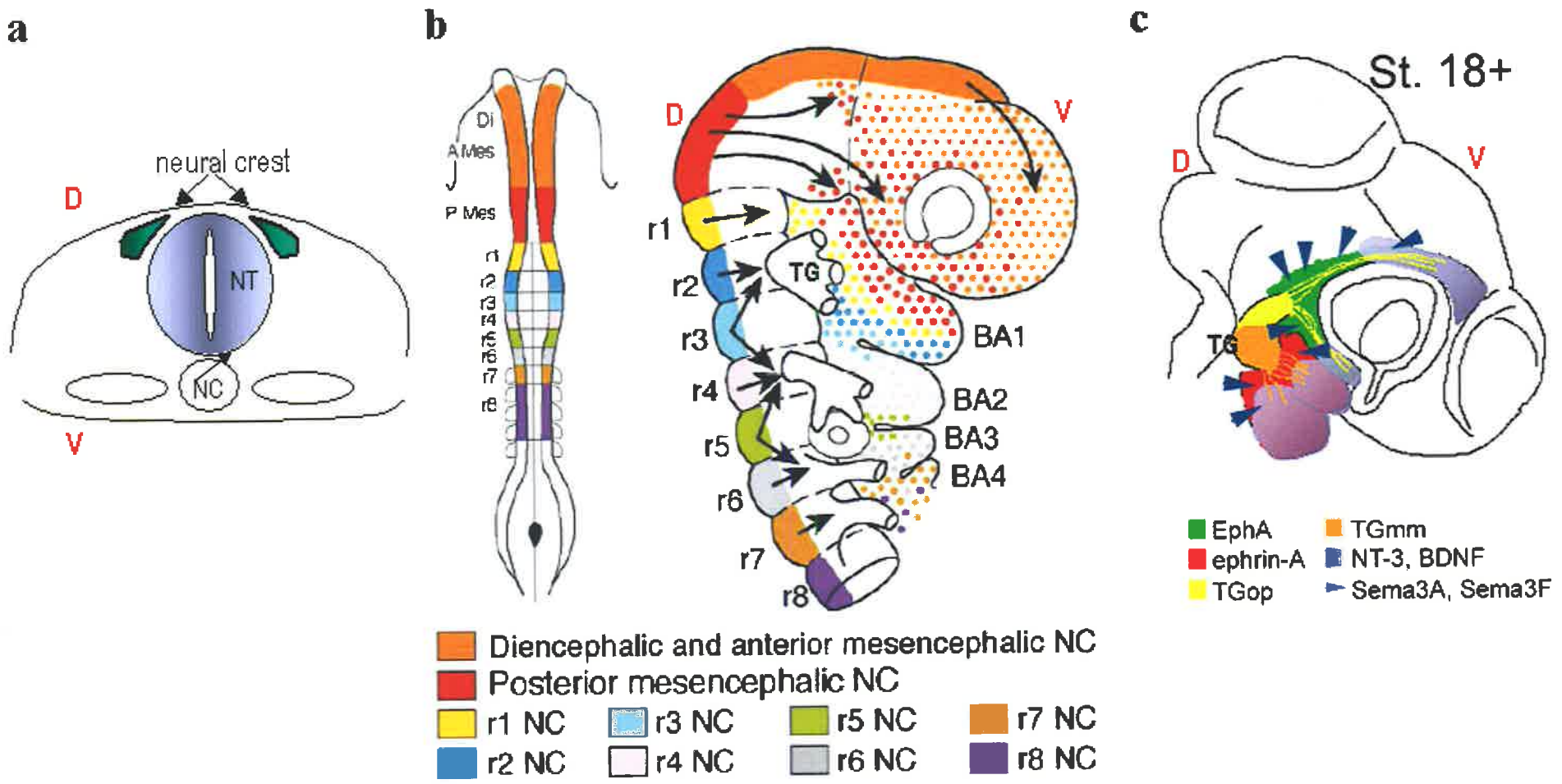
a
neural crest
D
NT
NC
V
b
Di
A Mes
P Mes
r1
r2
r3
r4
r5
r6
r7
r8
D
V
TG
BA1
BA2
BA3
BA4
Diencephalic and anterior mesencephalic NC
Posterior mesencephalic NC
r1 NC
r2 NC
r3 NC
r4 NC
r5 NC
r6 NC
r7 NC
r8 NC
c
St. 18+
D
V
TG
EphA
ephrin-A
TGop
TGmm
NT-3, BDNF
Sema3A, Sema3F

Importantly, neural crest cells have also been shown to give rise to the progeny within the dorsal neural tube, including the roof plate and commissural neurons (Bronner-Fraser, M., 2002). Neural crest and neural tube derivates commonly arise from the same precursor in the dorsal neural tube, this suggests the precursor cell could contribute to the CNS and PNS cell fate (Bronner-Fraser, M., 2002). However, the potential of CNC to contribute to CNS derivatives has not been explored further.

1.3.2 Migration of cranial neural crest cells in response to guidance cues

Neural crest cells undergo three distinct stages during their migration, the emigration from the neural tube, the migration along distinct pathways and the cessation of migration upon reaching their final destination (reviewed by (Bronner-Fraser, M., 2002)). Early migrating CNC that travel ventrally into the branchial arch differentiate predominately into cartilage and bone, while CNC that migrate later move dorsally into the branchial arches and form the neurons and glia of the cranial sensory ganglia such as the TG (Baker et al., 1997; Tosney, W., 1982).

Guidance molecules, both secreted and membrane-bound contact dependent signals, ensure the correct navigation of migrating cells to their intended destination. Four types of guidance molecules exist: secreted chemo-attractive or -repulsive signals and membrane attached contact dependent attractive or repulsive signals (Tessier-Lavigne et al., 1996). The specific expression of these guidance molecules within rhombomeres and branchial arches creates the migratory pathways for CNC cell navigation. Attractive cues are important to initiate the migration of CNC towards a particular target field, such as FGF8, which mediates a chemo-attractive response of migrating CNC in mouse (Kubota et al., 2000). Additionally, Nerve Growth factor (NGF), Brain Derived Growth Factor (BDNF) and Neurotrophin-3 (NT-3) attract TG axons (Fig. 1.3c), although this seems to be more permissive rather than instructive (O'Connor et al., 1999). It appears that repulsive signals are important for establishing migratory pathways by creating non-permissive regions for migration. The Semaphorin members and their receptors, the neuropilins, in addition to the Eph/ephrin molecules, function as repulsive guidance molecules and are essential for correct CNC migration (Osborne et al., 2005; Smith et al., 1997).

The Eph receptor tyrosine kinase family is involved not only in boundary formation of CNC (Mellitzer et al., 2000; Xu et al., 1995; Xu et al., 1999) within rhombomere segments, but also with the correct navigation of CNC to their respective branchial arches (Robinson et al., 1997) and the projection of TG axons to their target fields (Jayasena et al., 2005). The expression of ephrin-B2 in the second branchial arch and EphA4 and EphB1 in the third branchial arch prevent migrating CNC populations from invading the opposite target fields, by mediating cell repulsion between the Eph and ephrin expressing cells. Eph expressing CNC migrate towards Eph expressing branchial arches and avoid ephrin expressing branchial arches, thereby preventing the intermingling between CNC populations (Robinson et al., 1997).

1.4 Eph and ephrin molecules

The Eph family of receptor tyrosine kinases (RTKs) and their ligands, the ephrin molecules, are membrane-bound molecules that predominantly mediate a contact dependent inhibitory response. They are essential for a number of biological processes during development and post-natally, including cell shape and movement (Boyd et al., 2001; Noren et al., 2004b), the formation (Poliakov et al., 2004) and maintenance (Yamaguchi et al., 2004) of both the CNS and PNS and following injury or disease (Goldshmit et al., 2006). Eph/ephrin molecules are expressed by invertebrates and vertebrate species (Wilkinson, G., 2000), comprising 14 Eph receptors and 9 ephrin ligands.

The ephrin ligands are divided into two subclasses based on their structure, such that A subclass ephrin molecules are glycosylphosphatidylinositol (GPI) linked to the membrane, while ephrin-B molecules are transmembrane (Fig. 1.4). The receptors are functionally divided into two subclasses determined by the binding affinity for their cognate ligand (Gale et al., 1996b). The dogma has been that there is promiscuous binding within a subclass but not between them (Fig. 1.4). EphA receptors only interact with ephrin-A ligands and EphB receptors bind ephrin-B ligands, with the exception of EphA4, which is able to bind both A and B ephrin molecules (Gale et al., 1996b; Holland et al., 1998). Recently it has also been shown that EphB2 has strong binding affinity for ephrin-A5 (Himanen et al., 2004).

1.4.1 Structure

The Eph receptors of both subclasses share the same structural identity, consisting of an extracellular globular ephrin binding domain, a cysteine-rich region and two fibronectin III repeats. Intracellularly, Eph receptors consist of a juxtamembrane motif, a kinase domain, a sterile alpha motif (SAM) domain and a postsynaptic density, discs-large, zona occludens-1 (PDZ) domain. The ligands of both subclasses differ in structure, where the ephrin-A molecules are GPI tethered to the plasma membrane, while ephrin-B ligands are transmembrane molecules containing a PDZ binding site Fig. 1.4 (Kalo et al., 1999; Zhou, R., 1998) (reviewed by (Kullander et al., 2002; Yamaguchi et al., 2004)).

1.4.2 Signalling mechanisms

The Eph RTK family does not fall into the conventional receptor ligand signalling mechanism, where the receptor mediates an intracellular signal upon ligand activation. While the family is able to function in this way, the terms 'receptor' and 'ligand' are somewhat artificial. Both are able to signal through the Eph and ephrin expressing cells and thus, can function as both receptors and ligands (Adams et al., 2001; Holland et al., 1996; Murai et al., 2003). Conventional signalling through the Eph receptor following ligand binding is referred to as "forward signalling" (Drescher et al., 1995; Krull et al., 1997; Wang et al., 1997); while activation of an ephrin ligand upon Eph receptor binding is considered "reverse signalling" (Fig. 1.4) (Birgbauer et al., 2000; Birgbauer et al., 2001; Cowan et al., 2002; Cutforth et al., 2003; Davy et al., 1999; Davy et al., 2000). While it was considered that the ephrin-A ligands could not function in this manner, as they are GPI linked to the membrane, *in vivo* genetic analysis and *in vitro* adhesion assays have demonstrated that ephrin-A proteins were able to promote adhesion, and hence able to signal through the ephrin-A ligand (Davy et al., 1999; Davy et al., 2000; Holmberg et al., 2000; Holmberg et al., 2002).

To increase the complexity of this RTKs family further, the Eph/ephrin molecules can mediate their response uni-directionally, through either the Eph or ephrin expressing cell, or bi-directionally, through both Eph and ephrin expressing cells simultaneously (Fig. 1.5) (Mellitzer et al., 1999), reviewed by (Gauthier et al., 2003; Kullander et al., 2002; Murai et al., 2003). Bi-directional signalling can be observed during the boundary formation of

rhombomere segments in the hindbrain (Xu et al., 2000), vascular network formation between arteries and veins (Gerety et al., 2002; Wang et al., 1998), during angiogenesis ((Nikolova et al., 1998) reviewed by (Zhang et al., 2006)), cell migration and adhesion (reviewed by (Cowan et al., 2002)).

As the Eph family are membrane bound, they can only mediate their response through cell-cell contact. X-ray crystallography has demonstrated that Eph receptors and ephrin ligands interact as dimers (high affinity binding) and tetramers (low affinity binding). The clustering of Eph and ephrin molecules is essential to provoke a specific response within a cell (reviewed by (Murai et al., 2003)). However, *in vitro* experiments have demonstrated that artificially clustering the extracellular portion of either an Eph receptor or a ligand to a fusion protein can activate its reciprocal ligand or receptor, respectively. This Eph or ephrin-Fc fusion protein interaction can elicit a biological response (Fig. 1.6) (Koblar et al., 2000; Wang et al., 1997). Furthermore, ephrin-B molecules have also been shown to interact with and be phosphorylated by other RTK molecules including platelet derived growth factor (PDGF) (Bruckner et al., 1997) and FGF (Chong et al., 2000). While EphB receptors directly bind with N-methyl D-aspartate (NMDA) synapses, upon ephrin-B activation, NMDA receptors cluster (Dalva et al., 2000), increasing NMDA receptor phosphorylation, which could be important for early synaptogenesis (Takasu et al., 2002).

1.4.2.1 Forward "Eph" signalling

X-ray crystallography analysis has shed light on the importance of the phosphorylation of the tyrosine residues within the juxtamembrane domain. When Eph receptors are in an inactive state, the juxtamembrane and kinase domains interact. This interaction results in the misalignment of ATP in the kinase domain and subsequent auto-inhibition of Eph receptor signalling. Upon ligand binding, Eph receptor dimers are auto-phosphorylated at two specific tyrosine residues within the juxtamembrane region. This region undergoes a conformational change, which relives the inhibition of the juxtamembrane domain on the kinase domain

Figure 1.4 The structure of Eph receptors and their cognate ligands, the ephrin molecules.

A schematic diagram illustrating a generic transmembrane EphA or EphB receptor expressed by one cell and a GPI-link ephrin-A or transmembrane ephrin-B ligand expressed by another cell. The extracellular globular domain of the Eph receptor (yellow) interacts with the globular domain of its cognate ligand (either ephrin-A – pink, or ephrin-B – blue). This interaction results in receptor/ligand dimerization or oligomerization, subsequently causing a conformational change and activating signalling through the Eph receptor (forward signalling) or through the ephrin ligand (reverse signalling). Glycosylphosphatidylinositol (GPI), sterile alpha motif (SAM) (adapted from (Kullander et al., 2002).

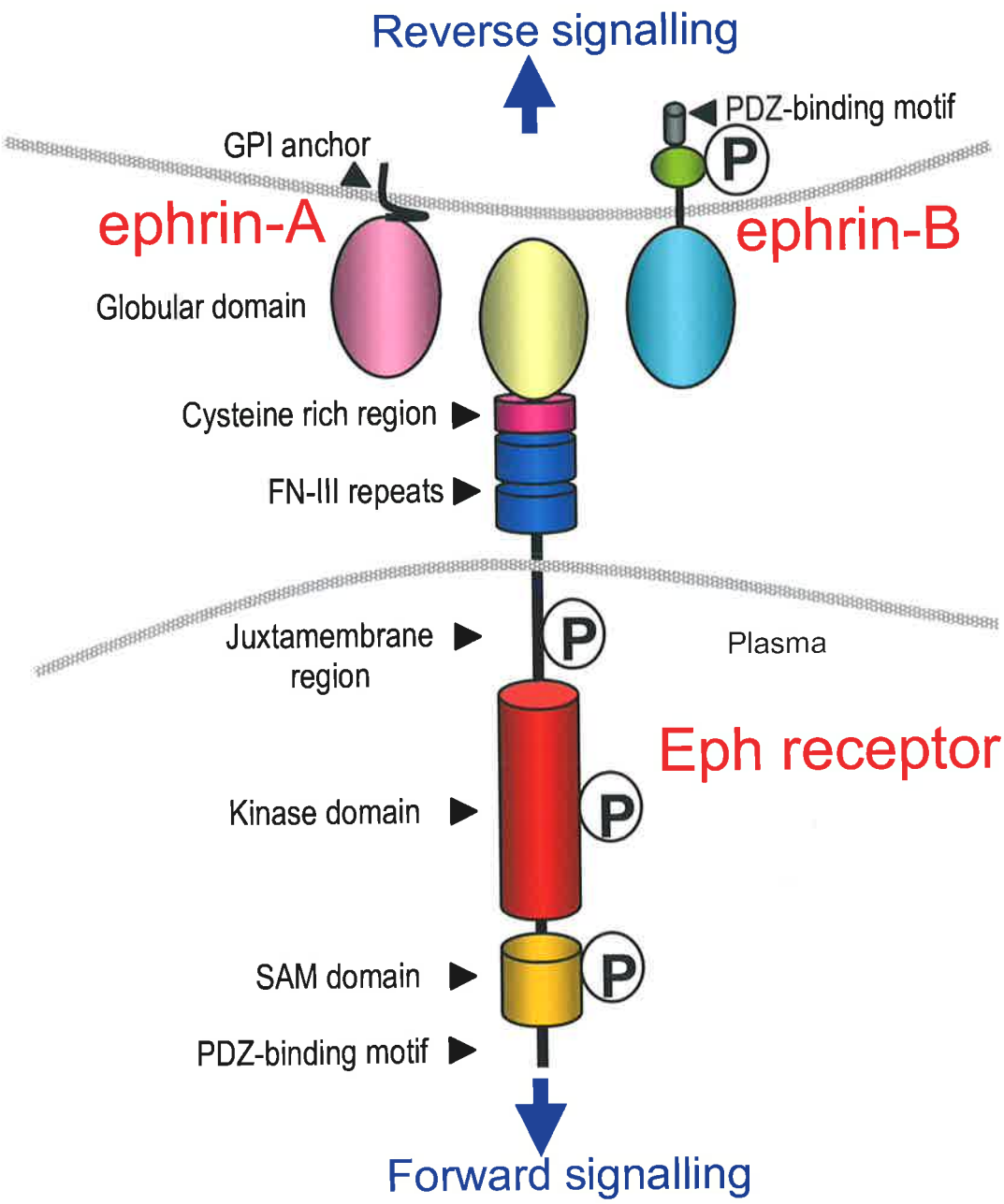
Reverse signalling
PDZ-binding motif
P
GPI anchor
ephrin-A
ephrin-B
Globular domain
Cysteine rich region
FN-III repeats
Juxtamembrane region
P
Plasma
Eph receptor
Kinase domain
P
SAM domain
P
PDZ-binding motif
Forward signalling

Figure 1.5 Eph/ephrin interaction can mediate uni-directional or bi-directional signalling.

(a) Upon Eph/ephrin interaction, uni-directional signalling results when either the Eph receptor or the ephrin ligand undergo a conformational change and stimulate a down-stream signalling cascade in the activated cell. When the Eph receptor alone is activated this is referred to as forward signalling, when the ephrin ligand mediates a response, this is called reverse signalling. (b) It has also been demonstrated that Eph/ephrin dimerization or oligomerization can result in simultaneous stimulation of both the Eph receptor and ephrin ligand, activating a response in the Eph expressing and ephrin expressing cells at the same time. This is referred to as bi-directional signalling.

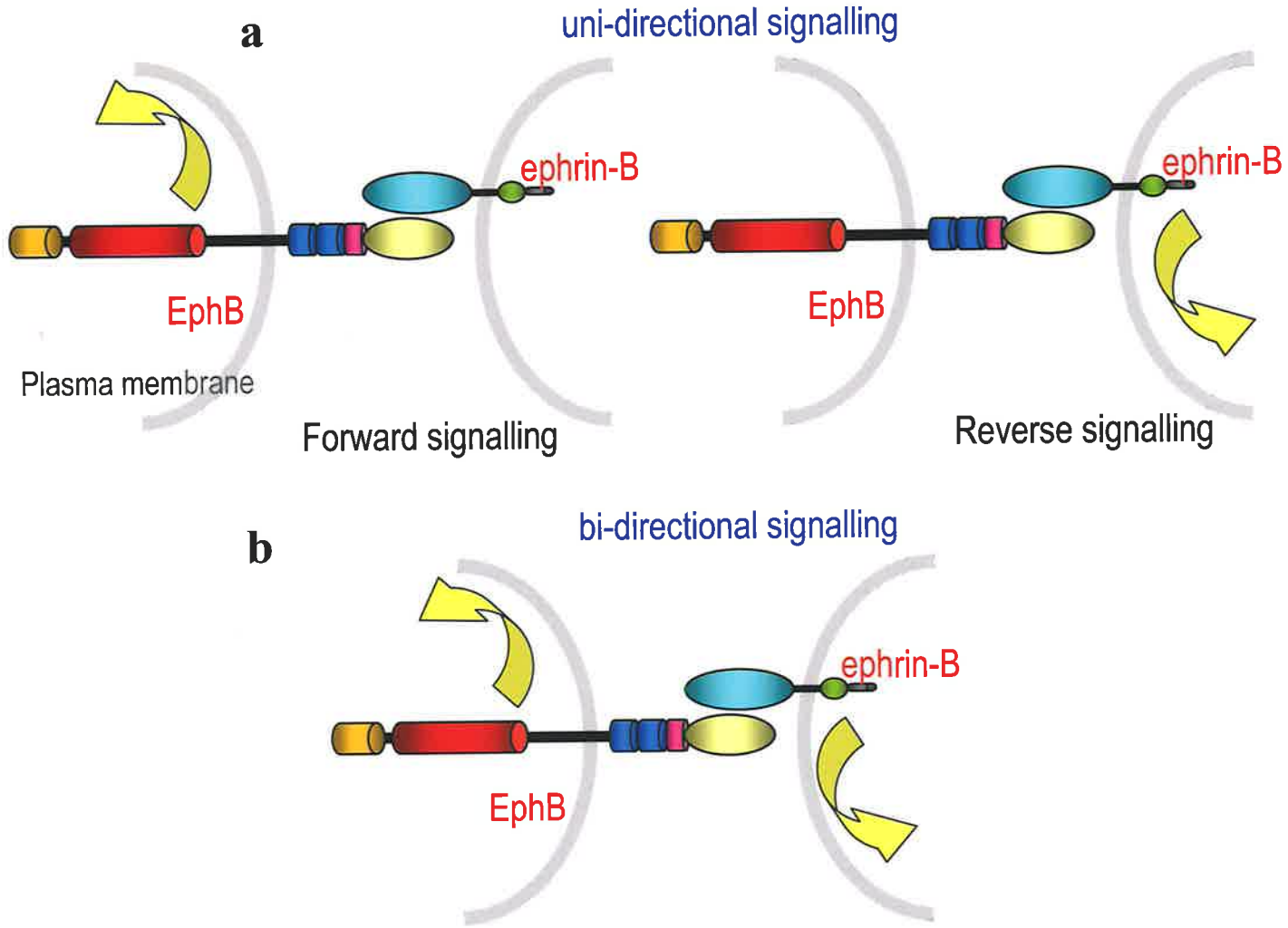
a
uni-directional signalling
ephrin-B
EphB
Plasma membrane
Forward signalling
ephrin-B
EphB
Reverse signalling
b
bi-directional signalling
ephrin-B
EphB

Figure 1.6 Eph or ephrin-Fc fusion protein interaction can elicit a biological response.

(a) For simplicity this schematic shows unclustered molecules and represents the B-subclass members. When the extracellular portion of the ephrin ligand is bound to the Fc portion of a human IgG molecule, it can bind to its cognate Eph receptor and mediate a conformational change in the ephrin bearing cell, resulting in forward signalling through the Eph bearing cell. Alternatively, the extracellular portion of the Eph receptor conjugated to the human Fc portion of an IgG molecule, when bound to its reciprocal ephrin ligand, can stimulate ephrin reverse signalling. (b) Depending on the tissue and the system, strong activation of the Eph receptor or ephrin ligand is attained through oligomerization with its reciprocal ligand or receptor. To achieve this, the Eph-Fc or ephrin-Fc can be clustered with an antibody that recognises the –Fc portion of the IgG molecule. This clustering allows the formation of tetrameric and multimeric structures that are able to interact with the reciprocal ligand or receptor, respectively.

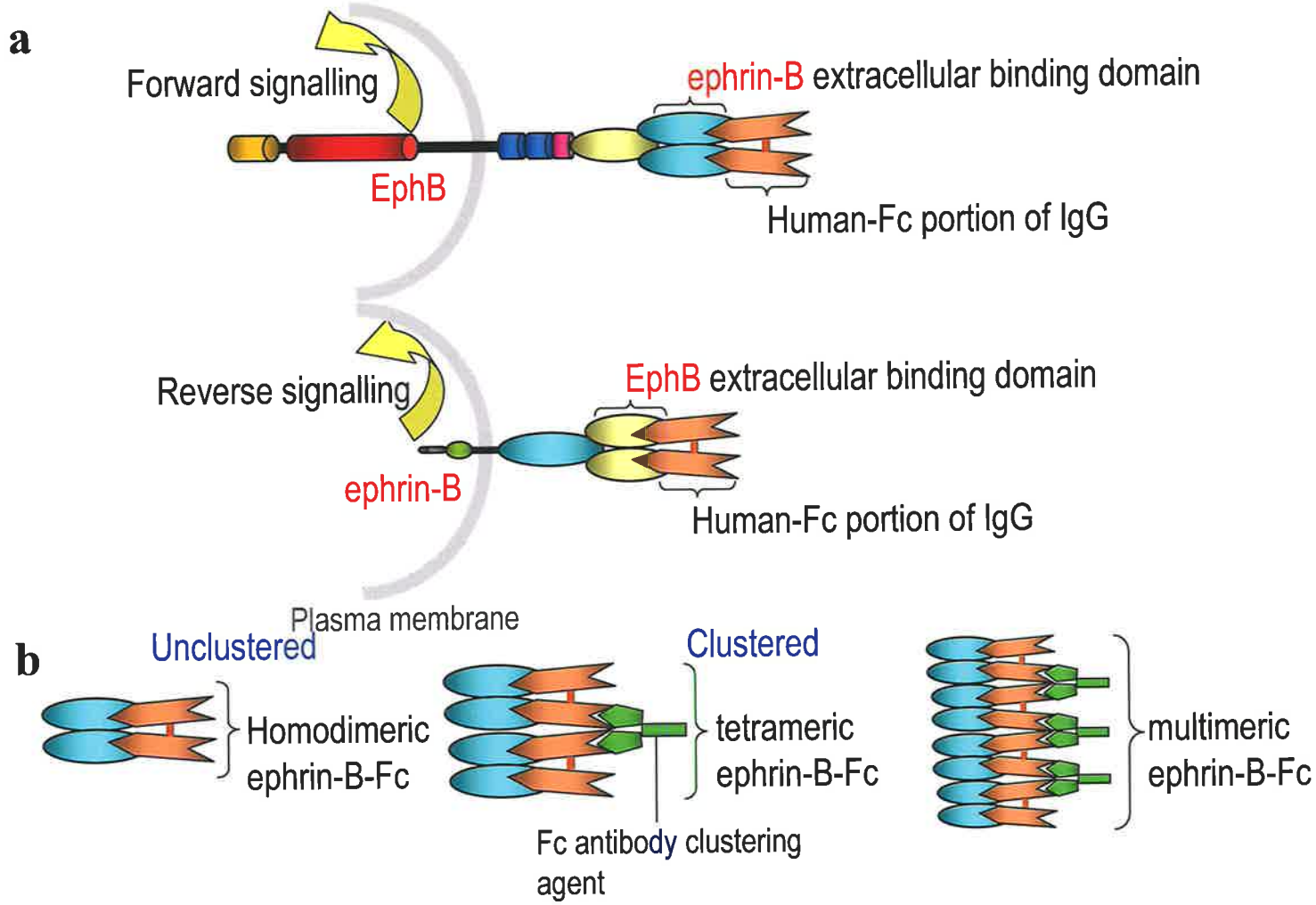
a
Forward signalling
ephrin-B extracellular binding domain
EphB
Human-Fc portion of IgG
Reverse signalling
EphB extracellular binding domain
ephrin-B
Human-Fc portion of IgG
Plasma membrane
b
Unclustered
Clustered
Homodimeric
ephrin-B-Fc
tetrameric
ephrin-B-Fc
multimeric
ephrin-B-Fc
Fc antibody clustering
agent

(Zisch et al., 2000) allowing the ATP to align correctly within the kinase domain and converting it to its active state. Activation of the kinase domain provides a docking site within the juxtamembrane domain for adaptor molecules that contain functional protein-interaction domains, such as Src homology (SH) SH2 and SH3 proteins. These adaptor proteins then mediate downstream signalling events (Pawson et al., 1997) that result in functional changes such as altered cell shape, adhesion, motility or proliferation (reviewed by (Kullander et al., 2002; Murai et al., 2003)).

Many of the activated signalling pathways that predominantly bind conserved phosphorylated tyrosine kinases residing within the Eph receptor result in changes to cytoskeletal dynamics and adhesion (Fig. 1.7) (reviewed by (Kullander et al., 2002; Noren et al., 2004b)). Briefly, this process involves small Rho GTPase molecules including Rho, Rac, cdc42 and Ephexin, that function to rearrange the cytoskeleton by extending or retracting stress fibres within lamellipodia and filopodia, or mediate downstream signalling pathways (Ogawa et al., 2006; Shamah et al., 2001). Suppression of the extracellular-signal related kinase (ERK)/mitogen activated protein kinase (MAPK) pathway not only influences changes in the cytoskeleton, but also inhibits proliferation and integrin mediated cell adhesion (Elowe et al., 2001; Miao et al., 2001).

1.4.2.2 Reverse "ephrin" signalling

Cells expressing ephrin ligands are also able to initiate an intracellular response through reverse signalling. It has been postulated that ephrin-A reverse signalling is carried out through the engagement of transmembrane co-receptors located in lipid rafts, known as caveolae, within the plasma membrane. Ephrin-A molecules localised to lipid rafts are known to associate with caveolins (Davy et al., 1999). Caveolins are proteins that generate one type of detergent-insoluble glycolipid-enriched complex that coats the cytoplasmic side of the plasma membrane invaginations (Anderson et al., 1998). G-proteins and members of protein tyrosine kinases, such as Fyn, also associate with caveolae, where Fyn is activated upon ephrin-A5 stimulation (Davy et al., 1999).

While the ephrin-A molecules have been shown to mediate reverse signalling, the B-subclass has been investigated more extensively. Ephrin-B ligands can be activated by either phosphorylation dependent or independent mechanisms. The activation by phosphorylation is

similar to Eph forward signalling in that conserved tyrosine residues are phosphorylated within the cytoplasmic region (Bruckner et al., 1997; Holland et al., 1996; Kalo et al., 2001). The phosphorylation also induces an intracellular conformational change at the hairpin structure of the C-terminal region, subsequently exposing sites for adaptor protein binding (Song et al., 2002) such as SH2 protein Grb4 (Cowan et al., 2001). The activation of ephrin-B reverse signalling through phosphorylation initiates a number of functional outcomes, including cytoskeletal changes (Fig. 1.7) (Cowan et al., 2001).

The intracellular region of ephrin-B ligands also contains a PDZ domain that is able to interact with PDZ-domain containing proteins, including PTP-BL, GRIP and the most recently identified PDZ-RGS3 (reviewed by (Gauthier et al., 2003)). The RGS3 domain of the PDZ-RGS3 is a GTPase activating protein that inhibits heterotrimeric G protein signalling. CXCR4 is a seven transmembrane heterotrimeric G protein, a receptor for the chemokine, stromal derived factor-1 (SDF-1) or CXCL12. Binding of SDF-1 to CXCR4 activates a heterotrimeric G protein signalling pathway, resulting in chemoattraction (reviewed by (Schmucker et al., 2001)). It has previously been shown that EphB2-Fc activation of ephrin-B1 silences the SDF-1 chemo-attractive signalling to granule cells in the cerebellum. These granular cells were no longer responsive to SDF-1 and migrated away from SDF-1 high expressing regions in response to EphB/ephrin-B interaction (Lu et al., 2001). Thus it appears that EphB/ephrin interactions could indirectly modulate chemo-attractive signalling mechanisms. Furthermore, SDF-1 and its receptor CXCR4, normally retain HSC within the bone marrow (Papayannopoulou, T., 2004). However, HSC are able to exit and re-enter their niche where chemokines are involved in the re-engagement of HSC following their exit (Pituch-Noworolska et al., 2003), and thus could also be implicated in the mobilisation of HSC from the niche. As EphB/ephrin-B molecules have been shown to inhibit SDF-1 signalling, they too may also be important for SC migration.

1.4.2.3 Termination of Eph/ephrin signalling

Following the initiation of a downstream signalling cascade, the interaction between the Eph receptors and ephrin ligands are subsequently disengaged. Two modes of disengagement have been demonstrated, cleavage by metalloprotease molecules and endocytosis.

Figure 1.7 Eph forward or ephrin reverse interaction activates a number of down-stream signalling pathways.

Eph/ephrin interaction stimulates the autophosphorylation of 2 tyrosine kinases within the juxtamembrane domain, resulting in a conformational change in the Eph bearing cell, and subsequently allowing the kinase domain to resume its active state. The schematic indicates a number of the adaptor proteins that interact with phosphorylated tyrosine kinases on both the Eph receptor and ephrin-B ligand. Binding of the adaptor binding protein activates or inhibits other down-stream proteins leading to changes in cell proliferation, cytoskeletal morphology, cell adhesion and migration. The ephrin-B ligand is also able to mediate phosphorylation independent signalling through the PDZ domain, which has implications for cell migration. Rho, Rac, Cdc42 are Rho-GTPases, Abelson (Abl); Abl-related gene (Arg); GTPase activating protein (GAP); phosphatidylinositol 3-kinase (PI3K); focal adhesion kinase (FAK); light molecular weight protein tyrosine phosphatase (LMW-PTP); Nck and Grb4, are both SH2-SH3 adaptor protein (adapted from (Kullander et al., 2002).

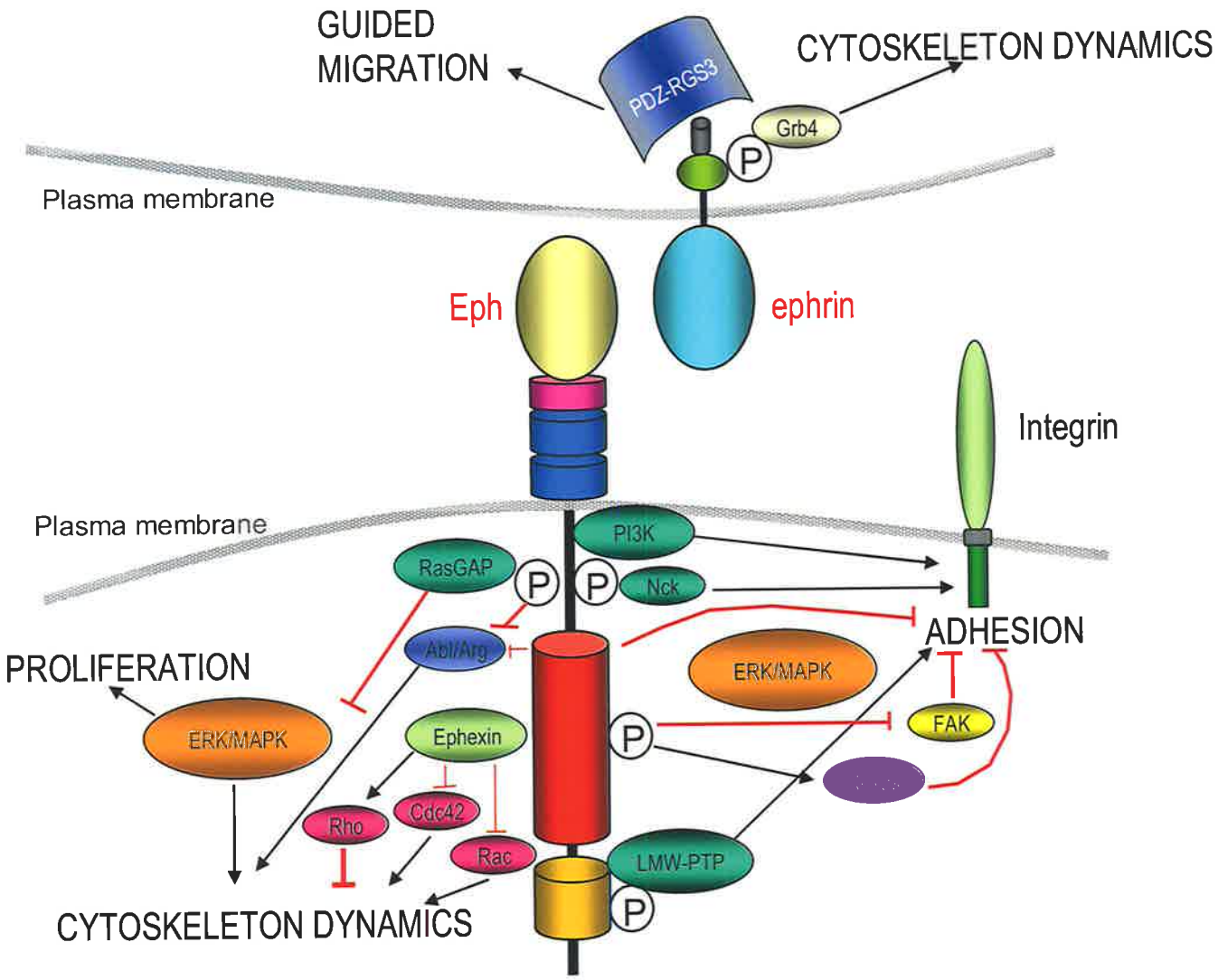
GUIDED
MIGRATION
PDZ-RGS3
CYTOSKELETON DYNAMICS
Grb4
P
Plasma membrane
Eph
ephrin
Integrin
Plasma membrane
PI3K
RasGAP
P
P
Nck
ADHESION
Abl/Arg
PROLIFERATION
ERK/MAPK
ERK/MAPK
Ephexin
P
FAK
Cdc42
Rho
Rac
LMW-PTP
P
CYTOSKELETON DYNAMICS

Metalloproteinase molecules Kuzbanian (Hattori et al., 2000) or ADAM10 (Janes et al., 2005), have been shown to cleave ephrin-A ligands at the juxtamembrane domain following EphA binding. Previous studies have implied that proteolytic cleavage is not very effective in terminating EphB/ephrin-B signalling. Recent investigation of EphB/ephrin-B2 interaction proposed that EphB stimulation of a metalloproteinase efficiently cleaves ephrin-B2. A soluble intracellular fragment was subsequently produced, that was further processed by precinilin-1, which led to activated Src auto-phosphorylation and consequently ephrin-B2 phosphorylation (Georgakopoulos et al., 2006). However, rather than terminating the signalling, the cleavage assists in the function of membrane bound ephrin-B2 phosphorylation and recruitment of downstream signalling molecules such as Grb4 (Georgakopoulos et al., 2006).

An alternative mode of terminating EphB/ephrin-B signalling postulates that B-subclass interactions are removed through endocytosis or transcytosis (Marston et al., 2003; Zimmer et al., 2003). These studies indicated that the membrane of the cell containing the EphB/ephrin-B complex was engulfed by either the EphB or ephrin-B expressing cell, depending which cell mediated the signal. Zimmer and colleagues demonstrated that for endocytose to take place, signalling through the cytoplasmic region of the respective receptor or ligand was required (Zimmer et al, 2003).

1.4.3 The role of Eph/ephrin molecules during development postnatally

The Eph/ephrin molecules mainly function as repulsive contact-dependent guidance molecules, but have also been identified as contact attractant molecules (Holmberg et al., 2000; Meima et al., 1997), promoting adhesion through integrins (Davy et al., 2000).

The Eph/ephrin molecules are essential for a number of processes (reviewed by Palmer and Klein, 2003) during embryonic development (Holder et al., 1999) and in postnatal tissue homeostasis (Conover et al., 2000). During development, the Eph/ephrin molecules have been implicated in axon guidance (Eberhart et al., 2000; Koblar et al., 2000; Krull et al., 2000), synaptogenesis (Grunwald et al., 2001; Lemke, G., 1998), migration of granular cells in the developing brain (Lu et al., 2001), the migration of trunk and cranial neural crest cells (Cooke et al., 2001; Krull, E., 1998; Krull et al., 1997), tooth development (Luukko et al.,

2005), boundary formation in the hindbrain (Xu et al., 1999), the intestinal epithelium (Sancho et al., 2003) and during angiogenesis (Adams et al., 2001; Cheng et al., 2002). Post-natally or in the adult, Eph/ephrin interactions have been identified in cancer tumorigenicity (Varelias et al., 2002), proliferation of endogenous neural SC (Conover et al., 2000; Holmberg et al., 2005) and maintenance of SC niches within the intestine (Holmberg et al., 2006).

Of particular interest to this study was the identification of the Eph/ephrin-A subclass during tooth development (Luukko et al., 2004). Radioactive *in situ* hybridisation demonstrated that *EphA2-A4*, *EphA7* and *ephrin-A1-A5* were differentially expressed at varying stages during tooth development, including the epithelial thickening, folding, the cuspal area of the dental papilla, during blood vessel and alveolar bone formation, odontogenesis and during trigeminal axon path finding (Luukko et al., 2004). However, EphA/ephrin-A protein expression patterns or function during tooth development were not assessed. Various Eph/ephrin members have also been found to be expressed by adult DPSC, based on a microarray study comparing adult human DPSC and BMSSC (personal communication Dr. Gronthos). However, the requirement of Eph/ephrin molecules by adult human DPSC has not been explored previously and requires further investigation.

1.4.3.1 Role of Eph/ephrin molecules in stem cell niche maintenance, proliferation and following injury

The expression of Eph/ephrin molecules within intestinal, hematopoietic, epidermal, neural and most recently identified dental pulp stem/progenitor populations (Conover et al., 2000; Holmberg et al., 2005; Holmberg et al., 2006; Okubo et al., 2006; Sakamoto et al., 2004), personal communication Dr. Gronthos), suggests that these molecules may control similar features in several organs, such as modulating tissue homeostasis or maintenance of SC niches.

Within the intestine there is a sheet of epithelial cells, the epithelial sheet convolves to form the intestinal crypt. Intestinal stem cells (ISC) reside at or near the bottom of the crypt, within a niche formed by neighbouring cells (Leedham et al., 2005). These cells release signals that orchestrate the maintenance, proliferation or migration of the SC within the niche (Fuchs et al., 2004). As ISC proliferate and subsequently differentiate, the majority of these cells

migrate out of the crypt and are shed into the lumen. The β-catenin pathway is required for the proliferation and positioning of the SC within the crypt. The β-catenin pathway in turn regulates the expression of Eph/ephrin molecules (Holmberg et al., 2006). Frisen and colleagues elegantly showed that ephrin-B expressed by the surrounding epithelium interacted with EphB expressing ISC based on gain- and loss-of-function studies following administration of soluble fusion proteins. These interactions were reported to maintain the position of ISC within the SC niche. Furthermore, the authors demonstrated that independent of the migratory response, dose-dependent EphB2/EphB3 forward kinase-dependent signalling promoted cell-cycle re-entry of intestinal progenitor cells within the crypt, controlling approximately 50% of the proliferation of ISC (Holmberg et al., 2006).

The observations of the Frisen et al. study were unexpected, considering that it was previously proposed that Eph forward signalling inhibited MAPK mitogen signalling and did not actively participate in cell proliferation responses (reviewed by (Kullander et al., 2002)). The same researchers who identified the positive regulation of ISC proliferation, described above had previously discovered that ephrin-A2 through EphA7 activated reverse signalling, which negatively regulated neural progenitor cell proliferation (Holmberg et al., 2005). The investigations by Vanderhaeghen and colleagues also support the role of Eph/ephrin molecules as negative regulators of neural SC proliferation (Depaepe et al., 2005). Genetic analysis demonstrated that ephrin-A2-/- mice displayed increased neurogenesis from neural SC niches within the adult brain. These proliferating cells also appeared to display a shorter cell cycle. Furthermore, greater numbers of cells accumulated in the olfactory bulb of these mice compared to littermate controls (Holmberg et al., 2005). Contrary to these findings, but consistent with the ISC observations, Alvarez-Buylla and colleagues illustrated that in the presence of soluble EphB2-Fc or ephrin-B2-Fc, SC within the adult mouse brain localised to the SVZ where they increased their proliferation (Conover et al., 2000). It may be that the A-subclass Eph RTK family members act as negative regulators of proliferation, while the B-subclass molecules may mediate positive proliferative responses. However, this notion remains to be elucidated. Understanding the role of Eph/ephrin molecules in SC niches, whether in determining position or location, migration or regulating proliferation, could have implications during SC repair following tissue injury.

Members of both subclasses of the Eph family of RTK and their ligands have been identified and shown to be up-regulated following neural injury (reviewed by (Goldshmit et al., 2006)),

presumably inhibiting axonal regeneration, while being conducive to glial scar formation. One such study observed that EphB2/ephrin-B2 protein levels initially decreased following spinal cord injury (1 day post-injury), allowing initial migration of fibroblasts into the lesion site. However, EphB2/ephrin-B2 protein levels increased significantly 14 days following injury. Bi-directional signalling between the EphB2 expressing fibroblasts and ephrin-B2 expressing astrocytes inhibited further cell migration and resulted in astrocytic scar formation (Bundesen et al., 2003). While the role of Eph/ephrin molecules in SC following injury has not been explored in detail, there is evidence to suggest that neural stem/progenitor cells do migrate to the injury site where they differentiate into astrocytes and may contribute to glial scar formation (Takahashi et al., 2003). The role of the Eph family members in SC niche maintenance, proliferation, SC migration and following neural injury, suggests that the Eph/ephrin molecules may participate in SC based repair following injury.

1.5 Factors that regulate stem cell mediated neurogenesis

Understanding the factors that influence neural differentiation during development and in postnatal tissue are the first steps in understanding and identifying the components that are essential for the neural differentiation of SC. This information is critical in determining whether SC are able to respond to endogenous neural environmental cues, or whether SC need to be stimulated along the neural pathway *in vitro* prior to *in vivo* transplantation.

1.5.1 Neural differentiation during development and neurogenic regions in the adult

The neural tube is the first structure to form following neural induction, where the development of the forebrain initiates from the most anterior end of the neural tube during neurulation. The forebrain is comprised of two main structures, the hypothalamus and the telencephalon and its vesicles. The telencephalon encompasses many structures including the olfactory bulb (OB), the rostral migratory stream (RMS), and the medial and lateral ganglionic eminence (MGE & LGE), which also comprise the ventricular zones (VZ). Progenitor cells in the VZ undergo proliferation, exist the cell cycle and migrate radially or tangentially from the VZ. The progenitors then differentiate into a mature phenotype to form

the cerebral hemispheres (fig. 1.8). These cells migrate through previously generated cell layers, contributing to new layers of the CNS, such that the brain is built from the inside-out (Marin and Rubenstein., 2002).

SC persist in the adult nervous system (reviewed by (Gritti et al., 2002)), within the same regions during embryonic neurogenesis, such as the SVZ, SGZ, hippocampal dentate gyrus (DG) and RMS (Martino et al., 2006). Studies investigating adult neurogenesis started with the canary and rodent (Goldman, A., 1998; Hidalgo et al., 1995); showing that the phases of neurogenesis during development also exist in the adult (Doetsch et al., 1999a; Doetsch et al., 1999b).

It appears that a number of mitogens and proliferative factors involved in the proliferation phase of embryonic neurogenesis are also employed during proliferation of adult neurogenesis. *In vitro* studies have demonstrated that mitogen EGF and FGF were able to induce proliferation of CNS SC, while still maintaining their multi-lineage potential (Doetsch et al., 2002; Gritti et al., 1996; Reynolds et al., 1996). Other intrinsic and extrinsic factors have also been implicated during proliferation and a continual role in differentiation; some of these include leukemia inhibitory factor (LIF) (Bauer et al., 2003), cyclin dependent kinases (cdks) and BMPs (Coskun et al., 2002). BMPs and one of its receptors, Noggin, appear to play a pivotal role in embryonic and adult neurogenesis, where BMP and Noggin are expressed on ependymal cells of the SVZ. BMP expression inhibits proliferation while Noggin promotes it (Lim et al., 2000). These factors are also important during differentiation (Palmer et al., 1999), where BMP initiates glial differentiation and Noggin instigates neuronal cell fates in the SVZ (Lim et al., 2000) and the OB (Coskun et al., 2002). Intrinsic factors have also been implicated during differentiation, including cdk $p19^{INK4d}$ which is regulated by BMPs in OB glial differentiation (Coskun et al., 2002) and suppressor of cytokine signalling (SOCS2), which promotes neuronal differentiation *in vitro*

Figure 1.8 The location of neural stem cells within the developing and adult rodent brain.

(a) Following the closure of the neural tube (dorsal view), vesicles develop from the most anterior portion of the neural tube. Neural stem cells line the vesicle; specifically within the lateral ventricle (LV), these stem cells proliferate and generate the specific structures within the central nervous system, whereby the brain grows from the vesicle and expands out from it. As the brain develops, the vesicles become smaller (arrows). The blue line denotes the layers of the developing forebrain in (b). A transverse view through the developing LV (blue line in (a)) shows the layers of the developing forebrain. Note that the ventricular zone (VZ) and sub-ventricular zone (SVZ) line the wall of the lateral ventricle. These stem cell regions remain in the adult brain (red line as a sagittal section in (c)) (adapted from (Jessell and Sanes., 2000)). (c) Neural stem cells persist in the VZ, the SVZ and the hippocampus of the adult brain. This image represents a sagittal view (red line in (b)) of an adult rodent brain. Neural stem cells within the SVZ proliferate, these progenitors travel along the rostral migratory stream (RMS) to the olfactory bulb (OB) where they differentiate into mature neurons.

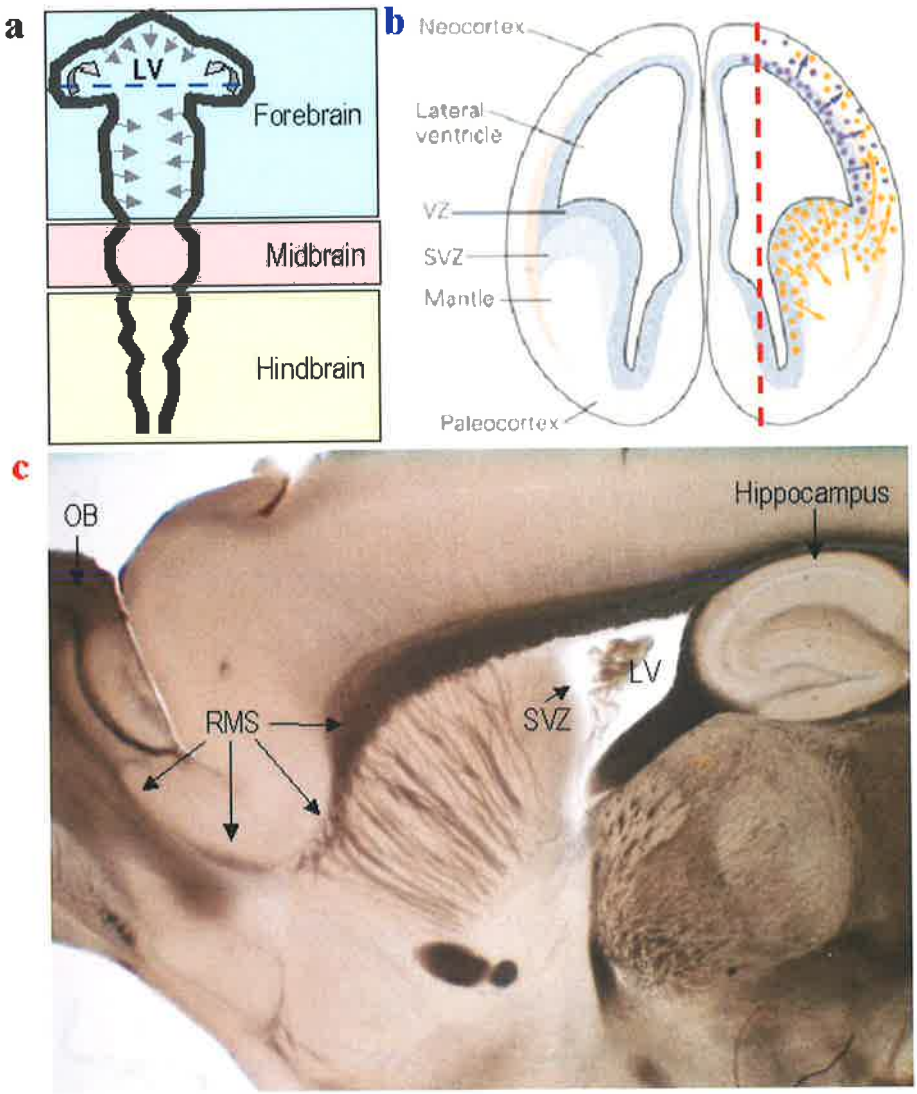
a
LV
Forebrain
Midbrain
Hindbrain
b
Neocortex
Lateral ventricle
VZ
SVZ
Mantle
Paleocortex
c
OB
Hippocampus
LV
SVZ
RMS

Figure 1.9 A schematic diagram depicts the structure of the NeuroD protein.

NeuroD belongs to the basic helix-loop-helix (bHLH) family of transcription factors. NeuroD members consist of a nuclear localisation signal (NLS) towards the N-terminus, a bHLH domain and an activation domain at the C-terminus that also overlaps with the co-activator p300/cAMP response element binding protein-binding protein (CBP) interaction domain. The bHLH domain is essential for DNA binding and dimerization. The bHLH dimers bind to a specific sequence (CANNTG), known as the E box, which is also expressed by other bHLH transcription factors. The interaction occurs through the basic domain of the BHLH, which activates specific gene transcription. NeuroD has been implicated in insulin production and neurogenesis developmentally and in the adult.

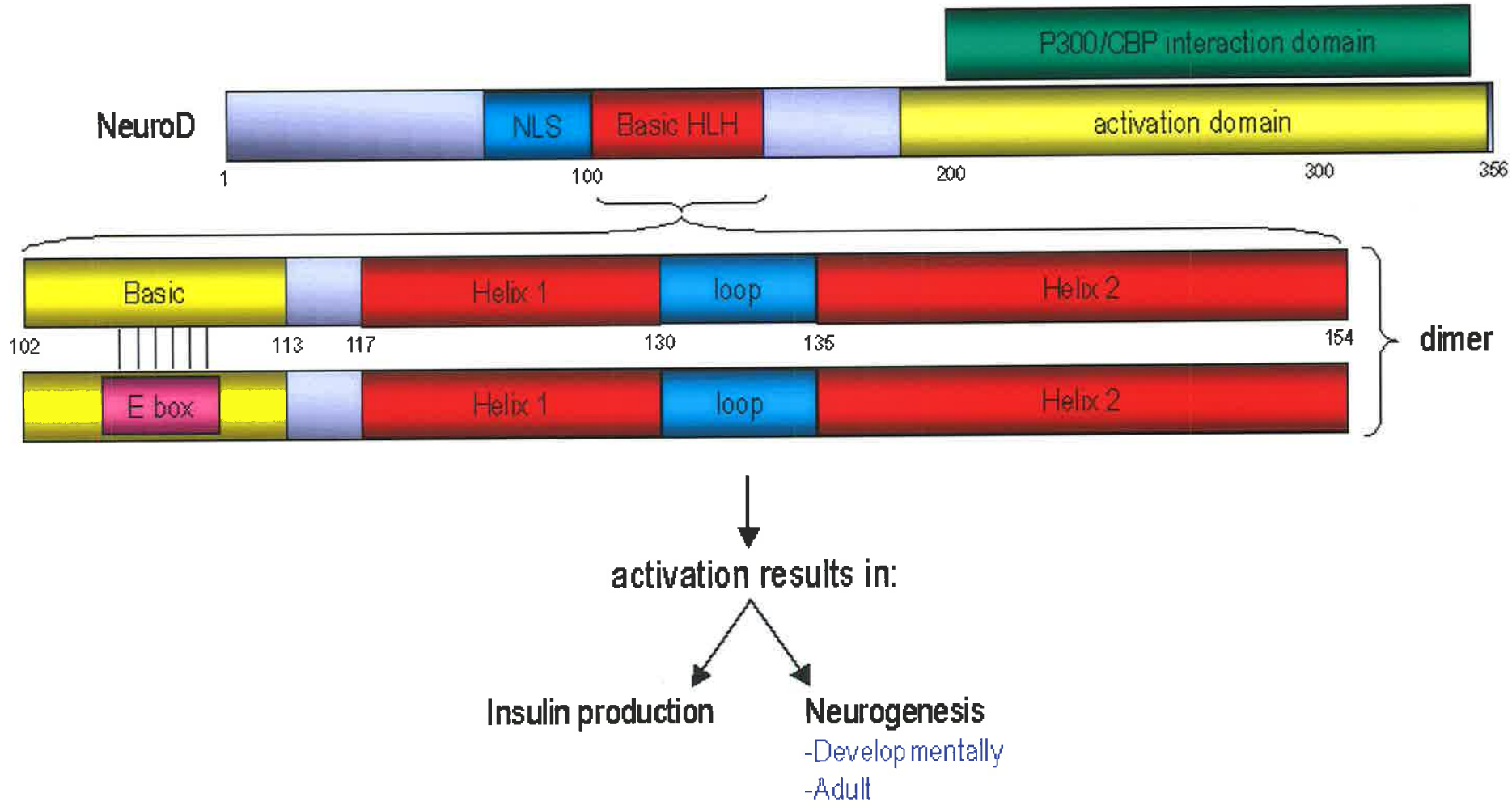
P300/CBP interaction domain
NeuroD
NLS
Basic HLH
activation domain
1
100
200
300
356
Basic
Helix 1
loop
Helix 2
102
113
117
130
135
154
dimer
E box
Helix 1
loop
Helix 2
activation results in:
Insulin production
Neurogenesis
-Developmentally
-Adult

and *in vivo* (Turnley et al., 2002). Transcription factors are also essential for neural differentiation. For instance, the expression of basic helix-loop-helix (bHLH) transcription factor, NeuroD, correlates both temporally and spatially during the active stages of embryonic (Lee et al., 1995) and adult (Elliott et al., 2001) neural differentiation.

1.5.1.1 Role of NeuroD in neural differentiation

The pro-neural gene, neurogenic differentiation, otherwise known as Beta2/ NeuroD/ NeuroD1, interchangeably, is a bHLH transcription factor family, comprising 3 members; NeuroD1 NeuroD2 and NeuroD3. These proteins function to activate the transcription of downstream target genes that determine the cell type. The HLH domain of the protein is essential for dimerization, while the basic domain makes specific contact with the DNA. The bHLH structure then binds the specific DNA recognition site, CANNTG, which is known as an E box (Kim et al., 2004b; Lee et al., 1995). The protein also consists of a nuclear localisation signal (NLS) upstream of the bHLH domain and an activation domain at the C-terminus of the protein, where together these domains activate downstream targets for neural differentiation (Fig. 1.9).

The NeuroD molecules are known to be positive regulators of neural differentiation during development (Korzh et al., 1998; Schwab et al., 2000) and neurogenesis (Lee et al., 1995). However, for NeuroD to mediate its neural differentiation function it first needs to be activated. This is regulated by a neural determination gene, Neurogenin-1 (Ngn-1), also a neural specific bHLH transcription factor (Ma et al., 1998). Following the activation by Ngn-1, it appears that NeuroD1 and NeuroD2 are involved in the primary stages of neural differentiation, where NeuroD1 regulates NeuroD2 expression (Westerman et al., 2004). Subsequently, NeuroD3 is believed to commit post-mitotic neural progenitors to the neuronal fate (Franklin et al., 2001).

Initial studies investigating the role of *NeuroD1* in mouse, demonstrated its mRNA expression primarily in the TG at embryonic day 9 (E9). By E11.5 *NeuroD* was expressed by sensory ganglia V to XI and dorsal root ganglion (DRG), where it appears that NeuroD participates in the neural rather than glial cell fate of neural crest cells (Deisseroth et al., 2004). At this stage, *NeuroD* was also observed in the cerebral cortex, the spinal cord and in sensory organs, such as the retina, during active neurogenesis. *NeuroD* expression

diminished by E14.5 within the cranial ganglia and DRG, at which time neurogenesis had stopped (Lee et al., 1995; Morrow et al., 1999). These observations suggest that NeuroD contributes to the differentiation process, possibly in terminal differentiation during neurogenesis, but is not required to maintain differentiated cell types (Lee et al., 1995). However, NeuroD has been shown to be important for the survival of a subset of rod photoreceptors in the adult (Morrow et al., 1999).

Since these initial observations, NeuroD has been shown to be expressed by a number of cell types during ear and eye development (Ahmad et al., 1998; Kim et al., 2001), and within various adult tissues, including pancreatic cells (Itkin-Ansari et al., 2005), hippocampal cells (Liu et al., 2000; Pleasure et al., 2000; Seki, T., 2002a), the cortex (Marin et al., 2001), SVZ (Lee, E., 1997), placode and neural crest cells (Schlosser et al., 2000).

Beta2/NeuroD knockout studies in mouse have noted abnormalities in the cerebellum and failure to form the granular cell layer of the DG (Liu et al., 2000; Miyata et al., 1999), resulting in epilepsy (Liu et al., 2000). The malformation of the DG was attributed to defective proliferation of precursor cells within the developing DG, with failure to differentiate into granular cells at the appropriate time. Subsequently, this resulted in a loosely packed and disorganised tertiary matrix that was unable to produce the appropriate number of postnatal granule neurons (Liu et al., 2000). However, these investigations failed to determined whether the resulting epilepsy observed in these mice occurred due to the lack of DG granule cells, change in DG structure, lack of Beta2/NeuroD or other associated but unidentified abnormalities. In another study, Tamura and colleagues investigated the role of NeuroD and NeuroD-related factor (NDRF) (homologous to mammalian NeuroD2) in mice, following seizure (Konishi et al., 2001). The seizure was induced by a chemi-convulsant, pentylenetetrazol (PTZ), which blocks GABA receptor-coupled chloride channels, where seizure stimulated neurogenesis to replace the damaged neurons (Parent et al., 2002a; Parent et al., 2002b). PTZ-induced seizure enhanced NDRF gene and protein expression 7-8 hours post seizure, and has been proposed to be involved in long-lasting neural activation (Konishi et al., 2001). Collectively, these studies suggest that NeuroD family members are important candidate molecules for the neural differentiation of SC.

1.5.2 Neural differentiation capacity of exogenous SC types

Primate and human studies demonstrate that adult macaque monkeys and humans appear to produce fewer newly generated neurons than rodents in the hippocampus (Eriksson et al., 1998; Kornack, R., 2000; Kornack et al., 1999). This may be reflective of the limited number of adult NSC in adult primates (Kornack et al., 2001). The majority of NSC studies have been conducted in the rodents, predominantly investigating the neural derivatives and migratory pathways of NSC within the SVZ and along the RMS to the OB. Given that rodents have a more pronounced olfactory system than humans, it is important to demonstrate that the same mode of neurogenesis exists between mammals. Investigations conducted by Alvarez-Buylla and colleagues have demonstrated that adult NSC exist in humans within the SVZ, however, these NSC did not display chain migration to the OB (Sanai et al., 2004). This is in contrast to other primate species, specifically adult macaque monkeys, which were able to generate neuroblasts in the sub-ventricular region that were capable of migrating to the OB (Kornack et al., 2001). Therefore, it remains to be determined whether the limited pool of endogenous human NSC can provide an adequate source of SC for therapy or have the potential for appropriate migration for tissue repair, following local neural injury.

Global brain ischemia is one type of brain injury that is caused by stroke; it is a neuronal injury model that can be used to explore the reparative function of endogenous NSC or exogenous SC sources. Ischemia induced in young adult macaque monkeys generated neural progenitor cells that differentiated and co-stained with neural markers within the CNS (Tonchev et al., 2003). Although SC from the SVZ also appear to be reactive to neural injury in rodent models, the newly generated neurons observed in the macaque monkey brain did not appear sufficient to replace the damaged neurons, nor did they represent a stable population (Picard-Riera et al., 2004). Similarly, in mice, 80% of newly generated neurons were found to undergo apoptosis between 2-6 weeks post-injury, with only approximately 0.2% of striatal neurons being replaced (Nakatomi et al., 2002).

An alternative and plausible approach to endogenous NSC as a SC therapy would be to utilise an exogenous source of SC with neural potential (reviewed by (Lindvall et al., 2004b)). Pluripotent ESC and multipotent BMSSC have been investigated predominantly. These SC have demonstrated their ability to differentiate into neural derivatives and improve

sensorimotor function following stroke in rodents (Chen et al., 2001a; Chen et al., 2001b; Ikeda et al., 2005; Leker et al., 2004; Li et al., 2001; Li et al., 2000; Wei et al., 2005). Crain and colleagues reported that human BMSSC were able to survive and differentiate into non-neuronal and neuronal cells within the human brain (Mezey et al., 2003). Briefly, four female patients were transplanted with human male donor BMSSC. These patients had underlying diseases, either, lymphocytic leukemia or genetic deficiency of the immune system and had died from their respective diseases 2-10 months following transplantation. The brains of the four patients were analysed for the potential contribution of transplanted BMSSC into the nervous system. While BMSSC were identified in non-neuronal cells within the white matter, neuronal differentiated BMSSC were located in the hippocampus and cerebral cortex (Mezey et al., 2003). These observations lend further support to the possibility of using exogenous human SC for the repair of human neurodegenerative diseases or trauma.

DPSC, a mesenchymal-like SC population, isolated by the same markers (STRO-1 and CD146) used to enrich for BMSSC, are another potential exogenous source of SC with neural potential. The postulated neural crest origin, the expression of neural markers by DPSC in normal growth media and the survival of damaged neurons in the presence of DPC (Gronthos et al., 2000; Laino et al., 2005; Laino et al., 2006; Nosrat et al., 2001), support the postulated neural potential of DPSC. Furthermore, the expression of a number of neurotrophic factors by DPC and dental pulp *in vivo* could play a dual role in DPSC therapy-based treatment, not only for neural differentiation to replace fatally damaged neural tissue, but possibly to assist in the survival and recovery of damaged endogenous neural cells that might otherwise die during an ischaemic event. This notion is supported by studies conducted by Nosrat and colleagues who demonstrated that a hemisected spinal cord in a rat model resulted in a 115% increase of surviving motor neurons when grafted with DPC compared to control (Nosrat et al., 2001). These encouraging findings beg the question as to the full developmental and therapeutic potential of DPSC beyond the constraints of dental tissues.

1.6 Use of DPSC as a stem-cell therapy-based treatment – Aims

1.6.1 Summary

DPSC residing in the pulp tissue of adult teeth are a novel population of SC that are hypothesized to be of neural crest origin. To date, there have been limited studies of DPSC suggesting these cells may have neural and regenerative potential, as they express a number of neural markers, mitogens and guidance factors during both embryonic and adult neurogenesis. Characterization of this SC population and its neural potential requires further investigation.

DPSC location within the tooth is unique and appears to reside within a restricted niche, in the perivasculature of the fibrous dental pulp tissue. Recently, different SC types, including neural and intestinal SC, have been localised to specialised niches within their respective tissues and are believed to respond to factors from the surrounding vasculature and neural environment. Additionally, it is emerging that SC within their niche also respond to paracrine factors, such as the Eph/ephrin molecules, which have been implicated in SC niche maintenance and regulating SC proliferation. The Eph family of RTK and their ligands participate in a diverse array of functions during development and in the adult. Specifically, the Eph family contributes significantly to CNC boundary formation in the hindbrain and migration to target fields. Therefore, DPSC may respond to Eph/ephrin interactions in a similar manner to CNC, with a possible role in maintenance of the SC niche. Furthermore, if DPSC do possess CNC-like properties then it is also plausible to suggest that DPSC may have neural potential. DPSC are already being explored for their possible role in therapy-base bone and dentine regeneration/repair treatment, therefore, there is the possibility that DPSC could be used for other types of therapy-based treatment if the correct environmental cues are determined.

1.6.2 Project aims

There were two aims for this PhD, the first was to explore the role of Eph/ephrin guidance molecules on DPSC, their possible role in DPSC niche maintenance and how they may assist DPSC in regenerating a damaged tooth. The second aim was to determine the neural potential of human adult DPSC, utilising both *in vitro* culture methods and an *in vivo* animal model. Understanding the DPSC niche and neural capacity of DPSC would help develop future strategies for manipulating DPSC as novel cellular-based therapies for the repair and regeneration of dental and neural tissues.

In order to fulfil these aims, it was necessary to:

(1) Characterise the gene and protein expression pattern of the EphB and ephrin-B molecules by cultured DPSC and, within the tooth.

(2) Determine the function of the relevant Eph/ephrin molecules within DPSC in culture and *in vivo*.

(3) Demonstrate that DPSC could respond to neural inductive factors, express neural specific markers and display a neuronal morphology, and

(4) Determine whether human adult DPSC were able to respond to endogenous neural environmental factors following *in vivo* transplantation, or whether they would first need to be stimulated along a neural pathway prior to engraftment.

Chapter 2 - Materials and Methods

2.1 Materials

2.1.1 Analgesics and gases

Table 2.1 Antibiotics, analgesics and gases

Name	*Company*
Cyclosporin A	*Novartis, NSW, Australia*
Halothane	*Veterinary Companies of Australia, NSW, Australia*
Lignocaine	*Gift from Institute of Medical and Veterinary Science (IMVS), SA, Australia*
Butorphanol (Dolorex)	*Intervet, NSW, Australia*
Nembutol	*International Veterinary Supplies*
Carbogen gas	*BOC*

2.1.2 Antibodies

Table 2.2 Primary antibodies

Name	Catalogue #	Raised Against	Company	Concentration
Eph/ephrin				
EphA3	AF640	Mouse	R&D Systems	100µg/mL
EphA4	Sek1/Cek8	Mouse	Gift Dr. D. Wilkinson	200µg/mL
EphA5	sc-1014	Rabbit	Santa Cruz	200µg/mL
ephrin-A1	sc-911	Rabbit	Santa Cruz	200µg/mL
ephrin-A2	sc-912	Rabbit	Santa Cruz	200µg/mL
EphB1	sc-9319	Goat	Santa Cruz	200µg/mL
EphB2	sc-1763	Goat	Santa Cruz	200µg/mL
EphB4	sc-5536	Rabbit	Santa Cruz	200µg/mL
ephrin-B1	sc-1001	Rabbit	Santa Cruz	200µg/mL
ephrin-B2	sc-1010	Rabbit	Santa Cruz	200µg/mL
ephrin-B3	sc-7281	Goat	Santa Cruz	200µg/mL

Table 2.2 continued.

Name	Catalogue #	Raised Against	Company	Concentration
DPSC markers				
STRO-1	N/A	Mouse IgM	Gronthos Lab	supernatant
CD146	N/A	Mouse IgG_{2a}	Gronthos Lab	10 µg/mL
Neural Markers				
β-tubulin (TUJ1)	MMS-435P	Mouse	Covance	1mg/mL
GFAP	Z 0334	Cow	DAKO	4.1g/L
Nestin	611658	Mouse	BD Bioscience	N/A
NeuroD1	sc-1084	Goat	Santa Cruz	200µg/mL
NeuroD2	N 8411	Rabbit	Sigma	100µg/mL
NeuN	MAB377	Mouse	Chemicon	1mg/mL
Neurofilament-M	13-0700	Mouse	Zymed	0.5mg/mL
Neurofilament -H	AB1991	Rabbit	Chemicon	50µL
O4	MAB1326	Mouse IgM	R&D Systems	1mg/mL
PSA-NCAM	MAb12E3	Mouse (IgM)	Gift Dr. T Seki	acites
Other				
GATA 4	SC-9052	Rabbit	Santa Cruz	200µg/mL
GFP	600-101-215	Goat	Rocklands	1mg/mL
Human Integrin-β1	MAB2000	Mouse (IgG)	Chemicon	1mg/mL
Vinculin	CBL 233	Mouse	Cymbus Biotechnology	100µg/mL

Table 2.2 continued.

Name	Catalogue #	Raised Against	Company	Concentration
Negative Controls				
1A6.12	N/A	Mouse IgM	Gronthos Lab	supernatant
1D4.5	N/A	Mouse IgG_{2a}	Gronthos Lab	1mg/mL
IB5	N/A	Mouse (IgG_1)	Gronthos Lab	1mg/mL
Mouse IgM	MGMOO	Mouse	CALTAG	1mg/mL
Rabbit IgG	10500	Rabbit	CALTAG	3mg/mL
Goat IgG	10200	Goat	CALTAG	3mg/mL

Table 2.3 Secondary and tertiary antibodies

Name	Catalogue #	Company	Concentration
Conjugated			
TRITC-Phalloidin	P1951	Sigma	500µg/mL
Annexin V-Fluos	1828 681	Roche	N/A
Mouse Secondary			
Donkey anti Mouse Cy3	715-165-150	Jackson Immunoresearch	1.5mg/mL
Goat anti Mouse Alexa 488	A11029	Jackson Immunoresearch	2mg/mL
Mouse IgG	1030-02	Southern Biotechnology	1mg/mL
Mouse IgM FITC	1020-02	Southern Biotechnology	1mg/mL
Mouse IgM PE	1021-09	Southern Biotechnology	1mg/mL
Mouse IgG Biotin	M32115	CALTAG	1.9mg/mL
Mouse IgM Biotin	10201-08	Southern Biotechnology	05mg/mL
Rabbit Secondary			
Donkey anti Rabbit Cy3	711-165-152	Jackson Laboratories	0.75mg/mL
Goat anti Rabbit Alexa 488	A11034	Molecular Probes	2mg/mL
Goat anti Rabbit Biotin	BA-1000	Vector	1.5mg/mL

Table 2.3 continued.

Name	Catalogue #	Company	Concentration
Goat Secondary			
Donkey anti Goat Cy3	711-165-147	Jackson Laboratories	0.75mg/mL
Donkey anti Goat Alexa 488	A11055	Molecular Probes	2mg/mL
Donkey ant Goat HRP	610-703-125	Rocklands	1mg/mL
Rabbit anti Goat Biotin	BA-5000	Vector	1.5mg/mL
Tertiary			
Streptavidin Alexa 488	S-11223	Molecular Probes	1mg/mL
Streptavidin TexasRed	SA1003	CALTAG	

2.1.3 Buffers, Solutions and Media

Table 2.4 Buffers and Solutions

Name	*Content*
Agar plates	*10g Tryptone –Peptone, 5g Yeast extract, 10g NaCl in 1L water, 7.5g Agar, autoclaved, cooled, ampicillin (100mg/mL final concentration), plated*
Blocking solution (IHC)	*10% Horse serum in either PBS-T or PBT*
Blocking solution (FACS)	*5% Horse serum, 10% BSA, 1%Penecillin/Streptamycin, 5% FCS in HEPES solution (GIBCO BRL, Grand Island, NY)*
Luria Broth (LB)	*10g Tryptone –Peptone, 5g Yeast extract, 10g NaCl in 1L water*
PUCKS-EDTA	*5mM KCl, 130mM NaCl, 3mM $NaHCO_3$, 5mM D-glucose, 10mM HEPES (pH 7.3), 1mM EDTA in ddH_2O*
4% paraformaldehyde (PFA)	*Paraformaldehyde powder (Sigma), 4M NaOH, 5M NaCl, 0.1M NaOP made up in milliQ water*
8% paraformaldehyde	*80g paraformaldehyde powder, 10M NaOH, made up in milliQ water*
Phosphate buffer	*811mL 0.5M Na_2HPO_4 pH 10.0, 187mL 0.5M $NaH_2PO_2.H_2O$ pH 5.0, when added together, pH 7.4*
Phosphate buffered saline (PBS)	*7.5mM Na_2HPO_4, 2.5mM NaH2PO_4, 145mM NaCl*
PBS-T	*PBS, 0.1% Tween-20*
PBS-TX	*PBS, 0.3% Triton-X 100*
Ringer's solution	*7.2g $NaCl_2$, 0.17g $CaCl_2$, 0.37g KCl, 0.115g Na_2HPO_4 in 1L ddH_2O, adjust to pH 7.4, filter sterilised*
TAE	*40mM Tris-acetate, 20mM sodium acetate, 1mM EDTA pH 8.2*
TE	*10mM Tris-HCL pH 7.4, 1mM EDTA*
Tris-Glycine	*25mM Tris, 250mM glycine (pH 8.3), 0.1% SDS*

Table 2.5 Media

Name	***Content***
Growth Media (MEM)	*alpha Modification of Eagle's Medium (alpha-MEM)* (JRH Biosciences, Inc., Lenexa, Kansas) *supplemented with: 15% fetal calf serum (FCS)* (JRH Biosciences, Inc., Lenexa, Kansas), *100 μM L-ascorbic acid 2-phosphate (WAKO, Tokyo, Japan), 200 mM (stock), 2mM (final) L-glutamine,* (JRH Biosciences, Inc., Lenexa, Kansas), *100 U/mL penicillin,* (JRH Biosciences, Inc., Lenexa, Kansas), *100 μg/mL streptomycin* (JRH Biosciences, Inc., Lenexa, Kansas) *(pen/strep)*
DME/High	*Dulbecco's Mod Eagles Media (DME/High* JRH Biosciences, Inc., Lenexa, Kansas), *10% FCS, 1% L-Glutamine, x1 penicillin/streptomycin*
Wash solution (HHF)	*HEPES solution (GIBCO BRL, Grand Island, NY), 5% fetal calf serum (Equitech-Bio Inc, Kerrville, TX)*
Media A	*Neurobasal A (Invitrogen, GIBCO BRL, Grand Island, NY), x1 B27 supplement (Invitrogen, GIBCO BRL), 1% Penicillin/Streptomycin, 20μg/mL EGF, 40μg/mL (Sigma) FGF* (CytoLab/PeproTech, Rehovot, Israel)
Media 1	*DMEM/F12* (JRH Biosciences, Inc., Lenexa, Kansas), *x1 ITSS (Roche Diagnostics), 1% Penicillin/Streptomycin,*
Media 2	*DMEM/F12, x1 ITSS, 1% Penicillin/Streptomycin, 40μg/mL FGF*
Media 3	*DMEM/F12, x1 ITSS, 1% Penicillin/Streptomycin, 0.5μM RA (Sigma)*
Media4	*DMEM/F12, x1 ITSS, 1% Penicillin/Streptomycin, 40μg/mL FGF, 0.5μM RA*
SOC Medium	*2.0% Tryptone, 0.5% Yeast extract, 10mM NaCl, 2.5mM KCl, 10mM* $MgCl_2$-$6H_20$, *20mM glucose*

2.1.4. Enzymes and Reagents

All chemicals used were of analytical grade or other grade suitable for use in molecular biological techniques.

Table 2.6 Enzymes

BamHI	*New England Biolabs*
BglII	*New England Biolabs*
EcoRI	*New England Biolabs*
HindIII	*New England Biolabs*
DNA Ligase	*Promega (M1801)*

Table 2.7 Fusion proteins and inhibitors

Reagent	***Company***
Fusion proteins	
Human-IgG-Fc 2.5 mg/mL,	*Rocklands(009-0103)*
EphA3-Fc 200 µg/mL	*R&D Systems*
EphB2-Fc 200 µg/mL	*R&D Systems (467-B2-200)*
ephrin-A5-Fc 200 µg/mL	*R&D Systems (374-EA-200)*
ephrin-B1-Fc 920 µg/mL	*Gift from Dr. Doug Cerretti, Vascular Biology Department, Immunex Corporation, Seattle, USA*
ephrin-B3-Fc 200 µg/mL	*R&D Systems (395-EB-200)*
Human anti-Goat IgG (2.4 mg/mL)	*Jackson ImmunoResearch (109-005-008)*
Inhibitors	
LY294002 – PI3K inhibitor	*Gift from Dr. Ravinder Ivell*
PP2 – Src inhibitor (migration)	*Gift from Dr. Ravinder Ivell*
U0126 – MEK inhibitor	*Cell Signaling Tech (#9903)*

Table 2.8 General reagents

Reagent	*Company*
Agar	*BD Bioscience (214010)*
Agarose	*Promega*
Alkaline Phosphatase	*Promega (M2A2A)*
Alkaline Phosphatase Buffer	*Promega (M2A2A)*
Alpha MEM Media	JRH Biosciences, Inc., Lenexa, Kansas
L- Ascorbic acid 2-phosphate	*WAKO, Tokyo, Japan*
Avindin/Biotin Blocking kit	*Vector Laboratories, Burlingame, CA (SP-2001)*
B27 Supplement	*Invitrogen (Gibco) (17504-044)*
Bone wax	*Ethicon, LTD. UK W810A*
Bovine Serum Albumin	*Sigma*
Calcein	*Molecular Probes (C1430)*
Cell strainer (70μM)	*Falcon, BD Labware, Franklin Lakes, NJ*
8-well Chamber Slides (plastic bottoms)	*Lab Teck (Nalge-Nunc) (177445)*
Chicken embryos	*Hi-Chick Breeding Company, South Australia*
Chloroform	*BDH (10077.6B)*
CIP Stock 20U/ul	*Promega (M2825)*
Collagenase type I	*Worthington Biochem, Freehold, NJ*
DAPI (4',6-Diamidino-2-phenylindole dihyrochloride hydrate)	*Sigma (D9542)*
Dispase	*Boehringer Mannheim, GMBH, Germany*
DMEM Media	*Invitrogen (Gibco) (12100-046)*
DMSO (dimethyl-sulfoxide)	*BDH (103234L)*
Dosper Liposomal Transfection Reagent	*Roche (1811 169)*
dNTP mix (10mM)	*Promega (U1330)*
0.1M DTT	*Invitrogen (18080544)*
Ethanol (absolute)	*Merck*
EDTA 0.5M	*Merck (K34433918520)*
Epidermal Growth Factor	*Pepro Tech (100-15)*

Table 2.8 continued.

Reagent	*Company*
Ethidium Bromide	*Sigma (G8751)*
F12 Media	*Invitrogen (Gibco) (21700-075)*
Fast green	*Sigma (F7252)*
Fetal Calf Serum	JRH Biosciences, Inc., Lenexa, Kansas
Fibroblast Growth Factor (FGF)	*Prospec Tany Techno Gene (#104FGFB01)*
Fibronectin	*Roche (1080938)*
Flasks (T25/T75/T175)	*Costar, Cambridge, MA*
Fluorescent Mount Media	*DAKO (S3023)*
G418	*Invitrogen (10131)*
Geletin	*Sigma G2500*
L-glutamine	JRH Biosciences, Inc., Lenexa, Kansas
Hanks balanced salt solution	*Invitrogen (Gibco) (14170-112)*
Horse Serum	*Institute of Medical and Veterinary Science, Gilles Plains, SA, Aust*
Hydrogen peroxidase	*Sigma (H0904)*
Indian ink	*Winsor and Newton, England*
Insulin-transferrin-sodium-selenite supplement (ITSS)	*Roche Diagnostics, Mannheim, Germany (11074547001)*
Glucose	*BDH (10117.4Y)*
Laminin	*Invitrogen (Gibco) (23017-015)*
Neurobasal A Media	*Invitrogen (Gibco) (10888-022)*
OligodT (500ng/μL)	*Promega (C1101)*
Optical caps (8/stripe)	*ABI (4323032)*
Optical plate adhesive covers	*ABI (4311971)*
Optical plates (96-well)	*ABI (N8010560)*
Optical tubes (8/stripe)	*ABI (4316567)*
Pap pen	*Zymed, (00-8888)*
Penicillin/Streptomycin	JRH Biosciences, Inc., Lenexa, Kansas
Polybrene (Hexadimethrine Bromide)	*Sigma (H9268)*
Poly-L-Lysine solution	*Sigma Diagnostics Inc. (P8920)*

Table 2.8 continued

Reagent	***Company***
Poly-L-Lysine TC grade	*Sigma (P4707)*
Poly-ornithine	*Sigma (P3655)*
Prolong Gold anti-fade with DAPI	*Invitrogen (Molecular Probes) (P36931)*
Protein ladder	*Invitrogen (10748-010)*
Random Heximers (500ng/μL)	*Promega (C1181)*
Retinoic Acid	*Sigma (R2625)*
Rnasin	*Promega (N2 111)*
Superscript III	*Invitrogen (180-80-044)*
Sybergreen	*ABI (4309155)*
Transwell® plates (8.0μm pore size, 6.5mm diameter)	*Costar, Corning Incorporated (3422)*
Triton-X-100	*Sigma*
TRIzol	*Invitrogen (15596-018)*
Tween-20	*Sigma (P1379)*
Tryptone	*BD Bioscience (211705)*
WST-1	*Roche (1644807)*
Yeast extract	*BD Bioscience (212750)*

2.1.5 Equipment

Table 2.9 Equipment

Equipment	*Company*
ABI SDS 7000 light cycler – Real Time PCR	*ABI prism SDS v1.1 (Applied Biosystems; California, USA*
Capillaries (Glass) thin wall Boorosilicate	*SDR Clinical Technology (GC100TF-10)*
Centrifuges	*cell culture - Eppendorf (5417R)*
	bench top - Eppendorf (5424)
	FACS samples - DiaCent-12 DiaMed
Engraver (for burr hole)	*Medalist (90960)*
ELIZA plate reader	*EL808 Ultra Microplate Reader, BIO-TEK INSTRUMENTS, INC*
Fluorescent Activator Cell	*Sorter – FACS Star plus, BD*
Sorter (FACS)	*Analyser – EPICS (XL-MCL), Beckman Coulter, ADC*
Forceps	*#5 = ,#55 = , World Precision Instruments*
Hamilton syringe	*SGE, Syringe Perfection (5µL)*
Incubators	*cell culture – Sanyo (MCO-18A1C), distributed by Quantum Scientific*
	Avian embryo incubator – Bellsouth
Microscalpel (Feather)	*Designs for Vision P/L*
Microscopes	*Confocal - BioRad (Radiance 2100)*
	Inverted - Nikon (TE300)
	Inverted – Olympus (CKX41)
	Olympus (AX70)
	Fluorescent dissecting microscope – Nikon (SMZ100)
	Dissecting scope (Olympus S240)
	Stereomicroscope
Mini-gel (1.5mm) glass plates	*Bio-Rad (165-3312)*
Mini-gel (1.5mm) combs	*Bio-Rad (165-3365)*
Mouse ear bars	*KOPF 921F and G*
Needle (micropipette) puller	*SutterInstruments Co (P-87)*

Table 2.9 continued.

Equipment	*Company*
Needle Holder and Manipulator (avian embryo experiments)	*Narishage, Japan*
Needle Holder (mouse injection experiments)	*KOPF*
Plate reader (Calcein)	*Luminescence spectrometer (LS 55), Perkin Elmer Instruments*
Semi-dri transfer cell	*Trans-blot® SD, Bio-Rad*
Scissors (for dissections)	*World Precision Instruments*
Scalpel – Feather microscalpel	*Designs for vision*
Spectrophotometer	*Eppendorf; Hamburg, Germany*
Stereotaxic Frame	*KOPF*
Sutures	*Ethilon 6.0 (697G), Ethicon, supplied by Johnson & Johnson Medical, NSW, Australia*
Thermocycler – PCR machine	*MJ Research (PTC-200)*
Tungsten wire (0.65mm)	*ACE Chemicals*
Typhoon	*Typhoon 9410 Variable Mode Imager, Molecular Dynamics, part of Amersham Pharmacia Biotech*

2.1.6 Kits

Table 2.10 Kits

Avidin/biotin blocking kit	*Vector Laboratories (SP-2001)*
QIAquick PCR purification kit	*Qiagen*
Rnasy kit	*Qiagen*
Plasmid Midi Kit	*Qiagen*
Plasmid Endotoxin Free Kit	*Qiagen*
QIAquick Gel Extraction Kit	*Qiagen*

2.1.7 Oligonucleotides

Table 2.11 Primer sequences for real time PCR and sequencing

Name	Accession	Forward	Reverse
GAPDH	NM_002046	5' GACCACAGTCCATGCCATCA 3'	5' CCATCACGCCACAGTTTCC 3'
β-actin		5' GATCATTGCTCCTCCTGAGC 3'	5' GTCATAGTCCGCCTAGAAGCAT 3'
TBP		5' CTGGAAAAGTTGTATTAACAGGTGCT 3'	5' CTTCATAAATTTCTGCTCTGACTTTAGC 3'
EphB1	AF037331	5' GTGGCTACGATGAAAACCTGAAC 3'	5' CTGGTTGGGCTCGAAGACAT 3'
EphB2	AF025304	5' ATGAACACGATCCGCACGTA 3'	5' TTGGTCCGTAGCCAGTTGTTCT 3'
EphB3	NM_004443	5' TGTGTAATGTGCGCGAGTCA 3'	5' TTGCAGTCACGCACAGTGAA 3'
EphB4	NM_004444	5' GCCGCAGCTTTGGAAGAG 3'	5' CATCCAGGCCGCTCAGTT 3'
EphB6	NM_004445	5' TGGGACGAGGTGAGTGTTCTG 3'	5' CCACATGACATGCCTCAAAGG 3'
ephrin-B1	NM_004429	5' AGCTCCCTCAACCCCAAGTT 3'	5' GGCAGATGATGTCCAGCTTGT 3'
ephrin-B2	NM_004093	5' CCTCTCCTCAACTGTGCCAAA 3'	5' CCCAGAGGTTAGGGCTGAATT 3'
ephrin-B3	NM_001406	5' TGTCTACTGGAACTCGGCGAAT 3'	5' TCCCCGATCTGAGGGTACAG 3'
β-tubulin	NM_006086	5' GGGCCAAGTTCTGGGAAGTC 3'	5' ATCCGCTCCAGCTGCAAGT 3'
GFAP	NM_002055	5' GCACTCAATGCTGGCTTCAAG 3'	5' CGGTCATTGAGCTCCATCATC 3'
NeuroD1	NM_002500	5' ACTGAACGCGGCGCTAGA 3'	5' TGGCCAAGCGCAGAGTCT 3'
NeuroD2	NM_006160	5' CAGACTCTGTGCAAGGGTCTGT 3'	5' CGTGAGGAAGTTGCGAGAGTT 3'
NF-M	NM_005382	5' GACGGCGCTGAAGGAAATC 3'	5' CTCTTCGCCCTGGTGCATAT 3'
Nestin	NM_006617	5' GTCCATCCTCAGTGGGTCAGA 3'	5' CCGATTGAGCTCCCACATCT 3'
pLNCX2	Clonetech	5' AGCTCGTTTAGTGAACCGTCAGATC 3'	5' ACCTACAGGTGGGGTCTTTCATTCCC 3'
pLXSN	Clonetech	5' CCCTTGAACCTCCTCGTTCGACC 3'	5' GAGCCTGGGGACTTTCCACACCC 3'

2.1.8 Plasmids

Table 2.12 Plasmids

Constructs	
pCS2+ containing NeuroD1	Gift from Dr. David Turner (Department of Biological Chemistry, University of Michigan Medical School, Ann Arbor, Michigan, U.S.A.)
pCS2+ containing NeuroD2	Gift from Dr. David Turner
Viral vectors	
pLNCX2	Clontech (#6102-1)
pLXSN	Clontech (#PT3134-5)
Viral packaging lines	
PT67	Clontech
PA317	Gift from Dr. Zannettino (Division of Haematology, Institute of Medical and Veterinary Science, Adelaide, SA, Australia)

2.2 Methods

2.2.1 Tissue Culture Methods

2.2.1.1 Isolating stem cells

2.2.1.1.1 Isolating DPSC and SHED

DPSC were isolated as described by (Shi et al., 2003) and SHED were isolated as described by (Miura et al., 2003). Briefly, discarded normal human impacted third molars were collected from adults (19-35 years of age) or exfoliated teeth (7-8 years of age) with their informed consent, undergoing routine extractions at the Dental Clinic of the University of Adelaide, under approved guidelines set by the University of Adelaide and IMVS Human Subjects Research Committees (H-73-2003). Tooth surfaces were cleaned and cracked open using a vice to reveal the pulp chamber. The pulp tissue was gently separated from the crown and root and then digested in a solution of 3 mg/mL collagenase type I and 4 mg/mL dispase for 1 hour at 37°C. Single cell suspensions were obtained by passing the cells through a 70 μM strainer. Cultures were established by seeding single cell suspensions (1 to 2 x 10^5) of dental pulp into T-25 flasks in growth media, (alpha-Modification of Eagle's Medium supplemented with 20% fetal calf serum, 100 μM L-ascorbic acid 2-phosphate, 2 mM L-glutamine, 100 U/mL penicillin and 100 μg/mL streptomycin), then incubated at 37°C in 5% CO_2.

The freezing procedure of DPSC or any other cell type was not described in the methods section. All cell types used were cryo-preserved in a similar manner. Cells were washed with HANKS balanced salt solution, liberated using 1% trypsin/ethylene-diamine tetraacetic acid (EDTA) solution, then washed with HHF. Cells were centrifuged *Eppendorf (5417R)* for six minutes at 1400rpm and resuspended in HFF followed by a cell count. Cells were centrifuged as described and resuspended in 500μL drop-wise of fetal calf serum (FCS) per 1 x 10^6 cells, followed by the addition of 500μL drop-wise of 20% DMSO in FCS per 1 x 10^6 cells for a final concentration of 10% DMSO. Cells were aliquoted 1mL/ampoule with 1 x 10^6 cells/ampoule, stored in a cooled (4°C) Mr. Frosty (Nalgene, Rochester, NY, Cat # 5100)

and placed at -80°C for a minimum of three hours. Ampoules were transferred to liquid nitrogen storage once frozen.

2.2.1.1.2 Isolating BMSSC

Bone marrow mononuclear cells used in this study were isolated in the Gronthos lab using the procedure previously described by (Gronthos et al., 2003). Briefly, bone marrow aspirates were obtained from the posterior iliac crest of normal adult volunteers (20-35 years old) following informed consent, according to procedures approved by the ethics committee of the Royal Adelaide Hospital, South Australia. Primary BMSSC cultures were established in growth media. BMSSC clonal cell lines were generated by limiting dilution from day 14 colonies derived from STRO-1^{BRIGHT}/VCAM-1^{+} sorted cells.

2.2.1.1.3 Isolating skin fibroblasts

Skin fibroblasts (SFB) cultures were already established in the Gronthos lab prior to the commencement of this study. Briefly, SFB were isolated by collagenase/dispase digestion from explants of foreskin biopsies from neonatal male donors, with informed parental consent.

2.2.2 Molecular Techniques

2.2.2.1 Total RNA Isolation

RNA was extracted from cells using a modified protocol combining the TRIzol method with the RNeasy extraction system RNA cleanup protocol. RNA samples were quantified by spectrophotometer and RNA integrity checked on 1% agarose gels using a deionised formamide based loading buffer. Briefly, TRIZOL was added to the sample and homogenised by passing several times through a 19 gauge needle, and then a 26 gauge needle. Samples were centrifuged at 13,000 rpm for 10 minutes at 4°C to remove cellular material. The liquid was decanted to a 2 mL tube where an additional 0.5 mL TRIZOL was added and incubate 15 minutes at room temperature. Chloroform (0.3 mL) was added and samples were vortex for 1 minute, then centrifuged for 15 minutes at 13,000 rpm. The upper aqueous phase

was collected and transferred to a fresh 2 mL tube. An equal volume of 100% ethanol was added to the sample, vortexed and loaded into an RNeasy column. Procedures were followed as per Qiagen instructions, briefly, the samples were then centrifuged 13,000 rpm for 30 seconds. The eluate was discarded, the column was washed with 0.7 mL RW1 buffer and centrifuged 13,000 rpm for 30 seconds. The column was transferred to a fresh collection tube, washed with 0.5 mL RPE buffer and centrifuged 13,000 rpm for 30 seconds. The elute was discard and centrifuged for 1 minute to remove the last traces of buffer. The column was then transferred to an RNase free 1.5 mL tube, 30 µL DEPC-treated dH_2O was added directly to the column membrane and incubated at room temperature for 1 minute to allow re-hydration of RNA. The sample was then centrifuged at 13,000 rpm for 1 minute.

2.2.2.2 cDNA synthesis

Stored RNA samples were thawed and heated to 37°C for 2 minutes, a maximum of 12 µL of total RNA was added to an RNase free 0.5 mL tube, 4 µL of Random Hexamers (500 ng/µL) and 2 µL of oligo-d(T) (500 ng/µL) was added to each sample and incubated at 70°C for 10 minutes in a thermal cycler with heated lid and then place on ice for 5 minute. A master mix was prepared containing: 5x Superscript III Buffer, 0.1 M DTT, Superscript III, dNTP mix (10mM) and RNasin, this solution was added to each sample. Samples were incubated for 2.5 hours at 50°C, following this, 10 µL of 0.25M NaOH and 10 µL of 0.5M EDTA were added to each sample. Samples were vortexed and incubated for 15 minutes at 65°C to degrade the RNA. Finally, 15 µL of 0.2 M acetic acid was added to each sample and mixed to neutralise the reaction. The cDNA was then purified using QIAquick PCR purification kit as follows: 325 µL of Buffer PB (5 volumes) was added to the cDNA and vortexed. The solution was transferred to a spin column and centrifuged 30 seconds; the flow-through was discarded, followed by the addition of 750 µL Buffer PE to the column and spun for 30 seconds. Again the flow-through was discard and centrifuged for 1 minute to remove residual fluid. The column was then transferred to a 1.5 mL tube and 30 µL dH_2O was added directly to membrane, incubated for 1 minute then spun 30 seconds. The purified cDNA sample was quantified using by spectrophotometer.

2.2.2.3 Real time polymerase chain reaction

The cDNA samples were diluted to a uniform concentration of 50 ng/μL. Real-time PCR reactions were performed using TaqMan master mix on an ABI SDS 7000 light cycler driven by ABI prism SDS v1.1. TaqMan primers were designed using Primer Express v2.0 (Applied Biosystems) and synthesized locally (GeneWorks; South Australia, Australia). Primers were used at a final concentration of 300 nM and reactions for each sample were performed in either triplicate or quadruplicate. TATA box binding protein (TBP) or β-actin were used as a positive control.

2.2.2.4 Molecular cloning

2.2.2.4.1 Restriction Digests and purification of DNA

NeuroD1 and *NeuroD2* were sub-cloned from the pCS2+ vector into pLNCX2 or pLXSN viral vectors, respectively, using a combination of restriction enzymes. Enzymes, BamHI and HindIII were used to cut *NeuroD1* (1294 bp from the PCS2+ vector, while BglII & HindIII were used to cut the viral vector pLNCX2, where BamHI & BglII have compatible ends. Enzyme BamHI was used to extract *NeuroD2* from the pCS2+ vector and also to linearise the viral vector pLXSN. Briefly, the DNA, specific enzyme(s), their corresponding buffer and water was combined, the samples were vortexed, pulse centrifuged and incubated at 37°C for at least 1 hour. Samples were loaded into a 0.7% agarose check gel, run at 82 V for 1-2 hours, the gel was stained with ethidium bromide, products were visualised use the typhoon (610 BP 30 / Green (532 nM) fluorescence, 500 V: Normal sensitivity). To maintain the integrity of the DNA, Image quant software was used to process the image, which was then printed onto an overhead plastic sheet, the agarose gel was laid directly on top of the overhead photocopy of the gel, the DNA product was then cut out of the gel using a scalpel blade and placed this in a 1.5 mL tube. To confirm that the DNA had been extracted the gel was visualised using a UV scanner. The digests were then purified using QIAquick gel extraction kit. Briefly, x3 volume of buffer QG was added to 1 volume of gel, incubated at 55°C for 10 minutes. The solution was transferred to a QIAquick spin column in 2 mL collection tube and centrifuged (13,000rpm) for 1 minute. Flow-through was discard, 0.5 mL of Buffer QG was then added to column and centrifuged (13,000 rpm) for 1 minute. The DNA was then washed

with 0.75 mL of Buffer PE and centrifuged (1,000 rmp) for 1 minute. Flow-through was once again discarded and centrifuged (13,000 rpm) column for an addition 1 minute. The column was then placed into a clean 1.5 mL eppendrof tube; the DNA was eluted with 30 uL of Buffer EB (10 mM Tris-Cl, pH 8.5), then centrifuge (13,000 rpm) for 1 minute. Purified DNA was quantified using a spectophetometer and stored at -20°C until required further; otherwise DNA underwent calf intestinal phosphatase (CIP) treatment.

2.2.2.4.2 CIP treatment

Firstly, CIP Stock (20 U/μL) was freshly diluted (1:20) in Alkaline Phosphatase Buffer to obtain a 1 U/μL final concentration. Purified DNA, x10 Alkaline Phosphatase Buffer, diluted CIP and water were combined and incubated at 37°C for 30 minutes, then incubated at 65°C for 20 minutes. CIP treated DNA was then placed on ice to cool down before purification. CIP treated DNA was again purified using Qiagen PCR purification kit as explained above (section 2.2.2.2 cDNA Synthesis). Purified CIP treated DNA was then stored at -20°C until required for ligation.

2.2.2.4.3 Ligation

The concentration of vector and DNA of interested was determined. A ligation reaction and re-ligation control were prepared on ice and incubated at 4°C for 72 hours. The vector was incubated with x10 Buffer, T4 DNA ligase and insert (for ligation reaction) or water (for relegation control).

2.2.2.4.4 Transformations

Chemical competent cells (DH5α) were placed on ice to thaw for 10 minutes. The ligation mix was added to DH5α (100 μL) and incubated on ice for 30 minutes, followed by incubation at 42°C for 1.5 minutes, cells where then placed on ice for 2 minutes. SOC medium (200 uL per sample) was added to the samples and then placed in a 37°C heating block for 30 minutes. While cells were incubating, agar plates were brought to room temperature and labeled. Spreading utensils were sterilized with ethanol and a blue flame. Transformations were plated onto agar plates using a sterile spreader. Plates were incubated

upside down at 37°C overnight and check for colonies the following day. Single colonies were picked, grown in luria broth (LB) containing ampicillin overnight at 37°C, the DNA was purified using the Fast Plasmid Mini Procedure (Eppendorf). Colonies were tested for correct orientation of the insertions using specific restriction enzymes, EcoRI for *NeuroD1* and HindIII for *NeuroD2* transfections. Those colonies that produced the correct sized and orientated products were then sequenced. Once the correct sequences were determined original colonies from glycerol stocks were streaked out onto LB plates and incubated overnight at 37°C. Colonies were picked and incubated in 5 mL LB+amp media shaking overnight at 37°C. These samples were then transferred to 500 mL LB+amp and again incubated at 37°C shaking overnight. DNA was purified using Qiagen Maxi Prep Endotoxin Free Protocol. DNA concentration was determined using a spectrophotometer.

2.2.2.4.5 DNA sequencing

Purified DNA was added to 100 μg/mL either forward or reverse *NeuroD1* or *NeuroD2* primer, determination mix version III and the remaining volume made up with water. The DNA sequences were amplified with a PCR reaction (96°C for 2 minutes, followed by 25 cycles of 96°C for 30 seconds, 50°C for 15 seconds, 60°C for 4 minutes, with a final incubation of 25°C for 10 minutes). The samples were then transferred to 1.5 mL tubes, 2.5 volumes of absolute ethanol was added to the sample, followed by $1/10^{th}$ initial reaction volume of Rnase free 3M sodium acetate. Samples were incubated at -80°C for 30 minutes, and then centrifuged at 14,000 rpm (Eppendorf 5417R) for 20 minutes at 4°C. The supernatant was aspirated; the pellet was washed with 500 μL of 70% ethanol, spun at 14,000 rpm (Eppendorf 5417R) for 5 minutes at 4°C. The DNA pellet was air-dried at room temperature for 5 minutes and then sequenced by the IMVS sequencing facility.

2.2.2.4.6 Preparation of glycerol stocks

For long-term storage of competent cells transformed with the vector of interest, 0.5 mL of overnight liquid cultures (LB containing ampicillin) containing the transformant was mixed with 0.5 mL sterile 80% glycerol. This was stored in 2 mL cryo-tubes at -80°C.

2.2.2.5 Transfection of retro viral packaging line

Packaging lines PT67 and PA317 were thawed and grown in DMEM/High Glucose media containing 10% FCS, x1 L-Glutamine, x1 pen/strep. Packaging cells were plated (1 x 10^5 cells/well) in 6-well plates. A water control, control vector only (pLNCX2 for *NeuroD1* and pLXSN for *NeuroD2*), vector containing *NeuroD1* or *NeuroD2* was added to a dosper solution (50 μL/reaction). Packaging cell lines were washed twice with 2 mL serum free DMEM media, 1 mL of DMEM media was then added to the cells. The dosper solution containing vector+*NeuroD1*, vector+*NeuroD2*, control vector or water control were added to the DMEM media covering the packaging cells in a drop by drop manner. The plate was then gently moved the mix the 2 solutions. Cells were incubated for 5 hours at 37°C after which time the media was removed and replaced with 2 mL DMEM/high Glucose media with supplements for 24 hours. Cells transfected with each viral vector were then re-plated into individual T25 flasks. DMEM/high Glucose media with supplements containing 600 μg/mL G418, which selects for transfected cells, was added to the packaging cells. When all the mock transfected packaging cells had died, G418 was reduced to 200 μg/mL. Once confluent, the G418 selected packaging cells were plated and expanded in T75 flasks, simultaneously, transfected packaging cells were cryoperserved for future use.

2.2.2.6 Transduction of DPSC with NeuroD1 or NeuroD2 retro virus

DPSC were thawed, expanded and plated (1 x 10^5 cells/well) in 6-well plates. Transfected packaging lines grown without G418 were plated (2.5 x 10^5 cells/flask) into T25 flasks. In preparation for infection, the supernatant of the packaging cells line transfected with either control vectors (pLNCX2, or pLXSN). *NeuroD1* or *NeuroD2* constructs were removed, polybrene (4 mg/mL stock, 1:1000 final) was added to the supernatant, which was then filtered (0.45 μM). Media only control was also prepared, using DMEM/High Glucose media and polybrene. Fresh DMEM/High Glucose media was used to re-feed the packaging cells. The supernatants were aspirated from DPSC cultures and replaced with the filtered supernatant from the packaging cell lines or media only control. This procedure was repeated after 5 hours and again the following day. Twenty-four hours following the last infection, the DPSC media was changed to growth media containing 600 μg/mL G418, to select for transduced DPSC. Transduced DPSC were grown in the 6-well plates until they were

confluent and then were transferred to T25 flasks. When all DPSC transduced with media only had died, G418 was reduced to 200 μg/mL. Transduced DPSC were then expanded in T75 flasks, when DPSC were confluent, they were cryo-preserved or processed for RNA isolation and protein isolation.

2.2.3 Protein Analysis

2.2.3.1 Immunocytochemistry of cultured cells preparations

Chamber slide or spreading assay cultures were fixed with 4% paraformaldehyde (PFA) for 30 minutes at room temperature and then washed with phosphate buffered saline plus 0.1% tween-20 (PBS-T). Cultures were blocked (10% horse serum in PBS-T and avidin-biotin blocking kit (SP-2001, Vector Laboratories) for 30 minutes at room temperature and then incubated with primary antibody in blocking solution overnight at 4°C. Mouse, goat and rabbit (Ig) controls; were treated under the same conditions. After washing, the secondary antibodies were added in blocking solution for 2 hours at room temperature in the dark. The cultures were then washed and incubated with tertiary reagents and Phalloidin-TRITC, in blocking solution for 2 hours at room temperature in the dark. Finally, cultures were washed; slides were cover slipped with 80% glycerol with DAPI, or culture plates were maintained in 100 μL PBS and DAPI.

2.2.3.2 In Situ Eph/ephrin staining – pulp tissue

Frozen sections (5 μM) of human pulp tissue were fixed with cold acetone at -20°C for 15 minutes then washed in PBS. The samples were blocked with either 5% non-immune goat serum or rabbit serum for 1 hour at room temperature. Samples were incubated with 2mg/mL primary antibodies (Eph/ephrin, STRO-1, CD146) overnight at 4°C. Mouse (IgM, IgG2a), goat and rabbit (Ig) controls; were treated under the same conditions. After washing in PBS the samples were incubated with the appropriate secondary antibodies, goat anti-rabbit biotin or rabbit anti-goat biotin for 1 hour at room temperature. Dual-fluorescence labelling was achieved by adding secondary antibodies; goat anti-mouse IgM or IgG FITC conjugated and tertiary antibody streptavidin-Texas Red for 1 hour at room temperature. After washing, the sections were covered slipped with fluorescence mountant.

2.2.3.3 Neural antibody staining - Chicken embryo staining

Following 4% PFA fixation and open book dissection, injected avian embryos were washed 5 times, 5 minutes per wash with PBS + 0.3% Triton-X (PBS-TX). Embryos were then incubated with constant movement in blocking solution (10% horse serum in PBS containing 1% Triton-X) for 5 hours at room temperature. The solution was then replaced with anti-goat GFP antibody and either anti-mouse TUJ1 or Neurofilament-M in 10% horse serum containing 0.1% Triton-X, samples were incubated with constant movement for 24 hours at room temperature. Embryos were washed with PBS-TX as mentioned above and incubated with corresponding secondary Donkey anti-goat Alexa 488 and Donkey anti-mouse Cy3 overnight at 4°C with constant movement in the dark. Samples were washed with PBS-TX as mentioned above, placed as open-book on a slide and cover slipped with prolong gold anti-fade with DAPI.

2.2.3.4 Neural antibody staining - Adult mouse brain

Free floating vibratome sectioned (100 μM) adult mouse brains were blocked with 10% horse serum in PBS-T for 1 hour at room temperature. Samples were stained with primary antibodies directed against neural markers (refer to 2.1.2.1 Primary Antibodies, Methods) in 10% horse serum in PBS-T overnight at 4°C. Mouse (IgG, IgM), goat and rabbit (Ig) controls were treated under the same conditions. Samples were washed prior to incubation with corresponding secondary antibody for 2 hours at room temperature. Samples were kept in the dark from this point forth. Samples was washed and incubated with human specific Integrin-β1 antibody in blocking solution, to detect injected human adult DPSC. Samples were washed and incubated for 2 hours at room temperature with corresponding secondary antibody. Brain sections were then washed, placed onto slides and cover slipped with prolong gold anti-fade with DAPI.

2.2.3.5 Imaging and image processing

The spreading assay cultures, time-lapse microscopy and whole-mount chicken embryo images were acquired using the Nikon inverted microscope (TE300), fitted with a cooled CCD camera and V++ v.4 software. Cultured DPSC and human dental pulp tissue sections were imaged using an Olympus AX70 microscope fitted with a cooled CCD camera, and V++

v.4 software. Whole-mount chicken embryos and adult mouse brain sections images were taken using confocal microscopy (BioRad Radiance 2100). Confocal images and z-images were processed and analysed using Confocal Assistant v.4.02. All digital images were processed using Adobe Photoshop 6 and only brightness and/or contrast were altered. Time-lapse movies were generated using Adobe Image Ready 3.0.

2.2.3.3 Flow Cytometric Analysis

Cells were prepared as a signal cell suspension using trypsin, cells were washed with HHF and past through a 70 μM cell strainer, centrifuged at 1400 rpm (Eppendorf, 5417R) for 5 minutes and resuspended in 10 mL blocking buffer (5% horse serum, 10% BSA, 1% penicillin/ streptomycin, 5% FCS in HEPES media). A cell count was performed and cells were incubated with blocking buffer for 30 minutes on ice. Cells were separated into 5 mL polypropylene tubes, corresponding to the antibodies being used. Samples were centrifuged (DiaCent-12) for 2 minutes; the blocking buffer was aspirated. Cells were resuspended in 200 μL of 20 μg/mL of purified primary antibody and incubated for 1 hour on ice, shaking. Samples were washed twice with HHF and then resuspended with the corresponding secondary antibody (1:50). Samples were incubated for 45 minutes on ice, washed twice in HHF, the supernatant was aspirated, samples were vortexed and resuspended in 500 μL of FACS FIX. Samples were analysed with EPICS XL-MCL (Beckman Coulter, ADC) and EXPO32 software.

2.2.4 Assays

2.2.4.1 Spreading Assay – with and without inhibitors

Fc-fusion proteins (Human-IgG-Fc 2.5 mg/mL, EphB2-Fc 200 μg/mL and ephrin-B1-Fc 920 μg/mL) at 1, 5 and 10 μg/ml were pre-clustered with a 10-fold concentration of Human anti-Goat IgG (2.4 mg/mL) in PBS for 1 hour at room temperature. Ninety-six-well flat-bottom plates, chamber slides or 4-well plates were coated with Poly-L-lysine (0.01% solution) for 5 minutes at room temperature. Following the pre-clustering of the Fc, the samples were incubated in the coated wells for 2 hours at 37°C in a 5% CO_2 incubator. The wells were

washed to remove unbound -Fc with PBS and incubated with 5 μg/mL laminin, fibronectin or growth media alone for 2 hours at 37°C in a 5% CO_2 incubator. Cells were prepared as a single cell suspension using PUCKS-EDTA, washed in HHF and resuspended in growth media. DPSC were either prepared as a single cell suspension for the original spreading assay, or cells were prepared for the inhibitor assay. For the original spreading assay, 2 x 10^4 cells/well were added to each well and incubated for 3 hours at 37°C in 5% CO_2. For the inhibitor assay, cells were incubated for 30 minutes at room temperature with signalling inhibitor U0126, PP2, LY294002 or 0.1% DMSO. Cells were then processed in the same way as for the spreading assay. The cultures were then fixed and stained with phalloidin-TRITC and/or vinculin as described above. For consistency, images of the cultures were taken in the centre of each well.

2.2.4.1.1 Time-lapse imaging

For Time lapse imaging, 1.28 x 10^5 cell/well were added to 4-well tissue culture plates. A very thin layer of sterile mineral oil was added to the surface of the media. The 4-well plate was placed on a heating plate mounted on a Nikon (TE300) inverted microscope. The plate was exposed to 5% Carbogen gas (BOC) for the duration of the experiment. Images were taken with V++ software at 1-minute intervals for 3 hours. Images were processed with Adobe photoshop 6.0 and created into to a movie using Adobe Image Ready 3.0.

2.2.4.2 Scion Image Analysis

Scion image software (National Institute of Health) was used to determine surface area and roundness of DPSC following the spreading assay. Briefly, images were inverted from black background/white cells to white background/black cells, and manipulated using "threshold" to segment objects (cells) of interest and background on the bases of grey levels. Surface area and major and minor axial values (to determine roundness) were calculated for objects greater than 200 pixels. Objects that were touching the edge of the image or an object that contained more than one cell (either overlapping cells or cells that were still touching) were removed from the cohort.

Roundness was determined by dividing the value of the major axis by the value of the minor axis, resulting in a value equal to or greater than one. A value of one suggested a round object, as both major and minor axial values were the same, any value great than one suggested that the object was elliptical; the great the value, the more elliptical the cell.

Spreading experiments were performed in triplicate per –Fc (EphB2, ephrin-B1 and Human-IgG) treatment, from three individual donors (n = 3). A 2-tailed, 2-sample unequal variance, Student t-test was performed at 10 μg/mL between Human-IgG-Fc and either EphB2-Fc or ephrin-B1-Fc. The graphs were determined using the mean value of surface area and elliptical value for each donor; the error bars are the standard error of the mean (SEM).

2.2.4.3 Adhesion Analysis

Fc-fusion proteins (Human-IgG-Fc 2.5 mg/mL, EphB2-Fc 200 μg/mL and ephrin-B1-Fc 920 μg/mL) at 1, 5 and 10 μg/ml were pre-clustered with a 10-fold concentration of Human anti-Goat IgG (2.4 mg/mL) in PBS for 1 hour at room temperature. Ninety-six-well flat-bottom plates were coated with Poly-L-lysine (0.01% solution) for 5 minutes at room temperature. Following the pre-clustering of the Fc, the samples were incubated in the coated wells for 2 hours at 37°C in a 5% CO_2 incubator. During the -Fc incubation, cells were liberated from the flask using PUCKS-EDTA, washed in HHF and resuspended in alpha-MEM and transferred to 14 mL polypropylene tubes. Cells were washed for 5 minutes, 3 times in alpha-MEM and 0.2% BSA. Following the final wash, cells were resuspended in alpha-MEM containing 0.2% BSA and 10 μM Calcein. Cells were incubated at 37°C for 1 hour in the dark and kept in the dark from this point forth, as Calcein is light sensitive. Following the incubation, cells were washed for 5 minutes, twice with alpha-MEM containing 0.2% BSA and then resuspended in growth media in a volume corresponding to 150 μL/well with 2×10^4 cells/well. The 96-well plate incubating with -Fc solution was then washed 3 times with PBS to remove unbound -Fc. Calcein labelled cells (2×10^4 cells/well, in 150 μL) were then added to the 96-well plate and incubated for 3 hours at 37°C in a 5% CO_2 incubator. Cells were then gently washed for 5 minutes, 3 times with alpha-MEM containing 0.2% BSA. Following the final wash, the wells were air-dried, 150 μL of 1% SDS in PBS was added to the wells, the release of the Calcein dye into the solution was measured using the luminescence spectrometer (LS 55).

The 96-well plate was placed in the plate reader; the FL Win Lab software was set specifically to detect the fluorescent Calcein dye. The excitation and emission wavelength parameters were set at 485 nm and 530 nm, respectively, with a reading time of 0.5 seconds per plate and cycle time of 1 second per plate. The raw data was then transferred to Microsoft Excel and analysed.

2.2.4.4 Migration Assay

Fc-fusion proteins (Human-IgG-Fc 2.5 mg/mL, EphB2-Fc 200 μg/mL and ephrin-B1-Fc 920 μg/mL) at 10 μg/mL were pre-clustered with a 10-fold concentration of Human anti-Goat IgG (2.4 mg/mL) in PBS for 1 hour at room temperature. The Fc-fusion protein solution (0.6 mL) was then added to the bottom well of the transwell plate. Cells were prepared as a single cell suspension using PUCKS-EDTA, washed in HHF and resuspended in growth media. DPSC (3×10^4 cells/well) were added to the top chamber of each transwell and incubated for 24 hours at 37°C in 5% CO_2. For the inhibitor assay, cells were incubated for 30 minutes at room temperature with signalling inhibitor 10 μM U0126, or 0.1% DMSO prior to being added to the transwell. Following the 24 incubation, the cultures were fixed with 4% PFA for 20 minutes at room temperature, then washed with PBS. The inside of the transwell was then cleaned using a cotton bud, to remove any cells that had not migrated through the well and then stained with DAPI to visualise the nucleus. The assay was repeated in duplicate wells and images were taken at 3 random positions within the well for each well. The number of nuclei were counted in each image and represented as the average cell count/field of view.

2.2.4.5 Neural Induction Assay

Tissue culture flasks or wells were coated with Polyornithine (10 ug/mL final concentration) overnight at room temperature. Flasks and wells were washed twice with water and then coated with Laminin (5 ug/mL final concentration) overnight at 37°C in a humid incubator. Flasks and wells were again washed twice with PBS; these flasks and plates were either used immediately or stored at -20°C with the last PBS wash. Prior to use in an experiment, the surface of the flask or plate was washed once with media before cells were added. Cells were thawed and grown in T25 coated-flasks until 80% confluent, then liberated from the flask

using trypsin. Cells were re-seeded at a density of 1.5 x 10^5/well in 2 mL/well growth media (α-MEM plus supplements), for 3 days in 6-well coated-plates, or 2 x 10^3 cells in 8-well coated-chamber slides. The media was then replaced with 2 mL/well Media A (refer to table 2.2.1) for 7 days. Media A was then replaced with 2 mL/well of one of the following 4 media for 7 days. Following this incubation all media conditions were replaced with Media 3 for 7 days. Note that media was changed twice weekly. Following the final incubation, the 8-well coated-chamber slides were fixed with 4% PFA, cells in 6-well plates were lysed with TRIzol® and stored for RNA isolation and RT-PCR analysis.

Table 2.2. 1 Media Components

Media A	Media 1	Media 2	Media 3	Media 4
Neurobasal A	DMEM/F12	DMEM/F12	DMEM/F12	DMEM/F12
B27 supplement	Pen/strep	Pen/strep	Pen/strep	Pen/strep
Pen/strep	ITSS	ITSS	ITSS	ITSS
EGF		FGF	RA	FGF
FGF				RA

2.2.4.6 Proliferation / Survival WST-1 Assay

Cells were liberated using PUCKS-EDTA, 2.5 x 10^3 cells/well were added to each well of a 96-well plate. Cells were incubated for 4 hours, during this incubation Fc-fusion proteins (Human-IgG-Fc 2.5 mg/mL, EphB1-Fc 1.22 mg/mL, EphB2-Fc 200 μg/mL, EphB4-Fc 1 mg/mL, ephrin-B1-Fc 920 μg/mL, ephrin-B2-Fc 1 mg/mL and ephrin-B3-Fc 200 μg/mL) at 1, 5 and 10 μg/ml were pre-clustered with a 10-fold concentration of Human anti-Goat IgG (2.4mg/mL) in growth media for 1 hour at room temperature. Following the 4 hour incubation, the growth media was aspirated from the wells and replaced with corresponding -Fc solution (150 μL/well) and incubated at 37°C in a 5% CO_2 incubator for 4 days. On the final day 2.5 x 10^3, 5 x 10^3 and 1 x 10^4 cells/well were plated in duplicate and incubated for 4 hours at 37°C in a 5% CO_2 incubator. WST-1 was diluted (1:10) in growth media just prior to the conclusion of the assay. The media was aspirated from the cells and replaced with diluted WST-1 solution; WST-1 was also added to duplicate empty wells to act as a blank during analysis. Samples were incubated for 2 hours with the WST-1 solution at 37°C in a 5% CO_2

incubator. Following the incubation, samples were analysed using an ELIZA plate reader, KC4 software was used to analyse the readings, blanks were established on the layout of the KC4 software, in addition to known cell concentrations of plated cells (2.5 x 10^3, 5 x 10^3 and 1 x 10^4 cells/well). Prior to the 450 nM-absorbance reading, samples were shaken for 3 seconds. Raw data was transferred to Microsoft Excel software and analysed further.

2.2.5 *In vivo* Injection Procedures

2.2.5.1 Avian Embryo Injections

Ethical approval was obtained from the University of Adelaide (Approval number S-59-2003). Chicken eggs (white leghorn, HICHICK Breeding Company, Bethal, SA, Aust.) were placed long ways in egg trays and incubated in a humidified incubator at 37°C for approximately 40 hours to reach Stage 10-12 (Hamburger et al., 1951) prior to injection. GFP labelled DPSC, SHED, BMSSC or SFB were liberated using trypsin and prepared at 5 x 10^3/μL. Fast green dye (1 μL) was added to the cells to visualise them during the injection procedure. Each egg was individually prepared for injection, firstly the egg was wiped over with 70% Ethanol, a 18-gauge needle attached to a 10 mL syringe gentle pierced through the egg shell at one end of the egg and was inserted into the egg, 6 mL of egg white was drawn into the syringe. A window was then cut into the top of the egg, the embryo was visualised by injecting Indian ink (1:10 prepared in Ringer's Solution was drawn up into a 1 mL syringe through a 26-gauge needle) underneath the embryo. A few drops of Ringer's Solution were placed on top of the embryo to maintain moisture. Cells (5 x 10^3/μL) were slowly drawn up into a 1 mL syringe through a 36-gauge needle and then gently expelled into a glass capillary that had been pooled into a needle. The cells and solution were flicked to the tip of the glass needle and then placed into a needle holder attached to pressure injector, set at 25 V. The pressure injector was also attached to an oxygen tank. The needle holder was then placed into a micromanipulator; the tip of the glass needle was removed with forceps. The egg was then placed under a dissecting microscope (Olympus S240); the vitelline membrane was removed from around head of the embryo, the micromanipulator was used to direct the glass needle into the embryo at regions adjacent to the hindbrain. Cells were injected into the embryo using a foot pump attached to the pressure injector. The glass needle was removed and a few

drops of Ringer's Solution were placed on top of the embryo. The egg was sealed with sticky tape and placed back in the humidified incubator for either 24/ 48 or 72 hours. Following the incubation period, embryos were cut out of the egg and placed in cold PBS, GFP injected cells were visualised using a fluorescent dissecting microscope. Embryos were then dissected below the heart. The head was cut as open-book, ie, cut from the nose to the hindbrain down the length of the head, along the ventral side. Dissected embryos were fixed in 4% PFA for either 2 hours at room temperature or overnight at 4°C, then washed twice with PBS prior to immunofluorescent staining.

2.2.5.2 Adult Mouse Brain Injections

Ethical approval was obtained from the University of Adelaide and the Institute of Medical and Vetinary Science, Adelaide (approval number 30/04). Prior to the injection procedure, the mouse cage was warmed on a heat pad, so that the animals were warm when recovering following the surgery. All surgical equipment was placed in Betadine. The stereotactic frame was assembled, in addition to the Hamilton syringe, its holder and ear bars. Animals were anaesthetised (1L oxygen and 3% Fluothane), when the animal was no longer responsive, the top of the skull was shaved, cleaned and the mouse was placed in the stereotactic frame. The head was positioned so that the skull was completely horizontal; this position was maintained with the ear-bars. The skull was swabbed with antiseptic; lignocaine (10 µL) was injected under the skin on both sides of the presumptive incision. A small incision was made at the midline slightly posterior of the eyes, as close to Bregma (the central point where the 4 plates of the brain meet, looks like a cross) as possible. The soft connective tissue between the skin and skull was gently scraped away; a stereomicroscope was used to locate Bregma. The Hamilton syringe connected to the stereotactic frame was used to determine the co-ordinates of Bregma for each individual animal. The co-ordinates of 3 axes were obtained, anterior-posterior (A-P), lateral-medial (L-M) and dorsal ventral (D-V). The stereotactic frame uses Vernier measurements, for instructions visit:
http://www.phy.ntnu.edu.tw/java/ruler/vernier.html

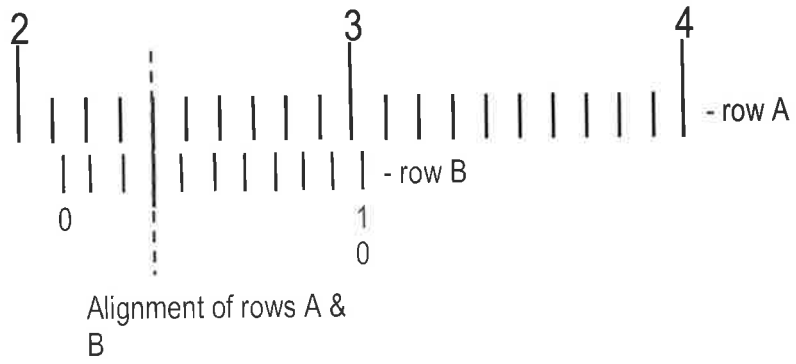

Briefly, the diagram above shows a measurement to 2 decimal places. The increments between 2 and 3 are 0.1; the increments of this row will be referred to as row A (black lines) for this explanation. The first decimal place is determined by the position of the '0' on the second set of increments, referred to as row B (blue lines). With vernier measurements, the second set of increments determines the first decimal place, as well as the second decimal place. To determine the second decimal place, increments of row A and B must align (red line). For the example presented, the first unit is '2', as the alignment is between '2' and '3'. The first decimal place is '1' as the '0' of row B is just past '1' in row A. The second decimal place is '3', as the alignment (red line) of increments between rows A and B is on increment '3' of row B, therefore the reading would be 2.13.

The coordinates for the RMS from Bregma were L-M -0.1, A-P -0.15, D-V –0.4, but injected at -0.2, the extra -0.2 was added to allow space for the injected cells. The coordinates for the hippocampal injections from Bregma were L-M -0.1, A-P -0.15, D-V -0.20, an extra -0.04 was added to allow space for injected cells.

The syringe was moved to the corresponding L-M and A-P position for either the RMS or hippocampal co-ordinates, a mark was left on the skull at this position. A Burr hole was made at the marked position on the skull. Five microliters of DPSC (2 x 10^4/μL) was placed in the Hamilton syringe, the syringe was placed into the syringe holder and returned to the previously marked injection site. The syringe was lowered very slowly to the determined D-V coordinates (including the extra -0.2 for RMS injections, -0.04 for hippocampal injections) and then up to the D-V injection coordinates. The cells were slowly expelled into the site at a rate of 1 μL/30 seconds. The Hamilton syringe was removed slowly, the burr hole was covered with bone wax and 2 μL of lignocaine was distributed over the surface of the skull.

The skin was sutured using nylon sutures. Butorphanol® (2 mg/kg) was administered intramuscularly into the hind leg muscle near the tail. The mouse was then removed from the stereotaxic frame and allowed to recover in a warmed cage. Animals were closely monitored for the first 30 minutes, and then daily. Mice were administered cyclosporinA (concentration) diluted in peanut oil daily for 3 weeks. The cyclosporin A was injected intraperitoneally, six different injection sites were used to prevent scaring of tissue and pain to the animal.

Following the 3-week incubation of DPSC in the adult mouse brain, the animals were killed by overdose of Nembutol (100 μL of 60 mg/mL stock concentration), via intraperitoneal injection. Once the animal was no longer responsive to pain the animal underwent transcardial perfusion.

2.2.5.3 Transcardial perfusion

This procedure was conducted in an area with scavenger airflow and protective eyewear was worn. Four percent PFA was made by combining 50 mL 8% PFA with 20 mL phosphate buffer (pH 7.4) and 20 mL water. Once the mouse was no longer responsive to pain, but the heart was still beating, the mouse was placed on its back and its limbs were pinned away from to body. The skin covering the abdomen was cut towards the head to expose the diaphragm and ribs. The sternum was clamped; the diaphragm and ribs were cut carefully, so that the liver and heart were not damaged. The sternum was then pulled up and towards the head to view the heart. A very small incision/cut was made into the right atrium (located on the left hand side when looking down at the animal). Very deep red blood flowed out of this chamber, once the blood was flowing, curved forceps were placed across the bottom half of the heart to apply pressure.

A blunt ended 21-gauge needle attached to a 50 mL syringe, containing saline was inserted into the left ventricle, as close to the interventricular septum as possible. Saline was administered into the heart at a steady pace until the liver had cleared of blood and the skin around the mouth had turned white. Once the blood had cleared from the animal, the needle was removed. Again pressure was applied to the bottom half of the heart, another blunt 21-gauge needle attached to a 50 mL syringe, containing 4% PFA was placed into the whole, in the left ventricle, previously made with the needle attached to the saline containing syringe.

The 4% PFA was injected at a steady pace into the heart until the muscles had stiffened, the legs and tail of the mouse had extended and the head had moved backwards, with the nose pointing upwards. The needle was then removed from the heart; the animal was turned ventrally, tested for the rigidity in the head, to determine the effectiveness of the transcardial perfusion. If the head was not stiff, then more 4% PFA was administered. If the head was stiff, it was removed from the rest of the body; the skin from the back of the head was cut along the midline, towards the nose and removed to expose the skull. Curved forceps were placed above and gently below the skull at the midline to break the skull. A portion of the skull was then gently peeled away from the brain, so that the brain was not damaged, but allowed access to fluid. For complete fixation, the head of the mouse, with the exposed brain were incubated further in 4% PFA overnight at room temperature or at 4°C for 3 days. Samples were then removed from the 4% PFA, washed in PBS and then processed for immunohistochemistry.

Chapter 3 - Characterisation of Eph/ephrin molecules on cultured DPSC and within the pulp tissue.

3.1 Introduction

Tooth development commences from the interaction between cranial neural crest (CNC) mesenchymal derived cells and the neighbouring epithelial tissue. These CNC derived cells are thought to persist within the adult tooth, mainly in the pulp tissue (Chai et al., 2000), which is the soft connective tissue in the central chamber of the tooth. A stem cell population was recently isolated from the pulp region of human adult third molar teeth, known as dental pulp stem cells (DPSC) (Gronthos et al., 2000) and the pulp of deciduous teeth (SHED) (Miura et al., 2003). DPSC and SHED have been demonstrated to possess self-renewal capacity, high proliferation potential and multi-lineage differentiation (Gronthos et al., 2002; Gronthos et al., 2000; Miura et al., 2003). These stem cells were identified with two early mesenchymal stem cell markers STRO-1 and CD146. These markers also localise around the blood vessels within the pulp, demonstrating that DPSC and SHED reside largely within perivascular niches within their respective tissues (Miura et al., 2003; Shi et al., 2003). More specifically DPSC have been shown to display a similar phenotype to pericytes (identified with antibodies to the pericyte marker, 3G5 antibody and to α-smooth muscle actin), which line the peri-vasculature, where pericytes are also thought to be derived from a neural crest origin (Schor et al., 1998). The co-localisation of DPSC with the pericyte marker 3G5 supports previous studies that hypothesize that pre-odontoblasts originate from perivascular niches (Alliot-Licht et al., 2001; Schor et al., 1998). While the ontogeny of DPSC is unknown, it has been proposed that DPSC themselves may be of neural crest origin, or at least possess neural crest properties, due to the neural crest origin of the tooth and the localisation of DPSC within the perivascular niche.

Recent studies by (Tecles et al., 2005) show that preodontoblasts migrate from blood vessels to dentine surfaces following injury. However, little is known about what regulatory cues DPSC respond to following disruption of the dentine matrix or how they are maintained or restricted within their niche under steady state conditions. Transcription factors, growth factors and guidance cues are all thought to be required and essential for the creation,

homeostasis and dynamic flux of stem cell niches (Fuchs et al., 2000). Some critical factors involved in maintaining stem cell niches and cell fate commitments have been described, including Wnt/β-catenin signalling and BMP signalling (Lowry et al., 2005; Niemann & C., 2006; Ohlstein et al., 2004; Song et al., 2004). It has also been suggested that Notch 1, Lunatic Fringe, Fibroblast Growth Factor-10 (FGF-10) may be important for DPSC maintenance due to their localisation and requirement during tooth development (Harada et al., 2004). The role of guidance cues has previously not been investigated in DPSC niche maintenance. However, a well-known family of guidance molecules, the Eph RTK family, have been implicated in neural stem cell proliferation and migration (Conover et al., 2000; Holmberg et al., 2005) and more recently demonstrated to controls the proliferation and migration of stem cells within the intestinal stem cell niche (Holmberg et al., 2006).

The Eph/ephrin family are contact-dependent molecules and well known for their role in mediating inhibitory or repulsive responses. The family are divided into two subclasses based on structure for the ephrin ligands, where the A-subclass is GPI-tethered to the membrane, while the B-subclass is transmembrane. The receptors are thus divided into two subclasses based on their binding affinity for their cognate ligand, with promiscuous binding within subclasses, but minimal interaction between subclasses, with the exception of EphA4 (Gale et al., 1996a) and EphB2 (Himanen et al., 2004). Both subfamilies have been shown to signal through both the receptor (forward signalling) and the ligand (reverse signalling), mediating various responses depending on the mode of signalling. The Eph family of molecules are expressed by most tissue types during development and are essential for the formation and maintenance of specific structures such as rhombomere formation in the hindbrain, angiogenesis, neural stem cell proliferation, axon guidance and migration of neural crest cells to name a few (Himanen et al., 2003; Kullander et al., 2002).

More specifically, Eph/ephrin molecules are essential for correct CNC cell compartmentalisation to specific rhombomeres (r) in the hindbrain and migration during embryo development (Smith et al., 1997). The Eph receptors and ligands are expressed in complementary rhombomeres, these molecules restrict intermingling of cells at rhombomere boundaries by initiating a repulsive signal at the boundary, which results in cell sorting between Eph and ephrin expressing cells (Robinson et al., 1997; Xu et al., 1999). EphA4/EphB receptors are expressed in r3 and r5, while ephrin-B2 is expressed in r2, r4 and r6. Additionally, CNC cells from r2, r4 and r6 migrate into the second, third and forth

branchial arches, respectively. They are restricted to these segmental paths via EphB/ephrin-B contact repulsive signalling, which restricts cell intermingling (Cooke et al., 2005; Cooke et al., 2001; Klein, R., 1999). A response can be mediated either uni-directionally through either Eph or ephrin expressing cell, or bi-directionally, where both Eph forward and ephrin reverse signalling occurs simultaneously through each cell (Cooke et al., 2002; Mellitzer et al., 1999).

The recognition of guidance factors expressed by DPSC has not been examined in detail. Thus far the Semaphorin family of secretary guidance molecules and the Eph RTK family have been identified during tooth development. Radioactive *in situ* hybridisation demonstrated that *EphA2-A4* and *EphA7*, *ephrin-A1-A5* were differentially expressed at varying stages during tooth development, including the epithelial thickening, folding, the cuspal area of the dental papilla, during blood vessel and alveolar bone formation, odontogenesis and during trigeminal axon pathfinding (Luukko et al., 2004). However, protein expression patterns or EphA/ephrin-A function was not determined in those studies. The B subclass have not been investigated during tooth development or in the adult, however personal communication with Dr. Gronthos revealed that after probing a cDNA microarray filter (Shi et al., 2001) with cDNA probes generated from total RNA derived from adult DPSC, EphB1, EphB2 and ephrin-B3 were identified (Fig. 3.1). However, no further characterisation or functional studies were conducted in relation to these molecules.

Whilst there appears to be an important role for Eph/ephrin interactions in regulating developmental processes, little is known about their role in tissue maintenance and repair in postnatal tissues. Eph/ephrin interactions are important for stem cell proliferation and migration and are fundamental for correct neural crest cell migration. Therefore, the expression pattern of the B-subclass Eph/ephrin molecules on DPSC was elucidated, to provide insight into the functional role in DPSC niche maintenance.

3.2 Results

3.2.1 *In vitro* expression

3.2.1.1 B subclass expression by adult human DPSC and within the pulp tissue

Luukko and colleagues were the first to study the expression of *EphA/ephrin-A* mRNA transcripts in teeth, in a mouse model (Luukko et al., 2004). However, there are no publications to date investigating the B-subclass Eph/ephrin molecules in teeth. Since EphB/ephrin-B molecules are important during CNC cells migration and localisation (Smith et al., 1997), the gene/protein expression and distribution pattern of the B-subclass Eph/ephrin molecules was investigated in DPSC.

cDNA microarray studies conducted by Gronthos and colleagues (Shi et al., 2001) indicated that *EphB1*, *EphB2* and *ephrin-B3* (Dr. Gronthos, unpublished observations) were expressed at the gene level at varying intensities by adult human DPSC (Fig. 3.1). Subsequent confirmative real time RT-PCR analysis indicated that the heterogeneous population of human DPSC expressed all *EphB* receptors and *ephrin-B* ligands, although at varying levels (Fig. 3.2). The results indicated that *EphB6* and *EphB4* were the most abundantly expressed receptors, as indicated by the lowest cycle threshold value, followed by *EphB2* and *EphB1*, whereas *EphB3* was the lowest expressed receptor. The mRNA expression of the ligands was lower than the receptors; *ephrin-B2* was the highest expressed ligand, followed by *ephrin-B1*, while *ephrin-B3* indicated the lowest mRNA expression of all the genes investigated.

Figure 3.1 Detection of *EphB/ephrin-B* genes by human adult ex vivo cultured DPSC using a cDNA microarray filter

The level of *EphB/ephrin-B* gene expression is represented as a percentage of hybridization intensity of DPSC cDNA to the microarray filter from 3 individual donors (n = 3) (Shi et al., 2001), error bars = SEM.

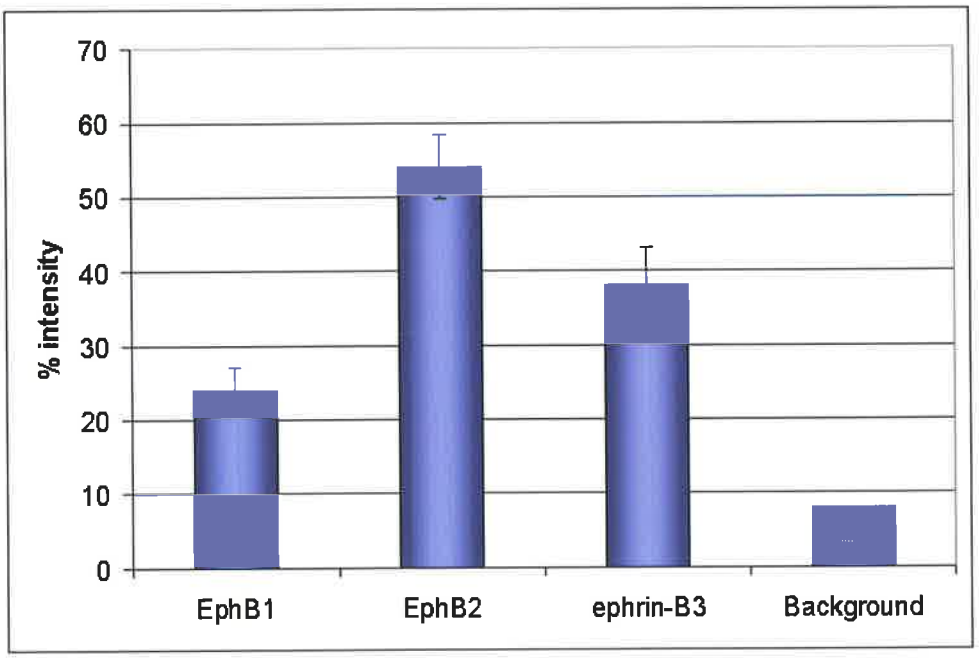
70
60
50
40
30
20
10
0
% intensity
EphB1
EphB2
ephrin-B3
Background

Figure 3.2 Gene expression of B-subclass Eph receptors and ephrin ligands on cultured DPSC.

Real time RT-PCR analysis of all *EphB* and *ephrin-B* transcripts in total RNA derived from *ex vivo* expanded DPSC (a). The graph represents the cycle threshold value during the exponential phase of replication, where the lower threshold value indicated higher mRNA expression; *TATA Binding Protein* (*TBP*) was used as a positive control. In order of highest to lowest mRNA expression by human DPSC: *EphB6*, *EphB4*, *EphB2*, *EphB1*, *ephrin-B2*, *ephrin-B1*, *EphB3* and *ephrin-B3* (error bars = SEM, n = 2 donors, 4 replicates per donor). Raw data of real time PCR of the Eph receptors (b) and ephrin ligands (c), indicating their linear range and cycle threshold values.

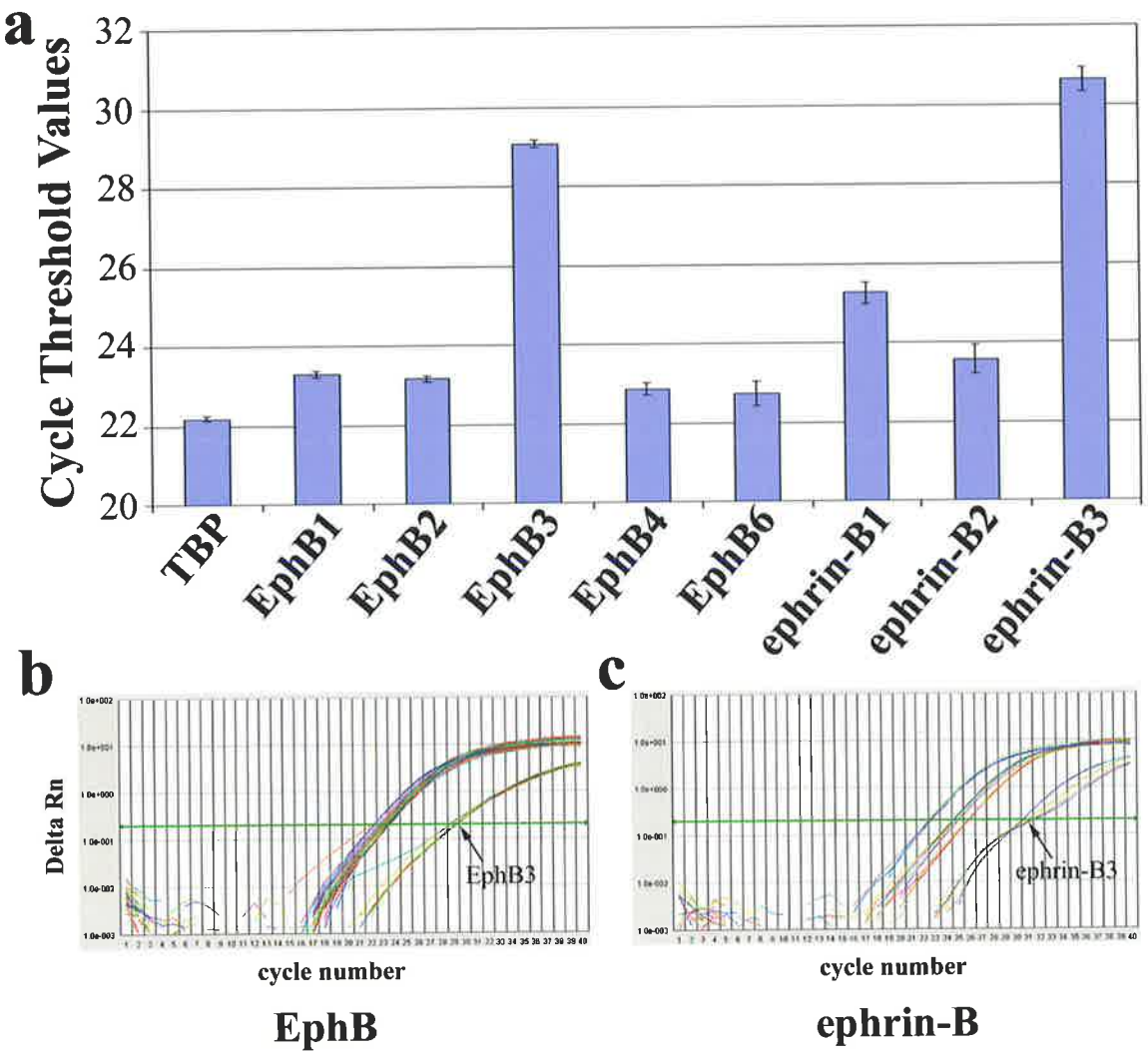
a
Cycle Threshold Values
32
30
28
26
24
22
20
TBP
EphB1
EphB2
EphB3
EphB4
EphB6
ephrin-B1
ephrin-B2
ephrin-B3
b
Delta Rn
EphB3
cycle number
EphB
c
ephrin-B3
cycle number
ephrin-B

To further develop our understanding of the distribution of the B-subclass Eph RTK family within the DPSC population *in vitro* and *in vivo*, protein expression was investigated. Immunocytochemistry was performed on cultured DPSC using commercially available anti-EphB1, B2 and B4 and anti-ephrin-B1, -B2 and -B3 antibodies (Fig. 3.3a-f). Two receptors, EphB3 and EphB6 were not investigated further in this study due to low mRNA expression and lack of kinase activity (Gurniak et al., 1996), respectively. No staining was observed in samples incubated with the corresponding rabbit or goat negative control immunoglobulins (Fig. 3.3h-i). The cellular expression patterns indicated that EphB4 (Fig. 3.3c-c') and ephrin-B1 (Fig. 3.3d-d') were most strongly expressed at the leading edge of the cell surface and on the extending protrusions (refer to arrows). Similar cellular staining patterns were observed for EphB1 and EphB2 (Fig. 3.3a-b'), albeit at lower levels. However, ephrin-B3 (Fig. 3. 3f-f') was differentially expressed within the population depending on the cellular density, with a greater proportion of cells expressing high levels of ephrin-B3 (19%) in semi-confluent cultures than in confluent cultures (8%). In contrast, ephrin-B2 (Fig. 3.3e-e') appeared to be expressed at the lowest levels irrespective of the cell density, which was contrary to the mRNA expression levels and may suggest post-translational modification for protein expression in the cell.

It has been observed that there is a strong perinuclear staining pattern within the stem cells *in vitro* which has not been reported previously. The only reference to such staining patterns has been by Varelias et al., (2002) and Pasquale (personal communication) where a similar staining pattern was found in tumour cells. The implications of this may relate to a link between stem cell biology and oncogenesis, which has recently been raised (Baker et al., 2007).

3.2.1.2 EphB/ephrin-B interaction in vitro

To investigate the possible role that the Eph/ephrin molecules may play in DPSC and within the tooth, it was important to determine what Eph/ephrin interactions maybe taking place. Due to the specific membrane localisation of the EphB/ephrin-B molecules, a more detailed investigation of the B-subclass was undertaken. Cultured DPSC were co-stained with an EphB and ephrin-B antibody to decipher whether the same or different cells expressed EphB/ephrin-B molecules, and to determine whether the cells were responding to the interaction in cis or trans. However, EphB4/ephrin-B interaction was unable to be

investigated, since all ephrin-B antibodies were raised in rabbit, included an anti-EphB4 antibody. As observed previously (Fig 3.3), ephrin-B1 expression was more prominent than either EphB1 (Fig 3.4a) or EphB2 (Fig 3.4b), although EphB1 was consistently at the leading edge of the cell, with some co-localisation with ephrin-B1 on the same cell (Fig 3.4a). It appeared that the co-localisation was at the cell junction. Alternatively, expression of EphB1 and ephrin-B1 was visualised separately on neighbouring cells (data not shown). While the overlapping expression between EphB2 and ephrin-B1 was moderate, punctate staining at the

Figure 3.3 Protein expression of EphB/ephrin-B molecules by adult cultured DPSC.

Representative images of EphB (a-c) receptors and ephrin-B (d-f) ligands stained with anti-rabbit or goat-Alexa488 and counterstained with TRITC-phalloidin, which binds to the F-actin, outlining the morphology of the cell. Arrows indicate the punctate staining of EphB1, B2, B4 and ephrin-B1 at the leading edge of the cell (a-d) arrowhead indicates the lack of ephrin-B3 staining by a sub-population of DPSC (f). Control staining no primary antibody (g), Rabbit IgG (h), control for Eph/ephrin antibodies raised in rabbit, Goat IgG (i), control for Eph/ephrin antibodies raised in goat, Alexa 488 secondary antibody was used to visualise any staining, TRITC-phalloidin was used to indicate the morphology of the cell. DAPI (blue) was used to identify the nucleus. Scale Bar = 20 μm.

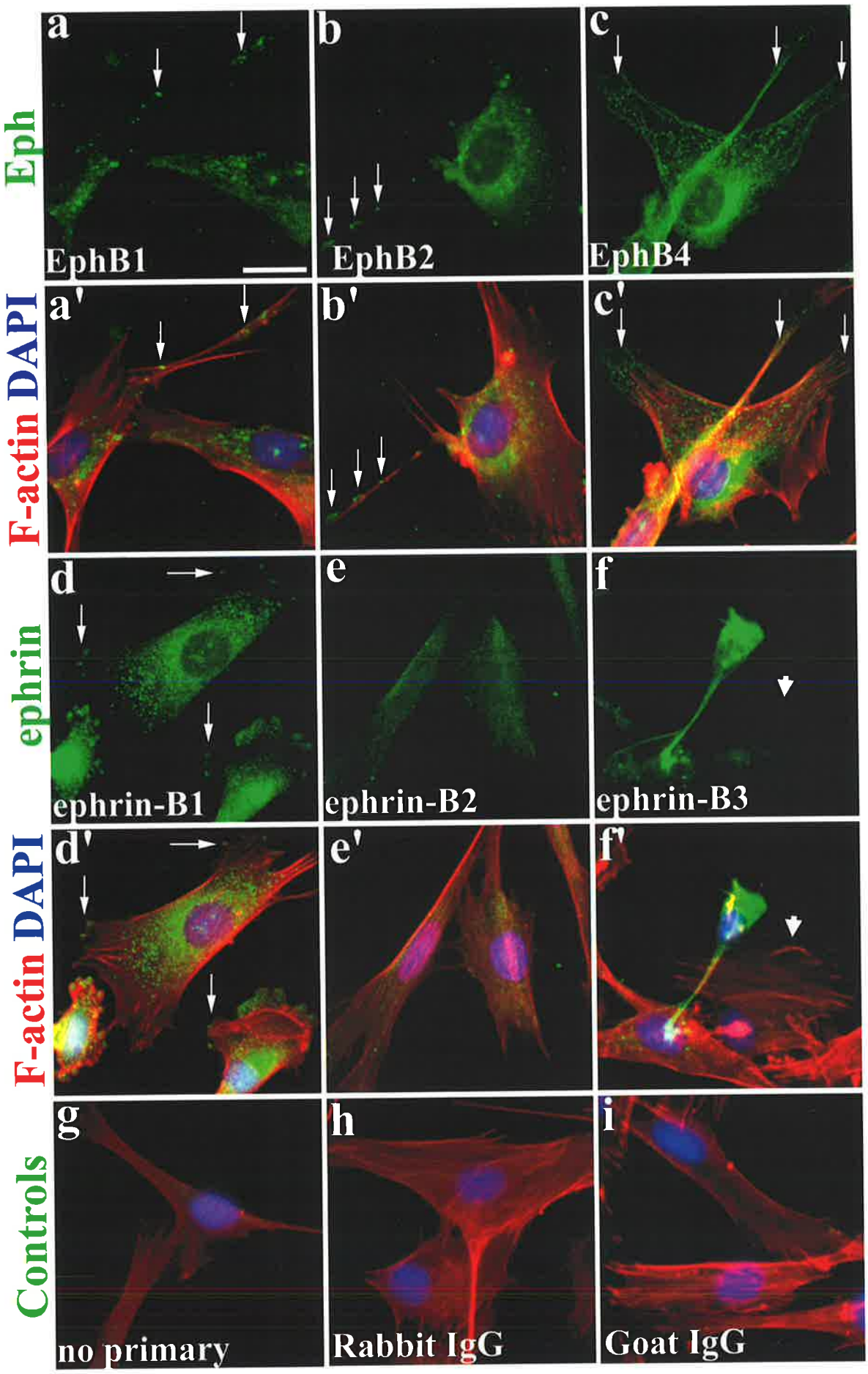
Eph
F-actin DAPI
ephrin
F-actin DAPI
Controls
a
b
c
EphB1
EphB2
EphB4
a'
b'
c'
d
e
f
ephrin-B1
ephrin-B2
ephrin-B3
d'
e'
f'
g
h
i
no primary
Rabbit IgG
Goat IgG

Figure 3.4 EphB/ephrin-B interactions within cultured DPSC.

EphB1 (a) or EphB2 (b-d, green) were counterstained with ephrin-B (red) ligands to decipher interacting partners within the DPSC population. EphB1/ephrin-B1 co-localised predominantly at cell junctions (a, arrows). Arrows indicate the punctate staining of EphB2 and ephrin-B1 on adjacent areas within the same cell (b), with low level of co-localisation at the cell junction (arrow head). EphB2/ephrin-B2 interaction was minimal, with diffuse staining of EphB2 within the cytoplasm of ephrin-B2 expressing cells (c). Strong punctate staining of EphB2 was detected at the leading edge of the cells at what appeared to be a cell junction, interacting with ephrin-B3 (d, arrows). Scale bar = 20 μm.

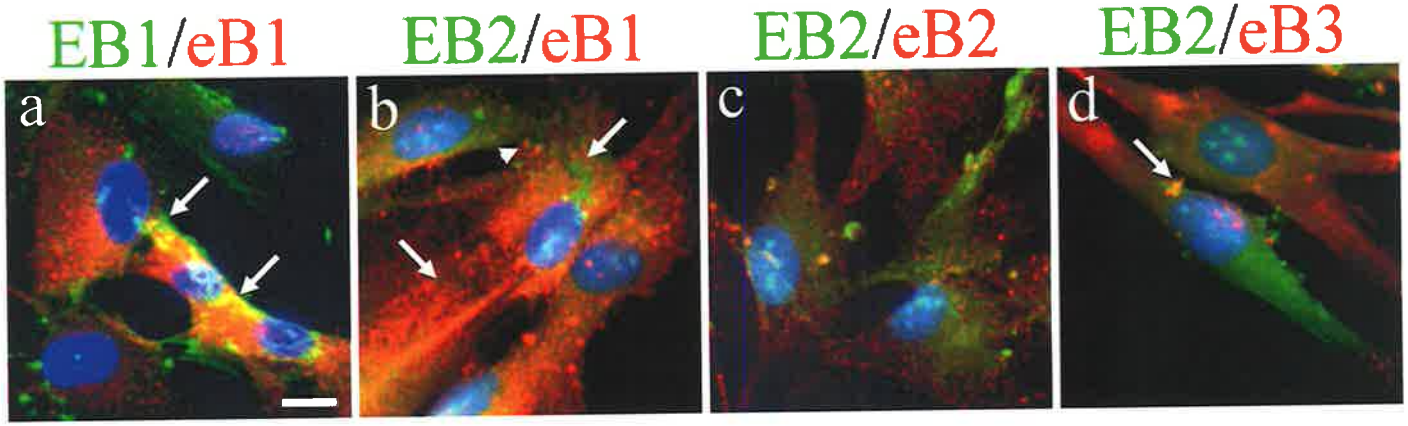
EB1/eB1
EB2/eB1
EB2/eB2
EB2/eB3
a
b
c
d

Figure 3.5 EphB/ephrin-B molecules were expressed by STRO-1 positive DPSC at varying levels as detected with FACS analysis.

EphB4 (18%), ephrin-B1 (13.1%) and ephrin-B2 (2.1%) were expressed by STRO-1 positive DPSC within the cultured population compared to the negative control.

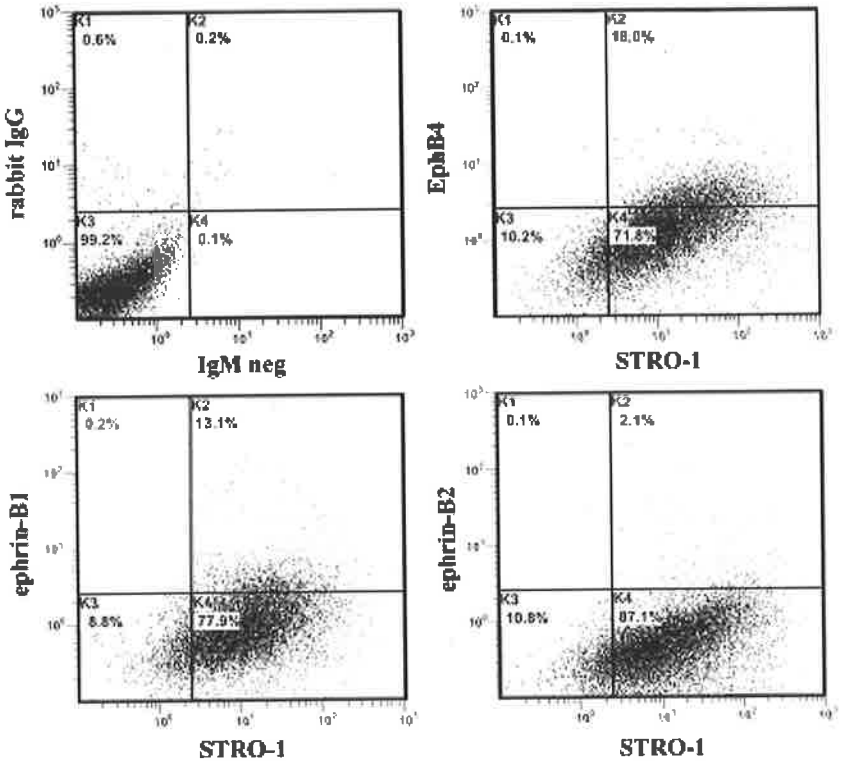
rabbit IgG
IgM neg
K1
0.6%
K2
0.2%
K3
99.2%
K4
0.1%
EphB4
STRO-1
K1
0.1%
K2
18.0%
K3
10.2%
K4
71.8%
ephrin-B1
STRO-1
K1
0.2%
K2
13.1%
K3
8.8%
K4
77.9%
ephrin-B2
STRO-1
K1
0.1%
K2
2.1%
K3
10.8%
K4
87.1%

leading edge of the cell was visualised with minimal co-localisation between EphB2 and ephrin-B1 (Fig 3.4b). Although EphB2 staining was considerably diffuse throughout the cell body, clusters at the leading edge were observed. However these did not seem to co-localise with ephrin-B2 (Fig 3.4c). Clusters of ephrin-B2 were observed throughout the cell, surrounded by diffuse EphB2 staining. While there was minimal co-localisation between EphB2/ephrin-B2 within the heterogeneous DPSC population, the alternating pattern of EphB2/ephrin-B2 within the same cells suggests the cis mode of signalling. Immunocytochemical staining for ephrin-B3 and EphB2 demonstrated the previously observed punctate clusters of EphB2 at the interface of two cells, with limited co-localisation with ephrin-B3 (Fig 3.4d). It was consistently observed that, while the same cell expressed EphB2 and ephrin-B3, the proteins localised to opposite ends of the cell (Fig 3.4d).

3.2.1.4 Cultured STRO-1 positive DPSC express EphB/ephrin-B molecules

As the immunocytochemical analysis was conducted on the heterogeneous population of DPSC, flow cytometric analysis was implemented to determine the proportion of EphB/ephrin-B molecules expressed by cells expressing the mesenchymal stem cell marker, STRO-1. Specifically, EphB4, ephrin-B1 and ephrin-B2 were investigated due to their involvement in CNC migration (Smith et al., 1997) and their expression pattern on cultured DPSC. EphB4 (Fig. 3.5b) and ephrin-B1 (Fig. 3.5c) were predominantly expressed by STRO-1 positive DPSC (18% and 13%, respectively), while only 2.1% of STRO-1 positive DPSC expressed ephrin-B2 (Fig. 3.5d). Consistent with the immuncytochemical analysis, the flow cytometric data suggested that a subset of STRO-1 positive cells were also positive for EphB4, ephrin-B1 and ephrin-B2. These results suggest that EphB/ephrin-B proteins are expressed by STRO-1 positive DPSC *in vitro*.

3.2.2 DPSC and the surrounding pulp tissue differentially express EphB/ephrin-B molecules.

Following the *in vitro* analysis we investigated the *in vivo* distribution of the EphB/ephrin-B molecules within the pulp tissue, to determine whether these receptors and/or ligands co-expressed with the mesenchymal stem cell/perivascular markers STRO-1 and CD146. Previous studies have demonstrated that STRO-1 positive DPSC reside in a perivascular niche within adult human dental pulp tissue (Shi et al., 2003). *In situ* immunohistochemical staining of frozen human dental pulp sections (Fig. 3.6) revealed that EphB1, ephrin-B1 and ephrin-B3 were strongly expressed by cells of the mature odontoblast layer and pulp fibroblasts, surrounding STRO-1 positive perivascular cells around blood vessels within the pulp tissue (Fig. 3.6). EphB2, EphB4, and ephrin-B2 were expressed predominantly on STRO-1 positive vascular cells (Fig. 3.6b, c, e), away from the differentiated odontoblast layer. More specifically, EphB4 and ephrin-B2 were present on vascular structures, as demonstrated by dual-colour co-staining with CD146 antigen (Fig. 3.6g, h). EphB4 appeared as punctate staining throughout the whole cell surrounded by either STRO-1 or CD146 staining. Similarly, punctate staining of ephrin-B2 was visualised within the perivasculature, localising with STRO-1 expressing cells along the outer perimeter of the blood vessel wall, with CD146 at the inner edge of the blood vessel wall lined with endothelial cells. The differential class B Eph/ephrin expression patterns observed within pulp tissue suggests that Eph/ephrin interactions may be involved in maintaining the STRO-1 positive DPSC within their perivascular niche possibly through a similar mechanism to CNC cell compartmentalisation (Cooke et al., 2002; Cooke et al., 2001; Mellitzer et al., 1999; Xu et al., 1999).

Figure 3.6 EphB/ephrin-B molecules are expressed in adult human third molar pulp tissue.

Human third molar pulp tissue, 5 μM frozen sections were co-stained with B-subclass Eph receptor or ephrin ligand (red), and mesenchymal stem cell marker, STRO-1 (green) (a-f) or perivascular marker, CD146 (green) (g-h). EphB1 (a), EphB2 (b), EphB4 (c) and ephrin-B2 (e) co-localised with STRO-1, while EphB1(a) in addition to ephrin-B1 (d) and ephrin-B3 (f) were strongly expressed by the surrounding fibrous pulp tissue (arrows). EphB4 (g) and ephrin-B2 (h) were also identified in the peri-vasculature. Scale Bar = 20 μm.

Eph/ephrin STRO-1
a
EphB1
b
EphB2
c
EphB4
d
ephrin-B1
e
ephrin-B2
f
ephrin-B3
Eph/ephrin CD146
g
EphB4
h
ephrin-B2

3.3 Discussion

The *in vitro* and *in vivo* expression data indicated that the class B Eph RTK family members were present on DPSC and within the pulp tissue, with the exception of ephrin-B2. The protein expression appears to be down regulated in culture, while staining of pulp tissue suggested that ephrin-B2 was expressed at relatively high levels. EphB4 and ephrin-B2 localized with perivascular markers in this study in accord with previous reports describing that EphB4/ephrin-B2 are required during angiogenesis or vasculogenesis throughout embryonic development and tumour growth (Adams et al., 2001; Bruhl et al., 2004; Noren et al., 2004a; Wang et al., 1998). The cytoplasmic domain of ephrin-B2 is required for correct vascular morphogenesis (Adams et al., 2001), while EphB4 stimulates endothelial cell proliferation and survival (Noren et al., 2004a; Steinle et al., 2003). The interaction between ephrin-B2 and EphB4 within the DPSC perivascular niche may signal bi-directionally to localise or prevent the movement of DPSC from the perivascular niche under steady state conditions. Subsequent interruptions to EphB4/ephrin-B2 signalling, brought about by damage to the pulp or dentin tissues, may lead to recruitment of odontoblast precursor cells towards the sites of injury.

The level of *EphB/ephrin-B* mRNA expression and the protein expression of numerous B-subclass Eph/ephrin molecules on *ex vivo* expanded DPSC was demonstrated. Intriguingly, the *in vivo* protein expression analysis suggests that the EphB expressing DPSC may be restricted to their niche through interaction with their cognate ephrin-B ligands expressed by the surrounding tissue. Eph/ephrin interactions primarily mediate a repulsive inhibitory response that can signal uni-or bi-directionally and result in repulsion, limiting cell intermingling and consequently compartmentalisation, or in the case of CNC cells, boundary formation (Xu et al., 1995; Xu et al., 1999).

EphB1, EphB2, EphB4 and ephrin-B1-B3 are required for boundary formation of the hindbrain and compartmentalisation of neural crest cells (Cooke et al., 2001; Smith et al., 1997; Xu et al., 1999; Xu et al., 2000). It has clearly been demonstrated that the predominant interacting partner for EphB4 is ephrin-B2 (Gale et al., 2001; Zhang et al., 2001), while EphB2/ephrin-B2 interaction is essential for correct trunk neural crest cell migration (Wang et al., 1997). Furthermore, ephrin-B1 is necessary for correct neural crest migration (Santiago et

al., 2002) acting through both forward and reverse signalling (Davy et al., 2004). Additionally, ephrin-B3 with the most restricted pattern of expression of the ephrin-B ligands is still required for correct neural crest migration (Gale et al., 1996a).

It was of interest in this study to determine the probable EphB/ephrin-B interactions of DPSC and the surrounding environment to provide an indication of a potential functional role of these molecules within the tooth. Our observations suggest that there is a complex mode of interaction between Eph receptor and ligand possibly acting cell autonomously (*cis*) and/or non-autonomously (*trans*) depending on the localisation, in addition to forward and/or bi-directional signalling. Interestingly, while there was minimal co-localisation of EphB2/ephrin-B3 at cell junctions, it appeared that EphB2/ephrin-B3 localised to opposite ends of the same cell. From this observation it could be postulated that either EphB2 or ephrin-B3 could be involved in directional movement or anchorage of DPSC, depending on whether the signal was mediated through the EphB2 or ephrin-B3 expressing region of the cell. In addition, limited co-localisation was observed between EphB2/ephrin-B2, thus it appears likely that the majority of EphB/ephrin-B communication requires ephrin-B1.

The staining pattern of EphB2/ephrin-B1 was consistent with the observations of Mellitzer and colleagues, where EphB and ephrin-B molecules were restricted to separate compartments (Mellitzer et al., 1999). While it is not clear at this stage whether DPSC are undergoing uni-or bi-directional signalling, it has been suggested that Eph/ephrin interaction restricts cellular intermingling through bi-directional signalling; and communication between adjoining cells via uni-directional, either forward or reverse signalling, through gap junctions (Mellitzer et al., 1999; Xu et al., 2000).

There was a strong co-localisation detected between EphB1/ephrin-B1 at what appeared to be gap junctions. Overlapping expression within the same cell was also observed, which suggests that EphB1/ephrin-B1 could be interacting in *cis*. Although there are no publications definitively demonstrating the *cis* interaction of EphB/ephrin-B molecules, it has been proposed that small lung cancer carcinomas co-express a number of B-subclass receptors and ligands and could act in an autocrine manner (Tang et al., 1999). While the *cis* interaction appears ambiguous, the co-localisation of EphB1/ephrin-B1 at cell junctions would be of *trans* interaction and was of interest, as it may provide insight into the possible interactions *in*

vivo. The above-mentioned observations suggest that the major interacting patterns *in vitro* are either EphB1 or EphB2 and ephrin-B1.

It was identified that ephrin-B1 was predominantly expressed *in vivo* by the surrounding pulp fibroblast like cells, with minimal co-localisation with the STRO-1 positive DPSC. However RT-PCR analysis, immunocytochemical staining and flow cytometric analysis all suggested that ephrin-B1 was expressed by a minor proportion (18%) of STRO-1 positive DPSC in culture. While ephrin-B1 expression was dominant on the pulp fibroblasts, the expression within the perivasculature may also be essential for the maintenance of DPSC within their niche. There is evidence to suggest that the environment surrounding a SC niche is important for stem cell fate decisions, while the microenvironment within the niche is thought to be important for self-renewal and maintenance of SC (Harada et al., 2004; Nishimura et al., 2002; Watt et al., 2000).

In summary, ephrin-B1 and -B3 were primarily expressed by the pulp tissue encapsulating the DPSC niche, and may act in a similar manner to CNC restricted intermingling (Cooke et al., 2001; Mellitzer et al., 1999; Robinson et al., 1997; Smith et al., 1997; Xu et al., 1999) acting to limit interaction of DPSC with the surrounding environment. Recently, there has been a strong emphasis on determining the properties of stem cells "niches" including the specific cues required to maintain those niches, determining stem cell quiescence, proliferation, future differentiation and mobilisation of stem cells/progenitors from the niche (Larsson et al., 2006; Niemann, C., 2006; Ohlstein et al., 2004). From the distribution pattern of EphB/ephrin-B proteins within the pulp tissue and the interaction between receptor and ligand observed *in vitro*, it is proposed that the B subclass Eph RTK family may be involved in maintaining the DPSC niche and required for DPSC decision-making processes such as SC maintenance, migration, and proliferation following a change in the environment, for example following injury or disease.

Chapter 4 - Eph/ephrin-B molecules maintain DPSC within their niche under normal conditions, and mediate DPSC migration following dentine/pulpal injury.

4.1 Introduction

It has been established that DPSC can regenerate a dentine-pulp-like complex composed of mineralised matrix with tubules lined with odontoblasts and fibrous tissue containing blood vessels, similar to the arrangement of the dentine-pulp complex found *in vivo* (Batouli et al., 2003; Gronthos et al., 2002; Gronthos et al., 2000). Blood vessels or more specifically the perivaculature within the pulp consists of pericytes that express smooth muscle actin. It has been demonstrated that DPSC co-localise with pericyte markers within the pulp and display smooth muscle pericyte like properties (Alliot-Licht et al., 2001; Gronthos et al., 2000). These observations suggest that DPSC reside within the perivascular niche of pulp tissue (Shi et al., 2003). More recently it has been shown that following pulp or dentin injury, BrdU positive cells, proliferate and migrate from the vasculature towards the injury site within a 4-week period (Tecles et al., 2005). These studies proposed that the BrdU positive cells may be migrating DPSC, recruited by environmental cues to facilitate tooth repair.

These findings raise several questions concerning the processes of dental tissue homeostasis and repair. Firstly, little is known about the mechanisms involved in maintaining DPSC within their niche under steady-state conditions. Secondly, which factors are critical in stimulating the growth and proliferation of DPSC. Thirdly, which guidance factors promote the migration of DPSC following injury. Guidance molecules are categorised into four groups, chemo- and contact-attractant molecules and chemo- and contact-repellent molecules, the Eph family of RTK predominantly fall into the contact-repulsive guidance molecule category (Tessier-Lavigne et al., 1996). It is well established that Eph and ephrin molecules are involved in cellular adhesion (Davy et al., 2000; Lawrenson et al., 2002) and consequently guidance during cell migration (Bruhl et al., 2004; Davy et al., 2000; Lawrenson et al., 2002; Santiago et al., 2002; Zimmer et al., 2003). The Eph/ephrin expression data within the tooth, the response of neural crest cells during compartmentalisation, boundary formation and

migration, and more recently the role of these molecules in proliferation of NSC; suggests that the Eph family of RTK could be required for similar processes during tooth repair.

The functional role of EphB/ephrin-B molecules on DPSC attachment and spreading was investigated in this study. A number of techniques were established or modified to investigate the restriction of DPSC to their niche, as well as examining the role of these molecules in DPSC migration and proliferation under normal conditions. More specifically an adhesion/spreading assay was developed (Fig. 4.1) as an attempt to mimic the *in vivo* microenvironment by plating EphB-Fc or ephrin-B-Fc molecules and binding them to the surface of the well. These fusion molecules encompass the extracellular globular region of the Eph or ephrin bound to the Fc portion of an IgG molecule. The globular region of the Eph or ephrin interacts with its reciprocal ligand or receptor, respectively, expressed by the cell to mediate a response as a model of the *in vivo* microenvironment. Upon plating into the culture wells, DPSC settled to the bottom of the well where they interacted with the EphB or ephrin-B molecules. This assay assessed the attachment, morphology and spreading of DPSC in response to EphB/ephrin-B-Fc molecules, while a transwell migration assay demonstrated the migration capacity of DPSC in response to ephrin-B molecules. These assays provided an insight into the role of EphB/ephrin-B molecule contribution to DPSC niche maintenance under normal conditions and their potential role following tooth injury.

4.2 Results

4.2.1 EphB/ephrin-B interactions inhibit DPSC attachment, spreading and migration in culture

4.2.1.1 EphB-ephrin-B interactions impair DPSC spreading in vitro.

The differential protein expression data of various EphB/ephrin-B molecules within dental pulp tissue lead to investigating the functional role of these molecules by DPSC, to determine whether Eph RTK family members contribute to maintaining DPSC niches by restricting the movement and communication of DPSC to their niche. A cell attachment and spreading assay (Fig. 4.1) was employed, which utilised Eph-Fc or ephrin-Fc molecules tethered to the surface of the well in order to determine whether EphB/ephrin-B interactions inhibit DPSC spreading and migration. Eph/ephrin-Fc molecules are able to physically interact with their reciprocal ephrin ligand or Eph receptor, respectively expressed by DPSC. EphB2-Fc and ephrin-B1-Fc were predominantly used in the assay as these molecules interact with a majority of the other B-subclass receptors and ligands (Pasquale, B., 2004) to help account for the promiscuous interactions between B class Eph and ephrins. Additionally, the immunohistochemical staining within the pulp tissue demonstrated that EphB2 was predominantly expressed by DPSC within their niche, while ephrin-B1 was highly expressed on the surrounding fibrous pulp tissue. EphA3-Fc and ephrin-A5-Fc were also utilised in the spreading assay to compare the functional response of DPSC to A versus B-subclass Eph/ephrin molecules.

The spreading assay demonstrated that there were no obvious changes in cellular morphology with increasing concentrations (1, 5, 10 μg/mL) of Human-IgG-Fc using the DPSC donor, NHT 6-99 (Fig. 4.2). In parallel experiments the morphology of DPSC substantially changed with increasing doses of either EphB2-Fc or ephrin-B1-Fc (Fig. 4.2). At 10 μg/mL the cells appeared smaller and rounder and displayed tight rings of actin at the edge of the cell, reminiscent of blebbing (Lawrenson et al., 2002). The blebbing was not attributed to cell death, as demonstrated by staining with the early cell death marker Annexin-V (Fig. 4.3). To determine whether this phenomenon was specific to the B class Eph/ephrin family, similar studies were performed with EphA3-Fc or ephrin-A5-Fc previously found to be expressed by

DPSC *in vitro* (Fig. 4.4). However, these studies showed that the cellular morphology of DPSC did not appear to differ dramatically in response to increasing concentrations of either EphA3-Fc or ephrin-A5-Fc, as demonstrated for the B-subclass molecules.

To confirm that the change in morphology was a general phenomenon of DPSC and not peculiar to one donor, the spreading assay was repeated at 10 μg/mL Human IgG, EphB2 and ephrin-B1-Fc, using DPSC derived from three independent donors (Fig. 4.5). These studies confirmed that DPSC exhibited a significantly rounder and smaller (almost half the size) morphology, when exposed to either EphB2-Fc (Student t-test, $p<0.04$ and $p<0.005$, respectively) or ephrin-B1-Fc (Student t-test, $p<0.04$ and $p<0.01$, respectively), when compared to the Human-IgG-Fc controls (Fig. 4.5j and k). In addition, their actin was no longer splayed with extending filopodia and lamellipodia, but rather displayed a blebbed morphology, as mentioned previously. Similar results were obtained in the presence of EphB4-Fc and ephrin-B3-Fc, however the response was not as uniform as observed with EphB2-Fc and ephrin-B1-Fc (Fig. 4.6).

Extracellular matrix (ECM) molecules, laminin and fibronectin are cell adhesion molecules, which are also classed as contact-dependent attractive molecules, are also expressed within the tooth (Sawada et al., 1998). To determine whether these ECM could influence the response of DPSC to Eph/ephrin molecules *in vivo*, EphB/ephrin-B containing wells were also coated with either laminin or fibronectin prior to adding the DPSC in the spreading assay. Even in the presence of laminin or fibronectin, DPSC rounded in response to EphB2-Fc and ephrin-B1-Fc in comparison to the Human-IgG-Fc controls, although, the response was not as pronounced (Fig. 4.7). Therefore, these findings confirmed that these ECM molecules do not alter the response of DPSC to EphB/ephrin-B molecules.

These data suggested that B-subclass receptors and ligands contributed to the attachment, adhesion and consequently spreading of DPSC *in vitro*. During this analysis fewer DPSC remained attached in the presence of EphB2-Fc or ephrin-B1-Fc, compared to Human-IgG-Fc in the absence of matrix molecules. The present study sought to determine whether DPSC were capable of spreading, retracting and subsequently losing their adhesion properties in response to bound –Fc, or whether they were restricted in the initial attachment and subsequent spreading process. Time lapse imaging indicated that the majority of DPSC remained rounded, only slightly extending and subsequently retracting their filopodia over the

3-hour duration when exposed to either 10μg/mL EphB2-Fc or ephrin-B1-Fc. (Fig. 4.8). Conversely, DPSC attached and spread substantially during the 3-hour incubation in the presence of Human-IgG-Fc. These findings indicated that the lack of attachment, adhesion and spreading was in response to either EphB2 or ephrin-B1 interaction with their reciprocal ligand or receptor expressed by DPSC and not the -Fc itself. Collectively, these results imply that B-subclass Eph/ephrin interactions may act to disrupt focal adhesions, which are essential for DPSC attachment and spreading.

4.2.1.2 EphB-ephrin-B interactions restrict the maturation of focal adhesions in cultured DPSC

To further investigate the underlying mechanisms of DPCS attachment in response to EphB/ephrin-B interactions, spreading assays were performed using two methods. Firstly, DPSC were pre-incubated with Calcein to fluorescently label the cells and cyclohexamide (CHX), to inhibit further formation of ECM proteins. DPSC adhesion was analysed using an enzyme-linked immunosorbent assay (ELIZA) plate reader that recognises fluorescence (picogreen) omitted by the lysed Calcein labelled DPSC. Secondly, the spreading assay was performed as previously described and DPSC co-immunostained for both vinculin and F-actin, to examine their distribution of focal adhesion complexes and cytoskeletal morphology, respectively.

The spreading assay conducted on CHX exposed DPSC with Calcein analysis, demonstrated that significantly fewer DPSC remained attached in the presence of 5μg/mL ephrin-B1-Fc (Student t-test, $p<0.05$), with a trend of decreased adhesion in the presence of 10μg/mL EphB2-Fc and ephrin-B1-Fc (data not shown). This data suggested that DPSC had lost their attachment properties in response to the B-subclass Eph receptor and ephrin ligand interactions. Additionally, without the influence of other ECM molecules, DPSC responded to ephrin-B1-Fc at a lower concentration, indicating that a greater response was mediated through forward EphB signalling than ephrin-B reverse signalling.

Furthermore, following the spreading assay, the distribution of vinculin on DPSC exposed to Human-IgG-Fc (Fig. 4.9a) appeared throughout and at the leading edge of the cells as

Figure 4.1 Schematic representation of the spreading/adhesion assay set up.

Cells were either pre-incubated with Calcein (fluorescent green dye that attaches to cell) or not pre-incubated. Pre-clustered Eph/ephrin-Fc or Human-Fc was plated onto the bottom of a tissue culture well. A single cell suspension of DPSC was added to each well and incubated for a 3-hour period. During this time the cells settled on the surface of the well and interacted with the –Fc. Three hours was sufficient for cells to settle, attach and spread. Following the 3-hour incubation, the growth media was removed from the wells and washed to remove any unbound cells. For the Calcein assay cells were lysed, which allowed for the release of the Calcein dye. The fluorescence was subsequently detected with an ELIZA plate reader. For the spreading assay, cells were fixed with 4% PFA and stained with TRITC-phalliodin, which binds F-actin, to observe the morphology of the cells. Images were taken in the center of each well for consistency. Images were analysed with software program, Scion image, for their size and morphological shape.

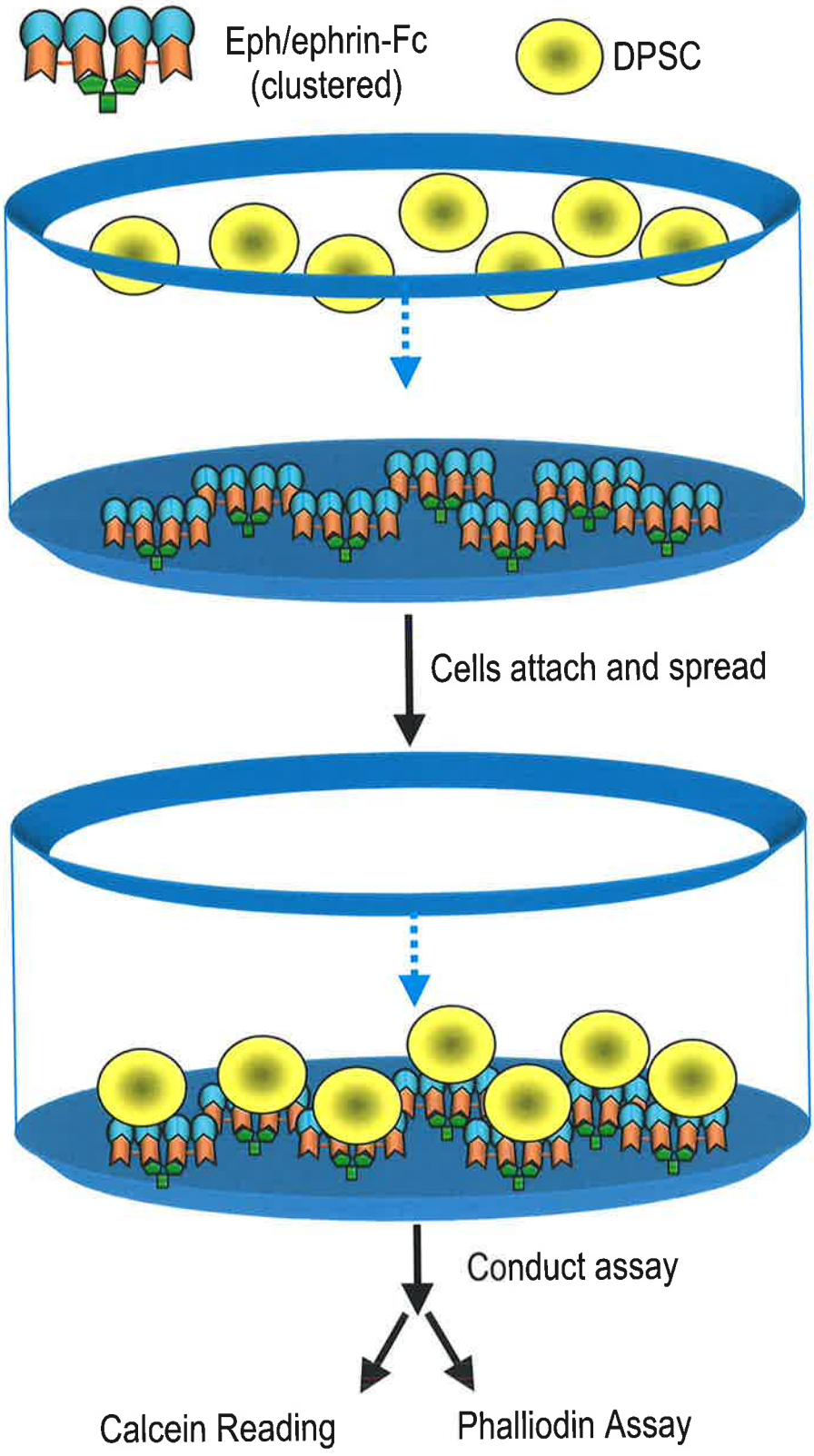
Eph/ephrin-Fc
(clustered)
DPSC
Cells attach and spread
Conduct assay
Calcein Reading
Phalliodin Assay

Figure 4.2 Cultured DPSC undergo rounding rather than spreading when exposed to EphB2-Fc or ephrin-B1-Fc in a dose-dependent manner.

DPSC from donor NHT 6-99 were exposed to 1, 5 or 10 μg/mL of surface bound Human-IgG-Fc (a-c), EphA3-Fc (d-f), ephrin-A5-Fc (g-i), EphB2-Fc (j-l) or ephrin-B1-Fc (m-o) for three hours, then stained with TRITC-phalliodin to observe F-actin distribution and cytoskeletal morphology. DPSC did not alter their morphology in response to any concentration of Human-IgG-Fc, although slight rounding of DPSC was observed with increasing concentrations of either EphA3-Fc or ephrin-A5-Fc. Cell rounding was visualised in response to 5μg/mL, with considerably more rounding at higher concentration of 10 μg/mL of either EphB2-Fc (f) or ephrin-B1-Fc (i), with complete loss of protrusions, where the F-actin appeared as a ring round the cell. Scale Bar = 20 μm.

1μg/ml
5μg/ml
10μg/ml
Human-Fc
EphA3-Fc
ephrin-A5-Fc
EphB2-Fc
ephrin-B1-Fc
a
b
c
d
e
f
g
h
i
j
k
l
m
n
o

Figure 4.3 Rounding and blebbing of DPSC in response to EphB2-Fc or ephrin-B1-Fc was not caused by cell death.

DPSC that underwent the spreading assay were stained with early cell death marker Annexin-V (green), images of cells were taken in bright field and overlaid with Annexin-V. Blebbed cells exposed to EphA3-Fc, ephrin-A5-Fc, EphB-Fc or ephrin-B-Fc were not Annexin-V positive. Scale bar = 20μm.

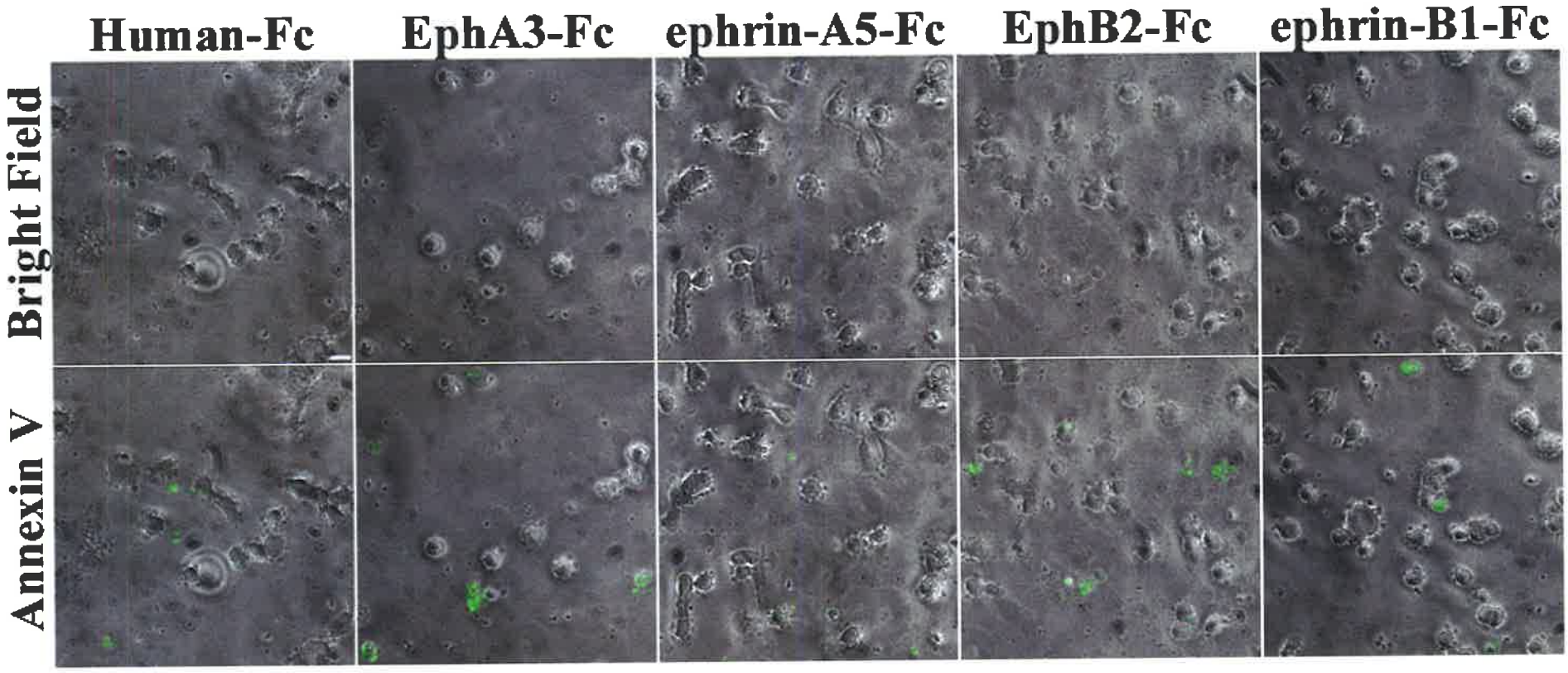
Human-Fc
EphA3-Fc
ephrin-A5-Fc
EphB2-Fc
ephrin-B1-Fc
Bright Field
Annexin V

Figure 4.4 Protein expression of EphA/ephrin-A molecules on DPSC

EphA/ephrin-A (green) molecules were counterstained with F-actin (red) to visualise the morphology of the cell. EphA3 (a-a') and EphA5 (b-b') were expressed throughout the cell, albeit lowly expressed at the leading edge of the cell. ephrin-A1 punctate staining was evident within the cytoplasm and at the leading edge of the cell (c-c'). ephrin-A2 protein expression was predominantly dispersed throughout the cell (d-d'). Negative controls rabbit IgG and goat IgG (green) were not detectable (e-f). Scale bar = 20μm.

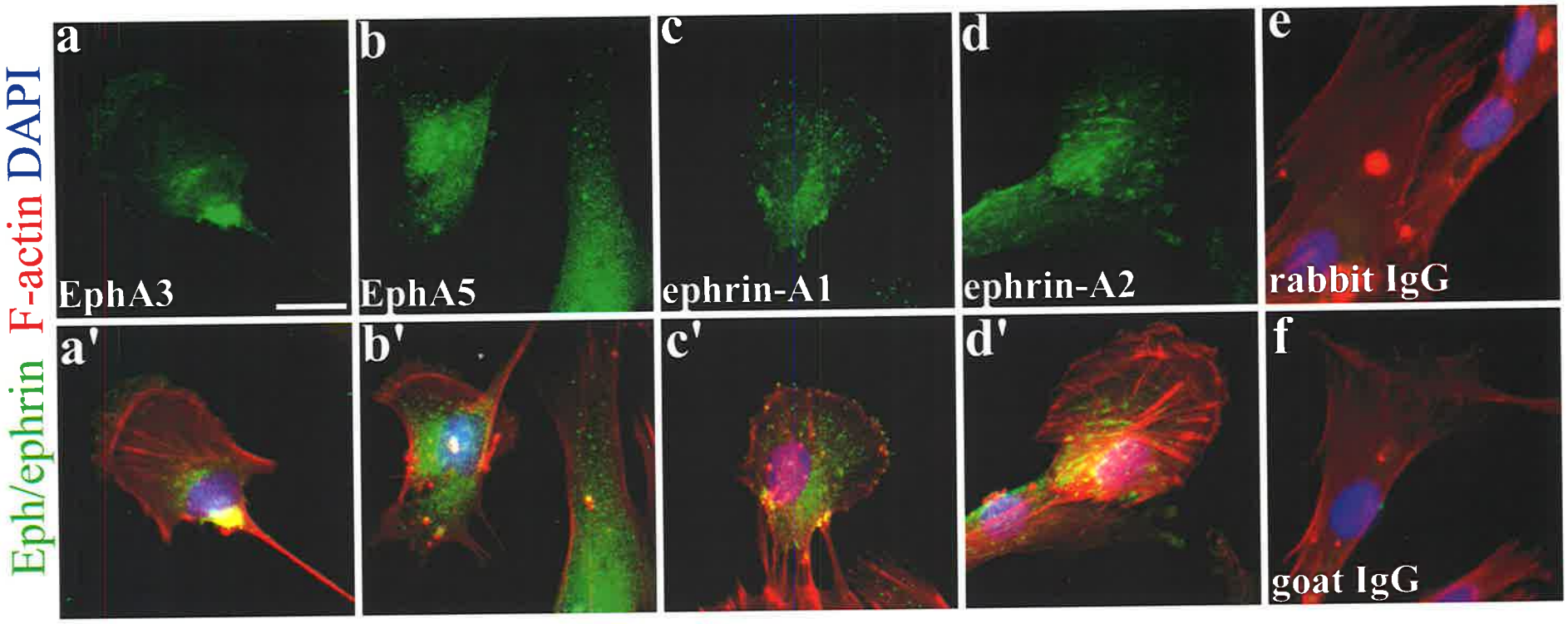
Eph/ephrin F-actin DAPI
a
EphA3
b
EphA5
c
ephrin-A1
d
ephrin-A2
e
rabbit IgG
a'
b'
c'
d'
f
goat IgG

Figure 4.5 Cultured DPSC were significantly rounder and smaller when exposed to EphB2-Fc or ephrin-B1-Fc.

A number of cell lines were investigated to determine the generality of the cell rounding phenomena in response to the B-subclass-Fc molecules. These DPSC underwent the spreading assay protocol and were stained with TRITC-phalloidin. NHT 6-99 (a, d, g), NHT 5-0 1 (b, e, h) and NHT 7-99 (c, f, i) demonstrated that DPSC from these cell lines rounded in response to 10 μg/mL EphB2-Fc (d-f) or ephrin-B1-Fc(g-i), but not Human-IgG-Fc (a-c). The roundness (j) and surface area (k) of DPSC from these three independent donors was analysed with Scion Image Software. In all three donors, DPSC were significantly rounder and smaller when exposed to EphB2-Fc or ephrin-B1-Fc compared to Human-IgG-Fc. Statistical analysis, Student t-test (* = $p < 0.04$, # = $p < 0.005$, ^ = $p < 0.01$). Scale Bar = 20 μm.

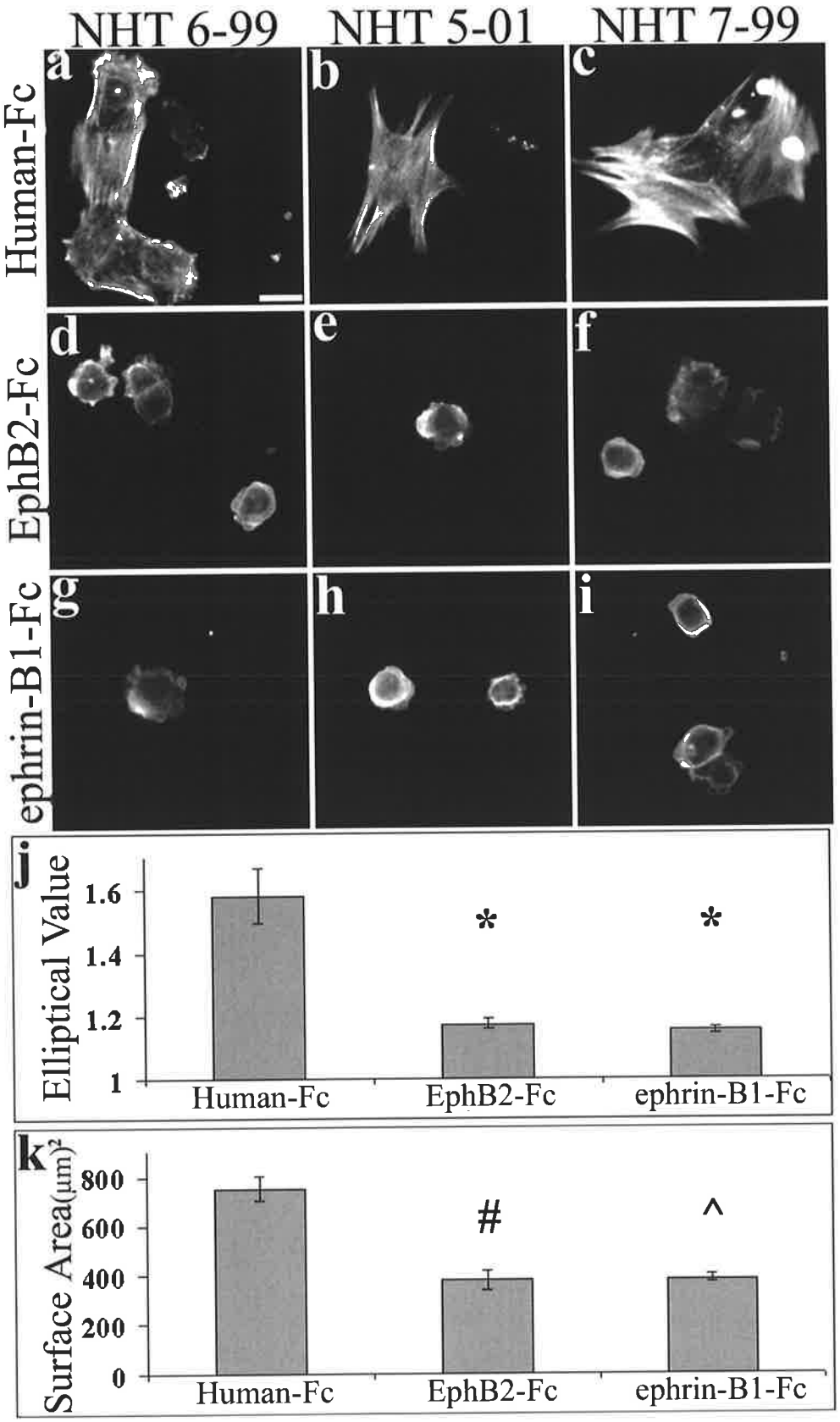
NHT 6-99
NHT 5-01
NHT 7-99
Human-Fc
EphB2-Fc
ephrin-B1-Fc
a
b
c
d
e
f
g
h
i
j
Elliptical Value
1.6
1.4
1.2
1
*
*
Human-Fc
EphB2-Fc
ephrin-B1-Fc
k
Surface Area(μm)²
800
600
400
200
0
#
^
Human-Fc
EphB2-Fc
ephrin-B1-Fc

Figure 4.6 DPSC rounded in response to increasing concentrations of ephrin-B3-Fc.

DPSC were exposed to increasing concentrations of 1, 5 and 10 μg/mL surface bound Human-Fc (a-c), EphB4-Fc (d-f) or ephrin-B3-Fc (g-i) for 3-hours. DPSC morphology did not vary substantially with increasing concentrations of Human-Fc (a-c), nor EphB4-Fc (d-f), although generally the cells were slightly rounder compared to Human-Fc. DPSC did round in response to increasing concentrations of ephrin-B3-Fc (g-i). Scale bar = 20μm.

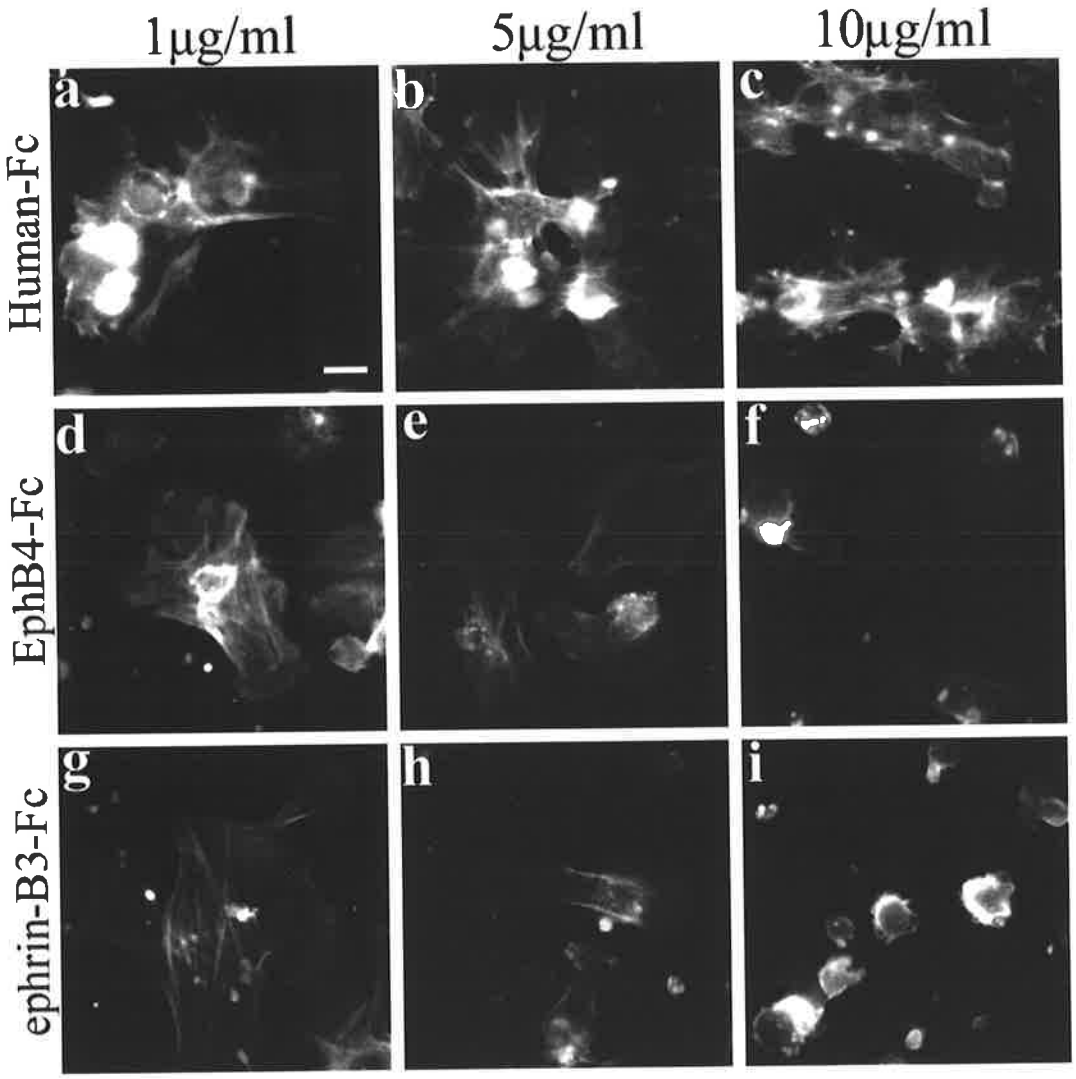
1μg/ml
5μg/ml
10μg/ml
Human-Fc
EphB4-Fc
ephrin-B3-Fc
a
b
c
d
e
f
g
h
i

Figure 4.7 The presence of ECM decreases DPSC rounding in response to EphB2-Fc or ephrin-B1-Fc.

ECM molecules laminin or fibronectin were plated on top of the –Fc molecules as a substrate that is permissive to cell spreading, bovine serum albumin (BSA) was used as a control substrate. Although DPSC exposed to Human-Fc in the presence or absence of ECM molecules appeared to have similar splayed morphology in all conditions (a-d), in the presence of laminin (a) or fibronectin (b), DPSC displayed more F-actin. The DPSC morphology appeared to be uniform when exposed to EphA3-Fc (e-h) or ephrin-A5-Fc (i-l) in the presence or absence of ECM molecules. However, in the presence of either EphB2-Fc (m-p) or ephrin-B1-Fc (q-t) DPSC rounding was reduced and more cells remained attached when exposed to laminin (m,q) or fibronectin (n,r), but not BSA (o,s) when compared to no substrate conditions (p,t). Scale bar = 50 μm.

Laminin
Fibronectin
BSA
Nothing
Human-Fc
EphA3-Fc
ephrin-A5-Fc
EphB2-Fc
ephrin-B1-Fc
a
b
c
d
e
f
g
h
i
j
k
l
m
n
o
p
q
r
s
t

Figure 4.8 Time-lapse video microscopy demonstrated that DPSC failed to spread when in contact with EphB2-Fc or ephrin-B1-Fc.

Representative still images at 1-hourly time points indicated that when DPSC were in contact with Human-IgG-Fc (a) they attached and spread their processes (arrowhead), connecting with surrounding cells. When DPSC were in contact with EphB2-Fc (b) or ephrin-B1-Fc (c), cells that attached were restricted in spreading their processes (arrowhead). Scale Bar = 20 μm.

ephrin-B1-Fc
EphB2-Fc
Human-Fc
c
b
a
0'
0'
0'
60'
60'
60'
120'
120'
120'
180'
180'
180'

diffuse staining, characteristic of normal attachment and spreading. In contrast, vinculin distribution appeared as circular patches, surrounded by rings of F-actin in the absence of ECM molecules following contact with EphB2-Fc (Fig. 4.9b) or ephrin-B1-Fc (Fig. 4.9c). A similar vinculin distribution was also observed when ECM molecules were present (data not shown). The aberrant dissemination of vinculin coincided with the appearance of spreading initiation centres (SIC), which are only present at early stages of cell spreading, as previously described by de Hogg and colleagues (Hoog et al., 2004). Three dimensional confocal imaging using z-serial analysis confirmed that F-actin distribution of DPSC exposed to EphB2-Fc (Fig. 4.9b') or ephrin-B1-Fc (Fig. 4.9c') formed ring structures surrounding vinculin (Fig. 4.9b"-c") or the SIC (Hoog et al., 2004) and was not actually part of the SIC itself.

The presence of early stage focal complexes and lack of mature focal adhesions correlated with the lack of spreading observed in the time-lapse studies (Fig 4.8), demonstrating that DPSC interacting with EphB2-Fc or ephrin-B1-Fc were severely restricted in their ability to attach and spread, while their counterparts interacting with Human-IgG-Fc demonstrated normal attachment and spreading. Thus the presence of either B-subclass Eph/ephrin molecules may act to restrict the maturation of focal adhesions required for cell spreading, where the immature state of the adhesion complex leads to reduced attachment, restricting cell spreading and migration and consequently the detachment of DPSC.

4.2.1.3 ephrin-B1 inhibits DPSC migration in vitro

To assess whether the Eph RTK family restricts DPSC migration under normal conditions, a Transwell migration assay was used. This well-established assay has been used previously to investigate endothelial cell migration in response to EphB/ephrin-B signalling (Steinle et al., 2003) and bone marrow derived MSC in response to SDF-1. DPSC plated in the top chamber were observed to migrate through the 8μm pore filter and adhere to the underside of the filter, in the presence of Human-IgG-Fc in the bottom chamber (Fig. 4.10 a, b). To confirm that the DPSC were responding appropriately during the migration assay, DPSC were incubated with known MSC chemo-attractive molecule, SDF-1. Pilot studies showed that DPSC expressing the SDF-1 receptor, CXCR4 (data not shown) appeared to increase their migration as a response to SDF-1 being present in the bottom chamber (Fig. 4.10 a,e). In parallel experiments, DPSC migration was significantly reduced (Student t-test, $p<0.0097$) in the

presence of ephrin-B1-Fc (Fig. 4.10 a, d). Interestingly, DPSC migration was not inhibited by EphB2-Fc (Fig 4.10 a,c), where this interaction was previously shown to inhibit DPSC attachment and spreading.

From these results it appears that both forward and reverse signalling are important for DPSC spreading and attachment, while forward signalling only was required for inhibiting DPSC migration, suggesting that the signalling response required for these processes must vary.

4.2.1.4 Signalling molecules that restrict cell attachment, spreading and migration

The Eph/ephrin family of RTK can activate a multitude of signalling pathways. To decipher which of these signalling pathways were responsible for the rounding and detachment of human adult DPSC in both forward and reverse Eph/ephrin signalling, inhibitors to specific signalling cascades were implemented. Inhibitors were added to the DPSC for 30 minutes prior to Eph or ephrin-Fc exposure. If a targeted signalling cascade was involved in rounding and detachment when activated by the Eph or ephrin, then the rounding and detachment response would be reversed in the presence of the specific signalling inhibitor.

When DPSC were incubated with MEK/ERK inhibitor U0126, which blocks the MAPK pathway, DPSC morphology reverted back to that of the control (fig. 4.11 a,c,d,f, Fig 4.12 a-d). Increasing doses of U0126 resulted in an increase in the attachment and spreading of human DPSC when in contact with ephrin-B1-Fc, with an optimal response occurring at a concentration of 10μM U0126 (data not shown). In contrast, neither P13 Kinase inhibitor LY294002 (Fig 4.11 a,c,j,l), nor Src family kinase inhibitor PP2 (Fig 4.11 a,c,g,i) influenced the attachment or spreading of human DPSC in response to ephrin-B1-Fc to the same extent as U0126. Although a few cells did spread slightly more in the presence of LY294002 compared with no inhibitor when in contact with ephrin-B1-Fc, this attachment and spreading was not pronounced. Whilst the restricted attachment and spreading of human DPSC was mainly mediated through MAPK pathway for Eph forward signalling, it was suggested that a combination of signalling pathways may be required to completely mediate this response.

Figure 4.9 Mature focal adhesion complexes do not form in DPSC when exposed to EphB2-Fc or ephrin-B1-Fc.

DPSC were treated with 10 μg/ml of Human-IgG-Fc (a), EphB2-Fc (b) or ephrin-B1-Fc (c). Cells were subsequently stained with TRITC-phalloidin (red) and anti-vinculin (green), indicating F-actin distribution and focal adhesion complexes, respectively. The same cell was visualised using confocal stacks of 1.5μm slices, demonstrating that vinculin remained as circular patches surrounded by F-actin when exposed to EphB2-Fc or ephrin-B1-Fc. Individual slices down through the cell (1.5μm, left to right) for (b'-c') F-actin and (b''-c'') vinculin distribution are illustrated. Scale Bar = 20 μm (a), 20 μm (b,c).

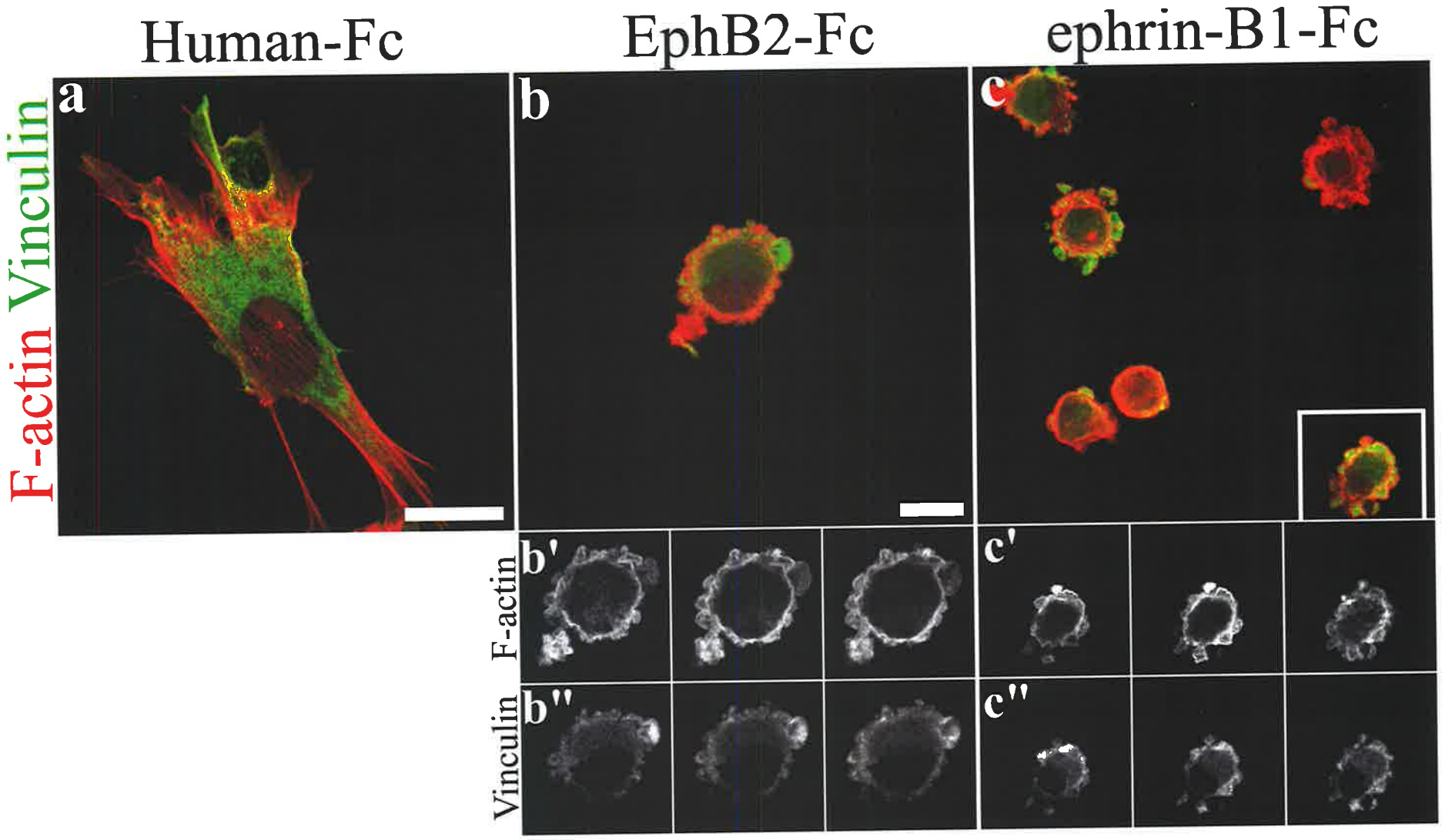
Human-Fc
EphB2-Fc
ephrin-B1-Fc
F-actin Vinculin
a
b
c
b'
c'
F-actin
b''
c''
Vinculin

Figure 4.10 EphB forward signaling inhibits DPSC migrating *in vitro*.

DPSC plated in the top chamber of a transwell migration assay that migrated through the 8μm pore membrane after 24hours to the bottom chamber were fixed, cells remaining in the top chamber removed and then stained with DAPI to visualise the nucleus. Images were taken in several random regions of the membrane and number of nuclei counted (a-d). The graph represents the average of 6 independent cell counts, 3 fields of view from duplicate membranes, error bars = SEM (a). DPSC exposed to 10μg/mL Human-Fc (a,b), and EphB2-Fc (a,c), significantly fewer cells migrated through the membrane in the presence of ephrin-B1-Fc ($p < 0.01$) (a,d), while relatively more DPSC migrated in response to chemokine SDF-1 (10ng/mL) (a,e).

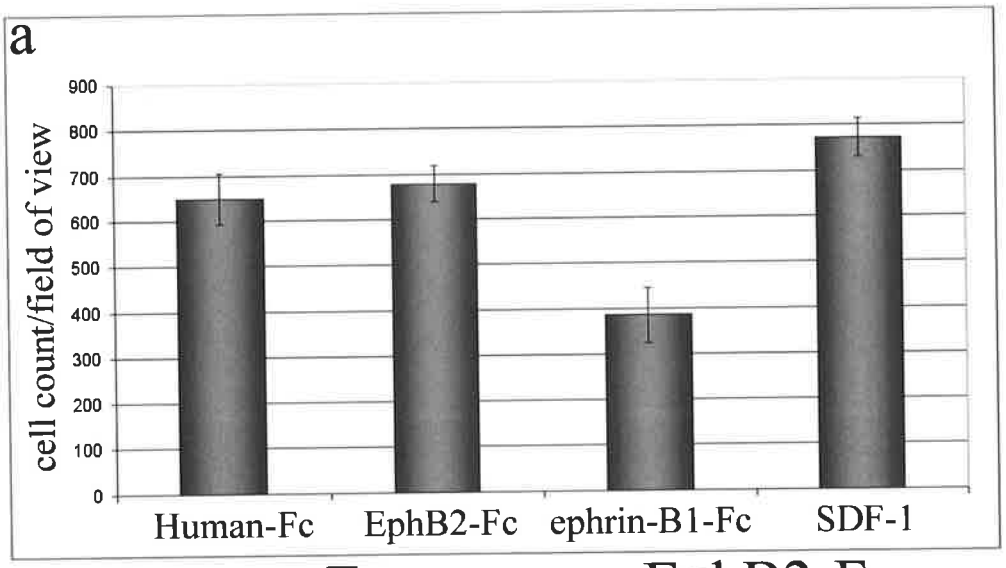

Human-Fc

EphB2-Fc

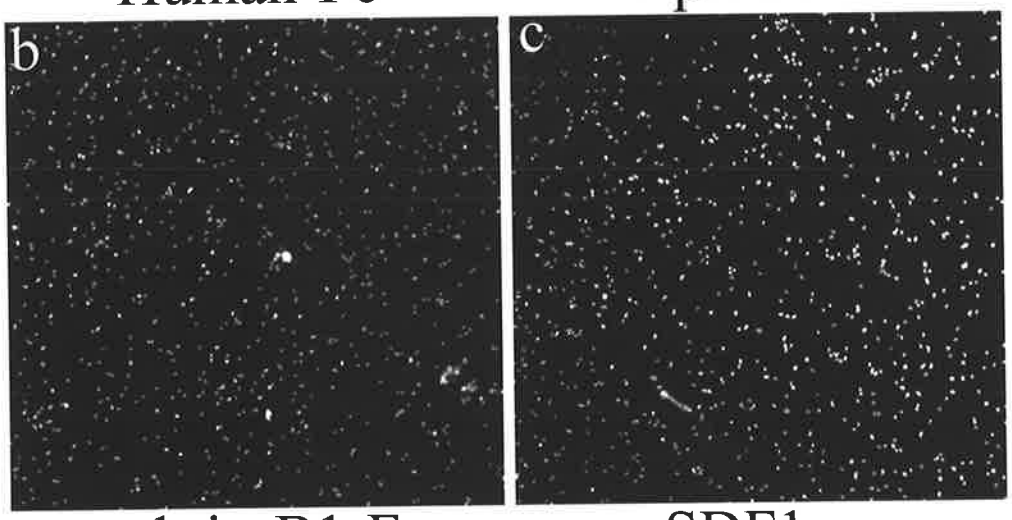

ephrin-B1-Fc

SDF1

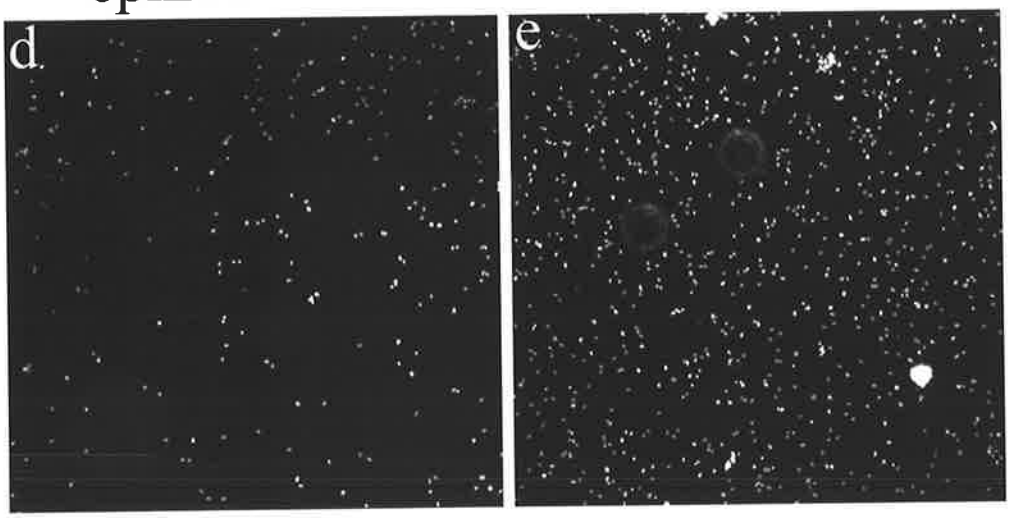

Figure 4.11 DPSC mediated their rounding response through specific signalling pathways.

The spreading assay was conducted with specific signalling pathway inhibitors U0126, which block the MEK/ERK pathway; PP2, which blocks SH2 phosphorylation when binding with tyrosine kinases, and LY294002 which blocks PI3 Kinase Eph forward signalling. DPSC pre-incubated with 0.1% DMSO when exposed to Human-Fc (a), EphB2-Fc (b) or ephrin-B1-Fc (c) did not change their morphology compared to previously conducted spreading assay. (d-f) DPSC pre-incubated with U0126 displayed normal morphology in response to Human-Fc (d), rounded cell morphology in response to EphB2-Fc (e), while reverting to splayed morphology in response to ephrin-B1-Fc (f), indicating that DPSC were no longer response to ephrin-B1. DPSC pre-incubated with PP2 displayed normal morphology in response to Human-Fc (g), rounded morphology in response to ephrin-B1-Fc (i), while more cells remained attached and spread in the presence of EphB2-Fc (h). There was very little difference in DPSC morphology compared to control samples when DPSC were pre-incubated with LY294002 (j-l). Scale bar = 20 μm.

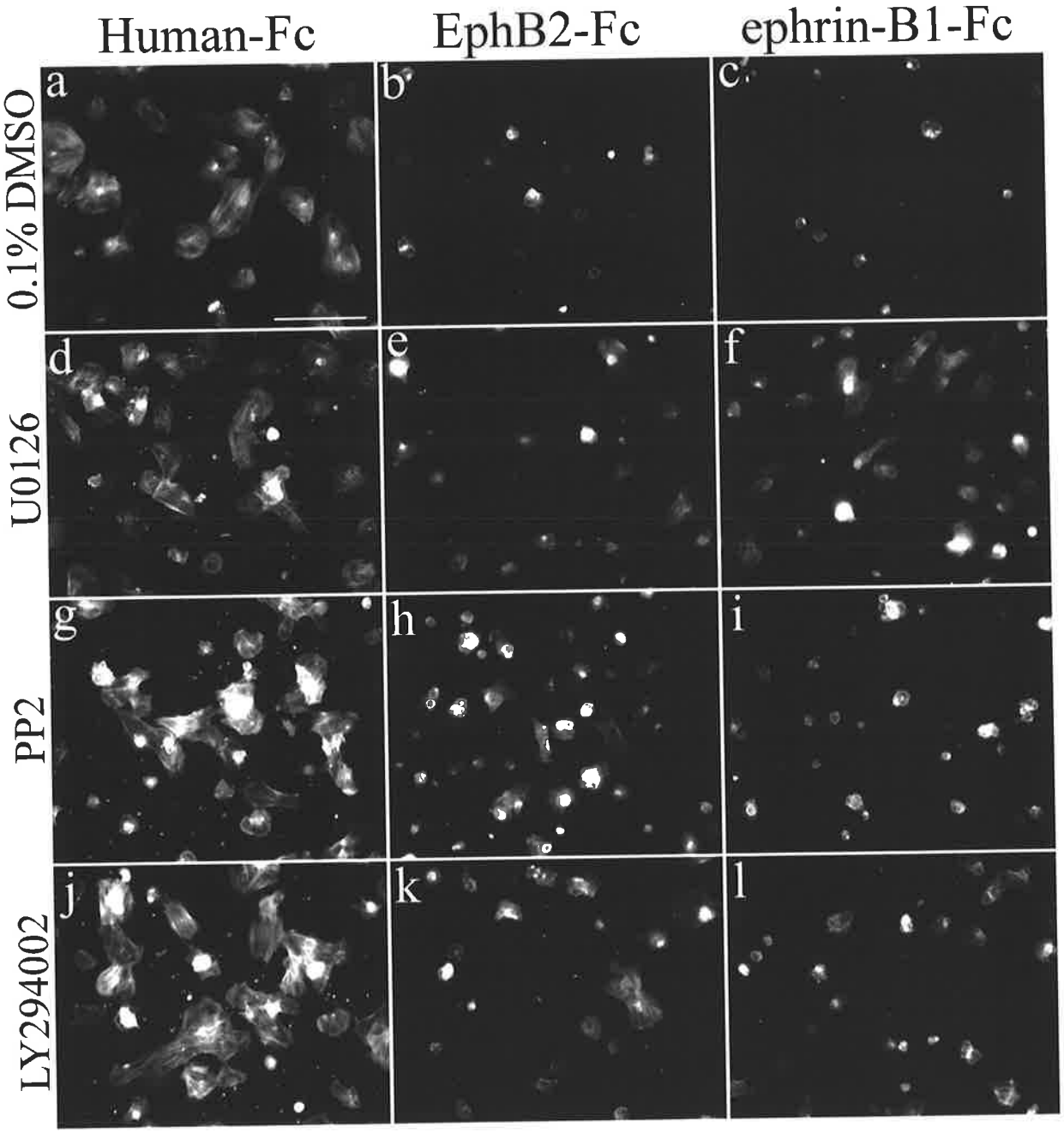
Human-Fc
EphB2-Fc
ephrin-B1-Fc
0.1% DMSO
U0126
PP2
LY294002
a
b
c
d
e
f
g
h
i
j
k
l

Figure 4.12 DPSC round and detach in response to EphB forward and ephrin-B reverse downstream signalling pathways.

EphB receptor predominantly mediated forward signalling through the MEK/ERK pathway (a-d). Representative images of cells pre-incubated with 0.1% DMSO in growth media did not change their previously observed morphology in response to either Human-Fc (a) or ephrin-B1-Fc (c). When DPSC were pre-incubated with U0126 and ephrin-B1-Fc (d), the cells no longer rounded and detached in response to the -Fc, instead displaying normal spreading morphology as observed with the Human-Fc (b). DPSC mediated ephrin-B reverse signalling in a phosphorylation dependent manner through the SH2 domains (e-h). Cells pre-incubated with 0.1% DMSO in growth media did not change their previously observed morphology in response to either Human-Fc (e) or EphB2-Fc (g). DPSC pre-incubated with PP2 did not round or detach in response to the EphB2-Fc (h), instead displaying a spread morphology as observed with the Human-Fc (f). Scale bar = 20 μm.

0.1% DMSO
U0126
0.1% DMSO
PP2
Human-Fc
ephrin-B1-Fc
Human-Fc
EphB2-Fc
a
b
c
d
e
f
g
h

Figure 4.13 ephrin-B1 interaction with EphB expressing DPSC inhibits their migration by signalling through the MAPK pathway.

DPSC were treated with either 0.1% DMSO or 10μM U0126 prior to their exposure to either 10μg/mL Human-Fc or ephrin-B1-Fc. The graph represents the average of 6 independent cell counts, 3 fields of view from duplicate membranes, error bars = SEM (a). DPSC exposed to Human-Fc migrated though the 8μm pore membrane (a,b), while DPSC in contact with ephrin-B1-Fc reduced their migration significantly compared to Human-Fc (Student t-test, $p < 0.00001$) (a, c). However, in the presence of MEK/ERK inhibitor U0126, DPSC were no longer responsive to ephrin-B1 interaction, significantly (Student t-test, $p < 0.0003$) increasing their migration through the membrane (a,d).

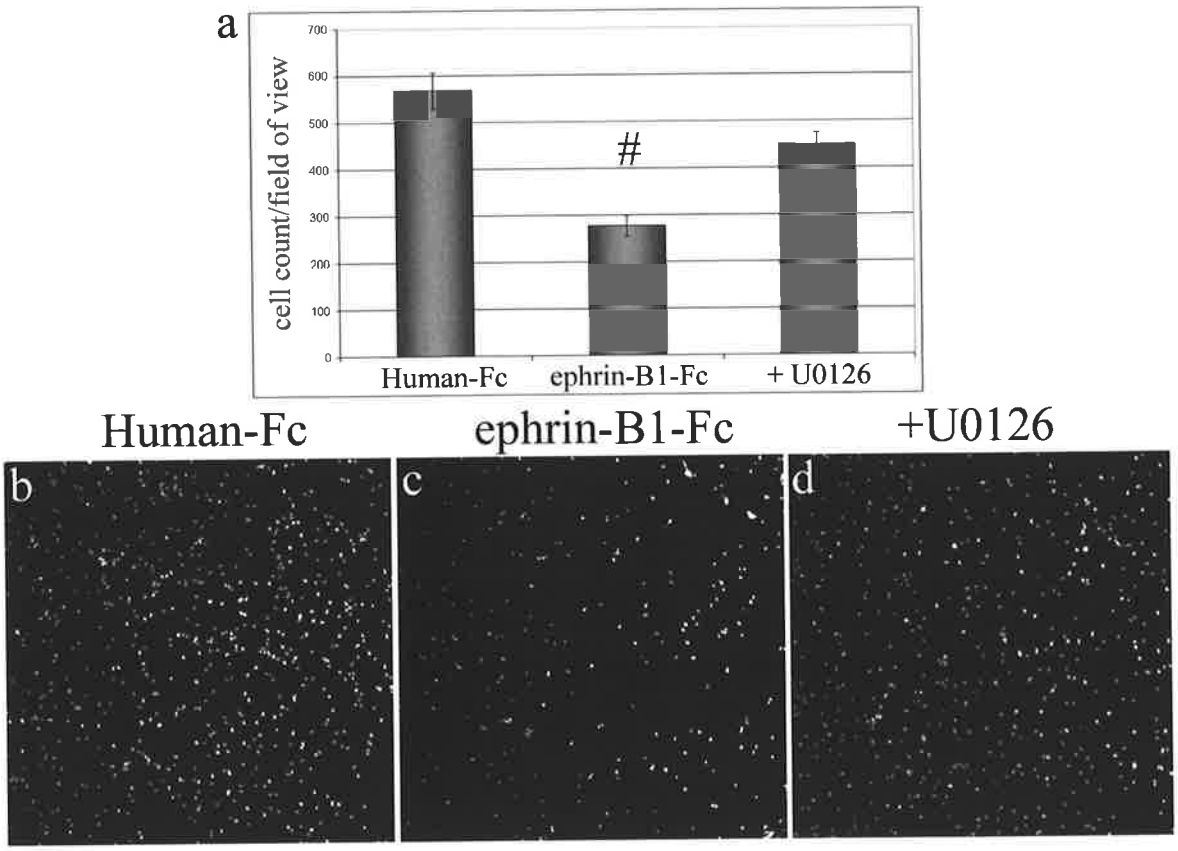
a
cell count/field of view
700
600
500
400
300
200
100
0
#
Human-Fc
ephrin-B1-Fc
+ U0126
Human-Fc
ephrin-B1-Fc
+U0126
b
c
d

Reverse ephrin signalling is mediated through either phosphorylation of Src family kinases, or via a phosphorylation independent pathway mediated by the ephrin PDZ domain (Kullander et al., 2002). Signalling through the phosphorylation dependent pathway was investigated using inhibitor, PP2 (4-amino-5-(4-chlorophenyl)-7-(*t*-butyl)pyrazolo[3,4-*d*]pyrimidine), which blocks phosphorylation of the Src family kinases. Src family kinases predominantly mediate their signalling through proteins containing Src homology (SH2) domains. A greater proportion of DPSC incubated with 10μM PP2 were found to undergo attachment and spreading on the EphB2-Fc coated surfaces over controls in the absence of PP2 (Fig. 4.11 a,b,g,h, Fig. 4.12 e-h). However, no change in DPSC morphology was observed in the presence of either U0126 (Fig 4.11 a,b,d,e) or LY294002 (Fig. 4.11 a,b,g,h) when in contact with EphB2-Fc. These data suggested that human DPSC rounding and detachment were mediated through an ephrin ligand instigated phosphorylation dependent ephrin-B reverse signalling pathway via an SH2 or SH3 containing protein or proteins.

Studies were conducted to examine the role of MAPK pathway during DPSC migration given the importance of forward Eph/ephrin signalling for DPSC spreading and attachment (Fig. 4.11). As previously shown, DPSC exposed to ephrin-B1-Fc significantly (Student t-test, $p<0.01$) reduced their migration (Fig 4.10 a,d, Fig 4.13). Forward signalling required the MAPK pathway (Fig 4.13 a,c), where significantly (Student t-test, $p<0.0003$) more DPSC migrated through the filter when pre-incubated with U0126 and in contact with ephrin-B1-Fc than when in contact with ephrin-B1-Fc alone. While the MAPK signalling pathway appeared to be the major signalling cascade involved in mediating the inhibitory response, the number of cells that were able to migrate through the membrane with U0126 was still less than in the presence of Human-IgG-Fc control, suggesting that there might be other signalling pathways involved during forward EphB signalling.

The findings of the adhesion, spreading and migration assays suggested that cell rounding and restricted movement due to B class Eph/ephrin interactions results in compartmentalising DPSC to their stem cell niche under normal steady-state conditions *in vivo*. However, teeth sometimes encounter injury or matrix degradation due to bacterial manifestation known as carries, which often results in a cellular response to try and repair the defect. It was proposed that under these conditions, DPSC are no longer restricted to their SC niches following interruption of B class Eph/ephrin interactions. However, this hypothesis has not been examined *in vivo* under steady-state or pathological conditions. While it has recently been

reported that putative DPSC undergo proliferation and mobilisation from their perivascular niche following injury (Tecles et al., 2005), the guidance cues required for their correct localisation to the injury site has not been investigated.

4.2.2 Down regulation of ephrin-B1 protein may be required for DPSC mobilisation following tooth injury

A number of molecules have been suggested to contribute to DPSC migration following injury including TGF, FGF, BMP and SDF-1 (Granjeiro et al., 2005; Harada et al., 2002a; Nakashima, M., 2005; Nie et al., 2006; Shimabukuro et al., 2005; Zhang et al., 2005). Eph RTK family of guidance molecules are required for correct migration of CNC cells. The findings of this study indicate that EphB/ephrin-B interactions restrict DPSC attachment, spreading and migration under normal steady-state conditions. Therefore, the role of Eph/ephrin molecules was further investigated following tooth injury.

4.2.2.1 ephrin-B1 gene expression decreases following pulpal injury

In the present study, EphB/ephrin-B gene expression levels were compared between normal and injured teeth. Paired normal unaffected, and damaged (carries affected) third molars were obtained from three individual donors undergoing normal extractions with informed consent. The pulp tissue from each tooth was removed and used to isolate total RNA. Following reverse transcription into cDNA, real time PCR was conducted comparing *EphB* and *ephrin-B* gene expression between paired normal and injured samples from each of the three donors. The average gene expression levels from the three comparisons showed no significant difference for *EphB1, EphB2* or *EphB4* expression between normal and injured pulp tissues (Fig. 4.14a). In contrast, a significant (Student t-test, $p < 0.012$) 1.8-fold decrease in *ephrin-B1* expression was observed in the paired injured teeth between all individuals in comparison to normal teeth (Fig. 4.14b). Although, *ephrin-B2* and *ephrin-B3* also appeared to be down regulated following injury, this difference was not found to be statistically significant.

In the previous Chapter, ephrin-B1 was shown to be strongly expressed on the pulp tissue surrounding DPSC within their perivascular niche, signifying that ephrin-B1 interaction with EphB expressing DPSC may restrict DPSC to their niche under steady-state conditions by

restricting DPSC attachment and spreading. The present study also support this notion where down regulation of ephrin-B1 may play an important role in DPSC mobilisation following injury.

4.2.3 Eph/ephrin involved in DPSC proliferation

The maintenance of quiescent stem cells or their proliferation when required, such as following mechanical or bacterial induced injury, is critical for the maintenance of stem cell niches (Harada et al., 2004; Larsson et al., 2006; Niemann, C., 2006; Ohlstein et al., 2004). Tecles et al., showed with their tooth injury model that DPSC proliferation increased following injury (Tecles et al., 2005). Recently it has been shown that EphB/ephrin-B molecules influence neural stem cell proliferation (Conover et al., 2000), while reverse signalling through EphA7/ephrin-A2 down-regulates proliferation in neural stem cell niches (Holmberg et al., 2005). Eph/ephrin molecules are also expressed by a number of other stem cell populations including epidermal, intestinal and hematopoietic (Batlle et al., 2002; Fuchs et al., 2004; Ivanova et al., 2002; Ramalho-Santos et al., 2002), suggesting that Eph/ephrin molecules may also influence DPSC quiescence or proliferation.

DPSC proliferation potential in response to EphB/ephrin-B interaction was first determined *in vitro*. DPSC were incubated for 4 days with 1, 5 and 10μg/mL of EphB1-Fc, EphB2-Fc, EphB4-Fc, ephrin-B1-Fc, ephrin-B2-Fc, ephrin-B3-Fc or Human-IgG-Fc, after which a WST-1 assay was used to identify viable cells by detecting the cleavage of tetrazolium salts from WST-1 to formazan. The absorbance of the colourimetric assay was measured with an ELIZA plate reader. There was no significant difference in the proliferation of DPSC in response to EphB2-Fc, EphB4-Fc, ephrin-B2-Fc or ephrin-B3-Fc at any concentration relative to Human-IgG-Fc (data not shown). In contrast, EphB1-Fc significantly enhanced DPSC proliferation at 5μg/mL (Student t-test, $p< 0.002$) and 10μg/mL (Student t-test, $p< 0.006$) relative to Human-Fc, at the corresponding concentration (data not shown). Increasing concentrations of ephrin-B1-Fc appeared to inhibit DPSC proliferation, although this was not significant compared to Human-IgG-Fc or between concentrations of ephrin-B1-Fc. These findings suggested that the expression of ephrin-B1 by pulp cells surrounding the stem cell niche may minimise DPSC proliferation under steady-state conditions. The interaction of

EphB expressing stem cells within the niches may possibly control stem cell quiescence and turn over under normal conditions.

Figure 4.14 *ephrin-B1* gene expression was significantly reduced following tooth injury.

Donors provided two molars, one normal and one damaged, the pulp was removed from the samples and mRNA was isolated. Real time PCR comparing *EphB* (a) *ephrin-B* (b) gene expression between normal and injured samples identified no significant difference in *EphB* gene expression, while a significant (Student t-test, $p < 0.012$) 1.8-fold decrease in *ephrin-B1* expression was observed following injury.

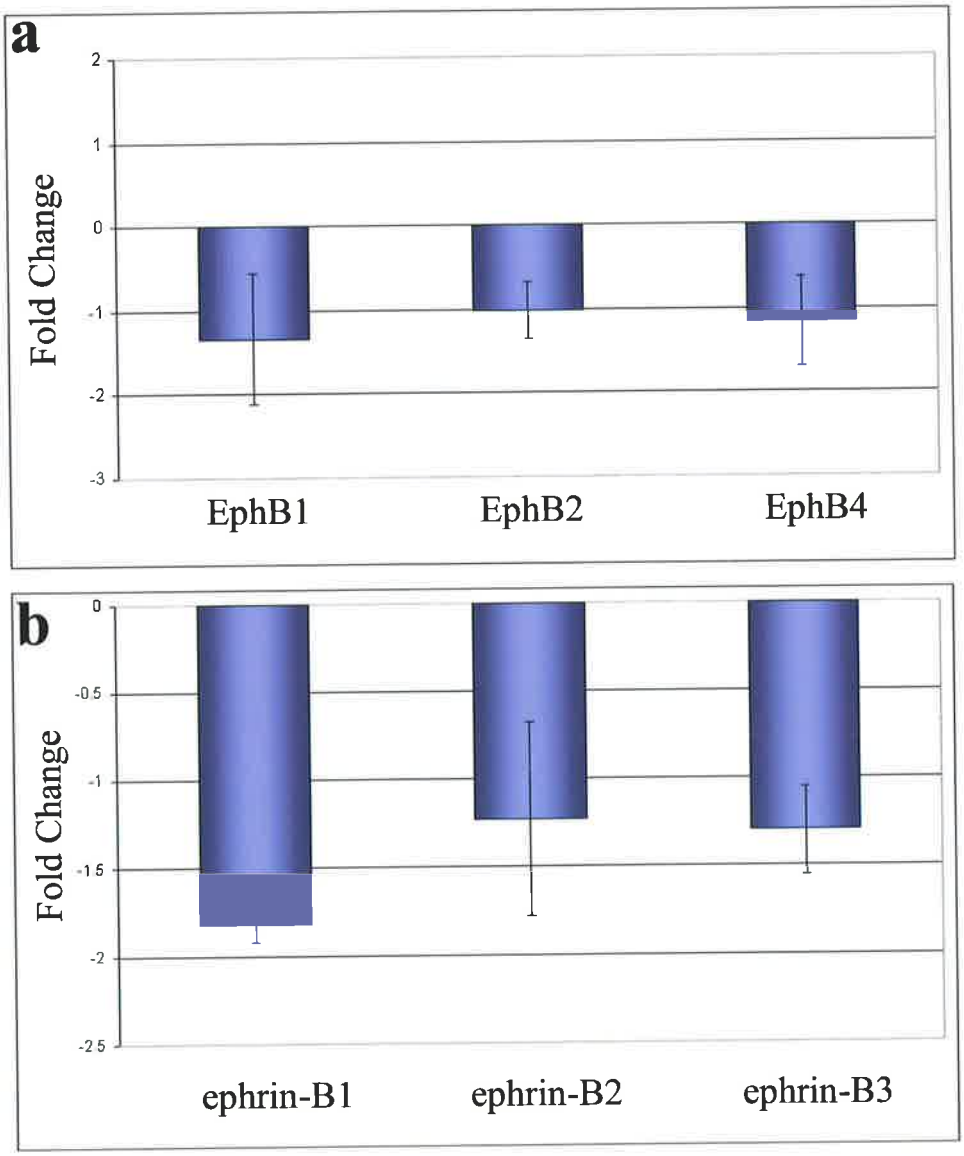
a
Fold Change
2
1
0
-1
-2
-3
EphB1
EphB2
EphB4
b
Fold Change
0
-0.5
-1
-1.5
-2
-2.5
ephrin-B1
ephrin-B2
ephrin-B3

4.3 Discussion

It has been clearly demonstrated that DPSC have the capacity to regenerate a dentine/pulp like structure in the absence or presence of endogenous environmental cues (Batouli et al., 2003; Gronthos et al., 2002; Gronthos et al., 2000). These findings suggest that this cell population may be a reservoir of odontogenic precursor cells required during tooth repair. Human DPSC have been identified to reside within perivascular sites of pulp tissue (Shi et al., 2003). More recently Tecles and colleagues demonstrated that BrdU positive, putative DSPC odontogenic precursors could be induced to migrate from their perivascular niche to the pulp or dentine injury site within 2-4 weeks (Tecles et al., 2005). The question still remained, how are DPSC mobilised following injury and what cues are responsible for initiating proliferation?

Previously, it has been shown that following spinal cord injury EphB/ephrin-B molecules initially down-regulate their expression while cells migrate and infiltrate the injury site and then up-regulate once migration has ceased (Bundesen et al., 2003). Furthermore, Eph/ephrin molecules of both subclasses have been implicated in stem cell proliferation responses (Conover et al., 2000; Holmberg et al., 2005; Holmberg et al., 2006). The findings of the present study indicate that ephrin-B1 may play an important role for DPSC niche maintenance under normal conditions and for allowing DPSC migration following injury (refer to the schematic in Fig. 4.15). Furthermore, this data suggests that increased concentrations of EphB1-Fc initiate proliferation, while increasing concentrations of ephrin-B1-Fc tended to reduce DPSC proliferation in culture. This implies that Eph-B1 positively regulates proliferation, while ephrin-B1 could negatively regulate proliferation; the latter proposal being inconsistent with that of Conover and colleagues (Conover et al., 2000). However, our data is consistent with the notion that ephrin-B1 maintains DPSC within their niche by limiting cell division under normal conditions. Alternatively, with decreased ephrin-B1 expression within the pulp tissue following injury, the negatively regulated proliferation response would also be reduced, thus inadvertently increasing DPSC proliferation and inducing migration. Therefore, it is important to decipher how these molecules could be utilised or manipulated to accelerate the repair processes, either through enhanced migration or proliferation of DPSC.

It was hypothesised that if the Eph/ephrin molecules were restricting DPSC to their niche, then DPSC would respond to Eph/ephrin molecules in a similar manner as other cell types

during boundary formation, restricting their intermingling between different cell populations by cell rounding. The spreading assay analysis and time-lapse imaging data suggested that DPSC were inhibited from spreading, remaining in a rounded state when in contact with either the EphB receptors or ephrin-B ligands. However, rather than losing focal adhesions, as previously shown during boundary formation, DPSC were limited in their ability to form mature focal adhesions. This is consistent with neural crest loss of focal adhesion complexes in response to 10 μg/mL ephrin-B1-Fc (Santiago et al., 2002), the same concentration used in the present study.

Importantly, our studies showed that while DPSC expressed various Eph/ephrin A subclass family molecules such as EphA3, EphA5, ephrin-A1 or ephrin-A2, no substantial change in DPSC morphology, attachment or spreading was observed using EphA3-Fc or ephrin-A5-Fc when compared to the control cultures treated with Human-IgG-Fc. Thus, the observed morphological and functional changes appeared to be mediated predominantly by B-subclass Eph/ephrin interactions. These findings are in agreement with previous reports describing how early migrating neural crest cells readily undergo rounding, when incubated with ephrin-B1-Fc (Santiago et al., 2002). In general, cells restrict their intermingling by losing focal adhesions, retracting their stress fibres and consequently round (Cowan et al., 2001).

Focal adhesion complexes comprise a multitude of proteins that together are essential for cell attachment/adhesion, spreading and migration (Gumbiner, M., 1996; Zamir et al., 2001). Vinculin, a major component of focal adhesion complexes specifically attaches the actin cytoskeleton (Huttelmaier et al., 1997) to various cell adhesion molecules/receptors (Zamir et al., 2001) associated with the process of cell adhesion, spreading and migration. Interestingly, vinculin distribution appeared as circular patches on DPSC exposed to EphB2-Fc or ephrin-B1-Fc, but not to the same extent with Human-IgG-Fc following the spreading assay. These circular patches appeared similar to the recently discovered SICs (Hoog et al., 2004), otherwise reported as dot-like adhesions (Zimerman et al., 2004), which are required for early stages of cell spreading, prior to the maturation of focal adhesions. In the present study, three-dimensional confocal microscopy imaging of double labelled F-actin and vinculin by DPSC treated with either EphB2-Fc or ephrin-B1-Fc revealed that the blebbing of actin was not caused by cell death, but the formation of actin ring structures possibly ensheathing vinculin expressing SICs. Time-lapse imaging further demonstrated that DPSC were inhibited from spreading on either EphB2-Fc or ephrin-B1-Fc, but not on Human-IgG-Fc.

Here DPSC continuously tried to extend their processes, but were retarded in doing so, inhibiting the maturation of focal adhesion complexes and thus the movement of DPSC.

The constant movement of the DPSC filopodia and lamellipodia in response to EphB/ephrin-B interaction suggested active signalling in both the EphB and ephrin-B expressing cells. These results demonstrated that DPSC signal bi-directionally through both the Eph and ephrin-expressing DPSC to restrict cell intermingling. Although it has not been directly shown that DPSC signal uni-directionally or bi-directional, Mellitzer and colleagues have reported that bi-directional and not uni-directional signalling is required for restricted cell intermingling (Mellitzer et al., 1999). Conversely, *in vitro* migration analysis suggested that DPSC mobilisation required uni-directional signalling, where only EphB expressing DPSC significantly reduced their ability to migrate in response to ephrin-B1-Fc. These finding are also consistent with our immunohistochemical observations of EphB's being expressed by DPSC within the putative DPSC perivascular niche, while the fibrous pulp tissue and odontoblast layer surrounding the niche predominantly expressed ephrin-Bs. Our data suggest that following injury to the dentine/pulp tissues, there is a down-regulation of *ephrin-B1* within the pulp tissue suggested a possible mechanism for regulating DPSC mobilisation. Hence it was proposed that the dynamic EphB/ephrin-B bi-directional signalling maintains DPSC within their niche, by limiting the intermingling with the surrounding environment and uni-directional signalling restricts DPSC movement. Had time permitted, the organ culture system developed by Tecles and colleagues would have been utilised to try and block BrdU positive DPSC mobilization in the presence of EphB/ephrin-B -Fc.

Previous studies have indicated that EphB expressing cells retract their processes and round through endocytosis (Zimmer et al., 2003), whereas rounding and detachment of ephrin-B expressing cells required tyrosine phosphorylation (Cowan et al., 2001). The present study indicated that restricted DPSC attachment, spreading and migration were all predominantly mediated through the extracellular signal-regulated kinase (ERK)/MAPK pathway, which is important not only for cytoskeletal reorganisation, but also for cell division. The de-adhesion and rounding response of DPSC was mostly reverted in the presence of MEK/ERK inhibitor, suggesting that the forward signalling cascade was primarily mediated through the MAPK pathway. Src family kinases predominantly mediate their signal through proteins containing Src homology (SH2) domains. When the phosphorylation of Src family kinases was blocked using PP2, there appeared to be more Eph expressing DPSC remaining attached following the

spreading assay. However, this was not to the same extent as observed with the MAPK inhibitor, suggesting that SH2 binding proteins may not be essential for DPSC rounding and cell adhesion.

Previous studies have reported that MAPK signalling is negatively regulated by SH2 domain containing protein RasGAP when bound to phosphorylated tyrosine within the juxtamembrane region of the EphB receptor (Miao et al., 2001; Tong et al., 2003). Alternatively, R-Ras indirectly represses MAPK function by blocking integrin mediated activation of the MAPK pathway (Zou et al., 1999). Interestingly, another SH2 domain containing protein, Grb2 adaptor protein, is a positive regulator of MAPK signalling when bound to the phosphorylated tyrosine within the kinase active loop of the EphB receptor (Tong et al., 2003). Thus using an inhibitor that blocks a number of regulatory signalling pathways did not provide a true representation of the signalling events that were taking place. While the MAPK pathway was shown to be essential for DPSC rounding and detachment, it is yet to be determined whether this response is mediated through RasGAP or R-Ras. Although it can be speculated that perhaps each pathways is required for alternative events. Potentially, the RasGAP mediated down-regulation of MAPK maybe required for DPSC rounding, as has previously been shown for neurite retraction (Elowe et al., 2001), while R-Ras, which inhibits integrin activation of MAPK regulates DPSC adhesion.

Further, it was observed that DPSC migration was inhibited through Eph forward signalling only. The MAPK inhibitor was able to rescue the inhibitory response, although, it could not be reverted to control levels. This suggested that at least for DPSC migration, other signalling pathways may also be vital. The PI3K signalling pathway is necessary for endothelial cells migration and proliferation through EphB receptors (Maekawa et al., 2003; Steinle et al., 2003; Steinle et al., 2002). Although it was surprising that the PI3K signalling pathway was not essential for DPSC attachment and spreading, it might be required in combination with MAPK signalling for DPSC migration. In addition, almost half as many DPSC migrated in response to ephrin-B1 than Human-IgG-Fc. There were also a number of cells that were not responsive to ephrin-B1 interaction, suggesting that the inhibitory response could be mediated through ephrin-B3 as well, where ephrin-B3 was predominantly expressed on pulp tissue surrounding the DPSC niche.

Reverse signalling of ephrin-B molecules can mediate through a phospho-tyrosine dependent or independent manner (Kalo et al., 2001; Lu et al., 2001; Xu et al., 2003). The data demonstrated that ephrin-B expressing DPSC mediate their signalling through a phospho-tyrosine dependent pathway via Src homology 2/3 (SH2/SH3) domains. Therefore, it was postulated that ephrin-B1 reverse phosphorylation-dependent signalling may be mediated by SH2/SH3 adaptor protein Grb4 as demonstrated by Cowan and colleagues. The Grb4 molecule is able to recruit CAP (Cbl-associated protein), resulting in loss of stress fibres via the lack of F-actin, the disassembly of focal adhesions and consequently cell rounding via ephrin-B1 reverse signalling (Cowan et al., 2001).

However, the phosphorylation independent pathways were not investigated; therefore the involvement of the JNK pathway (Xu et al., 2003) and the PDZ pathway are unknown. While the JNK pathway can induce cell rounding via ephrin-B1 activation (Xu et al., 2003), it is unlikely that this pathway is involved in DPSC rounding due to the contrasting observations between this study and that of Xu and colleagues in 2003. Phospho-tyrosine dependent signalling in conjunction with the PDZ pathway may be required to induce DPSC rounding. The PDZ domain binds with PDZ-RGS3, where the RGS3 domain inhibits heterotrimeric G protein signalling, CXCR4, a seven transmembrane heterotrimeric G protein, a receptor for stromal derived-factor 1 (SDF-1). CXCR4 is expressed at the mRNA level by DPSC in addition to SDF-1 within the pulp tissue (personal communication Dr. Stan Gronthos). It has previously been shown that EphB2-Fc activation of an ephrin-B inhibited SDF-1 chemo-attractive signalling of granule cells in the cerebellum (Lu et al., 2001). SDF-1 is also a chemokine that is up-regulated following injury or inflammation (Kucia et al., 2004; Sano et al., 2005; Togel et al., 2005) and is necessary for neural migration (Bagri et al., 2002; Chalasani et al., 2003). It was therefore postulated that ephrin-B reverse signalling inhibits DPSC chemo-attractive responsiveness to SDF-1, maintaining DPSC within their niche. However, following injury, the down-regulation of ephrin-B1 no longer masks SDF-1 signalling and thus DPSC would be mobilised to the site of injury in response to SDF-1.

The hypothesised events taking place within the DPSC niche under normal steady-state conditions and following injury to allow for DPSC mobilisation in response to caries are represented schematically (Fig. 4.15). Under normal conditions bi-directional signalling through both the Eph and ephrin expressing cells is required to restrict DPSC attachment and spreading, where the response is mediated predominately though the MAPK pathway for

forward signalling, while phosphorylation of the ephrin-B1 was required for reverse signalling (Fig. 4.15a). Inhibition of DPSC migration only requires uni-directional Eph forward signalling, again predominantly through the MAPK pathway when activated by ephrin-B1 (Fig. 4.15b). It was postulated that under normal conditions EphB expressing DPSC and ephrin-B1 expressing surrounding fibroblastic pulp tissue interaction sustains the DPSC niche by maintaining DPSC roundness, inhibiting attachment and spreading. This response is mediated through bi-directional signalling, while mobility of DPSC is repressed through uni-directional forward signalling. However, following tooth injury ephrin-B1 is down-regulated, thus eliminating the inhibitory signal, both bi-directional and uni-directional, allowing attachment, spreading and consequently migration of DPSC presumably to the injury sight in response to other attractive guidance cues, such as SDF1 (Fig. 4.15c).

The mechanisms of DPSC maintenance and recruitment of odontogenic precursor cells in postnatal tissue has yet to been previously defined. In this study it was shown that Eph/ephrin interaction contributes to the localisation of DPSC within their niche, as well as their proliferation and migration following injury within the adult dental pulp tissue. Thus restricting cell intermingling through Eph/ephrin interaction may be one potential mechanism of facilitating DPSC recruitment and maintenance. Eph/ephrin molecules are well known for their contribution to boundary formation during development as well as their role in migration of neural crest cells (Santiago et al., 2002) during branchial arch formation (Smith et al., 1997). In this study it was shown that DPSC respond to Eph/ephrin signalling in a similar way to neural crest cells. In addition to the contribution of neural crest cells to tooth development and persistence within the adult pulp tissue, it was suggested that DPSC possess neural crest properties. As neural crest cells are considered to be a stem cell population, giving rise to sensory ganglia, muscle, connective tissue (head, skin, heart), cartilage, bone, pulp and dentine (Chai et al., 2000; Morrison et al., 1999), it would be important to determine whether DPSC have the same lineage differentiation capacity as neural crest cells. Gronthos and colleagues have established that DPSC can regenerate a dentine-pulp-like complex composed of mineralised matrix with tubules lined with odontoblasts and fibrous tissue containing blood vessels, similar to the arrangement of the dentine-pulp complex found *in vivo* (Gronthos et al., 2000). DPSC possess the capacity to differentiate into fat laden adipocytes, and express neural lineage markers such as nestin and GFAP (Gronthos et al., 2002). When stem cells isolated from deciduous teeth were transplanted into the brains of mice, these cells co-localised with neurofilament antibody (Miura et al., 2003). Since DPSC

demonstrate a therapeutic potential for tooth repair (Batouli et al., 2003; Gronthos et al., 2002; Tecles et al., 2005), it would also be important to investigate whether DPSC possess any other therapeutic potential beyond dental structures. In particular, whether DPSC have the capacity to terminally differentiate into neuronal cells that could be used as an exogenous source of neural cells for neural degenerative disease or trauma.

Figure 4.15 Schematic representation of the DPSC niche under normal and injury conditions and the involvement of EphB/ephrin-B molecules.

EphB/ephrin bi-directional signaling is required to restrict DPSC intermingling with the surrounding environment, maintaining the DPSC within their niche under normal conditions (a), while inhibiting EphB-expressing DPSC migration through uni-directional signaling (b). Following injury, ephrin-B1 down-regulates expression by the surrounding pulp tissue, which results in DPSC mobilization to the injury site (c).

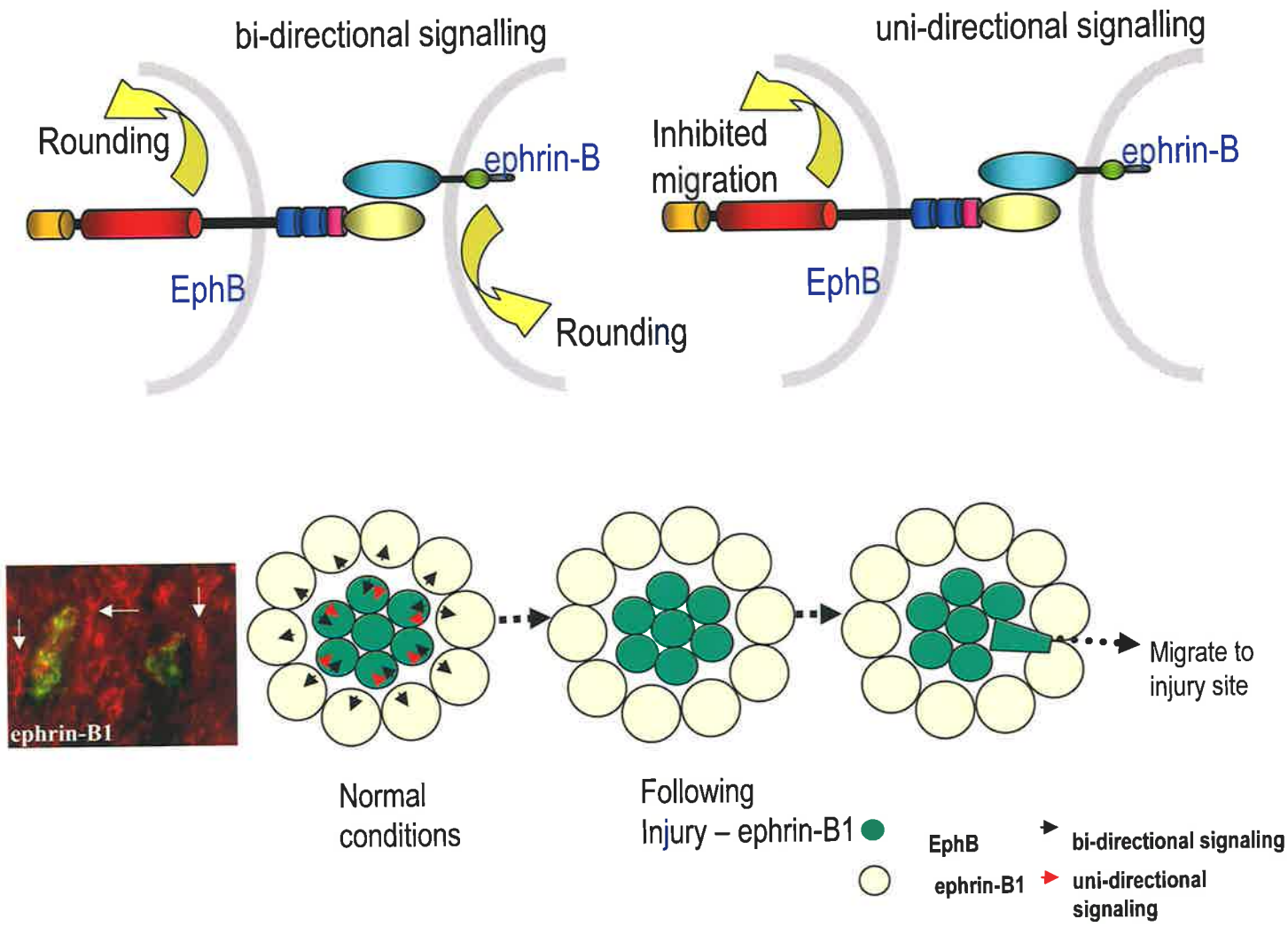
bi-directional signalling
Rounding
ephrin-B
EphB
Rounding
uni-directional signalling
Inhibited
migration
ephrin-B
EphB
ephrin-B1
Migrate to
injury site
Normal
conditions
Following
Injury – ephrin-B1
EphB
ephrin-B1
bi-directional signaling
uni-directional
signaling

Chapter 5 - Neuronal Potential of DPSC

5.1 Introduction

The treatment for stroke is limited to preventative measures in the form of tissue-type plasminogen activator (tPA), a thrombotic agent that can dissolve blood clots. To date there are no functional repair mechanisms clinically available for the treatment of strokes. SC therapy has recently been suggested as a possible treatment for neurological diseases (Henningson et al., 2003; Lindvall et al., 2004a; Lindvall et al., 2004b; Rossi et al., 2002). A review of the literature suggests that SC therapy needs to be expanded to include not only the repair and replacement of dead or damaged neurons or glia, but also preventing the death of existing neurons, as a consequence of the injury response or disease progression (reviewed by (Lindvall et al., 2006; Lindvall et al., 2004b)).

The ultimate goal for SC therapy-based research is the repair and regeneration of functional neurons and glia in order to facilitate functional improvement following injury. It has been postulated that the functional improvement observed following SC engraftment may be attributed to a number of underlying mechanisms; neurogenesis, growth factor production, immuno-modulation and modulation of intrinsic factors required for neural repair (reviewed by (Lindvall et al., 2004a)). Understanding these mechanisms and processes is paramount to achieving viable clinical outcomes using SC therapy-based treatments. Critical factors contributing to the repair/regeneration process may need to be modulated to facilitate the functional potential of SC following transplantation.

In model organisms, both endogenous and exogenous SC have been investigated for their capacity to repair or replace damaged neurons following injury. Due to limited knowledge and limited number of endogenous human adult NSC, a plausible approach to SC therapy would be to utilise an exogenous source of SC with neural potential. Pluripotent ESC and multipotent BMSSC or MSC have been investigated predominantly in the repair of neurons and glia following injury (reviewed by (Lindvall et al., 2006; Lindvall et al., 2004b)). These SC types have demonstrated some capacity to differentiate into neural derivatives and improve sensorimotor function following stroke (Chen et al., 2001a; Chen et al., 2001b; Ikeda et al., 2005; Leker et al., 2004; Li et al., 2001; Li et al., 2000; Wei et al., 2005). However, the

neural differentiation potential of these exogenous SC types is limited. In particular, the functional improvement observed following ESC transplantation required the ESC to be restricted to a specific cell type, such as oligodendrocytes prior to transplantation (Keirstead et al., 2005) to avoid the possible formation of teratomas (Itskovitz-Eldor et al., 2000). The use of ESC for SC therapy-based treatment requires further investigations to develop safer protocols that ensure no tumour development. Furthermore, the study of human ESC is restricted to a few cell lines due to ethical issues that still encumber human embryonic research. Whilst postnatal SC may avoid some of these problems, studies examining the neural differentiation capacity of BMSSC are limited and still require further investigation.

It was hypothesised that DPSC may provide an alternative SC source for therapy-based treatment of neuronal disorders, such as stroke. Four key studies suggest that DPSC may have neural potential (Gronthos et al., 2002; Miura et al., 2003; Nosrat et al., 2004). The first researchers to specifically investigate the neural potential of human adult DPSC showed that under non-neuronal inductive conditions, DPSC expressed the neural progenitor marker, Nestin, and glial marker, GFAP, at both the gene and protein level (Gronthos et al., 2002). Subsequent examination by the same researchers documented that DPSC under neural inductive conditions expressed post mitotic neuron-specific marker, neuronal nuclei (NeuN) (Gronthos et al., 2004), however, no further investigation was conducted into the neuronal potential of DPSC. The above-mentioned observations were further supported by the finding of Nosrat and colleagues who demonstrated that a sub-population of rat and human DPC maintain a neuronal morphology for up to 5 months, as demonstrated with neuron marker, protein gene product (PGP) 9.5 and β-tubulin expression, when cultured in DMEM/F12 media (Nosrat et al., 2004). Furthermore, Shi and colleagues showed that culturing SHED in neural inductive media conditions for 4 weeks resulted in the up-regulation of neural markers β-tubulin, glutamic acid decarboxylase (GAD) and NeuN, as well as the expression of many other neural specific markers (Miura et al., 2003). These studies imply that DPC (Nosrat et al., 2004) and SHED (Miura et al., 2003) have the ability to survive and express neural markers following transplantation into the rodent brain.

Importantly, DPC have also been shown to express a range of neurotrophic factors that improve the survival of damaged motoneurons following spinal cord hemi-section (Nosrat et al., 2001). It was observed that when DPC were grafted into the anterior chamber of the eye, they became vascularized with an increasing number of surviving motor neurons entering the

grafts over time. More importantly, the DPC were able to increase the number of surviving motor neurons by 115%, when grafted into a hemisected spinal cord of rats. It was proposed that GDNF was the principal survival factor, with strong gene expression in cells of the grafts day 1 post-injury, with a decreased expression after 1 week (Nosrat et al., 2001). Furthermore, *in vitro* co-cultures of DPC with trigeminal neurons resulted in sustained survival and intricate neurite outgrowth patterns from the trigeminal ganglia (TG), the axons of which innervate the face and teeth *in vivo*. Neurite outgrowths were not observed when the TG was co-cultured with skin fibroblasts. These findings propose that heterogeneous populations of DPC have the potential to facilitate survival of both sensory and motor neurons *in vitro* and *in vivo*, respectively. As previously mentioned, growth factor production may be an underlying mechanism for stem cell therapy based neural repair. These observations further suggests the plausible function of DPSC as a source for SC therapy for neurological disorders

The above-mentioned studies demonstrate that DPSC do express neural markers, although the knowledge of the neuronal potential of DPSC is limited. Three modes of DPSC neuronal differentiation were investigated in this chapter: (1) culturing DPSC with growth factors that induce neuronal differentiation; (2) forced neuronal differentiation by stably transfecting DPSC with a neuronal specific transcription factor; (3) transplanting DPSC into the head region of the developing avian embryo.

Growth factors such as epidermal growth factor (EGF) (Reynolds et al., 1996), fibroblast growth factor (FGF) (Palmer et al., 1999) and/or retinoic acid (RA) (Itoh et al., 1997) in certain culture media have induced neuronal differentiation. This has been shown for ESC (Nakayama et al., 2004), neural precursors, BMSSC (Scintu et al., 2006) and SHED (Miura et al., 2003). Additionally, it has been documented that these media conditions maintain neuronal cell types in culture (Ciccolini et al., 1998; Gritti et al., 1995; Weiss et al., 1996). Thus, such factors and neural media conditions may also instigate neural differentiation of human adult DPSC.

Basic helix-loop-helix (bHLH) transcription factor, NeuroD1, is a proneural gene known to be a positive regulator of neural differentiation during development (Korzh et al., 1998; Schwab et al., 2000) and important for neurogenesis (Lee et al., 1995). NeuroD1 expressed by hippocampal cells (Pleasure et al., 2000; Seki, T., 2002a), within the cortex (Marin et al.,

2001) and sub-ventricular zone (Lee, E., 1997), is also present following injury or seizure when neurogenesis of SC replaces damaged neurons (Konishi et al., 2001). NeuroD1 transcription is regulated by another neural specific bHLH transcription factor Neurogenin-1 (Ngn-1) (Ma et al., 1998). Ngn-1 has been shown to induce and commit neural differentiation of embryonic carcinoma P19 cells in the absence of RA (Kim et al., 2004a), possibly through the NeuroD pathway. Therefore, NeuroD1 was considered a suitable candidate that could induce neuronal differentiation of DPSC efficiently.

The avian embryo was employed to investigate neuronal differentiation capacity of human DPSC *in vivo*. The avian embryo is an *in ovo* animal model that is easily accessible, has rapid development and lacks an immune response to xeno-transplantation during the early stages of development. Additionally, the neurobiology of the developing embryo has been extensively studied and is well characterised. The chicken embryo has previously been used for quail-chicken (Douarin et al., 1999d) and mouse-chicken chimera (Mitsiadis et al., 2003) experiments and for transplantation of mouse embryonic endothelial progenitor cells into the chicken embryo (Hatzopoulos et al., 1998). Therefore, the avian embryo provides an excellent *in vivo* environment to investigate the neural potential of DPSC in response to endogenous neuronal cues. To our knowledge there have been no systematic studies to investigate human-chicken chimeras.

5.2 Results

5.2.1 Neuronal differentiation of DPSC by exogenous growth factors

To determining the neuronal differentiation potential of DPSC, neuronal inductive conditions, as well as growth and signalling factors were used. The main components of most media conditions include EGF, FGF and RA in either Neurobasal A media or 50:50 ratio of DMEM/F12 media; both media also contain growth factor supplements. The present study investigated which media formulation or additional components were most optimal for neural differentiation of DPSC (Fig. 5.1). Following preliminary analysis of 5 different media conditions, 3 neural media formulations (Media A, Media 2 and Media 4) were investigated further based on the *NF-M* gene expression analysis (data not shown). These media conditions were consistent with investigations of neural differentiation of DPSC from deciduous teeth, SHED (Miura et al., 2003) and embryonic stem cells (Gallo et al., 2002; Nakayama et al., 2004).

5.2.1.1 Neuronal inductive conditions rich in growth factors promote adult human DPSC neuronal differentiation

Three independent DPSC donors NHT 5_01, NHT 15_04 and NHT 1_04 were examined for their neuronal potential following incubation with one of three neural inductive conditions, Media A, Media 2 and Media 4 compared to control media conditions, alpha Modification of Eagle's Medium (MEM). To determine which of the media conditions would be most optimal for neuronal differentiation, DPSC exposed to the differing conditions were examined with neural progenitor, Nestin and neuronal markers β-tubulin III and Neurofilament, at both the gene and protein level using RT-PCR and immunocytochemistry. A trend was observed between the donors exposed to the three different neuronal inductive media, although at varying levels of gene expression. Neural progenitor, *Nestin*, was decreased by donor NHT 15_04, predominantly when cultured in Media 4, followed by Media 2 and then Media A, while donors NHT 5_01 and NHT 1_04 were unchanged. Early neuronal marker *β-tubulin III* was reduced by two of the donors (NHT 15_04 and NHT 1_04) and unchanged by donor NHT 5_01. Potentially, the DPSC may have differentiated past the expression of the early

Figure 5.1 Schematic representation of the Neural Induction Assay (NIA) set up for a 3-week time frame

DPSC from 3 independent donors were incubated on Polyornithine and Poly-L-lysine coated flasks, culture plates or chamber slides for the duration of the experiment, media was changed twice weekly. Initially DPSC were cultured in control growth media (MEM) for 3 days or until confluent, the culture media was then changed to Media A (Neuroblasal A media containing B27 supplement, epidermal growth factor (EGF) and basic fibroblast growth factor (FGF)) for the experimental group or maintained in MEM for the control group for 1 week. At the beginning of the second week, DPSC were liberated from the flasks and plated at 1.5×10^5 cells/well in a 6-well culture plate or 2×10^3 cells/well in 8-well chamber slides and incubated with Media A, Media 2 (DMEM/F12 containing insulin-transferrin-sulphate salute (ITSS) and FGF) or Media 4 (DMEM/F12 containing ITSS, FGF and retinoic acid (RA)) for the experimental group or maintained in MEM for the control group. At the commencement of the third week, the culture media was changed to DMEM/F12 containing ITSS and RA for all DPSC in the experimental group, while maintained in MEM for the control group. At the conclusion of the third week, cells plated in 6-well culture plates were used for gene expression analysis, while those in 8-well chamber slides were fixed with 4% PFA and stained with neural antibodies.

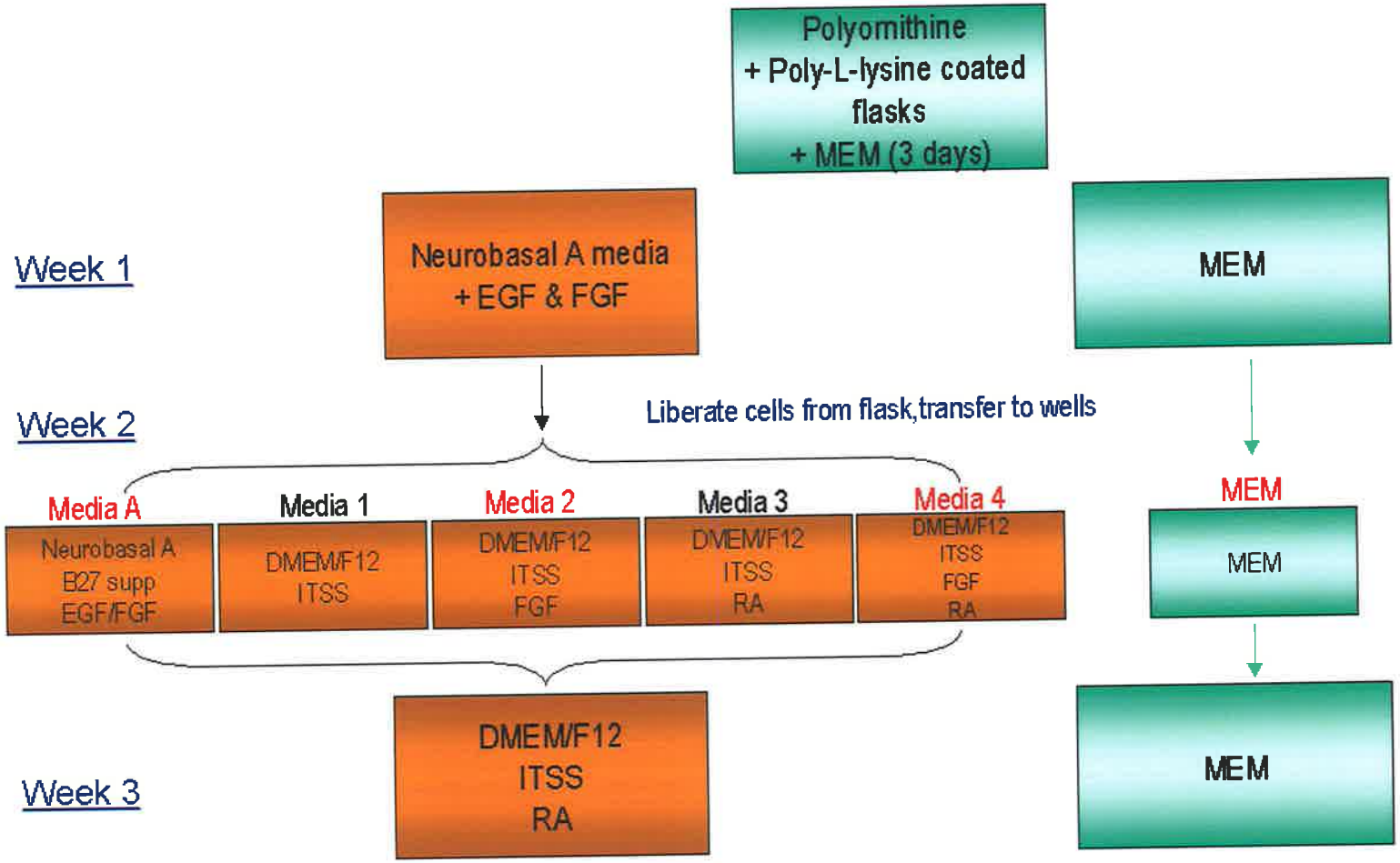
Polyornithine
+ Poly-L-lysine coated flasks
+ MEM (3 days)
Week 1
Neurobasal A media
+ EGF & FGF
MEM
Week 2
Liberate cells from flask,transfer to wells
Media A
Neurobasal A
B27 supp
EGF/FGF
Media 1
DMEM/F12
ITSS
Media 2
DMEM/F12
ITSS
FGF
Media 3
DMEM/F12
ITSS
RA
Media 4
DMEM/F12
ITSS
FGF
RA
MEM
MEM
Week 3
DMEM/F12
ITSS
RA
MEM

neural marker during the three-week incubation, which correlates with the increased expression of mature neuronal marker *Neurofilament-medium chain* (*NF-M*), found to be up-regulated by DPSC in all conditions, predominantly in Media 2 (Fig. 5.2).

Immunocytochemistry was employed to verify the neuronal differentiation of DPSC cultured in neuronal inductive conditions. Different markers ranging from neural progenitor to mature neural markers indicated that the morphology of DPSC exposed to neuronal inductive conditions was markedly different to those exposed to normal growth media conditions. DPSC exposed to neuronal inductive media appeared to acquire a bipolar morphology reminiscent of sensory neurons, while a number of DPSC displayed dendritic like processes (Fig. 5.3, arrows). However, this was not observed in the normal growth media control cultures (Fig. 5.3). Notably, while some DPSC in control growth media expressed neuronal proteins such as NF-M, the proportion of NF-M positive cells was considerably lower when exposed to MEM (22%) compared to Media A (74%), Media 2 (75%) or Media 4 (50%). Furthermore, Neurofilament – heavy chain (NF-H), a mature neural marker expressed by large projection or myelinated neurons *in vivo* (Giasson et al., 1997; Shea et al., 1997; Szebenyi et al., 2002), and an important determinant for axonal calibre; was lowly expressed by DPSC cultured in normal growth media (12%), while NF-H was visible on DPSC exposed to Media A (82%), Media 2 (78%) and Media 4 (58%) (Fig. 5.3). Additionally, the proliferation rate of DPSC was decreased in neural inductive cultures compared to control cultures. Fewer cells were observed in Media A (16-fold decrease), Media 2 (21-fold decrease) and Media 4 (21-fold decrease). These observations imply that both Media A and Media 2 produced relatively similar levels of DPSC displaying neuronal morphology and expressing mature neuronal markers, despite the substantial difference in media conditions.

5.2.2 Neuronal differentiation of DPSC by enforced transcriptional activation

5.2.2.1 Transduction of NeuroD1 into adult human DPSC

Adult human DPSC constitutively express low levels of *NeuroD1*, although the level of gene expression varied between donors (Fig 5.4a). Human *NeuroD1* cDNA was introduced into 2 different DPSC donors using retro-viral transduction. To achieve this, *NeuroD1* was firstly cloned into the retro-viral expression vector, pLNCX2. Two alternative packaging cell lines

PT67 and PA317 were generated following stable transfection with either the *NeuroD1* construct or pLNCX2 vector alone. Viral particle containing supernatant from each of the packaging lines was used to infect different DPSC donors to determine which packaging line produced the highest transduction efficiency. Packaging line PT67 resulted in more consistent and higher transduction efficiencies and was therefore used for subsequent experiments. Following the generation of G418 resistant stably transduced pooled clones of *NeuroD1* or control DPSC, *NeuroD1* gene expression was assessed relative to control gene TBP. RT-PCR analysis confirmed that incorporation of retro-virally transduced *NeuroD1* increased *NeuroD1* gene expression 8,713-fold for donor NHT 1_04 and 2,286-fold for donor NHT 5_01, when compared to the corresponding control transduced with vector alone (Fig. 5.4b). These results demonstrated that stably transfected DPSC up-regulated *NeuroD1*, at the gene level. To determine the level of NeuroD1 protein expressed by the transduced DPSC, immunocytochemical and western blot analysis were undertaken. However the NeuroD1 antibody used, which had previously been published to specifically detect NeuroD1 (Sen et al., 2002) did not yield any findings (data not shown). To confirm whether the antibody was working, positive controls, the olfactory bulb and hippocampus from post-natal rats (Liu et al., 2000; Manglapus et al., 2004) were used for western blot analysis, while adult mouse brain sections (Liu et al., 2000; Seki, T., 2002b) were used to detect NeuroD1 immunohistochemically. Both methods failed to detect the NeuroD1 protein (data not shown), indicating that the antibody was not functional. Therefore the level of NeuroD1 protein could not be determined in DPSC transduced with *NeuroD1*.

During retinal development, it has been suggested that NeuroD1 is capable of regulating the neuronal versus glial cell fate (Cai et al., 2000). Once these DPSC were transduced with *NeuroD1*, their morphology differed to their vector alone transduced counterparts. *NeuroD1* transduced DPSC displayed bipolar processes and large rounded soma, reminiscent of sensory neurons (Fig 5.5a). This was also consistent with the known function of NeuroD1 to induce terminal neural differentiation (Bertrand et al., 2002).

RT-PCR analysis indicated that both donors up-regulated gene expression of neural progenitor marker and early neuronal marker, *Nestin* and *β-tubulin III*, respectively, in response to NeuroD1. Surprisingly, gene expression of more mature neuronal marker *NF-M* was differentially expressed between the two donors. *NF-M* gene expression was increased 2-fold by NHT 1_04 DPSC and decreased 4-fold by NHT 5_01 DPSC. Glial marker, *GFAP*

expression was unchanged by both donors (Fig 5.5b), consistent with role of NeuroD1 in neuronal rather than glial differentiation. The neuronal gene expression variability between donors could be attributed to STRO-1 expression levels. Donor NHT 1_04, which has approximately 3-5% STRO-1 expression, demonstrated increased levels of *NF-M*, while donor NHT 5_01, with 30-50% STRO-1 expression, down-regulated *NF-M* expression. These observations imply that the higher the level of STRO-1 expression the less neuronal differentiated the DPSC appears. This is consistent with previous reports that demonstrated the immature state of STRO-1^+ expressing BMSSC over BMSSC populations that lost STRO-1 expression *in vitro* (Gronthos et al., 1999; Martens et al., 2006).

The findings of the *in vitro* growth factor or enforced transcriptional activation neuronal induction assay established that DPSC displayed both neuronal morphology and expressed early and mature neuronal markers at both the gene and protein levels. Collectively, these studies indicate that DPSC are endowed with the plasticity to differentiate into putative neuronal cell types *in vitro*. However, capacity of adult DPSC to undergo neuronal differentiation has not been demonstrated *in vivo*.

Figure 5.2 DPSC neural gene expression in response to neural media conditions.

RT-PCR analysis of total RNA isolated from 3 independent DPSC donors (NHT 5_01 – blue, NHT 15_04 – red, NHT 1_04 – yellow) exposed to differing neural and control media conditions, expressed as a fold change relative to control MEM media. Samples were normalized to control gene, *TBP*. (a) DPSC from all donors reduced expression of *Nestin* at varying levels, (b) down-regulated the expression of early neuronal marker, *β-tubulin III* gene, (c) but up-regulated the gene expression of more mature neuronal marker, *neurofilament-medium chain* (*Neurofilament-M*). n = 3 replications

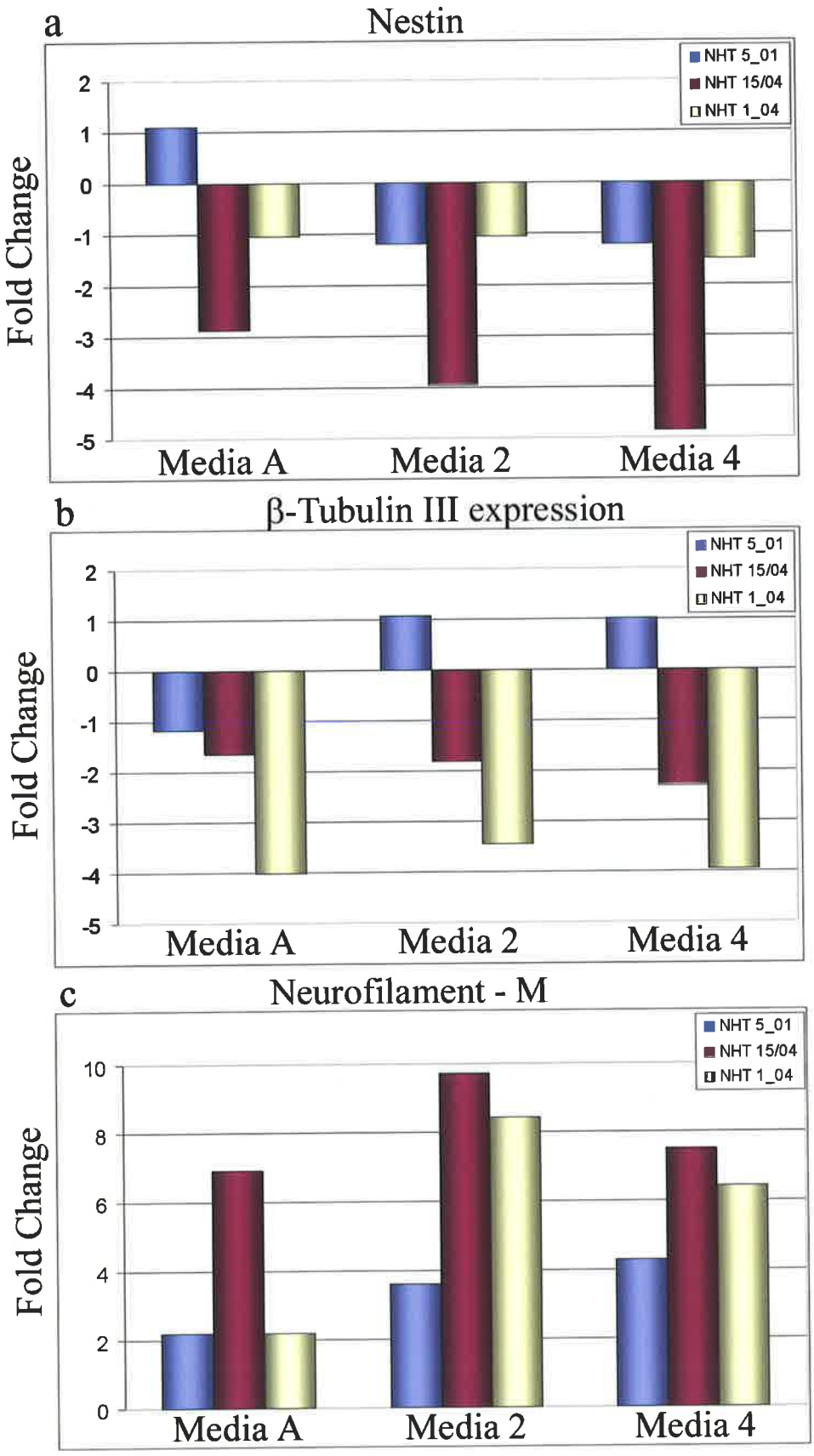
a
Nestin
NHT 5_01
NHT 15/04
NHT 1_04
Fold Change
2
1
0
-1
-2
-3
-4
-5
Media A
Media 2
Media 4
b
β-Tubulin III expression
NHT 5_01
NHT 15/04
NHT 1_04
Fold Change
2
1
0
-1
-2
-3
-4
-5
Media A
Media 2
Media 4
c
Neurofilament - M
NHT 5_01
NHT 15/04
NHT 1_04
Fold Change
10
8
6
4
2
0
Media A
Media 2
Media 4

Figure 5.3 DPSC cultured in neural inductive media displayed neural morphology and expressed neural proteins.

(a) Representative images of DPSC from 3 independent donors (NHT 5_01, NHT 15_04 and NHT 1_04) cultured in control MEM media, Media A, Media 2 and Media 4, and stained with Nestin, GFAP, neuroblast marker PSA-NCAM (PSA), β-tubulin III clone TUJ1, neurofilament-medium chain (NF-M) and mature neuronal marker neurofilament-heavy chain (NF-H). Scale bar = 20μm. (b) DPSC positive for Nestin, GFAP, PSA, TUJ1, NF-M and NF-H in response to the neural inductive media condition for all donors was counted (n=3 donors) and represented as a percentage of positive cell per field of view. There was a significant increase in neuronal protein expression by DPSC in response to both Media A and Media 2, but not Media 4 compared to MEM control media. In response to Media A there was a 3.5-fold (Student t-test, $p < 0.0004$) increase in NF-M positive cells and a 6.6-fold (Student t-test, $p < 0.0003$) increase in NF-H. In response to Media 2, a 3.6-fold (Student t-test, $p < 0.005$) increase in NF-M positive DPSC and a 6.3-fold (Student t-test, $p < 0.003$) increase in NF-H positive DPSC was observed, error bars = SEM.

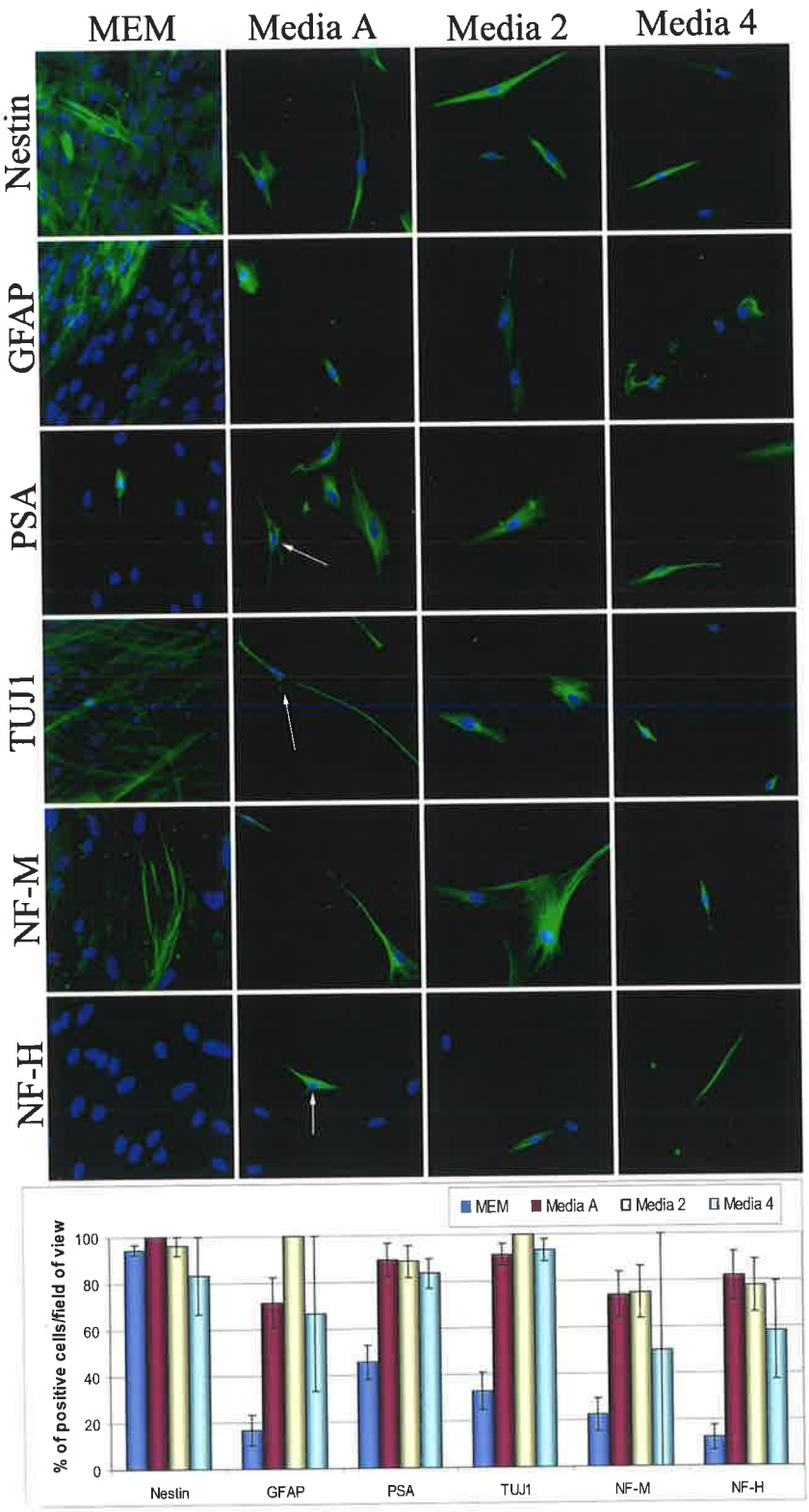
MEM
Media A
Media 2
Media 4
Nestin
GFAP
PSA
TUJ1
NF-M
NF-H
MEM
Media A
Media 2
Media 4
% of positive cells/field of view
100
80
60
40
20
0
Nestin
GFAP
PSA
TUJ1
NF-M
NF-H

Figure 5.4 Endogenous and retro-virally transduced level of *NeuroD1* expression by adult human DPSC.

(a) RT-PCR of cultured DPSC from 4 independent donors indicated from the cycle threshold level that *NeuroD1* was endogenously expressed by human adult DPSC, control gene, *β-actin*. (b) Retro-virally transfected adult human DPSC significantly up-regulate *NeuroD1* gene expression relative to the control vector alone. Multiple donor DPSC primary cultures (NHT 1_04 and NHT 5_01) were retro-virally transfected with either control vector alone (pLNCX2) or vector containing NeuroD1. RT-PCR analysis indicated that *NeuroD1* was up-regulated 8,000-fold relative to control vector alone for donor NHT 1_04, while *NeuroD1* was up-regulated 2,000-fold compared to control vector alone for donor NHT 5_01.

a

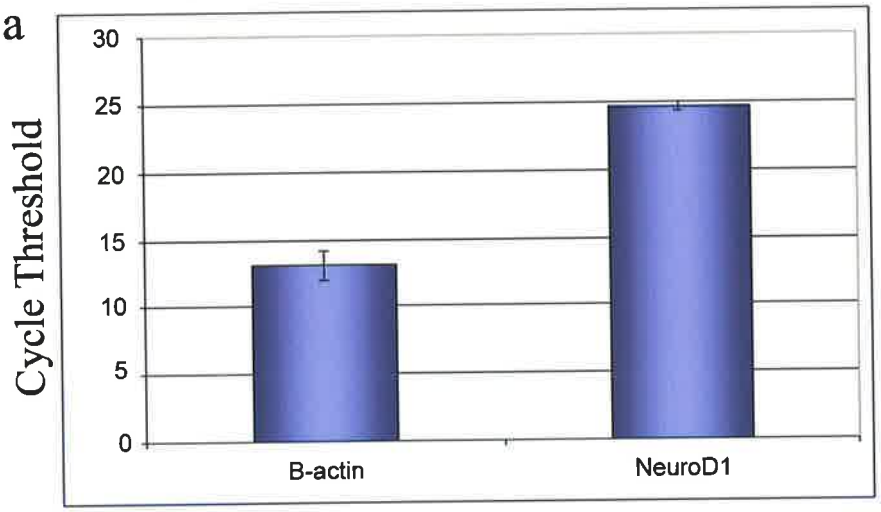
Cycle Threshold
30
25
20
15
10
5
0
B-actin
NeuroD1

b

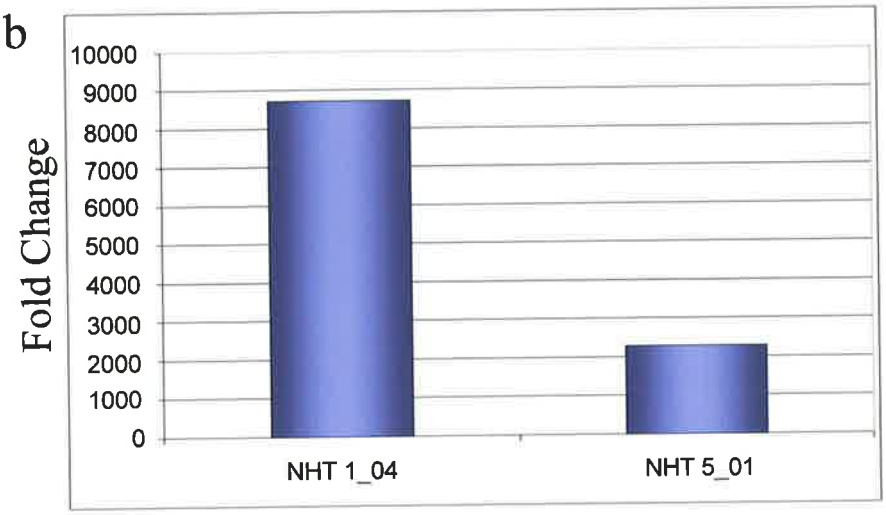
Fold Change
10000
9000
8000
7000
6000
5000
4000
3000
2000
1000
0
NHT 1_04
NHT 5_01

Figure 5.5 *NeuroD1* over-expressing DPSC display a neural morphology and neuronal differentiation potential.

(a) DPSC transduced with vector alone appear similar to untransduced DPSC, while *NeuroD1* over-expressing DPSC display a bipolar sensory neuronal morphology. Bright field representative images from donor NHT 1_04, taken by Simon Fallon. Scale bar = 50μm. (b) RT-PCR analysis indicated differential neuronal gene expression following transduction of DPSC with *NeuroD1* relative to vector alone transduced DPSC. *Nestin* and *β-tubulin III* gene expression was up-regulated in *NeuroD1* over-expressing samples while *neural specific enolase* (*NSE*) and *GFAP* were down-regulated. Interesting, *neurofilament-medium chain* (*Neurofilament-M*) was differentially expressed between donors.

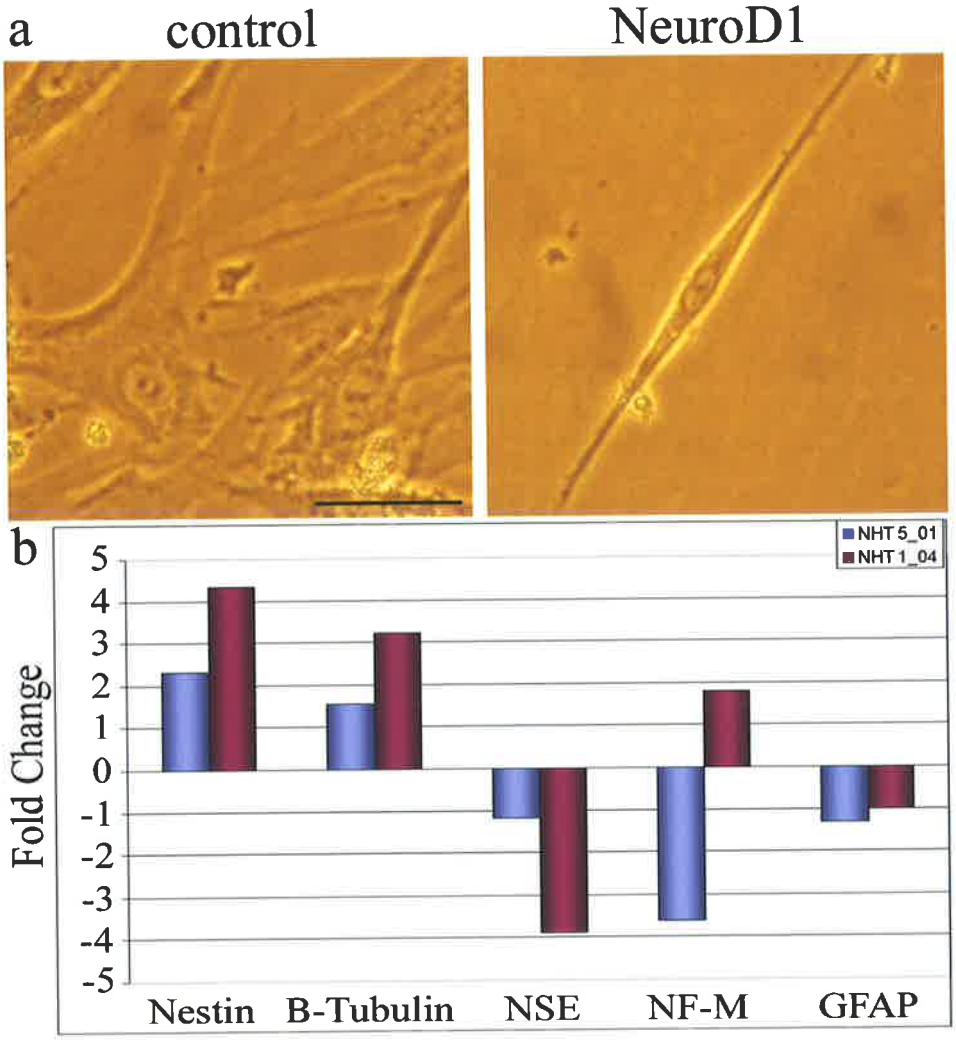
a
control
NeuroD1
b
Fold Change
5
4
3
2
1
0
-1
-2
-3
-4
-5
NHT 5_01
NHT 1_04
Nestin
B-Tubulin
NSE
NF-M
GFAP

5.2.3 Neuronal differentiation of DPSC in the chicken embryo

To date only one research group has demonstrated that SC from deciduous teeth, were able to respond to endogenous neural environmental factors following transplantation into the adult mouse brain (Miura et al., 2003). The present study aimed to extrapolate our understanding of whether human adult DPSC could respond to the endogenous neural environment and differentiate into neural derivatives. A developmental model organism, the avian embryo, was utilised because of its rapid development and the extensive knowledge of avian developmental neurobiology, where CNC migration and sensory neural differentiation is well documented in the avian embryo (Douarin et al., 1999c). The present study examined whether adult DPSC may respond in a similar manner when transplanted into a CNC rich region.

Stably transduced green fluorescent protein (GFP) expressing DPSC (n = 223 embryos) and control human cell types including SHED (n = 15 embryos), BMSSC (n = 84 embryos) and SFB (n = 18 embryos), were injected into regions adjacent to the developing neural tube in a time frame when CNC coalesce, migrate to their target tissue and differentiate into neural derivatives (LeDourine, 2004). All cell types were incubated for either 24, 48 or 72 hours post injection (PI) and then assessed for their migration, localisation, morphology and neural differentiation using immunohistochemistry to neuronal specific markers (Fig. 5.6).

5.2.3.1 Development of the Ikaros Assay - Method

GFP transduced adult human DPSC, SHED, BMSSC or SFB were injected into the developing avian embryo (white leghorn, Hi Chick Breeding Company) at stages 10-12 (approximately 40 hours incubation, as determined by (Hamburger et al., 1951). This equates to the formation of one the first ganglia in the embryo, the trigeminal ganglion (TG or V), which is located close to rhombomere 2. Embryos were visualised by injecting Indian ink (1:10 prepared in Ringer's Solution) underneath the embryo. The vitelline membrane was removed from around the head of the embryo, the cells (optimal concentration of $5 \times 10^3/\mu L$ for DPSC, SHED and SFB, and $2 \times 10^3/\mu L$ for BMSSC, as these are larger cells and block the pipette at higher concentrations) were injected through a glass pipette attached to a micromanipulator and pressure injector, set at 25 Volts, into the region directly adjacent to the

developing hindbrain (Fig. 5.6b). This region corresponds to the mesencephalon, specifically the anterior rhombencephalon region. CNC cells originating in this area at stages 10-12 migrate into the surrounding tissue and contribute to the formation of the trigeminal ganglion, first branchial arch and surrounding facial structures (Douarin et al., 1999a). Embryos were dissected 24, 48 and 72 hours post-injection (PI); the head was cut as open-book, ie, cut from the nose to the hindbrain down the length of the head, on the ventral side. Dissected embryos were fixed in 4% PFA for either 2 hours at room temperature or overnight at 4°C, then washed with PBS prior to immunofluorescent staining. Embryos were stained for GFP and CNC or neuronal markers at 24, 48 and 72 hours PI to investigate the survival, localisation, migration and differentiation of injected cells in the embryo (Fig. 5.6).

5.2.3.1 Transplanted DPSC follow neural CNC migratory pathways

Adult human DPSC injected into the avian embryo at stage 10-12 (Hamburger et al., 1951) from multiple donors (n = 7 donors) were able to survive when investigated up to 72 hours or stages 24-26 PI (Fig 5.7-5.9). After 24 hours DPSC had extended processes and localised to regions followed by migrating endogenous CNC. The TG is a CNC derived ganglia, which starts to develop into its recognised structure by approximately 60 hours post fertilization, this corresponds to St15 (Hamburger et al., 1951). Early neuronal marker β-tubulin III clone, TUJ1, is able to detect projecting axons from the TG by St 15, in addition to other developing neurons within the embryo (Jayasena et al., 2005). TUJ1 was used to visualise neurons and their axonal processes 24 hours PI (n = 8 embryos), corresponding to St16. DPSC appeared to have migrated along endogenous axonal pathways, particularly along the ophthalmic process (above the eye) of the trigeminal ganglion (TG) (Fig. 5.7a-b).

At 48 hours PI (n = 53 embryos), DPSC had primarily migrated into the CNS and along axonal pathways of the TG (Fig. 5.8, Fig. 5.11a-b), where the transplanted DPSC were found to lie within close proximity to endogenous sensory axons (Fig. 5.9c-f asterisks) by 72 hours PI (n = 26 embryos).

Figure 5.6 Experimental design: human adult DPSC injection into the hindbrain region of the developing avian embryo.

(a) Adult human DPSC, stained with human specific Integrin-β1 antibody, or green fluorescent protein (GFP) transfected DPSC (b) were injected into stage 10-12 (Hamburger et al., 1951) chicken embryos into the peripheral tissue surrounding the hindbrain (arrows), where cranial neural crest cells migrate from and contribute to the formation of cranial and neural structures. (c) Embryos incubated for 24 (n = 41), 48 (n = 139) and 72-hours (n = 43) post-injection (PI), which correlates to stages (St) 16, 20 and 26, respectively, in a humidified incubator. After which time embryos were removed from the egg, dissected, fixed and stained for early neuronal marker, β-tubulin III clone TUJ1 or intermediate neuronal marker, neurofilament-medium chain (NF-M). (d) Representative image of stage 20 embryo stained with NF-M. Embryos were mounted as open-book fashion with the E=eye to the left and right of image, indicating left and right side of embryo, HB=hindbrain in the middle of the embryo, TG=trigeminal ganglion to the left and right of the hindbrain. The TG is comprised of two lobes that migrate as 3 separate axonal processes. The ophthalmic (Op) process above the eyes, originating from the first lobe, the second lobe bifurcates into the maxillary (Mx) and mandibular (Md) processes, that navigate below the eye and into the branchial arches, respectively. (e-f) Injected human adult DPSC survived following injection and were identified with (e) human specific Integrin-β1 antibody 24 hours PI or (f) GFP staining 48 hours PI (green) and counterstained with a neural marker, in this representative image, NF-M (red). All subsequent images z-serial confocal images compressed to a single plane, unless otherwise stated.

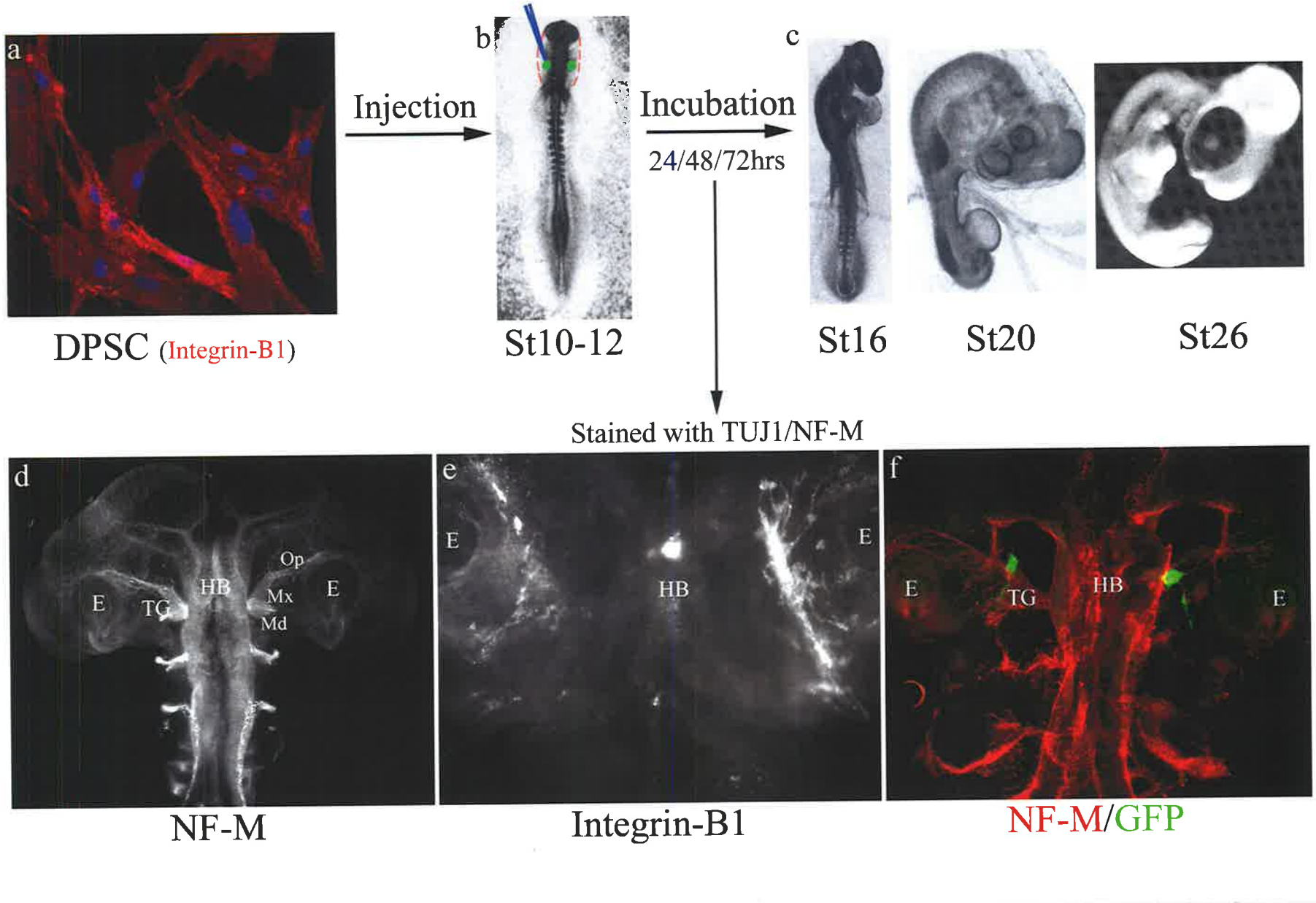
a
Injection
b
Incubation
24/48/72hrs
c
DPSC (Integrin-B1)
St10-12
St16
St20
St26
Stained with TUJ1/NF-M
d
E
TG
HB
Op
Mx
Md
E
e
E
HB
E
f
E
TG
HB
E
NF-M
Integrin-B1
NF-M/GFP

Figure 5.7 Twenty-four hours PI (stages 15-17) human adult DPSC survive and extend their processes in response to endogenous developmental cues.

(a-b) GFP labeled (green) DPSC were counter-stained with early neural marker TUJ1 (red, n=8) 24 hours PI and were visualized in close proximity to trigeminal axonal processes. All images were compressed confocal z-series. E=eye, HB=hindbrain, TG=trigeminal ganglion. Scale Bar = 100μm.

TUJ1

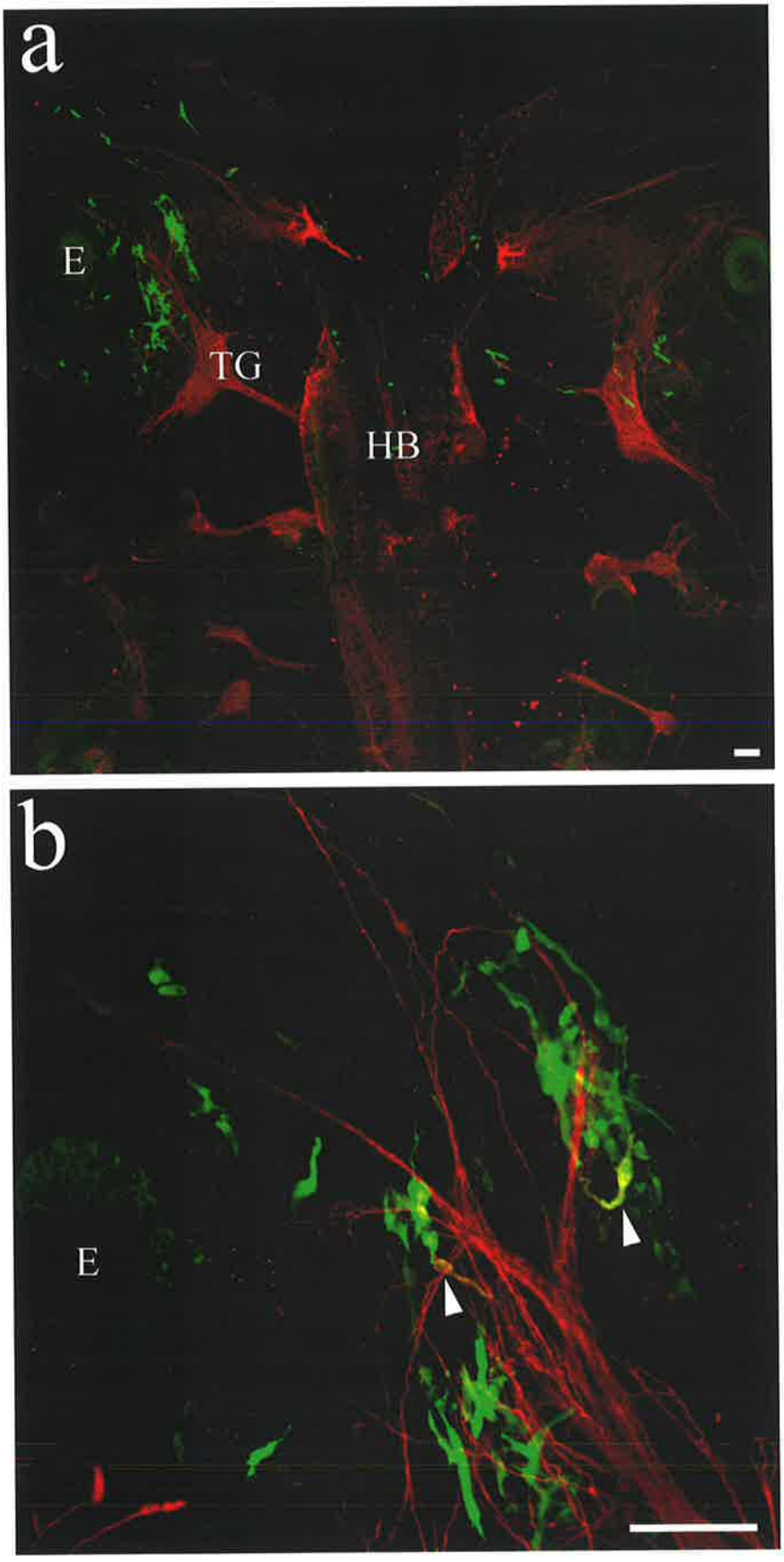

Figure 5.8 DPSC injected into the avian embryo displayed neural morphology and localized with neural markers 48 hours post injection (stages 19-23).

DPSC (green) migrated within the developing avian embryo into facial structures and into the central nervous system. DPSC displayed neural morphology, both bipolar (asterisk) and with multiple processes (arrow), localizing with (a-b) TUJ1 (red, n = 22) and (c-d'') NF-M (arrows) (red, n = 31). NF-M positive DPSC also displayed growth cones (asterisks, c-d''). (d'-d'') Compressed image of confocal z-series, slices 8-20 from image (d), demonstrating neurofilament staining by GFP labeled DPSC (arrows). E=eye, HB=hindbrain, TG=trigeminal ganglion. Scale Bar = 100μm.

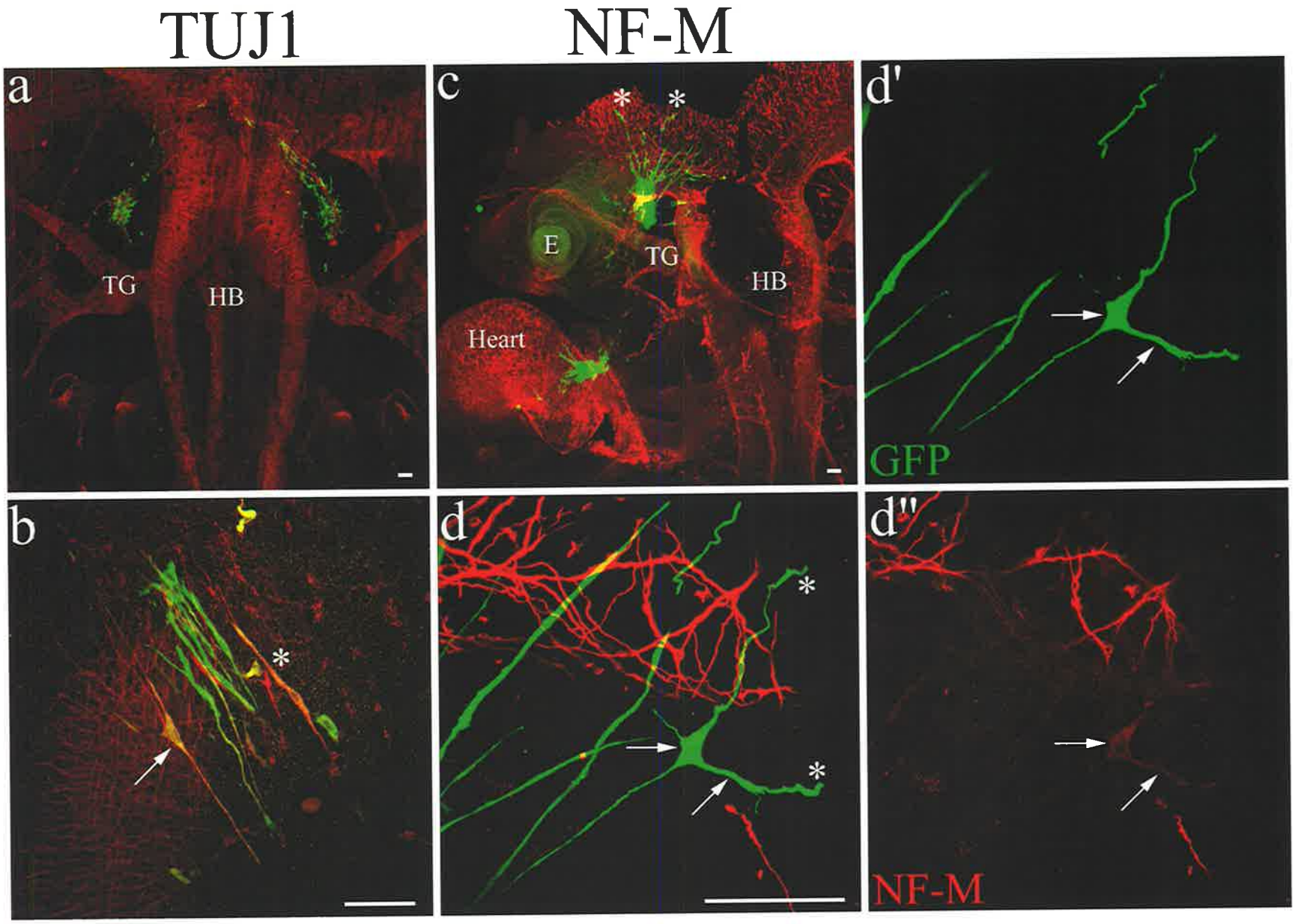
TUJ1
NF-M
a
TG
HB
c
E
TG
HB
Heart
d'
GFP
b
d
d''
NF-M

Figure 5.9 DPSC continued to display a neuronal morphology 72-hours post injection in the avian embryo.

GFP labeled DPSC (green) injected embryos were counterstained with (a-d) TUJ1 (red, n=5), or (e-h) NF-M (red, n=21). DPSC appeared to survive and localize to regions of axonal processes (c-f), migrate towards the heart near the mandibular (Md) process (a-b), and to the hindbrain (g-h). The transplanted DPSC appeared to display both bipolar (asterisk) and dendritic (arrowhead) morphology. All images were compressed confocal z-series. BA=branchial arch E=eye, HB=hindbrain, TG=trigeminal ganglion, Op ophthalmic process. Scale Bar = 100μm (a,c,e,g)(b,d,f,h).

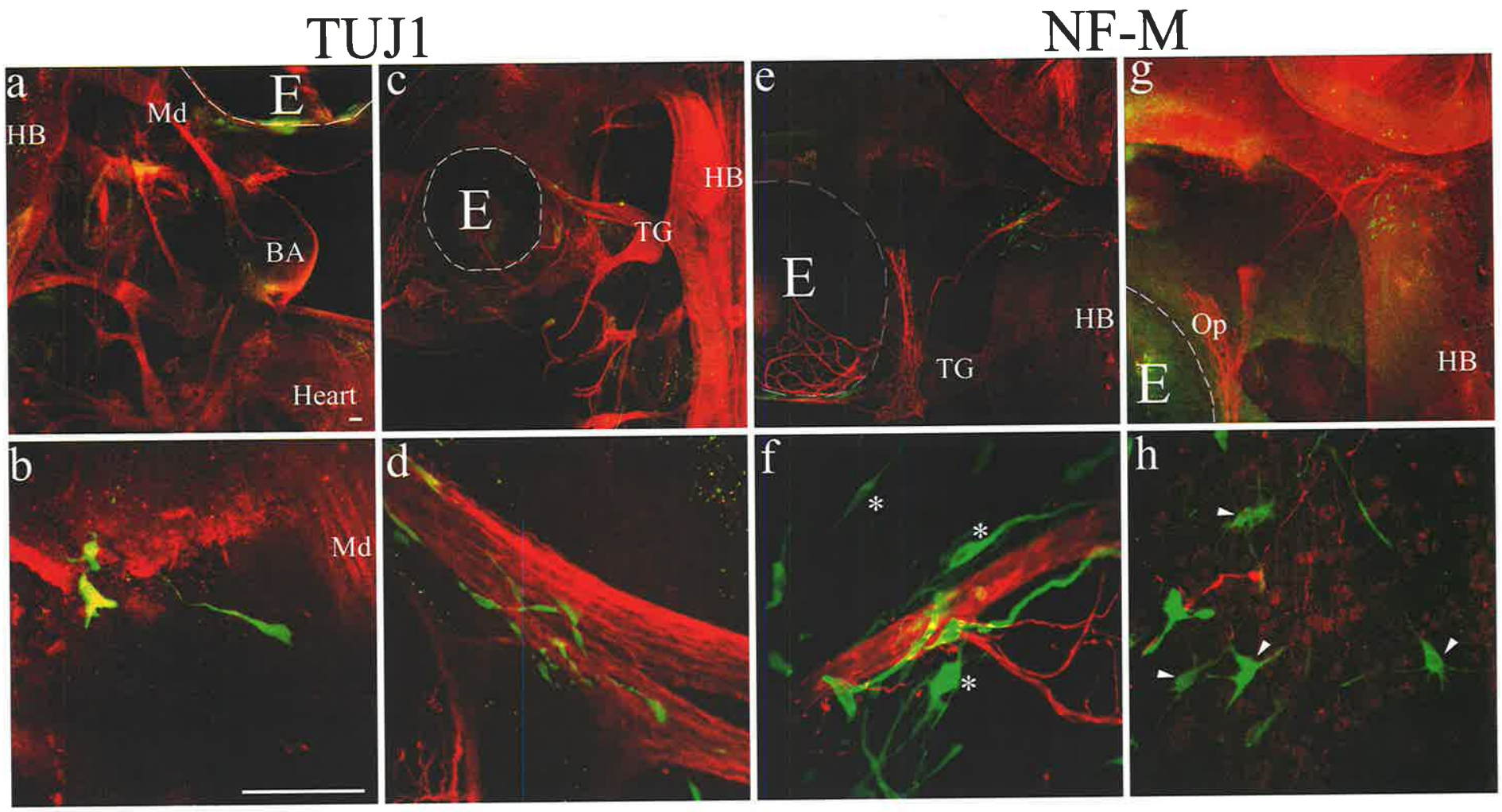
TUJ1
NF-M
a
Md
E
HB
BA
Heart
c
E
HB
TG
e
E
HB
TG
g
Op
E
HB
b
Md
d
f
*
*
*
h

To validate that the response of DPSC to the *in vivo* neural environment was specific to this cell type, alternative SC populations, SHED and BMSSC, and SFB were also investigated under the same conditions. Human SHED and BMSSC have previously been compared to DPSC, where all three SC types have been identified using the same early MSC markers, STRO-1 and CD146, despite their different tissue distributions (Miura et al., 2003; Shi et al., 2001). SFB were utilised to determine whether the migratory pathway followed by DPSC was specific to this population or whether all ectodermal derived cells were able to respond to the same embryonic environmental cues. All cell types were injected using the same method as described for human DPSC and then stained for either TUJ1 (Fig. 5.10) or NF-M (Fig. 5.11). SHED cells, which are most similar to DPSC, also responded in a similar manner to DPSC, where SHED cells migrated closely to the axons of the TG (Fig. 5.10c-d). BMSSC, originating from the mesodermal germ layer, exhibited a distinctly different morphology. BMSSC generally aggregated together (Fig. 5.10e-f), however, the few BMSSC that were mobile, tended to migrate into the CNS (Fig. 5.11e-f) rather than following the CNC migration pathway. Whilst SFB were found to migrate in the avian embryo, their migration appeared to be orientated towards the epidermal layer of the embryo rather than within the CNS or PNS or along axonal processes of the TG. These observations suggested that DPSC and their SHED counterparts specifically responded to endogenous migratory cues and followed neural CNC pathways, while BMSSC and SFB appeared to migrate indiscriminately.

5.2.3.2 DPSC traverse along non-neuronal CNC migratory pathways towards the heart

Injected DPSC were also observed to migrate to other regions within the embryo by 48 hours (Fig. 5.8c, Fig. 5.11a) and later, 72 hours (Fig. 5.9a, b) PI. In these studies only DPSC appeared to have migrated towards the heart, although this was observed in only a limited number of embryos (19%; n = 39/206). The migration to the heart was not detected for any of the other cell types investigated. This response by DPSC could be attributed to endogenous environmental cues, where some CNC cells from the third and fourth branchial arches contribute to the formation of large blood vessels of the common carotid arteries and the systemic aorta (Douarin et al., 1999f; Tallquist et al., 2003).

5.2.3.3 Transplanted DPSC differentiate into neuronal derivatives in the CNS and PNS of the avian embryo

To demonstrate that DPSC were able to respond to endogenous neural environmental cues and differentiate into neurons *in vivo*, embryos injected with GFP expressing DPSC were counterstained with neural markers 24 hours (Fig. 5.7), 48 hours (Fig. 5.8) and 72 hours (Fig. 5.9) PI. Few DPSC were found to co-localise with the early neuronal marker TUJ1 24 hours PI (Fig. 5.7c-d). However, at 48 hours PI, DPSC displayed the morphology of bipolar cells (Fig. 5.8b, asterisk) and neurons with multiple neurites (Fig. 5.8b, d, arrows), where the latter described DPSC appeared to have migrated into the CNS. The possibility of the neuronal multiple neurite morphology being attributed to multiple GFP expressing DPSC is highly unlikely as the images presented are a composite of merged z-series confocal images. Significantly, the DPSC that displayed the multiple neurite morphology also co-localised with both early and mature neural markers, TUJ1 (Fig. 5.8a-b) and NF-M (Fig. 5.8c-d", arrows), respectively. NF-M was lowly expressed (Fig. 5.8d'-d", arrows) by the differentiated DPSC in comparison to GFP staining. Structures reminiscent of growth cones were also observed with NF-M staining, suggesting that these DPSC cells had differentiated into neurons (Fig. 5.8c-d, asterisks), which appeared similar to endogenous axonal processes.

Transplanted embryos at 72 hours PI were analysed to determine whether further incubation with endogenous neural differentiation factors resulted in the progression of DPSC neural differentiation. DPSC survived and displayed bipolar processes when in close proximity to endogenous sensory axons (Fig. 5.9c-f asterisks), while exhibiting multi-neurite processes when localised to the CNS (Fig. 5.9g, h arrowheads). These observations were consistent with the 48-hour time point. However, due to the large size of the embryo at stages 24-26, there were technical difficulties in staining and imaging the embryos in whole-mounts. The intensity of the GFP signal was very strong, while NF-M staining was very weak, thus co-localisation was difficult to ascertain. Therefore, subsequent investigations were carried out at 48 hours PI.

Interestingly, injected SHED cells displayed bipolar neuron morphology 48 hours PI, co-staining with TUJ1 (Fig. 5.10c-d), consistent with the response of DPSC. Conversely, BMSSC within the CNS exhibited a distinctly different morphology that did not appear neuronal. For the BMSSC population dendritic processes were occasionally observed, where

the majority of cells displayed a large irregular shaped cytoplasm, consistent with the undifferentiated mesenchymal morphology (Fig. 5.11e-f). Although the morphology of SFB was thin and spindle-like, similar to bipolar neural cells, GFP labelled SFB did not localise with either TUJ1 (Fig. 5.10g-h) or NF-M (Fig. 5.11g-h) at 48 hours PI.

5.2.3.4 Avian embryo trigeminal ganglia axonal processes migrate towards transplanted DPSC

The TG is a bi-lobed structure in the avian embryo and consists of three axonal branches: the ophthalmic, maxillary and mandibular branch (Fig. 5.6d). The ophthalmic branch migrates above and below the eye, with the maxillary and mandibular branches of the second lobe migrating into the first branchial arch. These axonal processes navigate to their correct location in response to chemo- and contact-dependent guidance cues as represented in the schematic (Jayasena et al., 2005) (Fig. 5.12a).

Interestingly, while it was demonstrated that injected DPSC traversed along established axonal processes, it was also observed on a number of occasions (32%; n = 27/86) that additional endogenous axonal processes had migrated towards injected DPSC 48 hours PI (Fig. 5.8a, Fig. 5.10a, Fig. 5.12b-e asterisks). Changing the location of the injected DPSC, above (Fig. 5.12a-c) or below (Fig. 5.12d) the TG, did not alter the response of endogenous axons to migrate towards the cells. In a number of embryos injected with DPSC, a fourth axonal process migrated from the TG towards the DPSC (Fig. 5.12b, d, e). At other times established axonal processes, such as the ophthalmic nerve, which normally migrates above and round the eye, migrated in the opposite direction towards the injected DPSC (Fig. 5.12c asterisk).

The migration of additional endogenous axonal processes was also seen when SHED were transplanted into the embryo (Fig. 6.6c-d), albeit at a lower frequency than DPSC (20%; n = 3/15). Conversely, there was no detection of endogenous axonal processes migrating towards the injected BMSSC (Fig. 5.11e-f, 5.12e-f). Nor did any endogenous axonal processes deliberately navigate towards the injected SFB (Fig. 5.11g-h, 5.12g-h). These observations suggested that the neural morphology and attraction of endogenous axonal processes observed with DPSC and their SHED counterparts were specific to that SC type, rather than SC or ectoderm derived cells in general.

Figure 5.10 Neuronal differentiation in response to endogenous environmental cues was specific to human adult DPSC or those derived from deciduous teeth following 48-hour incubation.

(a-b) As previously observed DPSC (green) co-localised with β-tubulin III clone, TUJ1 (red), displaying neural morphology, (c-d) SHED (green, n = 6) also co-localized with TUJ1 (red), while (e-f) BMSSC (green, n = 15) nor (g-h) skin fibroblasts (green, n =6) appeared neuronal or localized with β-tubulin (red). All images were compressed confocal z-series. E=eye, HB=hindbrain, TG=trigeminal ganglion. Scale Bar = 100μm (a,e,g)(c)(b,d,f,h).

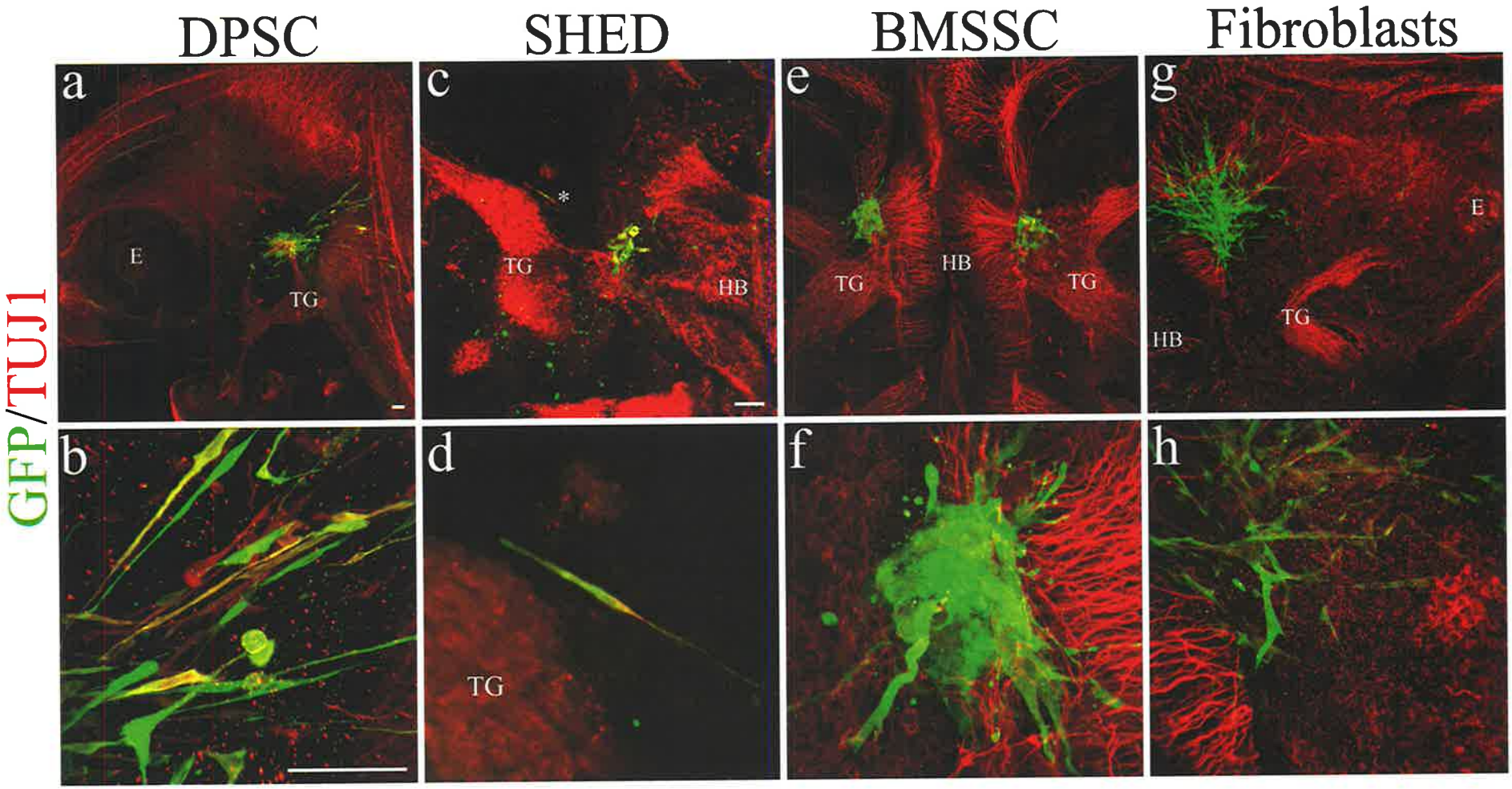
DPSC
SHED
BMSSC
Fibroblasts
GFP/TUJ1
a
b
c
d
e
f
g
h
E
TG
HB
*

Figure 5.11 Following injection into the avian embryo, SHED respond in a similar manner to DPSC.

(a-b) DPSC (green), (c-d) SHED (green, n=8), (e-f) BMSSC (green, n = 19) and (g-h) skin fibroblasts (green, n = 7) were injected into the avian embryo and incubated for 48 hours, then stained with neurofilament (red). (c-d) Addition trigeminal axonal process was observed in the presence to SHED as shown for DPSC. (e-f) When BMSSC survive and migrate to the CNS they do not differentiate into neurons nor do they express neural markers, (g-h) while skin fibroblasts are able to migrate and do display spinal-like processes, these to not localize with neurofilament, the skin fibroblasts as appear to be in a different plane to neurofilament positive cells. All images were compressed confocal z-series. E=eye, HB=hindbrain, TG=trigeminal ganglion. Scale Bar = 100μm.

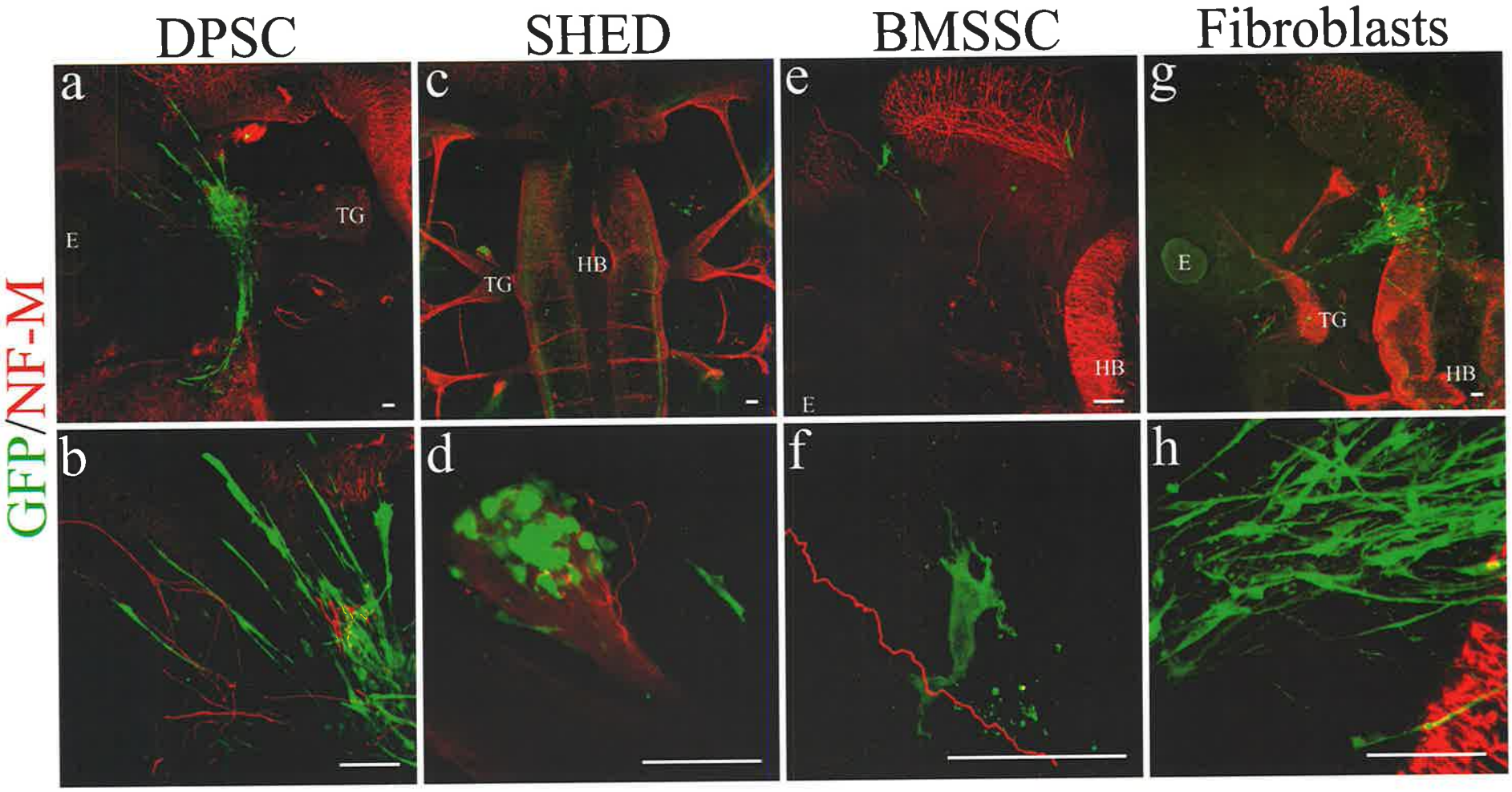
DPSC
SHED
BMSSC
Fibroblasts
GFP/NF-M
a
b
c
d
e
f
g
h
E
TG
HB
TG
HB
E
E
TG
HB

Figure 5.12 DPSC appeared to attract endogenous axonal processes.

(a) Schematic representation of avian embryo, the trigeminal ganglion is bi-lobed, the first lobe, the ophthalmic process (TGop) traverses above and below the eye. The second lobe (TGmm) eventually bifurcates into the maxillary and mandibular processes. These axonal processes migrate in response to neurotrophic factor-3 (NT-3), brain derived neurotrophic factor (BDNF), semaphorin (sema3a, 3f) and EphA/ephrin-A guidance cues, from (Jayasena et al., 2005) (b-e) Forty-eight hours post injection into the avian embryo endogenous trigeminal axonal processes (asterisk) stained with TUJ1 (red) migrated towards injected DPSC (green) regardless of injection site (n = 27). E=eye, HB=hindbrain, TG=trigeminal ganglion. Scale Bar = 200μm.

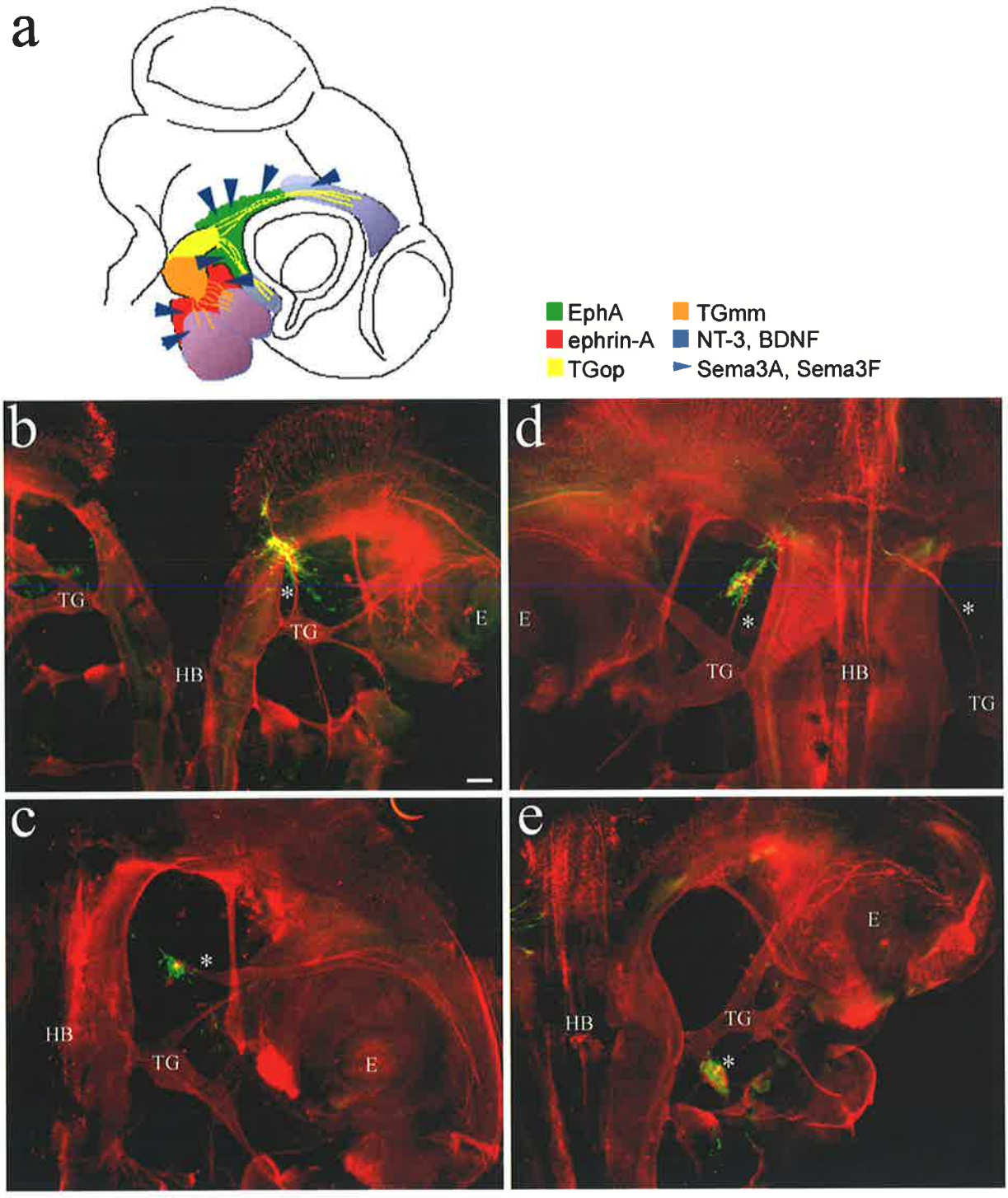
a
EphA
ephrin-A
TGop
TGmm
NT-3, BDNF
Sema3A, Sema3F
b
TG
HB
TG
E
d
E
TG
HB
TG
c
HB
TG
E
e
E
HB
TG

5.3 Discussion

In this chapter the neuronal differentiation potential of adult DPSC was investigated utilising extrinsic growth factors, transcriptional regulation and an endogenous neural environment. The results from all of these approaches suggested that DPSC had neuronal potential. The present study also confirmed the observations of Gronthos and colleagues that DPSC under normal growth conditions possess the ability to differentiate into neural derivatives, albeit at low levels (Gronthos et al., 2002).

5.3.1 *In vitro* neuronal differentiation capacity of adult human DPSC

Many types of neural inductive/maintenance conditions have been investigated and published with slight variations between them, however, most comprise at least EGF, FGF and/or RA (Gritti et al., 1995; Horiuchi et al., 2005; Itoh et al., 1997; Nakayama et al., 2004; Scintu et al., 2006). In the present study, it was important to elucidate which combination of these neural inductive conditions was the most appropriate and efficient for DPSC neural differentiation. Although all media conditions investigated induced neural differentiation to some degree, Media 2 indicated highest *NF-M* gene expression, where NF-M is a mature neuronal marker. Morphologically it appeared that in response to Media A, DPSC produced neurons with multiple processes, consistent with neural differentiation of SHED cells (Miura et al., 2003), while those in Media 2 or 4 were predominantly bipolar. Importantly, Media A consisted of Neurobasal A media and B27 supplement and Media 2 and 4 contained DMEM/F12 Media and ITSS as the supplement, the differing morphology of DPSC in Media A compared to Media 2 maybe attributed to the base media and supplements. Interestingly, while the components differed between Media A and Media 2, similar numbers of NF-M and NF-H expressing cells were produced compared to either MEM or Media 4. Media 2 and 4 contained the most similar factors, with only slight variation to the neural inductive media conditions used for ESC neural differentiation (Smith et al., 2003; Ying et al., 2003). The only difference between Media 2 and Media 4 was RA, cells exposed to media 4 were exposed to RA for 7 days longer than those in Media 2. While RA has been shown to induce neuronal differentiation, the observations of the present study suggested that prolonged expose to RA is not favourable for neuronal differentiation of DPSC.

5.3.1.1 STRO-1 expression may influence neuronal differentiation

DPSC donors either exposed to extrinsic growth factors or stably transduced with NeuroD1, demonstrated differential expression of neural genes. However, DPSC donors varied in their STRO-1 expression, where NHT 5_01 has 30-50% STRO-1 expression, while NHT 1_04 and NHT 15_04 have 3-5% STRO-1. It is proposed that the differential neural gene expression may be attributed to the expression of early mesenchymal stem cell marker, STRO-1. The STRO-1 monoclonal antibody was generated by Simmons and Torok-Storb, who showed that this reagent could identify a cell surface antigen expressed by BMSSC (Simmons et al., 1991). STRO-1 has since been used to select different mesenchymal SC populations (Bensidhoum et al., 2004; Dennis et al., 2002; Gronthos et al., 1994; Seo et al., 2004), including DPSC (Shi et al., 2003). Moreover, previous investigations have shown that continued expression of STRO-1 by BMSSC in vitro appears to maintain a more immature phenotype and function in comparison to stromal cells that exhibited a more differentiated phenotype corresponding to a loss in expression of STRO-1 (Gronthos et al., 1999; Martens et al., 2006; Stewart et al., 1999).

Interestingly, NeuroD1 over-expressing NHT 5_01 (high STOR-1) cells demonstrated an increase in the early neuronal marker, *β-tubulin III*, gene expression, but not for the mature marker *NF-M*, while NHT 1_04 (low STRO-1) NeuroD1 transduced cells appeared to display higher levels of early and mature neuronal markers. As with NeuroD1 transduced donors, the response of DPSC varied in the differing media conditions, which also correlated with STRO-1 expression levels. The response of DPSC exposed to extrinsic growth factors was consistent to the findings of NeuroD1 transduced DPSC. Interestingly, low STRO-1 expressing donors decreased their expression of early neuronal marker, while up regulating gene expression of mature neuronal marker *NF-M*. Conversely, the high STRO-1 expressing donor displayed an unchanged level of *β-tubulin III*, and although NF-M was up regulated it was less than for either of the low STRO-1 donors. This observation suggests that low STRO-1 expressing donors potentially differentiate into more mature neurons than the high STRO-1 expressing donor. However, to confirm that functional neurons can be generated *in vitro*, functional action potential studies need to be conducted.

Although the function of STRO-1 is unclear, the results of this study are consistent with the findings that the level of STRO-1 expression by DPSC appears to influence neuronal differentiation. It was postulated that the low STRO-1 expressing DPSC could be more committed to neuronal differentiation than high STRO-1 expressing DPSC.

5.3.2 Exposure of DPSC to an endogenous neural environment

In this study, the *in vivo* neural differentiation potential of DPSC was established utilising the avian embryo model, which was termed the 'Ikaros Assay'. Forty-eight hours PI into the avian embryo, DPSC expressed neural markers and displayed a neuronal morphology. The Ikaros Assay is a rapid, robust, and reliable model organism to investigate the neural differentiation potential of adult human DPSC. Transplanted DPSC expressed neuronal markers within 48 hours PI, indicating the timely response of DPSC to endogenous environmental cues. Furthermore, the robustness and reliability of the assay was demonstrated with over 200 embryos injected with either adult human DPSC, other human SC or ectodermal cell types, which survived for the duration of the experiments at 24, 48 or 72 hours. This is the first study to have successfully engrafted adult human SC populations into the avian embryo. *In vivo* neural differentiation experiments investigating the integration of grafted cells have predominantly been conducted in the rodent brain, for prolonged periods rather than days (Arnhold et al., 2006; Nosrat et al., 2004; Uchida et al., 2000). This model could be expanded further to investigate additional questions that have arisen from this study, such as which factors mediate DPSC migration and differentiation, or which factors are involved in the migration of endogenous axons towards injected DPSC?

5.3.2.1 Differentiation potential of human adult DPSC

From a therapeutic perspective, DPSC and SHED may be more adaptable and responsive to the surrounding neural environment than other SC types. The location of DPSC within the embryo appeared to be important for their specific neural morphology and differentiation capacity. DPSC located near sensory TG neurons displayed a bipolar morphology, whereas in the CNS, DPSC exhibited multi-dendritic processes and in the heart demonstrated a strikingly different, splayed morphology. These observations suggest that DPSC could respond to the cues of the microenvironment and differentiate into the appropriate neuronal

cell types. Consistent with the cell derivatives observed for DPSC, CNC differentiated into multiple cell types in response to the microenvironment. These cell types included sensory neurons of the PNS, Schwann cells, melanocytes, cartilage and CNC also contribute to major blood vessels within the heart (Bronner-Fraser, M., 1995; Douarin et al., 1999a; Graham et al., 2004). The observations of the present study demonstrated DPSC survival and differentiation potential 72 hours PI. However, to definitely demonstrate that DPSC are an appropriate candidate for SC therapy-based treatment for neurological diseases, DPSC survival, neuronal differentiation and integration into neuronal networks within the chicken embryo would be required. Therefore follow up long term incubations of DPSC exposed to the chicken embryo neuronal microenvironment would be vital.

Furthermore, while it is not common for CNC to exhibit CNS neural morphology, Bronner-Fraser and colleagues have observed that neural crest cells exhibit the capacity to differentiate and express markers specific for neurons of the CNS, when transplanted into the ventral neural tube (Ruffins et al., 1998). The study demonstrated that neural crest cells are flexible in their fate, by retaining the ability to respond to local environmental factors rather than being committed to a specific fate, even after migrating from the neural tube. It has been proposed that neural crest and neural tube derivatives originate from the same precursor within the dorsal neural tube, which contributes to both CNS and PNS derivatives (Bronner-Fraser, M., 2002). If DPSC do retain neural crest properties, it is not surprising then, that DPSC displayed characteristics of both PNS and CNS neurons in response to the environmental cues.

5.3.2.2 Correlation between the migration of CNC and human adult DPSC

Guidance cues dictate the direction cells migrate. The guidance cues that mediated the migration of engrafted DPSC to specific regions within the avian embryo were of particular interest. It appeared that DPSC followed recognised CNC pathways, whereas BMSSC and SFB failed to do so. Confocal imaging demonstrated DPSC near axonal processes of the TG, migrating towards branchial arches and the heart, analogous to the migration pathways of CNC (Baker et al., 1997). Thus it may be postulated that DPSC could respond to the same cues as endogenous CNC cells. More specifically, this thesis has established that DPSC are responsive to Eph/ephrin guidance molecules (chapters 3 and 4), which are essential for correct migration of neural crest cells (Baker et al., 2003; Santiago et al., 2002) and their

axonal processes (Jayasena et al., 2005). Eph/ephrin molecules, although important, mediate their response through cell contact (Himanen et al., 2003). Alternatively, chemotaxis factors may influence DPSC migration in the avian embryo. Semaphorin family of guidance molecules (Gammill et al., 2006; Lillesaar et al., 2004; Ulupinar et al., 1999), and neurotrophic factors such as BDNF (Douarin, M., 1988; Lindsay et al., 1985; Sieber-Blum et al., 1993; Zhou et al., 1998), are present during CNC migration. This is represented in the schematic of guidance molecules involved in TG axonal process migration, Fig. 5.12a, modified from (Jayasena et al., 2005). Curiously, only SHED displayed similar migratory and differentiation capacity to DPSC, while BMSSC and SFB did not. It could be speculated that SC isolated from the pulp are more responsive to cues in the developing avian embryo, or that factors responsive to these guidance molecules are uniquely expressed by SC isolated from the dental pulp, or perhaps other craniofacial tissue.

It was surprising, however, that DPSC and BMSSC did not exhibit a similar migratory path, considering a microarray study comparing gene expression between DPSC and BMSSC indicated that of the 10% of known human genes present on the microarracy filter, DPSC and BMSSC expressed the same repertoire of genes, with few genes expressed at differential levels (Shi et al., 2001). Genes highly expressed by BMSSC included collagen type I and insulin-like growth factor binding protein 7 (IGFBP7). DPSC highly expressed six genes including collagen type XVIII, Insulin-like growth factor 2 (IGF2), Discoidin domain tyrosine kinase 2 (DDR2), NAD(P)H: menadione oxidoreductase (NMOR1), Homolog 2 of Drosophila large disk (DGL) and cyclin-dependent kinase (Shi et al., 2001).

The high expression of the above-mentioned genes expressed by DPSC and BMSSC further supports the notion of DPSC as a potential cellular source for SC therapy-based treatment. The greater proliferation potential of DPSC over BMSSC, may be attributed to the up-regulation of IGF2 and CDK6, where BMSSC proliferation was up to 28% lower than for DPSC (Shi et al., 2001). Furthermore, the migration capacity of DPSC and SHED in the chicken embryos was more prevalent compared to BMSSC, which often clustered together. Extensive BMSSC migration was rarely observed, although when BMSSC did migrate, it seemed to be random within the CNS. This difference in migration responses between the two SC types may be attributed to the differential expression of the above-mentioned genes or alternatively, the origin of the different SC populations.

5.3.2.3 Attraction of endogenous axonal processes towards engrafted human adult DPSC

The migration and differentiation capacity of DPSC is both interesting and exciting. Serendipitously, DPSC exhibited the capacity to attract endogenous axonal processes towards them. Again, this observation was seen with SHED, but not with BMSSC or SFB. It could be postulated that DPSC that expressed higher levels of Collagen XVIII and/or DDR2 (Shi et al., 2001), which interact with a number of growth factors, their receptors and adhesion molecules (Iozzo, V., 2005; Vogel et al., 2006), could be attracting endogenous axons towards the DPSC. Furthermore, the axonal processes that were attracted towards the DPSC and SHED from the TG, were either a newly generated branch or an existing branch redirected in its development towards the transplanted DPSC. These observations suggest that the additional axonal outgrowths originated from endogenous axons and not the transplanted DPSC. While, these observations appear convincing, DiI labelling of endogenous axons would determine the origin of the additional processes.

Although the specific factors expressed by DPSC, that are responsible for the attraction of endogenous axons are not known, the response of TG axons to endogenous guidance factors may provide insight on this aspect. During normal TG migration, TG axons are responsive to a number of guidance factors including BDNF, NT-3 and semaphorins, as well as Eph/ephrin molecules, as represented in schematic Fig. 5.12a, (modified from (Jayasena et al., 2005)). More specifically, TG axons enter the dental pulp at late stages of tooth development, during and after tooth eruption (Fristad et al., 1994) and are responsive to soluble factors expressed within the pulp tissue (Lillesaar et al., 1999). A number of guidance molecules, both inhibitory and permissive, are expressed during this time and are believed to be required for correct TG axonal migration into the pulp. Such factors include semaphorins, NT-3 and NT-4, NGF, p75, TrkA, BDNF, and GDNF, SDF-1 (Lillesaar et al., 1999; Lillesaar et al., 2004; Luukko et al., 1997; Matsuo et al., 2001; Nosrat et al., 1998; Nosrat et al., 1997; Nosrat et al., 1996; Pan et al., 2000). It could be suggested that following DPSC engraftment, TG axonal processes were responsive to guidance factors expressed by DPSC that may have normally attracted them to the dental pulp tissue *in situ*. However, *Aves* do not produce teeth (Huysseune et al., 1998), only remnants of them. This implies that the factors secreted by DPSC may be highly conserved between species, and that the TG axonal processes could potentially be induced to navigate towards a presumptive tooth or in this case, transplanted DPSC. It has been shown previously that while *Aves* do not express BMP-4, a critical factor

required for odontogenesis (Chen et al., 1996; Ohazama et al., 2005; Peters et al., 1998; Tucker et al., 1998), exogenous BMP-4 induction activated down-stream factors required for tooth formation. This resulted in additional epithelial appendages (Chen et al., 2000), which supported the suggestion that latent signalling pathways may be reactivated.

Alternatively, Nosrat and colleagues have shown that *in vivo* adult DPC express neurotrophic factors (NF), including NGF, BDNF, and GDNF, which were up-regulated during cell culture. *In vitro*, these NF expressing DPC attracted neurons from trigeminal explants. Additionally, severed TG axons survived and migrated towards subcultured DPC. Therefore, DPC were able to assist in the survival of damaged axonal processes *in vivo* (Nosrat et al., 2001). Although the expression of NF has not been deciphered for DPSC specifically, these SC may act in a similar manner to DPC, possibly attracting endogenous TG axons towards them in response to NF.

Furthermore, if DPSC were to display NF characteristics similar to DPC, then DPSC could also aid in the survival, migration or replacement of damaged or dead neurons following injury. Whilst beyond the scope of the present thesis, the data presented in this study will help develop future strategies to determine the factors expressed by DPSC and SHED, which cause the attraction of endogenous axonal processes.

Chapter 6 - Concluding Remarks

6.1 Summary

DPSC were isolated in 2000 at the National Institutes of Health, Bethesda, USA by Dr. Gronthos and colleagues (Gronthos et al., 2000). Whilst the origin of DPSC is unknown, these SC may be derived from cranial neural crest derived mesenchyme (Imai et al., 1996; Miletich et al., 2004). Supportive evidence comes from reports showing that the pulp and dentine retain cranial neural crest markers in the adult (Chai et al., 2000; Miletich et al., 2004). However, DPSC were originally isolated using early mesenchymal stem cell/vascular markers, STRO-1 and CD146, also used to isolate BMSSC (Gronthos et al., 2000), where BMSSC are thought to be mesodermal derived. Given the wide spread distribution of STRO-1 and CD146 in different tissues (Bianco et al., 2001) it is likely that these markers are not limited to cells derived from one specific embryonic germ layer.

A limited number of studies have been published investigating the differentiation potential of these stem cells. DPSC are a diverse stem cell population, with the ability to recapitulate a developing tooth-like structure following sub-cutaneous transplantation into nude mice. This implies that DPSC could contribute to tooth repair following injury. DPSC also have been shown to be a multipotent SC population, expressing markers associated with fat-laden adipocytes and neural precursors (Gronthos et al., 2002). However, there is limited knowledge as to the neural capacity of DPSC (Gronthos et al., 2002; Gronthos et al., 2004). The diverse potential of DPSC, suggests that they may be a useful SC source for SC therapy based treatment for different tissues. The present study examined factors that regulate DPSC migration and retention in the pulp tissue and factors that mediate neuronal differentiation of DPSC.

The bacterial degradation of the dentine matrix also known as caries, is often repaired in the clinic by replacing the dead or damaged tissue with artificial material rather than replacing the tissue with viable cells. As DPSC have been shown to differentiate into all cell types of the dentine/pulp complex (Gronthos et al., 2002), the question arises as to why the tooth is unable to completely repair the caries themselves? One possibility is that DPSC are not able to reach and repair the damage in sufficient time. Tecles and colleagues indicated that BrdU positive

proliferating cells required up to four weeks to migrate to the injury site (Tecles et al., 2005). While this is a considerable amount of time, it is clear that these cells do have the capacity to respond to guidance signals. The findings of this study have demonstrated that B-subclass Eph/ephrin molecules are differentially expressed by DSPC and the surrounding pulp tissue under steady-state conditions, while down-regulation of ephrin-B1 following injury may assist in the migration of DPSC following injury. This information could contribute to the development of treatments that target Eph/ephrin expression in order to induce an earlier migration of DPSC to the injury site and potentially tooth repair. However, investigations into other chemo-attractive guidance molecules would also be beneficial.

The second aspect of this thesis focused on the neural potential of DPSC, which could lead to their possible role in repair following neural damage. This study confirmed *in vitro* and *in vivo* that DPSC have neural differentiation capacity. DPSC appeared to respond and behave similar to CNC cells following transplantation into the avian embryo, supporting the possibility for the neural crest origin of DPSC.

Furthermore, it was observed that endogenous axonal processes were stimulated to migrate towards the transplanted DPSC, where BMSSC and SFB were not able to elicit the same response following transplantation. It is known that DPC express a number of neurotrophic factors that maintain the survival of severed spinal cord neurons, where the spinal cord processes migrated towards the transplanted DPC (Nosrat et al., 2001). Although DPC and DPSC are cultured differently, they may contain a similar population of cells. It is proposed that DPSC may be a subpopulation within the heterogeneous DPC population. Potentially, DPSC may also express the same neurotrophic factors, and thus attain another important characteristic, cell survival. However, neurotrophic factor expression and cell survival of DPSC requires further investigation.

From the analysis of this thesis it is postulated that DPSC are a suitable source of SC to pursue investigation for SC therapy-based treatment following injury. More specifically, DPSC could function to maintain the survival of damaged neurons and subsequently replace dead neurons following neural trauma, such as stroke.

6.2 Future Directions

6.2.1 Are DPSC able to migrate to an injury site within the tooth and contribute to tooth repair?

Following injury it has been documented that BrdU positive cells migrate towards the injury site (Tecles et al., 2005). While it has been speculated that these BrdU positive cells are DPSC, this has not been shown conclusively. Therefore, it would be pertinent to repeat the tooth injury model described by Tecles and colleagues and co-stain with BrdU and DPSC stem cell markers STRO-1 and CD146, in order to confirm whether the BrdU positive cells express a phenotype consistent with DPSC. Moreover, functional studies could provide insight into the factors that mediate DPSC mobilisation and responsiveness following injury.

The observations of this study have indicated that Eph/ephrin interactions may restrict DPSC to their niche under steady state conditions in the pulp. The *in vivo* tooth injury model outlined by (Tecles et al., 2005) could be utilised further to incorporate the association of Eph/ephrin interactions by DPSC by the addition of EphB-Fc or ephrin-B-Fc molecules in the media. Therefore it could be speculated that incubating damaged teeth in a solution containing ephrin-B1-Fc would result in decreased DPSC migration. Conversely, the incubation of injured teeth with EphB1-Fc, may result in increased proliferation and enhanced migration. These experiments would help define whether Eph/ephrin guidance molecules contribute to DPSC migration, proliferation and differentiation following tooth injury.

A number of other guidance molecules, growth factors and ECM molecules are expressed within the pulp tissue. Previous studies (Lillesaar et al., 2004) have reporteded that semaphorin molecules, which mediate an inhibitory guidance signal, repel TG axons during tooth development, although the response in DPC or DPSC to semaphorins has not been investigated. Other molecules such as endothelin (Casasco et al., 1994), PDGF, IGF-1 (Denholm et al., 1998), TGF-β1 (Shirakawa et al., 1994) and basic FGF (Shiba et al., 1995), have been shown to increase DPC proliferation. The pulp expresses mRNA for all neurotrophins, including nerve growth factor and GDNF, which enhance TG axonal migration

(Lillesaar et al., 2003; Lillesaar et al., 2001; Lillesaar et al., 1999; Nosrat et al., 2004). Furthermore, cytokine and chemo-attractant SDF-1, expressed by DPSC (personal communication Dr. Gronthos), have previously been shown to influence migration of endogenous stem cells under normal conditions and towards an injury site (Claps et al., 2005; Pituch-Noworolska et al., 2003). To further augment DPSC proliferation and migration to the injury site, the tooth injury model could be utilised to investigate DPSC responsiveness to these and other factors.

6.2.2 What is the differentiation and migration capacity of human adult DPSC in the avian embryo?

During this study the avian *in ovo* transplantation model was used to determine the neural potential of human DPSC. This study provided interesting and exciting results, indicating that DPSC were able to survive, migrate and differentiate in the avian embryo. However, the avian embryo experiments raised a more complex question. Which guidance factors are DPSC responding to in the avian embryo? What factors do DPSC express that attract avian axonal processes towards them? Into which specific neural cell types are DPSC differentiating? Are these cells functional and can they integrate into neural networks?

The avian embryo is an excellent model organism to examine these questions. The location and morphology of transplanted DPSC within the avian embryo suggest a range of neural crest derivatives, including sensory neurons, neurons of the CNS, possibly Schwann cells that myelinated axonal processes and cardiac cell types. Transplanted embryos would undergo immunohistochemical analysis, using specific markers to confirm these cell types. Some of these markers would include stage specific embryonic antigen 1 (SSEA1) and SSEA4, which are specific markers for spinal sensory neurons and expressed by neural crest in the quail embryo (Sieber-Blum, M., 1989a; Sieber-Blum, M., 1989b). Peripherin is an intermediate filament that belongs to the same family as GFAP; peripherin is not only expressed by sensory neurons of the PNS, but also neurons of the CNS (Escurat et al., 1990; Rhrich-Haddout et al., 1997) and by neural crest. More specifically, to detect efferent neurons an antibody against inhibitory neurotransmitter, gamma-aminobutyric acid (GABA) (Fabian-Fine et al., 2000; Fabian-Fine et al., 1999) would be used. To detect Schwann cells, Schwann cell myelin protein (SMP) antibody, expressed at early stages of Schwann cell differentiation

would be used (Dulac et al., 1988). While cardiac specific antibodies GATA4 and troponin were investigated (data not shown), neither was expressed within the avian embryo, or could be detected by transplanted DPSC. Other cardiac specific markers that would be examined include myosin, light or heavy chain and myoglobin.

Chicken embryo explants are a very powerful tool to analyse the contribution of specific factors, involved in explicit processes. The embryo is removed from the egg and grown on a millipore membrane bathed in media (Krull et al., 1995); specific factors are added to the media to inhibit the function of the particular molecule or process. This explant experiment has been used previously to demonstrate that neural crest cells and motor axons migrate through the rostral half of each somite, in response to the inhibitory signal of ephrin-B1, expressed in the caudal half somite (Koblar et al., 2000; Krull et al., 1997).

There are a number of guidance molecules expressed in the avian embryo to which DPSC could be responsive. Candidate molecules include Eph/ephrins, semaphorin family members, neurotrophin and BDNF (Jayasena et al., 2005). Neural crest cells migrate along Eph/ephrin established migratory paths (Baker et al., 2003; McLennan et al., 2002; Smith et al., 1997), where the present study has demonstrated that DPSC are also responsive to Eph/ephrin molecules. To determine whether DPSC interact with Eph/ephrin molecules *in ovo*, cells would be injected into the embryo, the embryo would then be placed on the millipore membrane, bathed in media containing EphB-Fc or ephrin-B-Fc for 48 hours, and then undergo immunohistochemical analysis (Fig. 6.1). Furthermore, to verify the signalling pathways required for DPSC migration *in vivo*, explanted embryos would be incubated in the presence of MAPK inhibitor U0126, involved in Eph forward signalling, or PP2 implicated in ephrin-B reverse signalling.

The explant assay would also be used to determine the factors responsible for endogenous axons migration towards transplanted DPSC. The same experimental design explained above would be employed. Candidate molecules, collagen XVII and DDR2 would be examined initially, as they were more highly expressed by DPSC compared to BMSSC following microarray analysis (Shi et al., 2001). Alternatively, other candidates include growth factors NGF, BDNF and GDNF, which are required for TG axonal migration (Lillesaar et al., 2003; Lillesaar et al., 1999; Lillesaar et al., 2004; Nosrat et al., 2001) and are expressed by DPC (Nosrat et al., 2004; Nosrat et al., 2001). Inhibitors to these growth factors would be added to

the explant media until the molecule/s responsible for TG axonal redirected migration have been determined. In addition, overexpression and siRNA knockdown experiments for specific genes could be conducted under the same assay conditions. These genetically modified DPSC would then be transplanted into an avian embryo, to demonstrate that endogenous axonal processes migrate appropriately. This information would provide a better understanding of how DPSC may contribute to the survival or migration of endogenous nerves to potential sites of injury, to help improve functional recovery following neural injury, such as stroke.

6.2.3 Are DPSC able to differentiate into *bono fide* neurons in response to neural inductive culturing conditions?

Many studies have been conducted investigating the neural properties of a specific SC type when exposed to neural inductive conditions containing factors such as EGF, FGF and/ or RA. This study demonstrated that a combination of EGF, FGF and RA were required to attain a neural morphology and expression of neural specific markers. Alternatively, retro-viral transduction with transcript factors NeuroD1 or NeuroD2 also acquired a neural morphology. However, neither of these approaches to neural differentiation showed irrefutably that these morphologically neural cells were in fact *bono fide* neurons.

Neurons, smooth, skeletal and cardiac muscle are the few cells types that are able to produce an action potential, although others do have the ability to produce a current. Nosrat and colleagues have suggested from their preliminary results that DPC could generate an inward and outward current (Nosrat et al., 2004). Electrophysiology patch clamping is a technique that measures an action potential. This would be essential to demonstrate whether DPSC could differentiate into *bono fide* neurons in response to defined neural-inductive conditions, or following enforced expression of neural inductive transcription factors. These studies would further identify the critical factors important for neural differentiation of DPSC and other SC populations.

Following neural trauma there are a number of events that take place, including an inflammatory response, the removal of debris tissue, expression of neurotrophic factors and cytokines (Ebadi et al., 1997; Liao et al., 2001; Sugiura et al., 2000). For SC therapy-based

treatments, SC would need to be transplanted near to or at the injury site, where SC would be exposed to the array of factors expressed within that area. One possibility to establish neural differentiation and integration of these SC following neural trauma, could be to expose them to factors such as EGF, FGF and RA, to mediate partial neural differentiation prior to transplantation. The neural differentiation/integration process may be accelerated in these pre-neural inductive cultured SC and assist in recovery following injury.

6.2.4 Can DPSC survive and respond to adult neural cues following transplantation into the adult rodent brain?

The origin of this work stems from the interest in using SC in repair/therapy for neural trauma, disorder or disease, eg, stroke. A stroke or an ischaemic brain injury is a cerebrovascular disease, which results from a blood clot in the brain, blocking blood flow between the heart and brain. The cell death caused by lack of oxygen to neural tissue can impair cognitive and motor function. Stroke is the second greatest killer in Australia, with 12,201 deaths in 2001. It is also the leading cause (63,530 Australians) of long-term disability in adults, with an incidence of 40,000 strokes in Australia per year (http://www.aihw.gov.au/cvd/majordiseases/stroke.html). At present there is no cure or repair for stroke suffers, only preventative treatments and maintenance of the condition. Recently studies have been conducted investigating the use of SC as a therapeutic agent to repair damaged areas of the brain. While some have shown functional improvement when transplanted with BMSSC or ESC (Chen et al., 2001a; Chen et al., 2001b; Li et al., 2001; Lindvall et al., 2005; Wei et al., 2005), the present study suggests that DPSC may be a beneficial source of SC. The present study has also shown that DPSC have a greater capacity to survive, migrate and differentiate in response to endogenous environmental cues in the avian embryo, when compared to BMSSC. However, prior to investigating DPSC in a rodent stroke model, it appears more pertinent to confirm that human adult DPSC have the capacity to survive and respond to neural environmental cues in the adult rodent brain. The present study has performed preliminary experiments to confirm DPSC survival and differentiation in the adult rodent brain.

Previous studies have suggested that DPC were able to survive and migrate following six weeks incubation in the adult rat caudate nucleus (Nosrat et al., 2004), while SHED co-

localised with NF-M in response to mouse hippocampal endogenous environmental cues ten days post-transplantation (Miura et al., 2003). Preliminary evidence suggests that adult human DPSC were also able to survive, migrate and differentiate in response to endogenous environmental cues in the adult rodent brain. DPSC from multiple donors were injected into the adult mouse rostral migratory stream (RMS) or hippocampus and incubated for three weeks (Fig. 6.2a). The RMS and hippocampus were chosen because these are regions of neurogenesis in the adult rodent brain (Alvarez-Buylla et al., 2002; Bedard et al., 2002; Kuhn et al., 1996; Peretto et al., 1999; Smith et al., 2001). Normal mice were immuno-suppressed with an immuno-suppressant, cyclosporine A, to avoid rejection of the human cells transplants by the host animal (Nawa et al., 2006). Cyclosporin-A has also been used in other animal studies during xeno-transplantation without any adverse affects (Modo et al., 2002; Vescovi et al., 1999). Pilot studies demonstrated that Cyclosporin-A did not inhibit DPSC survival or proliferation *in vitro* within the range (0.1-1 μg/mL) used in previous xeno-transplanation experiments (Daadi et al., 2001; Modo et al., 2002). DPSC proliferation was significantly increased (Student t-test, $p < 0.05$) at 0.2, 0.4, 0.5, 0.7-1 μg/mL of Cyclosporin-A (Fig. 6.2b), while 5 μg/mL of Cyclosporin-A resulted in cell death, where 5 μg/mL is well in excess of the concentration injected into the mouse.

Following transplantation into the adult mouse brain, DPSC appeared to survive and co-express neural markers including TUJ1, NF, but not glial marker GFAP in both the hippocampus and RMS (Fig. 6.3). However, further experimentation using GFP labelled cells would be required to confirm these observations. In these preliminary experiments, adult human DPSC were identified with human specific Integrin-β1 antibody, as previously described (Gronthos et al., 2002).

6.2.5 Do DPSC have the capability to repair neural damage following stroke in a rodent stroke model?

DPSC, are a readily accessible source of SC isolated from a non-controversial source, predominantly from wisdom teeth, by less invasive methods. These cells show considerable proliferation and neural potential *in vitro* and *in vivo*, and may offer an alternate source of progenitors to ESC, BMSSC and endogenous NSC (Chen et al., 2001a; Chen et al., 2001b; Li

et al., 2001; Lindvall et al., 2005; Wei et al., 2005) for the treatment of neurological conditions.

From our preliminary data, where DPSC appear to survive in the adult rodent brain further studies may investigate the functional recovery of Nude rats that received DPSC therapy over sham controls following induced stroke. Motor and cognitive functions would be assessed using the rotarod test, bilateral asymmetry test and Barnes' circular maze (Stroemer et al., 2005). Thus behavioural testing would be conducted prior to and following stroke induction. The most common type of ischaemic stroke in humans is caused by occlusion of the middle cerebral artery, which leads to loss of many neural cell types: cortical neurons (motor and sensory), interneurons (e.g. GABA-ergic), oligodendrocytes and astrocytes. Therefore, a stroke would be induced in Nude rats by middle cerebral artery occlusion. This procedure involves blocking the blood flow to the brain for a short period of time. Following ischaemia, rats would be given post-operative care, and then undergo neurosurgery to deliver adult human GFP labelled DPSC to the site of injury. The animals would be tested both for functional improvement, with the above-mentioned tests. The integration of human DPSC into the rodent brain would be assessed by histological analysis at a number of time points including one month post injection, followed by two week intervals for a six month period.

Furthermore, if DPSC do not respond as predicted to the endogenous environmental cues, it might be necessary to evoke neural differentiation, by pre-incubating DPSC in neural inductive media prior to transplantation to elicit functional recovery. Once the DPSC population resulting in functional recovery following stroke has been identified in a rodent model, the findings could be examined in a pre-clinical non-human primate model.

Figure 6.1 Outline of the Ikoras Assay

Human adult green fluorescently (GFP) labelled DPSC incubated with –Fc molecules or inhibitors to specific guidance factors (a) were injected into stage 10-12 (Hamburger et al., 1951) chicken embryos. (b) Injected embryos were removed from the egg; the integrity of the vitelline membrane and the orientation of the embryo were maintained. The embryos were washed in Ringer's solution and then placed onto the millipore membrane bathed in Neurobasal A media containing –Fc molecules or specific inhibitors for guidance molecules. The embryos were orientated so that the vitelline membrane was in contact with the millipore membrane. (c) Embryos were incubated for 48 hours in a 5% carbon dioxide incubator. (d) Embryos were imaged in brightfield and (e) fluorescently to identify the injected GFP DPSC. Embryos were fixed and then underwent immunohistochemistry to identify the response of the endogenous axonal processes when inhibiting guidance molecules.

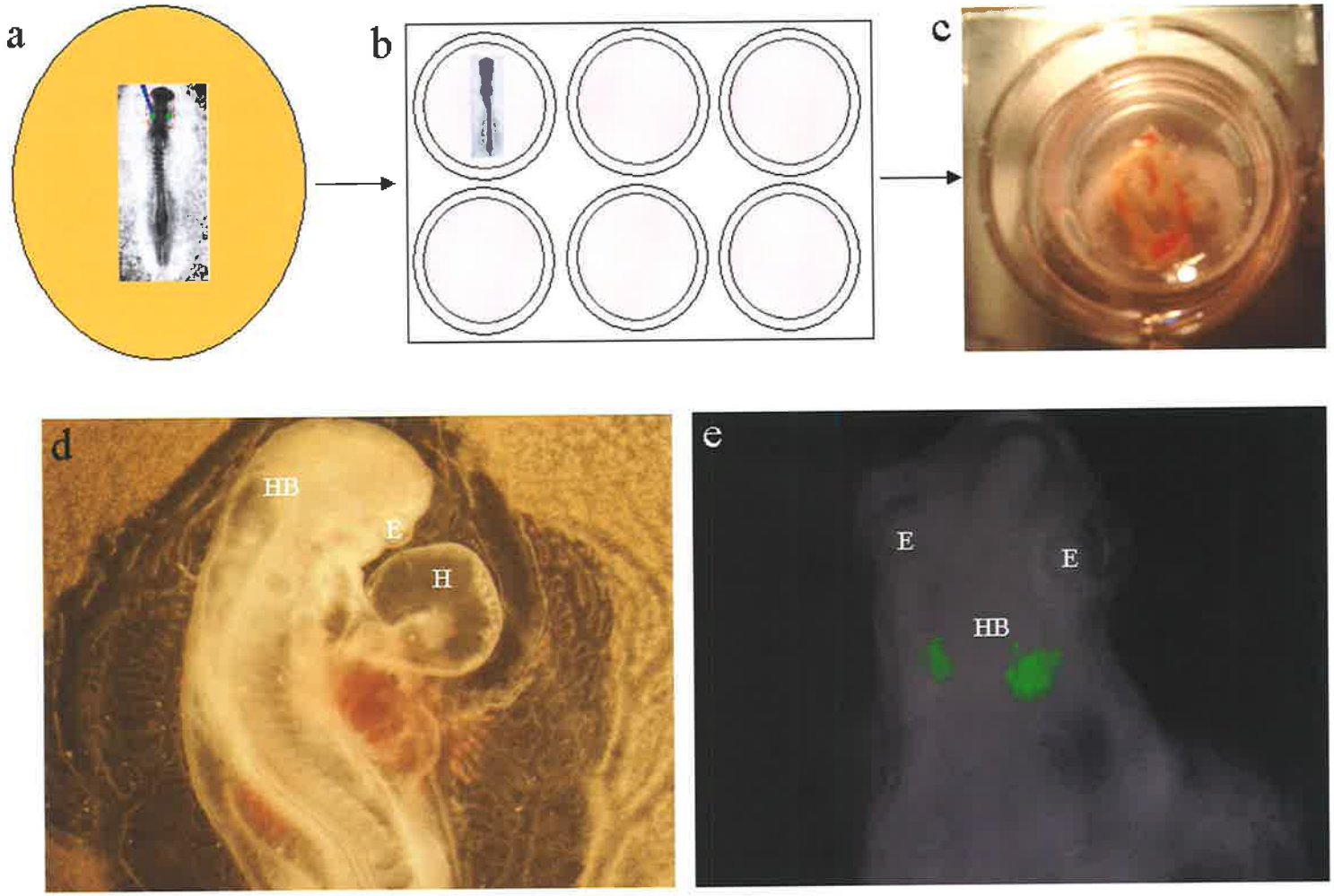
a
b
c
d
HB
E
H
e
E
E
HB

Figure 6.2 Cyclosporin-A does not inhibit DPSC survival in culture.

(a) Human adult DPSC were injected into the rostral migratory stream (RMS) or the hippocampus of the C57black mice. DPSC survival, migration and differentiation were investigated 3 weeks post injection. Mice were injected daily with 10 mg/kg Cyclosporin-A to avoid rejection of human DPSC by the host. (b) Human adult DPSC were cultured in the presence of 0.1-1 and 5 μg/mL Cyclosporin-A for 5 days. Cyclosporin-A at 0.2-1 μg/mL significantly enhanced DPSC proliferation (* = $p < 0.01$; # = $p < 0.05$), while excessive concentrations of Cyclosporin-A at 5μg/mL resulted in cell death.

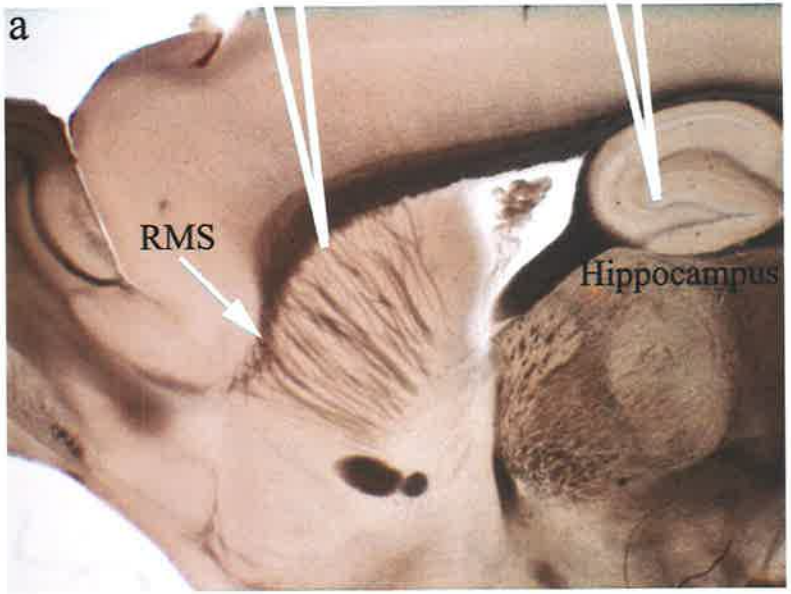

Injection site

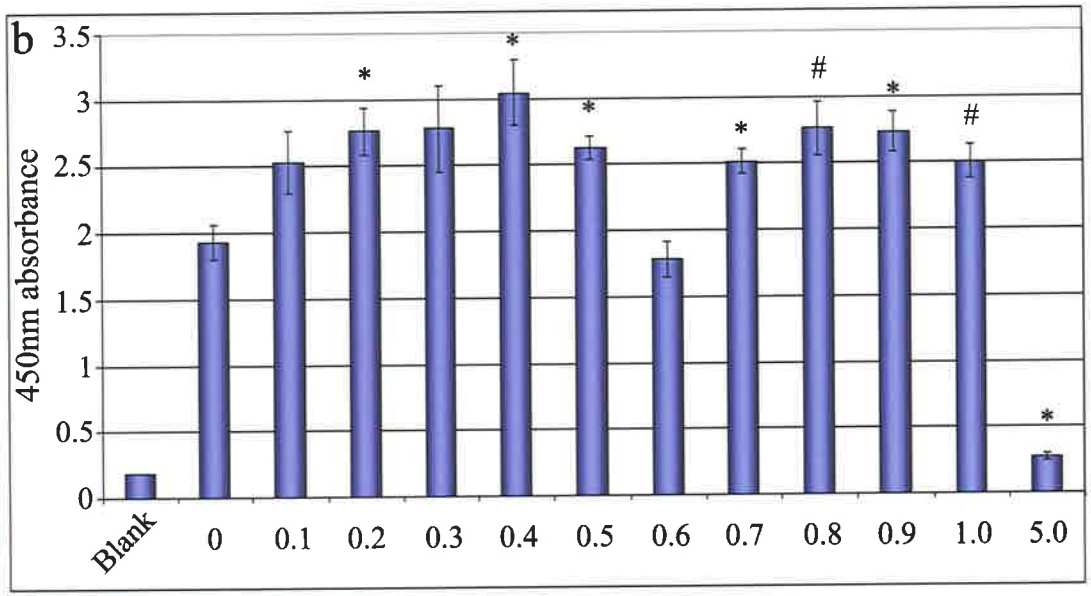

Concentration of Cyclosporin A (μg/mL)

Figure 6.3 DPSC survive for three weeks following injection into the adult mouse hippocampus or rostral migratory stream.

NHT 1_04 DPSC were injected into the hippocampus (a,c,e, arrowhead) or NHT 5_01 DPSC were injected into the rostral migratory stream (RMS) (b,d,f) of C57 black mice. Three weeks post injection, mice underwent transcardial perfusion, brains were vibratome sectioned (100μM) and stained with human specific Integrin-β1 (green) and either β-tubulin III clone, TUJ1 (a-b), Neurofilament, medium (NF-M, c) or heavy (NF-H, d) chain, or GFAP (e-f) (red). Injected DPSC appeared to co-localise with TUJ1 and NF-M in the hippocampus and RMS, but not with NF-H in the RMS or GFAP in the hippocampus. However, it seemed that GFAP positive cell in the RMS engulfed the human specific Integrin-β1 positive DPSC. Scale Bar = 100 μm.

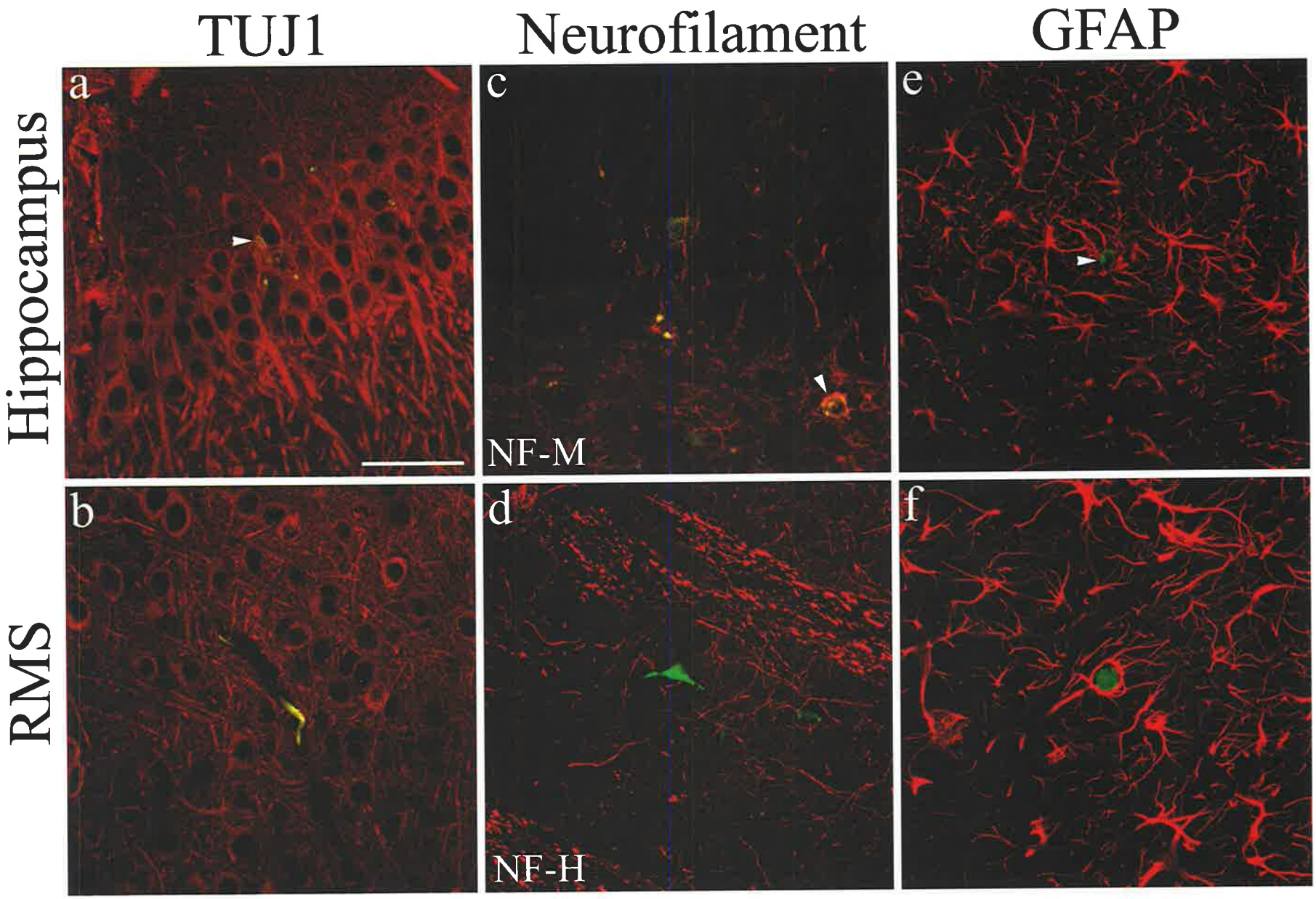
TUJ1
Neurofilament
GFAP
Hippocampus
RMS
a
b
c
d
e
f
NF-M
NF-H

Chapter 7 - Bibliography

Abzhanov, A., Tzahor, E., Lassar, B., A., Tabin, J., C. 2003. Dissimilar regulation of cell differentiation in mesencephalic (cranial) and sacral (trunk) neural crest cells in vitro. *Development* **130:**4567-79

Adams, H., R., Diella, F., Hennig, S., Helmbacher, F., Deutsch, U., Klein, R. 2001. The cytoplasmic domain of the ligand ephrinB2 is required for vascular morphogenesis but not cranial neural crest migration. *Cell* **104:**57-69.

Ahmad, I., Acharya, R., H., Rogers, A., J., Shibata, A., Smithgall, E., T., Dooley, M., C. 1998. The role of NeuroD as a differentiation factor in the mammalian retina. *J Mol Neurosci* **11:**165-78

Alliot-Licht, B., Hurtrel, D., Gregoire, M. 2001. Characterization of alpha-smooth muscle actin positive cells in mineralized human dental pulp cultures. *Arch Oral Biol* **46:**221-8.

Alvarez-Buylla, A., Garcia-Verdugo, M., J. 2002. Neurogenesis in adult subventricular zone. *J Neurosci* **22:**629-34.

Alvarez-Buylla, A., Lim, A., D. 2004. For the long run: maintaining germinal niches in the adult brain. *Neuron* **41:**683-6

Anderson, A., H., Chen, Y., Norkin, C., L. 1998. MHC class I molecules are enriched in caveolae but do not enter with simian virus 40. *J Gen Virol* **79 (Pt 6):**1469-77

Anderson, J., D. 1997. Cellular and molecular biology of neural crest cell lineage determination. *Trends Genet* **13:**276-80

Aquino, B., J., Hjerling-Leffler, J., Koltzenburg, M., Edlund, T., Villar, J., M., Ernfors, P. 2006. In vitro and in vivo differentiation of boundary cap neural crest stem cells into mature Schwann cells. *Exp Neurol* **198:**438-49

Arnhold, S., Klein, H., Klinz, J., F., Absenger, Y., Schmidt, A., Schinkothe, T., Brixius, K., Kozlowski, J., Desai, B., Bloch, W., Addicks, K. 2006. Human bone marrow stroma cells display certain neural characteristics and integrate in the subventricular compartment after injection into the liquor system. *Eur J Cell Biol*

Bagri, A., Gurney, T., He, X., Zou, R., Y., Littman, R., D., Tessier-Lavigne, M., Pleasure, J., S. 2002. The chemokine SDF1 regulates migration of dentate granule cells. *Development* **129:**4249-60.

Baker D.E., Harrison N.J., Maltby E., Smith K., Moore H.D., Shaw P.J., Heath P.R., Holden H., Andrews P.W. 2007. Adaptation to culture of human embryonic stem cells and oncogenesis in vivo. Nat Biotechnol. **25**:207-15.

Baker, K., R., Antin, B., P. 2003. Ephs and ephrins during early stages of chick embryogenesis. *Dev Dyn* **228:**128-42

Baker, V., C., Bronner-Fraser, M. 2001. Vertebrate cranial placodes I. Embryonic induction. *Dev Biol* **232:**1-61

Baker, V., C., Bronner-Fraser, M., Douarin, L., M., N., Teillet, A., M. 1997. Early- and late-migrating cranial neural crest cell populations have equivalent developmental potential in vivo. *Development* **124:**3077-87.

Baroffio, A., Dupin, E., Douarin, L., M., N. 1991. Common precursors for neural and mesectodermal derivatives in the cephalic neural crest. *Development* **112:**301-5

Batlle, E., Henderson, T., J., Beghtel, H., Born, v.d., M., M., Sancho, E., Huls, G., Meeldijk, J., Robertson, J., Wetering, v.d., M., Pawson, T., Clevers, H. 2002. Beta-catenin and TCF mediate cell positioning in the intestinal epithelium by controlling the expression of EphB/ephrinB. *Cell* **111:**251-63

Batouli, S., Miura, M., Brahim, J., Tsutsui, W., T., Fisher, W., L., Gronthos, S., Robey, G., P., Shi, S. 2003. Comparison of stem-cell-mediated osteogenesis and dentinogenesis. *J Dent Res* **82:**976-81

Bauer, S., Rasika, S., Han, J., Mauduit, C., Raccurt, M., Morel, G., Jourdan, F., Benahmed, M., Moyse, E., Patterson, H., P. 2003. Leukemia inhibitory factor is a key signal for injury-induced neurogenesis in the adult mouse olfactory epithelium. *J Neurosci* **23:**1792-803.

Bedard, A., Levesque, M., Bernier, J., P., Parent, A. 2002. The rostral migratory stream in adult squirrel monkeys: contribution of new neurons to the olfactory tubercle and involvement of the antiapoptotic protein Bcl-2. *Eur J Neurosci* **16:**1917-24.

Bensidhoum, M., Chapel, A., Francois, S., Demarquay, C., Mazurier, C., Fouillard, L., Bouchet, S., Bertho, M., J., Gourmelon, P., Aigueperse, J., Charbord, P., Gorin, C., N., Thierry, D., Lopez, M. 2004. Homing of in vitro expanded Stro-1- or Stro-1+ human mesenchymal stem cells into the NOD/SCID mouse and their role in supporting human CD34 cell engraftment. *Blood* **103:**3313-9

Bertrand, N., Castro, S., D., Guillemot, F. 2002. Proneural genes and the specification of neural cell types. *Nat Rev Neurosci* **3:**517-30

Bianco, P., Cossu, G. 1999. Uno, nessuno e centomila: searching for the identity of mesodermal progenitors. *Exp Cell Res* **251:**257-63.

Bianco, P., Riminucci, M., Gronthos, S., Robey, G., P. 2001. Bone marrow stromal stem cells: nature, biology, and potential applications. *Stem Cells* **19:**180-92

Birgbauer, E., Cowan, A., C., Sretavan, W., D., Henkemeyer, M. 2000. Kinase independent function of EphB receptors in retinal axon pathfinding to the optic disc from dorsal but not ventral retina. *Development* **127:**1231-41

Birgbauer, E., Oster, F., S., Severin, G., C., Sretavan, W., D. 2001. Retinal axon growth cones respond to EphB extracellular domains as inhibitory axon guidance cues. *Development* **128:**3041-8.

Bjornson, R., C., Rietze, L., R., Reynolds, A., B., Magli, C., M., Vescovi, L., A. 1999. Turning brain into blood: a hematopoietic fate adopted by adult neural stem cells in vivo. *Science* **283:**534-7.

Boyd, W., A., Lackmann, M. 2001. Signals from Eph and ephrin proteins: a developmental tool kit. *Sci STKE* **2001:**RE20

Bronner-Fraser, M. 1995. Origins and developmental potential of the neural crest. *Exp Cell Res* **218:**405-17

Bronner-Fraser, M. 2002. Molecular analysis of neural crest formation. *J Physiol Paris* **96:**3-8

Bruckner, K., Pasquale, B., E., Klein, R. 1997. Tyrosine phosphorylation of transmembrane ligands for Eph receptors. *Science* **275:**1640-3

Bruhl, T., Urbich, C., Aicher, D., Acker-Palmer, A., Zeiher, M., A., Dimmeler, S. 2004. Homeobox A9 transcriptionally regulates the EphB4 receptor to modulate endothelial cell migration and tube formation. *Circ Res* **94:**743-51

Bundesen, Q., L., Scheel, A., T., Bregman, S., B., Kromer, F., L. 2003. Ephrin-B2 and EphB2 regulation of astrocyte-meningeal fibroblast interactions in response to spinal cord lesions in adult rats. *J Neurosci* **23:**7789-800

Cai, L., Morrow, M., E., Cepko, L., C. 2000. Misexpression of basic helix-loop-helix genes in the murine cerebral cortex affects cell fate choices and neuronal survival. *Development* **127:**3021-30

Carlile, J., M., Sturrock, G., M., Chisholm, M., D., Ogden, R., G., Schor, M., A. 2000. The presence of pericytes and transitional cells in the vasculature of the human dental pulp: an ultrastructural study. *Histochem J* **32:**239-45.

Casasco, A., Maserati, E., Giordano, M., Casasco, M., Ciuffreda, M., Sander, S., Danova, M., Scappaticci, S., Calligaro, A., Springall, R., D., al., e. 1994. Stimulation of DNA synthesis by endothelin-1 in primary cultures of human dental pulp. *Arch Oral Biol* **39:**245-9.

Cate, T., R., A. 1989. Development of the Tooth and its Supporting Tissue. *In:* Oral Histology, Development, Structure and Function. T. Cate and A. R., editors. pp. 57-79. The C. V. Mosby Company, United States if America

Chai, Y., Jiang, X., Ito, Y., Bringas, P., Jr., Han, J., Rowitch, H., D., Soriano, P., McMahon, P., A., Sucov, M., H. 2000. Fate of the mammalian cranial neural crest during tooth and mandibular morphogenesis. *Development* **127:**1671-9.

Chalasani, H., S., Sabelko, A., K., Sunshine, J., M., Littman, R., D., Raper, A., J. 2003. A chemokine, SDF-1, reduces the effectiveness of multiple axonal repellents and is required for normal axon pathfinding. *J Neurosci* **23:**1360-71.

Chen, C., S., Marino, V., Gronthos, S., Bartold, M., P. 2006. Location of putative stem cells in human periodontal ligament. *J Periodontal Res* **41:**547-53

Chen, J., Li, Y., Wang, L., Lu, M., Zhang, X., Chopp, M. 2001a. Therapeutic benefit of intracerebral transplantation of bone marrow stromal cells after cerebral ischemia in rats. *J Neurol Sci* **189:**49-57.

Chen, J., Li, Y., Wang, L., Zhang, Z., Lu, D., Lu, M., Chopp, M. 2001b. Therapeutic benefit of intravenous administration of bone marrow stromal cells after cerebral ischemia in rats. *Stroke* **32:**1005-11.

Chen, Y., Bei, M., Woo, I., Satokata, I., Maas, R. 1996. Msx1 controls inductive signaling in mammalian tooth morphogenesis. *Development* **122:**3035-44.

Chen, Y., Zhang, Y., Jiang, X., T., Barlow, J., A., Amand, S., R., T., Hu, Y., Heaney, S., Francis-West, P., Chuong, M., C., Maas, R. 2000. Conservation of early odontogenic signaling pathways in Aves. *Proc Natl Acad Sci U S A* **97:**10044-9

Cheng, N., Brantley, M., D., Chen, J. 2002. The ephrins and Eph receptors in angiogenesis. *Cytokine Growth Factor Rev* **13:**75-85.

Chong, D., L., Park, K., E., Latimer, E., Friesel, R., Daar, O., I. 2000. Fibroblast growth factor receptor-mediated rescue of x-ephrin B1-induced cell dissociation in Xenopus embryos. *Mol Cell Biol* **20:**724-34

Christensen, R., L., Janas, S., M., Mollgard, K., Kjaer, I. 1993. An immunocytochemical study of the innervation of developing human fetal teeth using protein gene product 9.5 (PGP 9.5). *Arch Oral Biol* **38:**1113-20.

Ciccolini, F., Svendsen, N., C. 1998. Fibroblast growth factor 2 (FGF-2) promotes acquisition of epidermal growth factor (EGF) responsiveness in mouse striatal precursor cells: identification of neural precursors responding to both EGF and FGF-2. *J Neurosci* **18:**7869-80

Claps, M., C., Corcoran, E., K., Cho, J., K., Rameshwar, P. 2005. Stromal derived growth factor-1alpha as a beacon for stem cell homing in development and injury. *Curr Neurovasc Res* **2:**319-29

Conover, C., J., Doetsch, F., Garcia-Verdugo, M., J., Gale, W., N., Yancopoulos, D., G., Alvarez-Buylla, A. 2000. Disruption of Eph/ephrin signaling affects migration and proliferation in the adult subventricular zone. *Nat Neurosci* **3:**1091-7.

Cooke, E., J., Kemp, A., H., Moens, B., C. 2005. EphA4 is required for cell adhesion and rhombomere-boundary formation in the zebrafish. *Curr Biol* **15:**536-42

Cooke, E., J., Moens, B., C. 2002. Boundary formation in the hindbrain: Eph only it were simple. *Trends Neurosci* **25:**260-7

Cooke, J., Moens, C., Roth, L., Durbin, L., Shiomi, K., Brennan, C., Kimmel, C., Wilson, S., Holder, N. 2001. Eph signalling functions downstream of Val to regulate cell sorting and boundary formation in the caudal hindbrain. *Development* **128:**571-80.

Coskun, V., Luskin, B., M. 2002. Intrinsic and extrinsic regulation of the proliferation and differentiation of cells in the rodent rostral migratory stream. *J Neurosci Res* **69:**795-802.

Couly, G., Creuzet, S., Bennaceur, S., Vincent, C., Douarin, L., M., N. 2002. Interactions between Hox-negative cephalic neural crest cells and the foregut endoderm in patterning the facial skeleton in the vertebrate head. *Development* **129:**1061-73

Cowan, A., C., Henkemeyer, M. 2001. The SH2/SH3 adaptor Grb4 transduces B-ephrin reverse signals. *Nature* **413:**174-9

Cowan, A., C., Henkemeyer, M. 2002. Ephrins in reverse, park and drive. *Trends Cell Biol* **12:**339-46

Crittenden, L., S., Bernstein, S., D., Bachorik, L., J., Thompson, E., B., Gallegos, M., Petcherski, G., A., Moulder, G., Barstead, R., Wickens, M., Kimble, J. 2002. A conserved RNA-binding protein controls germline stem cells in Caenorhabditis elegans. *Nature* **417:**660-3

Cutforth, T., Moring, L., Mendelsohn, M., Nemes, A., Shah, M., N., Kim, M., M., Frisen, J., Axel, R. 2003. Axonal ephrin-As and odorant receptors: coordinate determination of the olfactory sensory map. *Cell* **114:**311-22.

Daadi, M., M., Saporta, S., Willing, E., A., Zigova, T., McGrogan, P., M., Sanberg, R., P. 2001. In vitro induction and in vivo expression of bcl-2 in the hNT neurons. *Brain Res Bull* **56:**147-52

Dalva, B., M., Takasu, A., M., Lin, Z., M., Shamah, M., S., Hu, L., Gale, W., N., Greenberg, E., M. 2000. EphB receptors interact with NMDA receptors and regulate excitatory synapse formation. *Cell* **103:**945-56.

Davy, A., Aubin, J., Soriano, P. 2004. Ephrin-B1 forward and reverse signaling are required during mouse development. *Genes Dev* **18:**572-83

Davy, A., Gale, W., N., Murray, W., E., Klinghoffer, A., R., Soriano, P., Feuerstein, C., Robbins, M., S. 1999. Compartmentalized signaling by GPI-anchored ephrin-A5 requires the Fyn tyrosine kinase to regulate cellular adhesion. *Genes Dev* **13:**3125-35.

Davy, A., Robbins, M., S. 2000. Ephrin-A5 modulates cell adhesion and morphology in an integrin-dependent manner. *Embo J* **19:**5396-405.

Deisseroth, K., Singla, S., Toda, H., Monje, M., Palmer, D., T., Malenka, C., R. 2004. Excitation-neurogenesis coupling in adult neural stem/progenitor cells. *Neuron* **42:**535-52

Denholm, A., I., Moule, J., A., Bartold, M., P. 1998. The behaviour and proliferation of human dental pulp cell strains in vitro, and their response to the application of platelet-derived growth factor-BB and insulin-like growth factor-1. *Int Endod J* **31:**251-8.

Dennis, E., J., Carbillet, P., J., Caplan, I., A., Charbord, P. 2002. The STRO-1+ marrow cell population is multipotential. *Cells Tissues Organs* **170:**73-82

Depaepe, V., Suarez-Gonzalez, N., Dufour, A., Passante, L., Gorski, A., J., Jones, R., K., Ledent, C., Vanderhaeghen, P. 2005. Ephrin signalling controls brain size by regulating apoptosis of neural progenitors. *Nature* **435:**1244-50

Dexter, M., T., Allen, D., T., Lajtha, G., L. 1977. Conditions controlling the proliferation of haemopoietic stem cells in vitro. *J Cell Physiol* **91:**335-44

Doetsch, F., Caille, I., Lim, A., D., Garcia-Verdugo, M., J., Alvarez-Buylla, A. 1999a. Subventricular zone astrocytes are neural stem cells in the adult mammalian brain. *Cell* **97:**703-16.

Doetsch, F., Garcia-Verdugo, M., J., Alvarez-Buylla, A. 1999b. Regeneration of a germinal layer in the adult mammalian brain. *Proc Natl Acad Sci U S A* **96:**11619-24.

Doetsch, F., Petreanu, L., Caille, I., Garcia-Verdugo, M., J., Alvarez-Buylla, A. 2002. EGF converts transit-amplifying neurogenic precursors in the adult brain into multipotent stem cells. *Neuron* **36:**1021-34.

Doherty, J., M., Ashton, A., B., Walsh, S., Beresford, N., J., Grant, E., M., Canfield, E., A. 1998. Vascular pericytes express osteogenic potential in vitro and in vivo. *J Bone Miner Res* **13:**828-38

Douarin, L., M., N. 1988. [Differentiation of the neural crest. Influence of growth factors]. *Ann Endocrinol (Paris)* **49:**256-69

Douarin, L., M., N. 2004. The avian embryo as a model to study the development of the neural crest: a long and still ongoing story. *Mech Dev* **121:**1089-102

Douarin, L., M., N., Creuzet, S., Couly, G., Dupin, E. 2004. Neural crest cell plasticity and its limits. *Development* **131:**4637-50

Douarin, L., M., N., Kalcheim, C. 1999a. The Autonomic Nervous System and the Endocrine Cells of Neural Crest Origin. *In:* The Neural Crest. pp. 197-251. Cambridge University Press

Douarin, L., M., N., Kalcheim, C. 1999b. Cell Lineage Segregation During Neural Crest Ontogeny. pp. 304-335. Cambridge University Press

Douarin, L., M., N., Kalcheim, C. 1999c. From Neural Crest to the ganglia of the peripheral nervous system: the sensory ganglia. *In:* The Neural Crest. pp. 153-196. Cambridge University Press

Douarin, L., M., N., Kalcheim, C. 1999d. Methods for Identifying Neural Crest Cells and Their Derivatives. *In:* The Neural Crest. pp. 1-22. Cambridge University Press

Douarin, L., M., N., Kalcheim, C. 1999e. The Migration of Neural Crest Cells. pp. 23-59. Cambridge University Press

Douarin, L., M., N., Kalcheim, C. 1999f. The Neural Crest: A Source of Mesenchymal Cells. *In:* The Neural Crest. pp. 60-151. Cambridge University Press

Drescher, U., Kremoser, C., Handwerker, C., Loschinger, J., Noda, M., Bonhoeffer, F. 1995. In vitro guidance of retinal ganglion cell axons by RAGS, a 25 kDa tectal protein related to ligands for Eph receptor tyrosine kinases. *Cell* **82:**359-70.

Duailibi, T., M., Duailibi, E., S., Young, S., C., Bartlett, D., J., Vacanti, P., J., Yelick, C., P. 2004. Bioengineered teeth from cultured rat tooth bud cells. *J Dent Res* **83:**523-8

Dulac, C., Cameron-Curry, P., Ziller, C., Douarin, L., M., N. 1988. A surface protein expressed by avian myelinating and nonmyelinating Schwann cells but not by satellite or enteric glial cells. *Neuron* **1:**211-20

Dunn, J., K., Williams, O., B., Li, Y., Pavan, J., W. 2000. Neural crest-directed gene transfer demonstrates Wnt1 role in melanocyte expansion and differentiation during mouse development. *Proc Natl Acad Sci U S A* **97:**10050-5

Ebadi, M., Bashir, M., R., Heidrick, L., M., Hamada, M., F., Refaey, E., H., Hamed, A., Helal, G., Baxi, D., M., Cerutis, R., D., Lassi, K., N. 1997. Neurotrophins and their receptors in nerve injury and repair. *Neurochem Int* **30:**347-74

Eberhart, J., Swartz, M., Koblar, A., S., Pasquale, B., E., Tanaka, H., Krull, E., C. 2000. Expression of EphA4, ephrin-A2 and ephrin-A5 during axon outgrowth to the hindlimb indicates potential roles in pathfinding. *Dev Neurosci* **22:**237-50.

Elliott, C., R., Khademi, S., Pleasure, J., S., Parent, M., J., Lowenstein, H., D. 2001. Differential regulation of basic helix-loop-helix mRNAs in the dentate gyrus following status epilepticus. *Neuroscience* **106:**79-88

Elowe, S., Holland, J., S., Kulkarni, S., Pawson, T. 2001. Downregulation of the Ras-mitogen-activated protein kinase pathway by the EphB2 receptor tyrosine kinase is required for ephrin-induced neurite retraction. *Mol Cell Biol* **21:**7429-41.

Eriksson, S., P., Perfilieva, E., Bjork-Eriksson, T., Alborn, M., A., Nordborg, C., Peterson, A., D., Gage, H., F. 1998. Neurogenesis in the adult human hippocampus. *Nat Med* **4:**1313-7

Escurat, M., Djabali, K., Gumpel, M., Gros, F., Portier, M., M. 1990. Differential expression of two neuronal intermediate-filament proteins, peripherin and the low-molecular-mass neurofilament protein (NF-L), during the development of the rat. *J Neurosci* **10:**764-84

Fabian-Fine, R., Meinertzhagen, A., I., Seyfarth, A., E. 2000. Organization of efferent peripheral synapses at mechanosensory neurons in spiders. *J Comp Neurol* **420:**195-210

Fabian-Fine, R., Volknandt, W., Seyfarth, E. 1999. Peripheral synapses at identifiable mechanosensory neurons in the spider Cupiennius salei: synapsin-like immunoreactivity. *Cell Tissue Res* **295:**13-9

Fejerskov, Josephsen, O.a., K. 1986. Odontogenesis. *In:* Human Oral Embryology and Histology. Mjor, I.A.a. Fejerskov, and O., editors. pp. 31-49. Munksgaard, Denmark

Feng, Q., J., Luan, X., Wallace, J., Jing, D., Ohshima, T., Kulkarni, B., A., D'Souza, N., R., Kozak, A., C., MacDougall, M. 1998. Genomic organization, chromosomal mapping, and promoter analysis of the mouse dentin sialophosphoprotein (Dspp) gene, which codes for both dentin sialoprotein and dentin phosphoprotein. *J Biol Chem* **273:**9457-64.

Francis-West, P., Ladher, R., Barlow, A., Graveson, A. 1998. Signalling interactions during facial development. *Mech Dev* **75:**3-28

Franklin, A., Kao, A., Tapscott, S., Unis, A. 2001. NeuroD homologue expression during cortical development in the human brain. *J Child Neurol* **16:**849-53

Fristad, I., Heyeraas, J., K., Kvinnsland, I. 1994. Nerve fibres and cells immunoreactive to neurochemical markers in developing rat molars and supporting tissues. *Arch Oral Biol* **39:**633-46

Fuchs, E., Segre, A., J. 2000. Stem cells: a new lease on life. *Cell* **100:**143-55

Fuchs, E., Tumbar, T., Guasch, G. 2004. Socializing with the neighbors: stem cells and their niche. *Cell* **116:**769-78

Gage, H., F. 2000. Mammalian neural stem cells. *Science* **287:**1433-8.

Gale, W., N., Baluk, P., Pan, L., Kwan, M., Holash, J., DeChiara, M., T., McDonald, M., D., Yancopoulos, D., G. 2001. Ephrin-B2 selectively marks arterial vessels and neovascularization sites in the adult, with expression in both endothelial and smooth-muscle cells. *Dev Biol* **230:**151-60.

Gale, W., N., Flenniken, A., Compton, C., D., Jenkins, N., Copeland, G., N., Gilbert, J., D., Davis, S., Wilkinson, G., D., Yancopoulos, D., G. 1996a. Elk-L3, a novel transmembrane ligand for the Eph family of receptor tyrosine kinases, expressed in embryonic floor plate, roof plate and hindbrain segments. *Oncogene* **13:**1343-52

Gale, W., N., Holland, J., S., Valenzuela, M., D., Flenniken, A., Pan, L., Ryan, E., T., Henkemeyer, M., Strebhardt, K., Hirai, H., Wilkinson, G., D., Pawson, T., Davis, S., Yancopoulos, D., G. 1996b. Eph receptors and ligands comprise two major specificity subclasses and are reciprocally compartmentalized during embryogenesis. *Neuron* **17:**9-19.

Gallo, R., Zazzeroni, F., Alesse, E., Mincione, C., Borello, U., Buanne, P., D'Eugenio, R., Mackay, R., A., Argenti, B., Gradini, R., Russo, A., M., Maroder, M., Cossu, G., Frati,

L., Screpanti, I., Gulino, A. 2002. Ren: a novel, developmentally regulated gene that promotes neural cell differentiation. *J Cell Biol* **158:**731-40.

Gammill, S., L., Gonzalez, C., Gu, C., Bronner-Fraser, M. 2006. Guidance of trunk neural crest migration requires neuropilin 2/semaphorin 3F signaling. *Development* **133:**99-106

Gauthier, R., L., Robbins, M., S. 2003. Ephrin signaling: One raft to rule them all? One raft to sort them? One raft to spread their call and in signaling bind them? *Life Sci* **74:**207-16

Georgakopoulos, A., Litterst, C., Ghersi, E., Baki, L., Xu, C., Serban, G., Robakis, K., N. 2006. Metalloproteinase/Presenilin1 processing of ephrinB regulates EphB-induced Src phosphorylation and signaling. *Embo J* **25:**1242-52

Gerety, S., S., Anderson, J., D. 2002. Cardiovascular ephrinB2 function is essential for embryonic angiogenesis. *Development* **129:**1397-410.

Giasson, I., B., Mushynski, E., W. 1997. Study of proline-directed protein kinases involved in phosphorylation of the heavy neurofilament subunit. *J Neurosci* **17:**9466-72

Golding, P., J., Dixon, M., Gassmann, M. 2002. Cues from neuroepithelium and surface ectoderm maintain neural crest-free regions within cranial mesenchyme of the developing chick. *Development* **129:**1095-105

Goldman, A., S. 1998. Adult neurogenesis: from canaries to the clinic. *J Neurobiol* **36:**267-86.

Goldshmit, Y., McLenachan, S., Turnley, A. 2006. Roles of Eph receptors and ephrins in the normal and damaged adult CNS. *Brain Res Brain Res Rev*

Graham, A., Begbie, J., McGonnell, I. 2004. Significance of the cranial neural crest. *Dev Dyn* **229:**5-13

Granjeiro, M., J., Oliveira, C., R., Bustos-Valenzuela, C., J., Sogayar, C., M., Taga, R. 2005. Bone morphogenetic proteins: from structure to clinical use. *Braz J Med Biol Res* **38:**1463-73

Gritti, A., Cova, L., Parati, A., E., Galli, R., Vescovi, L., A. 1995. Basic fibroblast growth factor supports the proliferation of epidermal growth factor-generated neuronal precursor cells of the adult mouse CNS. *Neurosci Lett* **185:**151-4.

Gritti, A., Parati, A., E., Cova, L., Frolichsthal, P., Galli, R., Wanke, E., Faravelli, L., Morassutti, J., D., Roisen, F., Nickel, D., D., Vescovi, L., A. 1996. Multipotential stem cells from the adult mouse brain proliferate and self-renew in response to basic fibroblast growth factor. *J Neurosci* **16:**1091-100.

Gritti, A., Vescovi, L., A., Galli, R. 2002. Adult neural stem cells: plasticity and developmental potential. *J Physiol Paris* **96:**81-90.

Gronthos, S. 2004. Reconstruction of human mandible by tissue engineering. *Lancet* **364:**735-6

Gronthos, S., Brahim, J., Li, W., Fisher, W., L., Cherman, N., Boyde, A., DenBesten, P., Robey, G., P., Shi, S. 2002. Stem cell properties of human dental pulp stem cells. *J Dent Res* **81:**531-5.

Gronthos, S., Cherman, N., Robey, P.G., Shi, S. 2004. Human Dental Pulp Stem Cells: Characterization and Developmental Potential. Humana Press Inc, NJ

Gronthos, S., Graves, E., S., Ohta, S., Simmons, J., P. 1994. The STRO-1+ fraction of adult human bone marrow contains the osteogenic precursors. *Blood* **84:**4164-73

Gronthos, S., Mankani, M., Brahim, J., Robey, G., P., Shi, S. 2000. Postnatal human dental pulp stem cells (DPSCs) in vitro and in vivo. *Proc Natl Acad Sci U S A* **97:**13625-30

Gronthos, S., Zannettino, C., A., Graves, E., S., Ohta, S., Hay, J., S., Simmons, J., P. 1999. Differential cell surface expression of the STRO-1 and alkaline phosphatase antigens on discrete developmental stages in primary cultures of human bone cells. *J Bone Miner Res* **14:**47-56

Gronthos, S., Zannettino, C., A., Hay, J., S., Shi, S., Graves, E., S., Kortesidis, A., Simmons, J., P. 2003. Molecular and cellular characterisation of highly purified stromal stem cells derived from human bone marrow. *J Cell Sci* **116:**1827-35

Grunwald, C., I., Korte, M., Wolfer, D., Wilkinson, A., G., Unsicker, K., Lipp, P., H., Bonhoeffer, T., Klein, R. 2001. Kinase-independent requirement of EphB2 receptors in hippocampal synaptic plasticity. *Neuron* **32:**1027-40.

Gumbiner, M., B. 1996. Cell adhesion: the molecular basis of tissue architecture and morphogenesis. *Cell* **84:**345-57

Gurniak, B., C., Berg, J., L. 1996. A new member of the Eph family of receptors that lacks protein tyrosine kinase activity. *Oncogene* **13:**777-86.

Hackney, A., J., Charbord, P., Brunk, P., B., Stoeckert, J., C., Lemischka, R., I., Moore, A., K. 2002. A molecular profile of a hematopoietic stem cell niche. *Proc Natl Acad Sci U S A* **99:**13061-6.

Hainfellner, A., J., Voigtlander, T., Strobel, T., Mazal, R., P., Maddalena, S., A., Aguzzi, A., Budka, H. 2001. Fibroblasts can express glial fibrillary acidic protein (GFAP) in vivo. *J Neuropathol Exp Neurol* **60:**449-61.

Hall, K., B. 2000. The neural crest as a fourth germ layer and vertebrates as quadroblastic not triploblastic. *Evol Dev* **2:**3-5

Hamburger, V., Hamilton, H.L. 1951. A series of normal stages in the development of the chick embryo. *J Embryol Exp Morphol* **88:**49-92

Harada, H., Kettunen, P., Jung, S., H., Mustonen, T., Wang, A., Y., Thesleff, I. 1999. Localization of putative stem cells in dental epithelium and their association with Notch and FGF signaling. *J Cell Biol* **147:**105-20

Harada, H., Ohshima, H. 2004. New perspectives on tooth development and the dental stem cell niche. *Arch Histol Cytol* **67:**1-11

Harada, H., Toyono, T., Toyoshima, K., Ohuchi, H. 2002a. FGF10 maintains stem cell population during mouse incisor development. *Connect Tissue Res* **43:**201-4

Harada, H., Toyono, T., Toyoshima, K., Yamasaki, M., Itoh, N., Kato, S., Sekine, K., Ohuchi, H. 2002b. FGF10 maintains stem cell compartment in developing mouse incisors. *Development* **129:**1533-41

Hattori, M., Osterfield, M., Flanagan, G., J. 2000. Regulated cleavage of a contact-mediated axon repellent. *Science* **289:**1360-5.

Hatzopoulos, K., A., Folkman, J., Vasile, E., Eiselen, K., G., Rosenberg, D., R. 1998. Isolation and characterization of endothelial progenitor cells from mouse embryos. *Development* **125:**1457-68

Henningson, T., C., Jr., Stanislaus, A., M., Gewirtz, M., A. 2003. 28. Embryonic and adult stem cell therapy. *J Allergy Clin Immunol* **111:**S745-53.

Hess, A., R., Cooke, S., P., Hofmann, C., M., Murphy, M., K. 2006. Mechanistic insights into the regulation of the spermatogonial stem cell niche. *Cell Cycle* **5:**1164-70

Hidalgo, A., Barami, K., Iversen, K., Goldman, A., S. 1995. Estrogens and non-estrogenic ovarian influences combine to promote the recruitment and decrease the turnover of new neurons in the adult female canary brain. *J Neurobiol* **27:**470-87.

Himanen, P., J., Chumley, J., M., Lackmann, M., Li, C., Barton, A., W., Jeffrey, D., P., Vearing, C., Geleick, D., Feldheim, A., D., Boyd, W., A., Henkemeyer, M., Nikolov, B., D. 2004. Repelling class discrimination: ephrin-A5 binds to and activates EphB2 receptor signaling. *Nat Neurosci* **7:**501-9

Himanen, P., J., Nikolov, B., D. 2003. Eph receptors and ephrins. *Int J Biochem Cell Biol* **35:**130-4

Holder, N., Klein, R. 1999. Eph receptors and ephrins: effectors of morphogenesis. *Development* **126:**2033-44.

Holland, J., S., Gale, W., N., Mbamalu, G., Yancopoulos, D., G., Henkemeyer, M., Pawson, T. 1996. Bidirectional signalling through the EPH-family receptor Nuk and its transmembrane ligands. *Nature* **383:**722-5.

Holland, J., S., Peles, E., Pawson, T., Schlessinger, J. 1998. Cell-contact-dependent signalling in axon growth and guidance: Eph receptor tyrosine kinases and receptor protein tyrosine phosphatase beta. *Curr Opin Neurobiol* **8:**117-27.

Holmberg, J., Armulik, A., Senti, A., K., Edoff, K., Spalding, K., Momma, S., Cassidy, R., Flanagan, G., J., Frisen, J. 2005. Ephrin-A2 reverse signaling negatively regulates neural progenitor proliferation and neurogenesis. *Genes Dev* **19:**462-71

Holmberg, J., Clarke, L., D., Frisen, J. 2000. Regulation of repulsion versus adhesion by different splice forms of an Eph receptor. *Nature* **408:**203-206

Holmberg, J., Frisen, J. 2002. Ephrins are not only unattractive. *Trends Neurosci* **25:**239-43

Holmberg, J., Genander, M., Halford, M., M., Anneren, C., Sondell, M., Chumley, J., M., Silvany, E., R., Henkemeyer, M., Frisen, J. 2006. EphB receptors coordinate migration and proliferation in the intestinal stem cell niche. *Cell* **125:**1151-63

Hoog, d., L., C., Foster, J., L., Mann, M. 2004. RNA and RNA binding proteins participate in early stages of cell spreading through spreading initiation centers. *Cell* **117:**649-62

Horiuchi, M., Tomooka, Y. 2005. An attempt to generate neurons from an astrocyte progenitor cell line FBD-104. *Neurosci Res* **53:**104-15

Huttelmaier, S., Bubeck, P., Rudiger, M., Jockusch, M., B. 1997. Characterization of two F-actin-binding and oligomerization sites in the cell-contact protein vinculin. *Eur J Biochem* **247:**1136-42

Huysseune, A., Sire, Y., J. 1998. Evolution of patterns and processes in teeth and tooth-related tissues in non-mammalian vertebrates. *Eur J Oral Sci* **106 Suppl 1:**437-81

Ikeda, N., Nonoguchi, N., Zhao, Z., M., Watanabe, T., Kajimoto, Y., Furutama, D., Kimura, F., Dezawa, M., Coffin, S., R., Otsuki, Y., Kuroiwa, T., Miyatake, S. 2005. Bone marrow stromal cells that enhanced fibroblast growth factor-2 secretion by herpes simplex virus vector improve neurological outcome after transient focal cerebral ischemia in rats. *Stroke* **36:**2725-30

Imai, H., Osumi-Yamashita, N., Ninomiya, Y., Eto, K. 1996. Contribution of early-emigrating midbrain crest cells to the dental mesenchyme of mandibular molar teeth in rat embryos. *Dev Biol* **176:**151-65.

Iozzo, V., R. 2005. Basement membrane proteoglycans: from cellar to ceiling. *Nat Rev Mol Cell Biol* **6:**646-56

Itkin-Ansari, P., Marcora, E., Geron, I., Tyrberg, B., Demeterco, C., Hao, E., Padilla, C., Ratineau, C., Leiter, A., Lee, E., J., Levine, F. 2005. NeuroD1 in the endocrine pancreas: localization and dual function as an activator and repressor. *Dev Dyn* **233:**946-53

Itoh, F., Nakane, T., Chiba, S. 1997. Gene expression of MASH-1, MATH-1, neuroD and NSCL-2, basic helix-loop-helix proteins, during neural differentiation in P19 embryonal carcinoma cells. *Tohoku J Exp Med* **182:**327-36

Itskovitz-Eldor, J., Schuldiner, M., Karsenti, D., Eden, A., Yanuka, O., Amit, M., Soreq, H., Benvenisty, N. 2000. Differentiation of human embryonic stem cells into embryoid bodies compromising the three embryonic germ layers. *Mol Med* **6:**88-95.

Ivanova, B., N., Dimos, T., J., Schaniel, C., Hackney, A., J., Moore, A., K., Lemischka, R., I. 2002. A stem cell molecular signature. *Science* **298:**601-4.

Janes, W., P., Saha, N., Barton, A., W., Kolev, V., M., Wimmer-Kleikamp, H., S., Nievergall, E., Blobel, P., C., Himanen, P., J., Lackmann, M., Nikolov, B., D. 2005. Adam meets Eph: an ADAM substrate recognition module acts as a molecular switch for ephrin cleavage in trans. *Cell* **123:**291-304

Jayasena, S., C., Flood, D., W., Koblar, A., S. 2005. High EphA3 expressing ophthalmic trigeminal sensory axons are sensitive to ephrin-A5-Fc: implications for lobe specific axon guidance. *Neuroscience* **135:**97-109

Jessell, Sanes, T.M.a., R., J. 2000. The Induction and Patterning of the Nervous System. *In:* Principles of Neural Science. Kandel, E. R, Schwartz, J.H.a. Jessell, and T. M., editors. McGraw-Hill Companies, United States of America

Jiang, Y., Jahagirdar, N., B., Reinhardt, L., R., Schwartz, E., R., Keene, D., C., Ortiz-Gonzalez, R., X., Reyes, M., Lenvik, T., Lund, T., Blackstad, M., Du, J., Aldrich, S., Lisberg, A., Low, C., W., Largaespada, A., D., Verfaillie, M., C. 2002. Pluripotency of mesenchymal stem cells derived from adult marrow. *Nature* **418:**41-9

Kalo, S., M., Pasquale, B., E. 1999. Signal transfer by eph receptors. *Cell Tissue Res* **298:**1-9.

Kalo, S., M., Yu, H., H., Pasquale, B., E. 2001. In vivo tyrosine phosphorylation sites of activated ephrin-B1 and ephB2 from neural tissue. *J Biol Chem* **276:**38940-8.

Katayama, Y., Battista, M., Kao, M., W., Hidalgo, A., Peired, J., A., Thomas, A., S., Frenette, S., P. 2006. Signals from the sympathetic nervous system regulate hematopoietic stem cell egress from bone marrow. *Cell* **124:**407-21

Keirstead, S., H., Nistor, G., Bernal, G., Totoiu, M., Cloutier, F., Sharp, K., Steward, O. 2005. Human embryonic stem cell-derived oligodendrocyte progenitor cell transplants remyelinate and restore locomotion after spinal cord injury. *J Neurosci* **25:**4694-705

Kim, E., Cho, W., S., Yang, Y., J., Cai, J., Lee, L., S., Ohshima, H., Jung, S., H. 2006. Tooth survival and periodontal tissues healing of allogenic-transplanted teeth in the mice. *Oral Dis* **12:**395-401

Kim, S., Yoon, S., Y., Kim, W., J., Jung, M., Kim, U., S., Lee, D., Y., Suh-Kim, H. 2004a. Neurogenin1 is sufficient to induce neuronal differentiation of embryonal carcinoma P19 cells in the absence of retinoic acid. *Cell Mol Neurobiol* **24:**343-56

Kim, Y., J., Chu, K., Kim, J., H., Seong, A., H., Park, C., K., Sanyal, S., Takeda, J., Ha, H., Shong, M., Tsai, J., M., Choi, S., H. 2004b. Orphan nuclear receptor small heterodimer partner, a novel corepressor for a basic helix-loop-helix transcription factor BETA2/neuroD. *Mol Endocrinol* **18:**776-90

Kim, Y., W., Fritzsch, B., Serls, A., Bakel, A., L., Huang, J., E., Reichardt, F., L., Barth, S., D., Lee, E., J. 2001. NeuroD-null mice are deaf due to a severe loss of the inner ear sensory neurons during development. *Development* **128:**417-26

Klein, R. 1999. Bidirectional signals establish boundaries. *Curr Biol* **9:**R691-4.

Koblar, A., S., Krull, E., C., Pasquale, B., E., McLennan, R., Peale, D., F., Cerretti, P., D., Bothwell, M. 2000. Spinal motor axons and neural crest cells use different molecular guides for segmental migration through the rostral half-somite. *Journal of Neurobiology* **42:**437-447

Kollet, O., Dar, A., Shivtiel, S., Kalinkovich, A., Lapid, K., Sztainberg, Y., Tesio, M., Samstein, M., R., Goichberg, P., Spiegel, A., Elson, A., Lapidot, T. 2006. Osteoclasts degrade endosteal components and promote mobilization of hematopoietic progenitor cells. *Nat Med* **12:**657-64

Konishi, Y., Matsu-ura, T., Mikoshiba, K., Tamura, T. 2001. Stimulation of gene expression of NeuroD-related factor in the mouse brain following pentylenetetrazol-induced seizures. *Brain Res Mol Brain Res* **97:**129-36

Kopen, C., G., Prockop, J., D., Phinney, G., D. 1999. Marrow stromal cells migrate throughout forebrain and cerebellum, and they differentiate into astrocytes after injection into neonatal mouse brains. *Proc Natl Acad Sci U S A* **96:**10711-6.

Kornack, R., D. 2000. Neurogenesis and the evolution of cortical diversity: mode, tempo, and partitioning during development and persistence in adulthood. *Brain Behav Evol* **55:**336-44

Kornack, R., D., Rakic, P. 1999. Continuation of neurogenesis in the hippocampus of the adult macaque monkey. *Proc Natl Acad Sci U S A* **96:**5768-73

Kornack, R., D., Rakic, P. 2001. The generation, migration, and differentiation of olfactory neurons in the adult primate brain. *Proc Natl Acad Sci U S A* **98:**4752-7.

Korzh, V., Sleptsova, I., Liao, J., He, J., Gong, Z. 1998. Expression of zebrafish bHLH genes ngn1 and nrd defines distinct stages of neural differentiation. *Dev Dyn* **213:**92-104

Kruger, M., G., Mosher, T., J., Bixby, S., Joseph, N., Iwashita, T., Morrison, J., S. 2002. Neural crest stem cells persist in the adult gut but undergo changes in self-renewal, neuronal subtype potential, and factor responsiveness. *Neuron* **35:**657-69.

Krull, E., C. 1998. Inhibitory interactions in the patterning of trunk neural crest migration. *Ann N Y Acad Sci* **857:**13-22.

Krull, E., C., Collazo, A., Fraser, E., S., Bronner-Fraser, M. 1995. Segmental migration of trunk neural crest: time-lapse analysis reveals a role for PNA-binding molecules. *Development* **121:**3733-43

Krull, E., C., Koblar, A., S. 2000. Motor axon pathfinding in the peripheral nervous system. *Brain Res Bull* **53:**479-87.

Krull, E., C., Lansford, R., Gale, W., N., Collazo, A., Marcelle, C., Yancopoulos, D., G., Fraser, E., S., Bronner-Fraser, M. 1997. Interactions of Eph-related receptors and ligands confer rostrocaudal pattern to trunk neural crest migration. *Curr Biol* **7:**571-80.

Krumlauf, R., Marshall, H., Studer, M., Nonchev, S., Sham, H., M., Lumsden, A. 1993. Hox homeobox genes and regionalisation of the nervous system. *J Neurobiol* **24:**1328-40

Kubota, Y., Ito, K. 2000. Chemotactic migration of mesencephalic neural crest cells in the mouse. *Dev Dyn* **217:**170-9

Kucia, M., Dawn, B., Hunt, G., Guo, Y., Wysoczynski, M., Majka, M., Ratajczak, J., Rezzoug, F., Ildstad, T., S., Bolli, R., Ratajczak, Z., M. 2004. Cells expressing early cardiac markers reside in the bone marrow and are mobilized into the peripheral blood after myocardial infarction. *Circ Res* **95:**1191-9

Kuhn, G., H., Dickinson-Anson, H., Gage, H., F. 1996. Neurogenesis in the dentate gyrus of the adult rat: age-related decrease of neuronal progenitor proliferation. *J Neurosci* **16:**2027-33

Kullander, K., Klein, R. 2002. Mechanisms and functions of Eph and ephrin signalling. *Nat Rev Mol Cell Biol* **3:**475-86

Laino, G., d'Aquino, R., Graziano, A., Lanza, V., Carinci, F., Naro, F., Pirozzi, G., Papaccio, G. 2005. A new population of human adult dental pulp stem cells: a useful source of living autologous fibrous bone tissue (LAB). *J Bone Miner Res* **20:**1394-402

Laino, G., Graziano, A., d'Aquino, R., Pirozzi, G., Lanza, V., Valiante, S., Rosa, D., A., Naro, F., Vivarelli, E., Papaccio, G. 2006. An approachable human adult stem cell source for hard-tissue engineering. *J Cell Physiol* **206:**693-701

Larsson, J., Scadden, D. 2006. Nervous activity in a stem cell niche. *Cell* **124:**253-5

Lawrenson, D., I., Wimmer-Kleikamp, H., S., Lock, P., Schoenwaelder, M., S., Down, M., Boyd, W., A., Alewood, F., P., Lackmann, M. 2002. Ephrin-A5 induces rounding, blebbing and de-adhesion of EphA3-expressing 293T and melanoma cells by CrkII and Rho-mediated signalling. *J Cell Sci* **115:**1059-72

Lee, E., J. 1997. Basic helix-loop-helix genes in neural development. *Curr Opin Neurobiol* **7:**13-20

Lee, E., J., Hollenberg, M., S., Snider, L., Turner, L., D., Lipnick, N., Weintraub, H. 1995. Conversion of Xenopus ectoderm into neurons by NeuroD, a basic helix-loop-helix protein. *Science* **268:**836-44

Leedham, J., S., Brittan, M., McDonald, A., S., Wright, A., N. 2005. Intestinal stem cells. *J Cell Mol Med* **9:**11-24

Leker, R., R., McKay, D., R. 2004. Using endogenous neural stem cells to enhance recovery from ischemic brain injury. *Curr Neurovasc Res* **1:**421-7

Lemke, G. 1998. Eph receptors and ligands in axon pathway choice, target recognition, and synaptogenesis. *Prog Brain Res* **117:**171-6

Li, Y., Chen, J., Wang, L., Lu, M., Chopp, M. 2001. Treatment of stroke in rat with intracarotid administration of marrow stromal cells. *Neurology* **56:**1666-72.

Li, Y., Chopp, M., Chen, J., Wang, L., Gautam, C., S., Xu, X., Y., Zhang, Z. 2000. Intrastriatal transplantation of bone marrow nonhematopoietic cells improves functional recovery after stroke in adult mice. *J Cereb Blood Flow Metab* **20:**1311-9.

Liao, L., S., Chen, Y., W., Raung, L., S., Kuo, S., J., Chen, J., C. 2001. Association of immune responses and ischemic brain infarction in rat. *Neuroreport* **12:**1943-7

Lillesaar, C., Arenas, E., Hildebrand, C., Fried, K. 2003. Responses of rat trigeminal neurones to dental pulp cells or fibroblasts overexpressing neurotrophic factors in vitro. *Neuroscience* **119:**443-51

Lillesaar, C., Eriksson, C., Fried, K. 2001. Rat tooth pulp cells elicit neurite growth from trigeminal neurones and express mRNAs for neurotrophic factors in vitro. *Neurosci Lett* **308:**161-4

Lillesaar, C., Eriksson, C., Johansson, S., C., Fried, K., Hildebrand, C. 1999. Tooth pulp tissue promotes neurite outgrowth from rat trigeminal ganglia in vitro. *J Neurocytol* **28:**663-70

Lillesaar, C., Fried, K. 2004. Neurites from trigeminal ganglion explants grown in vitro are repelled or attracted by tooth-related tissues depending on developmental stage. *Neuroscience* **125:**149-61

Lim, A., D., Tramontin, D., A., Trevejo, M., J., Herrera, G., D., Garcia-Verdugo, M., J., Alvarez-Buylla, A. 2000. Noggin antagonizes BMP signaling to create a niche for adult neurogenesis. *Neuron* **28:**713-26.

Lindsay, M., R., Barde, A., Y., Davies, M., A., Rohrer, H. 1985. Differences and similarities in the neurotrophic growth factor requirements of sensory neurons derived from neural crest and neural placode. *J Cell Sci Suppl* **3:**115-29

Lindvall, O., Kokaia, Z. 2004a. Recovery and rehabilitation in stroke: stem cells. *Stroke* **35:**2691-4

Lindvall, O., Kokaia, Z. 2005. Stem cell therapy for human brain disorders. *Kidney Int* **68:**1937-9

Lindvall, O., Kokaia, Z. 2006. Stem cells for the treatment of neurological disorders. *Nature* **441:**1094-6

Lindvall, O., Kokaia, Z., Martinez-Serrano, A. 2004b. Stem cell therapy for human neurodegenerative disorders-how to make it work. *Nat Med* **10 Suppl:**S42-50

Liu, H., Li, W., Shi, S., Habelitz, S., Gao, C., Denbesten, P. 2005. MEPE is downregulated as dental pulp stem cells differentiate. *Arch Oral Biol* **50:**923-8

Liu, M., Pleasure, J., S., Collins, E., A., Noebels, L., J., Naya, J., F., Tsai, J., M., Lowenstein, H., D. 2000. Loss of BETA2/NeuroD leads to malformation of the dentate gyrus and epilepsy. *Proc Natl Acad Sci U S A* **97:**865-70

Lowry, E., W., Blanpain, C., Nowak, A., J., Guasch, G., Lewis, L., Fuchs, E. 2005. Defining the impact of beta-catenin/Tcf transactivation on epithelial stem cells. *Genes Dev* **19:**1596-611

Lu, Q., Sun, E., E., Klein, S., R., Flanagan, G., J. 2001. Ephrin-B reverse signaling is mediated by a novel PDZ-RGS protein and selectively inhibits G protein-coupled chemoattraction. *Cell* **105:**69-79.

Lumsden, A., Sprawson, N., Graham, A. 1991. Segmental origin and migration of neural crest cells in the hindbrain region of the chick embryo. *Development* **113:**1281-91

Lumsden, G., A. 1988. Spatial organization of the epithelium and the role of neural crest cells in the initiation of the mammalian tooth germ. *Development* **103 Suppl:**155-69

Luukko, K., Arumae, U., Karavanov, A., Moshnyakov, M., Sainio, K., Sariola, H., Saarma, M., Thesleff, I. 1997. Neurotrophin mRNA expression in the developing tooth suggests multiple roles in innervation and organogenesis. *Dev Dyn* **210:**117-29.

Luukko, K., Loes, S., Kvinnsland, H., I., Kettunen, P. 2004. Expression of ephrin-A ligands and EphA receptors in the developing mouse tooth and its supporting tissues. *Cell Tissue Res*

Luukko, K., Loes, S., Kvinnsland, H., I., Kettunen, P. 2005. Expression of ephrin-A ligands and EphA receptors in the developing mouse tooth and its supporting tissues. *Cell Tissue Res* **319:**143-52

Lyaruu, M., D., Croonenburg, v., J., E., Duin, v., A., M., Bervoets, J., T., Woltgens, H., J., Blieck-Hogervorst, d., M., J. 1999. Development of transplanted pulp tissue containing epithelial sheath into a tooth-like structure. *J Oral Pathol Med* **28:**293-6.

Ma, Q., Chen, Z., Barrantes, d.B., I., Pompa, d.l., L., J., Anderson, J., D. 1998. neurogenin1 is essential for the determination of neuronal precursors for proximal cranial sensory ganglia. *Neuron* **20:**469-82

Maekawa, H., Oike, Y., Kanda, S., Ito, Y., Yamada, Y., Kurihara, H., Nagai, R., Suda, T. 2003. Ephrin-b2 induces migration of endothelial cells through the phosphatidylinositol-3 kinase pathway and promotes angiogenesis in adult vasculature. *Arterioscler Thromb Vasc Biol* **23:**2008-14

Manglapus, L., G., Youngentob, L., S., Schwob, E., J. 2004. Expression patterns of basic helix-loop-helix transcription factors define subsets of olfactory progenitor cells. *J Comp Neurol* **479:**216-33

Marin, O., Blanco, J., M., Nieto, A., M. 2001. Differential expression of Eph receptors and ephrins correlates with the formation of topographic projections in primary and secondary visual circuits of the EMBRYONIC chick forebrain. *Dev Biol* **234:**289-303.

Marin, Rubenstein, O.a., R., J.L. 2002. Patterning, Regionalization, and Cell Differentiation in the Forebrain. *In:* Mouse Development: Patterning, Morphogenesis, and Organogenesis. Rossant, J.a. Tam, and P.P.L., editors. Academic Press, Canada

Marston, J., D., Dickinson, S., Nobes, D., C. 2003. Rac-dependent trans-endocytosis of ephrinBs regulates Eph-ephrin contact repulsion. *Nat Cell Biol* **5:**879-88

Martens, P., T., See, F., Schuster, D., M., Sondermeijer, P., H., Hefti, M., M., Zannettino, A., Gronthos, S., Seki, T., Itescu, S. 2006. Mesenchymal lineage precursor cells induce vascular network formation in ischemic myocardium. *Nat Clin Pract Cardiovasc Med* **3 Suppl 1:**S18-22

Martino, G., Pluchino, S. 2006. The therapeutic potential of neural stem cells. *Nat Rev Neurosci* **7:**395-406

Matsuo, S., Ichikawa, H., Henderson, A., T., Silos-Santiago, I., Barbacid, M., Arends, J., J., Jacquin, F., M. 2001. trkA modulation of developing somatosensory neurons in oro-facial tissues: tooth pulp fibers are absent in trkA knockout mice. *Neuroscience* **105:**747-60

McLennan, R., Krull, E., C. 2002. Ephrin-as cooperate with EphA4 to promote trunk neural crest migration. *Gene Expr* **10:**295-305

Meima, L., Moran, P., Matthews, W., Caras, W., I. 1997. Lerk2 (ephrin-B1) is a collapsing factor for a subset of cortical growth cones and acts by a mechanism different from AL-1 (ephrin-A5). *Mol Cell Neurosci* **9:**314-28.

Meirelles, d.S., L., Chagastelles, C., P., Nardi, B., N. 2006. Mesenchymal stem cells reside in virtually all post-natal organs and tissues. *J Cell Sci* **119:**2204-13

Mellitzer, G., Xu, Q., Wilkinson, G., D. 1999. Eph receptors and ephrins restrict cell intermingling and communication. *Nature* **400:**77-81.

Mellitzer, G., Xu, Q., Wilkinson, G., D. 2000. Control of cell behaviour by signalling through Eph receptors and ephrins. *Curr Opin Neurobiol* **10:**400-8

Mezey, E., Key, S., Vogelsang, G., Szalayova, I., Lange, D., G., Crain, B. 2003. Transplanted bone marrow generates new neurons in human brains. *Proc Natl Acad Sci U S A* **100:**1364-9.

Miao, H., Wei, R., B., Peehl, M., D., Li, Q., Alexandrou, T., Schelling, R., J., Rhim, S., J., Sedor, R., J., Burnett, E., Wang, B. 2001. Activation of EphA receptor tyrosine kinase inhibits the Ras/MAPK pathway. *Nat Cell Biol* **3:**527-30

Miletich, I., Sharpe, T., P. 2004. Neural crest contribution to mammalian tooth formation. *Birth Defects Res Part C Embryo Today* **72:**200-12

Mitsiadis, A., T., Cheraud, Y., Sharpe, P., Fontaine-Perus, J. 2003. Development of teeth in chick embryos after mouse neural crest transplantations. *Proc Natl Acad Sci U S A* **100:**6541-5.

Miura, M., Gronthos, S., Zhao, M., Lu, B., Fisher, W., L., Robey, G., P., Shi, S. 2003. SHED: stem cells from human exfoliated deciduous teeth. *Proc Natl Acad Sci U S A* **100:**5807-12

Miyata, T., Maeda, T., Lee, E., J. 1999. NeuroD is required for differentiation of the granule cells in the cerebellum and hippocampus. *Genes Dev* **13:**1647-52

Modo, M., Rezaie, P., Heuschling, P., Patel, S., Male, K., D., Hodges, H. 2002. Transplantation of neural stem cells in a rat model of stroke: assessment of short-term graft survival and acute host immunological response. *Brain Res* **958:**70-82.

Mooney, J., D., Powell, C., Piana, J., Rutherford, B. 1996. Engineering dental pulp-like tissue in vitro. *Biotechnol Prog* **12:**865-8.

Moore, A., K., Lemischka, R., I. 2006. Stem cells and their niches. *Science* **311:**1880-5

Morrison, J., S., White, M., P., Zock, C., Anderson, J., D. 1999. Prospective identification, isolation by flow cytometry, and in vivo self-renewal of multipotent mammalian neural crest stem cells. *Cell* **96:**737-49.

Morrow, M., E., Furukawa, T., Lee, E., J., Cepko, L., C. 1999. NeuroD regulates multiple functions in the developing neural retina in rodent. *Development* **126:**23-36

Murai, K., K., Pasquale, B., E. 2003. 'Eph'ective signaling: forward, reverse and crosstalk. *J Cell Sci* **116:**2823-32

Nakashima, M. 2005. Bone morphogenetic proteins in dentin regeneration for potential use in endodontic therapy. *Cytokine Growth Factor Rev* **16:**369-76

Nakatomi, H., Kuriu, T., Okabe, S., Yamamoto, S., Hatano, O., Kawahara, N., Tamura, A., Kirino, T., Nakafuku, M. 2002. Regeneration of hippocampal pyramidal neurons after ischemic brain injury by recruitment of endogenous neural progenitors. *Cell* **110:**429-41.

Nakayama, T., Momoki-Soga, T., Yamaguchi, K., Inoue, N. 2004. Efficient production of neural stem cells and neurons from embryonic stem cells. *Neuroreport* **15:**487-91

Nawa, Y., Hara, M., Tanimoto, K., Nakase, K., Kozuka, T., Maeda, Y. 2006. Single-dose daily infusion of cyclosporine for prevention of Graft-versus-host disease after allogeneic bone marrow transplantation from HLA allele-matched, unrelated donors. *Int J Hematol* **83:**159-63

Nie, X., Tian, W., Zhang, Y., Chen, X., Dong, R., Jiang, M., Chen, F., Jin, Y. 2006. Induction of transforming growth factor-beta 1 on dentine pulp cells in different culture patterns. *Cell Biol Int* **30:**295-300

Niemann, C. 2006. Controlling the stem cell niche: right time, right place, right strength. *Bioessays* **28:**1-5

Nikolova, Z., Djonov, V., Zuercher, G., Andres, C., A., Ziemiecki, A. 1998. Cell-type specific and estrogen dependent expression of the receptor tyrosine kinase EphB4 and its ligand ephrin-B2 during mammary gland morphogenesis. *J Cell Sci* **111:**2741-51.

Nishimura, K., E., Jordan, A., S., Oshima, H., Yoshida, H., Osawa, M., Moriyama, M., Jackson, J., I., Barrandon, Y., Miyachi, Y., Nishikawa, S. 2002. Dominant role of the niche in melanocyte stem-cell fate determination. *Nature* **416:**854-60

Noren, K., N., Lu, M., Freeman, L., A., Koolpe, M., Pasquale, B., E. 2004a. Interplay between EphB4 on tumor cells and vascular ephrin-B2 regulates tumor growth. *Proc Natl Acad Sci U S A* **101:**5583-8

Noren, K., N., Pasquale, B., E. 2004b. Eph receptor-ephrin bidirectional signals that target Ras and Rho proteins. *Cell Signal* **16:**655-66

Nosrat, A., C., Fried, K., Ebendal, T., Olson, L. 1998. NGF, BDNF, NT3, NT4 and GDNF in tooth development. *Eur J Oral Sci* **106 Suppl 1:**94-9

Nosrat, A., C., Fried, K., Lindskog, S., Olson, L. 1997. Cellular expression of neurotrophin mRNAs during tooth development. *Cell Tissue Res* **290:**569-80

Nosrat, A., C., Tomac, A., Lindqvist, E., Lindskog, S., Humpel, C., Stromberg, I., Ebendal, T., Hoffer, J., B., Olson, L. 1996. Cellular expression of GDNF mRNA suggests multiple functions inside and outside the nervous system. *Cell Tissue Res* **286:**191-207

Nosrat, V., I., Smith, A., C., Mullally, P., Olson, L., Nosrat, A., C. 2004. Dental pulp cells provide neurotrophic support for dopaminergic neurons and differentiate into neurons in vitro; implications for tissue engineering and repair in the nervous system. *Eur J Neurosci* **19:**2388-98

Nosrat, V., I., Widenfalk, J., Olson, L., Nosrat, A., C. 2001. Dental pulp cells produce neurotrophic factors, interact with trigeminal neurons in vitro, and rescue motoneurons after spinal cord injury. *Dev Biol* **238:**120-32.

O'Connor, R., Tessier-Lavigne, M. 1999. Identification of maxillary factor, a maxillary process-derived chemoattractant for developing trigeminal sensory axons. *Neuron* **24:**165-78.

Ogawa, K., Wada, H., Okada, N., Harada, I., Nakajima, T., Pasquale, B., E., Tsuyama, S. 2006. EphB2 and ephrin-B1 expressed in the adult kidney regulate the cytoarchitecture of medullary tubule cells through Rho family GTPases. *J Cell Sci* **119:**559-70

Ohazama, A., Tucker, A., Sharpe, T., P. 2005. Organized tooth-specific cellular differentiation stimulated by BMP4. *J Dent Res* **84:**603-6

Ohlstein, B., Kai, T., Decotto, E., Spradling, A. 2004. The stem cell niche: theme and variations. *Curr Opin Cell Biol* **16:**693-9

Ohshima, H., Yoshida, S. 1992. The relationship between odontoblasts and pulp capillaries in the process of enamel- and cementum-related dentin formation in rat incisors. *Cell Tissue Res* **268:**51-63

Okubo, T., Yanai, N., Obinata, M. 2006. Stromal cells modulate ephrinB2 expression and transmigration of hematopoietic cells. *Exp Hematol* **34:**330-8

Osborne, J., N., Begbie, J., Chilton, K., J., Schmidt, H., Eickholt, J., B. 2005. Semaphorin/neuropilin signaling influences the positioning of migratory neural crest cells within the hindbrain region of the chick. *Dev Dyn* **232:**939-49

Palmer, D., T., Markakis, A., E., Willhoite, R., A., Safar, F., Gage, H., F. 1999. Fibroblast growth factor-2 activates a latent neurogenic program in neural stem cells from diverse regions of the adult CNS. *J Neurosci* **19:**8487-97.

Palmer, D., T., Willhoite, R., A., Gage, H., F. 2000. Vascular niche for adult hippocampal neurogenesis. *J Comp Neurol* **425:**479-94

Pan, M., Naftel, P., J., Wheeler, F., E. 2000. Effects of deprivation of neonatal nerve growth factor on the expression of neurotrophin receptors and brain-derived neurotrophic factor by dental pulp afferents of the adult rat. *Arch Oral Biol* **45:**387-99

Papayannopoulou, T. 2004. Current mechanistic scenarios in hematopoietic stem/progenitor cell mobilization. *Blood* **103:**1580-5

Parent, M., J., Lowenstein, H., D. 2002a. Seizure-induced neurogenesis: are more new neurons good for an adult brain? *Prog Brain Res* **135:**121-31.

Parent, M., J., Valentin, V., V., Lowenstein, H., D. 2002b. Prolonged seizures increase proliferating neuroblasts in the adult rat subventricular zone-olfactory bulb pathway. *J Neurosci* **22:**3174-88.

Pasquale, B., E. 2004. Eph-ephrin promiscuity is now crystal clear. *Nat Neurosci* **7:**417-8

Pawson, T., Scott, D., J. 1997. Signaling through scaffold, anchoring, and adaptor proteins. *Science* **278:**2075-80

Peretto, P., Merighi, A., Fasolo, A., Bonfanti, L. 1999. The subependymal layer in rodents: a site of structural plasticity and cell migration in the adult mammalian brain. *Brain Res Bull* **49:**221-43.

Peters, H., Balling, R. 1999. Teeth. Where and how to make them. *Trends Genet* **15:**59-65.

Peters, H., Neubuser, A., Kratochwil, K., Balling, R. 1998. Pax9-deficient mice lack pharyngeal pouch derivatives and teeth and exhibit craniofacial and limb abnormalities. *Genes Dev* **12:**2735-47

Picard-Riera, N., Nait-Oumesmar, B., Evercooren, B.-V., A. 2004. Endogenous adult neural stem cells: limits and potential to repair the injured central nervous system. *J Neurosci Res* **76:**223-31

Pituch-Noworolska, A., Majka, M., Janowska-Wieczorek, A., Baj-Krzyworzeka, M., Urbanowicz, B., Malec, E., Ratajczak, Z., M. 2003. Circulating CXCR4-positive stem/progenitor cells compete for SDF-1-positive niches in bone marrow, muscle and neural tissues: an alternative hypothesis to stem cell plasticity. *Folia Histochem Cytobiol* **41:**13-21

Pleasure, J., S., Collins, E., A., Lowenstein, H., D. 2000. Unique expression patterns of cell fate molecules delineate sequential stages of dentate gyrus development. *J Neurosci* **20:**6095-105.

Poliakov, A., Cotrina, M., Wilkinson, G., D. 2004. Diverse roles of eph receptors and ephrins in the regulation of cell migration and tissue assembly. *Dev Cell* **7:**465-80

Ramalho-Santos, M., Yoon, S., Matsuzaki, Y., Mulligan, C., R., Melton, A., D. 2002. "Stemness": transcriptional profiling of embryonic and adult stem cells. *Science* **298:**597-600.

Reynolds, A., B., Weiss, S. 1992. Generation of neurons and astrocytes from isolated cells of the adult mammalian central nervous system. *Science* **255:**1707-10.

Reynolds, A., B., Weiss, S. 1996. Clonal and population analyses demonstrate that an EGF-responsive mammalian embryonic CNS precursor is a stem cell. *Dev Biol* **175:**1-13.

Rhrich-Haddout, F., Klosen, P., Portier, M., M., Horvat, C., J. 1997. Expression of peripherin, NADPH-diaphorase and NOS in the adult rat neocortex. *Neuroreport* **8:**3313-6

Robinson, V., Smith, A., Flenniken, M., A., Wilkinson, G., D. 1997. Roles of Eph receptors and ephrins in neural crest pathfinding. *Cell Tissue Res* **290:**265-74

Ross, J., Li, L. 2006. Recent advances in understanding extrinsic control of hematopoietic stem cell fate. *Curr Opin Hematol* **13:**237-42

Rossi, F., Cattaneo, E. 2002. Opinion: neural stem cell therapy for neurological diseases: dreams and reality. *Nat Rev Neurosci* **3:**401-9.

Ruffins, S., Artinger, B., K., Bronner-Fraser, M. 1998. Early migrating neural crest cells can form ventral neural tube derivatives when challenged by transplantation. *Dev Biol* **203:**295-304

Rutherford, B., R. 2001. BMP-7 gene transfer to inflamed ferret dental pulps. *Eur J Oral Sci* **109:**422-4.

Sakamoto, H., Zhang, Q., X., Suenobu, S., Ohbo, K., Ogawa, M., Suda, T. 2004. Cell adhesion to ephrinb2 is induced by EphB4 independently of its kinase activity. *Biochem Biophys Res Commun* **321:**681-7

Sanai, N., Tramontin, D., A., Quinones-Hinojosa, A., Barbaro, M., N., Gupta, N., Kunwar, S., Lawton, T., M., McDermott, W., M., Parsa, T., A., Verdugo, M.-G., J., Berger, S., M., Alvarez-Buylla, A. 2004. Unique astrocyte ribbon in adult human brain contains neural stem cells but lacks chain migration. *Nature* **427:**740-4

Sancho, E., Batlle, E., Clevers, H. 2003. Live and let die in the intestinal epithelium. *Curr Opin Cell Biol* **15:**763-70

Sano, R., Tessitore, A., Ingrassia, A., d'Azzo, A. 2005. Chemokine-induced recruitment of genetically modified bone marrow cells into the CNS of GM1-gangliosidosis mice corrects neuronal pathology. *Blood* **106:**2259-68

Santiago, A., Erickson, A., C. 2002. Ephrin-B ligands play a dual role in the control of neural crest cell migration. *Development* **129:**3621-32

Sawada, T., Inoue, S. 1998. Basement membrane-like structures occurring on the surface of dental papilla mesenchymal cells during odontogenesis in the monkey Macaca fuscata. *Eur J Oral Sci* **106 Suppl 1:**126-31

Scadden, T., D. 2006. The stem-cell niche as an entity of action. *Nature* **441:**1075-9

Schilling, F., T., Kimmel, B., C. 1994. Segment and cell type lineage restrictions during pharyngeal arch development in the zebrafish embryo. *Development* **120:**483-94

Schlosser, G., Northcutt, G., R. 2000. Development of neurogenic placodes in Xenopus laevis. *J Comp Neurol* **418:**121-46

Schmucker, D., Zipursky, L., S. 2001. Signaling downstream of Eph receptors and ephrin ligands. *Cell* **105:**701-4

Schofield, R. 1978. The relationship between the spleen colony-forming cell and the haemopoietic stem cell. *Blood Cells* **4:**7-25

Schofield, R. 1983. The stem cell system. *Biomed Pharmacother* **37:**375-80

Schor, Canfield, A.M.a., E., A. 1998. Ostergenic Potential of Vascular Pericytes. *In:* Marrow Stromal Cell Culture. Beresford, J.a. Owen, and M., editors. Cambridge University Press, United Kingdom

Schor, M., A., Canfield, E., A., Sutton, B., A., Arciniegas, E., Allen, D., T. 1995. Pericyte differentiation. *Clin Orthop*:81-91.

Schwab, H., M., Bartholomae, A., Heimrich, B., Feldmeyer, D., Druffel-Augustin, S., Goebbels, S., Naya, J., F., Zhao, S., Frotscher, M., Tsai, J., M., Nave, A., K. 2000. Neuronal basic helix-loop-helix proteins (NEX and BETA2/Neuro D) regulate terminal granule cell differentiation in the hippocampus. *J Neurosci* **20:**3714-24

Scintu, F., Reali, C., Pillai, R., Badiali, M., Sanna, A., M., Argiolu, F., Ristaldi, S., M., Sogos, V. 2006. Differentiation of human bone marrow stem cells into cells with a neural phenotype: diverse effects of two specific treatments. *BMC Neurosci* **7:**14

Seki, T. 2002a. Expression patterns of immature neuronal markers PSA-NCAM, CRMP-4 and NeuroD in the hippocampus of young adult and aged rodents. *J Neurosci Res* **70:**327-34

Seki, T. 2002b. Hippocampal adult neurogenesis occurs in a microenvironment provided by PSA-NCAM-expressing immature neurons. *J Neurosci Res* **69:**772-83.

Semerad, L., C., Christopher, J., M., Liu, F., Short, B., Simmons, J., P., Winkler, I., Levesque, P., J., Chappel, J., Ross, P., F., Link, C., D. 2005. G-CSF potently inhibits osteoblast activity and CXCL12 mRNA expression in the bone marrow. *Blood* **106:**3020-7

Sen, A., Kallos, S., M., Behie, A., L. 2002. Expansion of mammalian neural stem cells in bioreactors: effect of power input and medium viscosity. *Brain Res Dev Brain Res* **134:**103-13.

Seo, M., B., Miura, M., Gronthos, S., Bartold, M., P., Batouli, S., Brahim, J., Young, M., Robey, G., P., Wang, Y., C., Shi, S. 2004. Investigation of multipotent postnatal stem cells from human periodontal ligament. *Lancet* **364:**149-55

Shah, M., N., Groves, K., A., Anderson, J., D. 1996. Alternative neural crest cell fates are instructively promoted by TGFbeta superfamily members. *Cell* **85:**331-43

Shamah, M., S., Lin, Z., M., Goldberg, L., J., Estrach, S., Sahin, M., Hu, L., Bazalakova, M., Neve, L., R., Corfas, G., Debant, A., Greenberg, E., M. 2001. EphA receptors regulate growth cone dynamics through the novel guanine nucleotide exchange factor ephexin. *Cell* **105:**233-44.

Shea, B., T., Dahl, C., D., Nixon, A., R., Fischer, I. 1997. Triton-soluble phosphovariants of the heavy neurofilament subunit in developing and mature mouse central nervous system. *J Neurosci Res* **48:**515-23

Shi, S., Bartold, M., P., Miura, M., Seo, M., B., Robey, G., P., Gronthos, S. 2005. The efficacy of mesenchymal stem cells to regenerate and repair dental structures. *Orthod Craniofac Res* **8:**191-9

Shi, S., Gronthos, S. 2003. Perivascular niche of postnatal mesenchymal stem cells in human bone marrow and dental pulp. *J Bone Miner Res* **18:**696-704

Shi, S., Robey, G., P., Gronthos, S. 2001. Comparison of human dental pulp and bone marrow stromal stem cells by cDNA microarray analysis. *Bone* **29:**532-9

Shiba, H., Fujita, T., Doi, N., Nakamura, S., Nakanishi, K., Takemoto, T., Hino, T., Noshiro, M., Kawamoto, T., Kurihara, H., Kato, Y. 1998. Differential effects of various growth factors and cytokines on the syntheses of DNA, type I collagen, laminin, fibronectin, osteonectin/secreted protein, acidic and rich in cysteine (SPARC), and alkaline phosphatase by human pulp cells in culture. *J Cell Physiol* **174:**194-205.

Shiba, H., Nakamura, S., Shirakawa, M., Nakanishi, K., Okamoto, H., Satakeda, H., Noshiro, M., Kamihagi, K., Katayama, M., Kato, Y. 1995. Effects of basic fibroblast growth factor on proliferation, the expression of osteonectin (SPARC) and alkaline phosphatase, and calcification in cultures of human pulp cells. *Dev Biol* **170:**457-66.

Shimabukuro, Y., Ueda, M., Ichikawa, T., Terashi, Y., Yamada, S., Kusumoto, Y., Takedachi, M., Terakura, M., Kohya, A., Hashikawa, T., Murakami, S. 2005. Fibroblast growth factor-2 stimulates hyaluronan production by human dental pulp cells. *J Endod* **31:**805-8

Shirakawa, M., Shiba, H., Nakanishi, K., Ogawa, T., Okamoto, H., Nakashima, K., Noshiro, M., Kato, Y. 1994. Transforming growth factor-beta-1 reduces alkaline phosphatase mRNA and activity and stimulates cell proliferation in cultures of human pulp cells. *J Dent Res* **73:**1509-14.

Sieber-Blum, M. 1989a. Commitment of neural crest cells to the sensory neuron lineage. *Science* **243:**1608-11

Sieber-Blum, M. 1989b. SSEA-1 is a specific marker for the spinal sensory neuron lineage in the quail embryo and in neural crest cell cultures. *Dev Biol* **134:**362-75

Sieber-Blum, M., Ito, K., Richardson, K., M., Langtimm, J., C., Duff, S., R. 1993. Distribution of pluripotent neural crest cells in the embryo and the role of brain-derived neurotrophic factor in the commitment to the primary sensory neuron lineage. *J Neurobiol* **24:**173-84

Simmons, J., P., Torok-Storb, B. 1991. Identification of stromal cell precursors in human bone marrow by a novel monoclonal antibody, STRO-1. *Blood* **78:**55-62

Smith, A., Robinson, V., Patel, K., Wilkinson, G., D. 1997. The EphA4 and EphB1 receptor tyrosine kinases and ephrin-B2 ligand regulate targeted migration of branchial neural crest cells. *Curr Biol* **7:**561-70.

Smith, R., Bagga, V., Fricker-Gates, A., R. 2003. Embryonic neural progenitor cells: the effects of species, region, and culture conditions on long-term proliferation and neuronal differentiation. *J Hematother Stem Cell Res* **12:**713-25

Smith, T., M., Pencea, V., Wang, Z., Luskin, B., M., Insel, R., T. 2001. Increased number of BrdU-labeled neurons in the rostral migratory stream of the estrous prairie vole. *Horm Behav* **39:**11-21.

Song, J., Vranken, W., Xu, P., Gingras, R., Noyce, S., R., Yu, Z., Shen, H., S., Ni, F. 2002. Solution structure and backbone dynamics of the functional cytoplasmic subdomain of human ephrin B2, a cell-surface ligand with bidirectional signaling properties. *Biochemistry* **41:**10942-9

Song, X., Wong, D., M., Kawase, E., Xi, R., Ding, C., B., McCarthy, J., J., Xie, T. 2004. Bmp signals from niche cells directly repress transcription of a differentiation-promoting gene, bag of marbles, in germline stem cells in the Drosophila ovary. *Development* **131:**1353-64

Steinle, J., J., Meininger, J., C., Chowdhury, U., Wu, G., Granger, J., H. 2003. Role of ephrin B2 in human retinal endothelial cell proliferation and migration. *Cell Signal* **15:**1011-7

Steinle, J., J., Meininger, J., C., Forough, R., Wu, G., Wu, H., M., Granger, J., H. 2002. Eph B4 receptor signaling mediates endothelial cell migration and proliferation via the phosphatidylinositol 3-kinase pathway. *J Biol Chem* **277:**43830-5

Stewart, K., Walsh, S., Screen, J., Jefferiss, M., C., Chainey, J., Jordan, R., G., Beresford, N., J. 1999. Further characterization of cells expressing STRO-1 in cultures of adult human bone marrow stromal cells. *J Bone Miner Res* **14:**1345-56

Stroemer, P., Hodges, H. 2005. Stem cell transplantation after middle cerebral artery occlusion. *Methods Mol Med* **104:**89-104

Sugiura, S., Lahav, R., Han, J., Kou, Y., S., Banner, R., L., Pablo, d., F., Patterson, H., P. 2000. Leukaemia inhibitory factor is required for normal inflammatory responses to injury in the peripheral and central nervous systems in vivo and is chemotactic for macrophages in vitro. *Eur J Neurosci* **12:**457-66

Szebenyi, G., Smith, M., G., Li, P., Brady, T., S. 2002. Overexpression of neurofilament H disrupts normal cell structure and function. *J Neurosci Res* **68:**185-98

Takahashi, M., Arai, Y., Kurosawa, H., Sueyoshi, N., Shirai, S. 2003. Ependymal cell reactions in spinal cord segments after compression injury in adult rat. *J Neuropathol Exp Neurol* **62:**185-94

Takasu, A., M., Dalva, B., M., Zigmond, E., R., Greenberg, E., M. 2002. Modulation of NMDA receptor-dependent calcium influx and gene expression through EphB receptors. *Science* **295:**491-5.

Tallquist, D., M., Soriano, P. 2003. Cell autonomous requirement for PDGFRalpha in populations of cranial and cardiac neural crest cells. *Development* **130:**507-18

Tang, X., X., Brodeur, M., G., Campling, G., B., Ikegaki, N. 1999. Coexpression of transcripts encoding EPHB receptor protein tyrosine kinases and their ephrin-B ligands in human small cell lung carcinoma. *Clin Cancer Res* **5:**455-60.

Tecles, O., Laurent, P., Zygouritsas, S., Burger, S., A., Camps, J., Dejou, J., About, I. 2005. Activation of human dental pulp progenitor/stem cells in response to odontoblast injury. *Arch Oral Biol* **50:**103-8

Tessier-Lavigne, M., Goodman, S., C. 1996. The molecular biology of axon guidance. *Science* **274:**1123-33.

Thesleff, I., Aberg, T. 1999. Molecular regulation of tooth development. *Bone* **25:**123-5.

Togel, F., Isaac, J., Hu, Z., Weiss, K., Westenfelder, C. 2005. Renal SDF-1 signals mobilization and homing of CXCR4-positive cells to the kidney after ischemic injury. *Kidney Int* **67:**1772-84

Tong, J., Elowe, S., Nash, P., Pawson, T. 2003. Manipulation of EphB2 regulatory motifs and SH2 binding sites switches MAPK signaling and biological activity. *J Biol Chem* **278:**6111-9

Tosney, W., K. 1982. The segregation and early migration of cranial neural crest cells in the avian embryo. *Dev Biol* **89:**13-24.

Trainor, A., P., Ariza-McNaughton, L., Krumlauf, R. 2002. Role of the isthmus and FGFs in resolving the paradox of neural crest plasticity and prepatterning. *Science* **295:**1288-91

Trentin, A., Glavieux-Pardanaud, C., Douarin, L., M., N., Dupin, E. 2004. Self-renewal capacity is a widespread property of various types of neural crest precursor cells. *Proc Natl Acad Sci U S A* **101:**4495-500

Tsai, Y., R., Kittappa, R., McKay, D., R. 2002. Plasticity, niches, and the use of stem cells. *Dev Cell* **2:**707-12.

Tucker, S., A., Matthews, L., K., Sharpe, T., P. 1998. Transformation of tooth type induced by inhibition of BMP signaling. *Science* **282:**1136-8.

Turnley, M., A., Faux, H., C., Rietze, L., R., Coonan, R., J., Bartlett, F., P. 2002. Suppressor of cytokine signaling 2 regulates neuronal differentiation by inhibiting growth hormone signaling. *Nat Neurosci* **5:**1155-62.

Uchida, N., Buck, W., D., He, D., Reitsma, J., M., Masek, M., Phan, V., T., Tsukamoto, S., A., Gage, H., F., Weissman, L., I. 2000. Direct isolation of human central nervous system stem cells. *Proc Natl Acad Sci U S A* **97:**14720-5.

Ulupinar, E., Datwani, A., Behar, O., Fujisawa, H., Erzurumlu, R. 1999. Role of semaphorin III in the developing rodent trigeminal system. *Mol Cell Neurosci* **13:**281-92.

Varelias, A., Koblar, A., S., Cowled, A., P., Carter, D., C., Clayer, M. 2002. Human osteosarcoma expresses specific ephrin profiles: implications for tumorigenicity and prognosis. *Cancer* **95:**862-9.

Vescovi, L., A., Gritti, A., Galli, R., Parati, A., E. 1999. Isolation and intracerebral grafting of nontransformed multipotential embryonic human CNS stem cells. *J Neurotrauma* **16:**689-93.

Vogel, F., W., Abdulhussein, R., Ford, E., C. 2006. Sensing extracellular matrix: An update on discoidin domain receptor function. *Cell Signal* **18:**1108-16

Wagers, J., A., Christensen, L., J., Weissman, L., I. 2002. Cell fate determination from stem cells. *Gene Ther* **9:**606-12.

Wang, H., Singh, R., S., Zheng, Z., Oh, W., S., Chen, X., Edwards, K., Hou, X., S. 2006. Rap-GEF signaling controls stem cell anchoring to their niche through regulating DE-cadherin-mediated cell adhesion in the Drosophila testis. *Dev Cell* **10:**117-26

Wang, U., H., Anderson, J., D. 1997. Eph family transmembrane ligands can mediate repulsive guidance of trunk neural crest migration and motor axon outgrowth. *Neuron* **18:**383-96

Wang, U., H., Chen, F., Z., Anderson, J., D. 1998. Molecular distinction and angiogenic interaction between embryonic arteries and veins revealed by ephrin-B2 and its receptor Eph-B4. *Cell* **93:**741-53.

Watt, M., S., Chan, Y., J. 2000. CD164--a novel sialomucin on CD34+ cells. *Leuk Lymphoma* **37:**1-25

Wei, L., Cui, L., Snider, J., B., Rivkin, M., Yu, S., S., Lee, S., C., Adams, D., L., Gottlieb, I., D., Johnson, M., E., Jr., Yu, P., S., Choi, W., D. 2005. Transplantation of embryonic stem cells overexpressing Bcl-2 promotes functional recovery after transient cerebral ischemia. *Neurobiol Dis* **19:**183-93

Weiss, S., Dunne, C., Hewson, J., Wohl, C., Wheatley, M., Peterson, C., A., Reynolds, A., B. 1996. Multipotent CNS stem cells are present in the adult mammalian spinal cord and ventricular neuroaxis. *J Neurosci* **16:**7599-609.

Weissman, L., I., Anderson, J., D., Gage, F. 2001. Stem and progenitor cells: origins, phenotypes, lineage commitments, and transdifferentiations. *Annu Rev Cell Dev Biol* **17:**387-403.

Westerman, A., B., Chhatta, A., Poutsma, A., Vegchel, v., T., Oudejans, B., C. 2004. NEUROD1 acts in vitro as an upstream regulator of NEUROD2 in trophoblast cells. *Biochim Biophys Acta* **1676:**96-103

Wilkinson, G., D. 2000. Eph receptors and ephrins: regulators of guidance and assembly. *Int Rev Cytol* **196:**177-244

Xie, T., Spradling, C., A. 2000. A niche maintaining germ line stem cells in the Drosophila ovary. *Science* **290:**328-30

Xu, Q., Alldus, G., Holder, N., Wilkinson, G., D. 1995. Expression of truncated Sek-1 receptor tyrosine kinase disrupts the segmental restriction of gene expression in the Xenopus and zebrafish hindbrain. *Development* **121:**4005-16

Xu, Q., Mellitzer, G., Robinson, V., Wilkinson, G., D. 1999. In vivo cell sorting in complementary segmental domains mediated by Eph receptors and ephrins. *Nature* **399:**267-71

Xu, Q., Mellitzer, G., Wilkinson, G., D. 2000. Roles of Eph receptors and ephrins in segmental patterning. *Philos Trans R Soc Lond B Biol Sci* **355:**993-1002.

Xu, Z., Lai, O., K., Zhou, M., H., Lin, C., S., Ip, Y., N. 2003. Ephrin-B1 reverse signaling activates JNK through a novel mechanism that is independent of tyrosine phosphorylation. *J Biol Chem* **278:**24767-75

Yamaguchi, Y., Pasquale, B., E. 2004. Eph receptors in the adult brain. *Curr Opin Neurobiol* **14:**288-96

Ying, L., Q., Stavridis, M., Griffiths, D., Li, M., Smith, A. 2003. Conversion of embryonic stem cells into neuroectodermal precursors in adherent monoculture. *Nat Biotechnol* **13:**13

Young, S., C., Terada, S., Vacanti, P., J., Honda, M., Bartlett, D., J., Yelick, C., P. 2002. Tissue engineering of complex tooth structures on biodegradable polymer scaffolds. *J Dent Res* **81:**695-700

Zamir, E., Geiger, B. 2001. Molecular complexity and dynamics of cell-matrix adhesions. *J Cell Sci* **114:**3583-90

Zhang, D., Y., Chen, Z., Song, Q., Y., Liu, C., Chen, P., Y. 2005. Making a tooth: growth factors, transcription factors, and stem cells. *Cell Res* **15:**301-16

Zhang, J., Hughes, S. 2006. Role of the ephrin and Eph receptor tyrosine kinase families in angiogenesis and development of the cardiovascular system. *J Pathol* **208:**453-61

Zhang, M., J., Hoffmann, R., Sieber-Blum, M. 1997. Mitogenic and anti-proliferative signals for neural crest cells and the neurogenic action of TGF-beta1. *Dev Dyn* **208:**375-86

Zhang, Q., X., Takakura, N., Oike, Y., Inada, T., Gale, W., N., Yancopoulos, D., G., Suda, T. 2001. Stromal cells expressing ephrin-B2 promote the growth and sprouting of ephrin-B2(+) endothelial cells. *Blood* **98:**1028-37.

Zhang, Y., Bai, F., X., Huang, X., C. 2003. Hepatic stem cells: existence and origin. *World J Gastroenterol* **9:**201-4

Zhou, F., X., Chie, T., E., Rush, A., R. 1998. Distribution of brain-derived neurotrophic factor in cranial and spinal ganglia. *Exp Neurol* **149:**237-42

Zhou, R. 1998. The Eph family receptors and ligands. *Pharmacol Ther* **77:**151-81.

Zimerman, B., Volberg, T., Geiger, B. 2004. Early molecular events in the assembly of the focal adhesion-stress fiber complex during fibroblast spreading. *Cell Motil Cytoskeleton* **58:**143-59

Zimmer, M., Palmer, A., Kohler, J., Klein, R. 2003. EphB-ephrinB bi-directional endocytosis terminates adhesion allowing contact mediated repulsion. *Nat Cell Biol* **5:**869-78

Zisch, H., A., Pazzagli, C., Freeman, L., A., Schneller, M., Hadman, M., Smith, W., J., Ruoslahti, E., Pasquale, B., E. 2000. Replacing two conserved tyrosines of the EphB2 receptor with glutamic acid prevents binding of SH2 domains without abrogating kinase activity and biological responses. *Oncogene* **19:**177-87

Zou, X., J., Wang, B., Kalo, S., M., Zisch, H., A., Pasquale, B., E., Ruoslahti, E. 1999. An Eph receptor regulates integrin activity through R-Ras. *Proc Natl Acad Sci U S A* **96:**13813-8.